

ABSTRACT

BERECZ, MICHAEL JOHN. The Disinfection and Protection of Microorganisms in Complex Water Systems. (Under the direction of Michael K. Stoskopf.)

The objective of this research was to characterize the antimicrobial properties of a derivatized C₆₀ fullerene as a potential supplement to disinfection in complex water systems. Microorganisms in complex water systems like those found in aquaculture and wastewater treatment operations present challenges to effective and efficient inactivation by ultraviolet light because of radiation attenuation by particulate matter in the form of scattering and absorption of electromagnetic energy. With the experimental conditions of these studies, a protective effect was found with increased concentration of the experimental compound fullerol. The evidence obtained in these studies suggested a shielding effect by fullerol aggregates resulted in ultraviolet light attenuation and led to the protective effect on microorganisms. The data were used to fit a sigmoidal dose response model and a deterministic EC50 dose-response model was created and evaluated to simplify the experimental system. Derivations of the model allowed for replacement of the $k \cdot I$ product in the traditional first order inactivation model for ultraviolet disinfection with the EC50 and dose variables. This model could be used to model disinfection or protection in experimental or applied systems where particle loads fluctuate or the intensity or first order kinetic rate constant (k) are unknown or difficult to accurately measure or calculate. These conditions can be common in complex water systems.

© Copyright 2010 by Michael John Berecz

All Rights Reserved

The Disinfection and Protection of Microorganisms in Complex Water Systems

by
Michael John Berez

A dissertation submitted to the Graduate Faculty of
North Carolina State University
in partial fulfillment of the
Requirements for the degree of
Doctor of Philosophy

Comparative Biomedical Sciences

Raleigh, North Carolina

2010

APPROVED BY:

Michael K. Stoskopf
Chair of Advisory Committee

Jay F. Levine

Thomas M. Losordo

Phillip E. Russell

DEDICATION

My entire work and infinitesimal existence are dedicated to my little family.

Amée, Tristan and Keira

Only through their innocence did I earn my salvation.

Only through their enduring love do I exist at this moment in time.

Only through their lives will I survive my own death

and witness the future for which I yearn.

“PEACE AND LONG LIFE, MY CHILDREN, PEACE AND LONG LIFE!”

...AND, LOGICALLY, THE HEAVENS RESOUND

FROM GALAXY TO GALAXY,

“LIVE LONG AND PROSPER ...”

BIOGRAPHY

Born in Alpha Quadrant, Sector 001, Earth, in an area currently known as Inglewood, California, Dr. Berecz developed juvenile neurons in Berrien Center, a small rural crossroads in southwest Michigan. He graduated high school from Andrews Academy in 1988 and attended undergraduate courses at Lake Michigan College, Andrews University, and finally, Michigan State University where he obtained his Bachelor of Science in Veterinary Science (1998) and Doctor of Veterinary Medicine (2001) degrees. He served in the United States Navy on board USS Shiloh (CG-67) from 1993 to 1997 as a sonar technician and made two deployments to the Persian Gulf. After he graduated from veterinary school, he continued active duty service in the United States Army Veterinary Corps. His first assignment was Branch Chief, Brunswick, Maine where he oversaw veterinary services in Massachusetts, New Hampshire, Vermont, Maine and Quebec, Canada. In 2003, he was reassigned to Hanau, Germany where he served as officer-in-charge of veterinary services for North Branch, Northern Europe Veterinary Detachment. His area of responsibility included Germany, Denmark, Sweden, Norway, Netherlands, Greenland, and South Africa where his expertise resided in food safety and sanitation inspections and audits of military and commercial facilities. In 2006, Dr. Berecz moved to Raleigh, North Carolina to pursue a Doctor of Philosophy degree in Comparative Biomedical Sciences with focus on aquatic animal medicine, preventive medicine and toxicology. Dr. Berecz continues research at the United States Army Medical Research Institute of Chemical Defense (USAMRICD) at Aberdeen Proving Ground, Maryland.

ACKNOWLEDGMENTS

Appreciation goes to my committee members for their support, encouragement and many helpful suggestions during my PhD program. I indebted myself to Dr. Michael Stoskopf for his patience with me, although I wish I could have garnered more of his vast knowledge while under his mentorship. I thank Dr. Jay Levine for my use of his laboratory and other significant resources. I am grateful to Dr. Phillip Russell who allowed me to use his instruments and personnel at Appalachian State University and for his technical expertise. Finally, I thank Dr. Thomas Losordo for his tours at the North Carolina State University aquaculture facility that let me learn more about the aquaculture industry and kept me realistic in terms of how things actually work in aquaculture.

In addition, I thank Ms. Susan Yun and Dr. Ronald Hedrick at the University of California at Davis for their supply of cell cultures and viruses. Appreciation also goes to Mr. Richard Sweeney at the United States Army Medical Research Institute of Chemical Defense (USAMRICD) for mathematical expertise. Also, I acknowledge Dr. Rattapan Pattanarangsarn's tender care of my bacteria and viruses in my absence and to the other members of Dr. Stoskopf's and Dr. Levine's laboratory groups for any suggestions and help along the way. Lastly, I thank Mr. Dennis DeLong at the NCSU aquaculture facility for his input on various aquaculture topics.

TABLE OF CONTENTS

LIST OF TABLES	viii
LIST OF FIGURES	x
PART I: LITERATURE REVIEW	1
CHAPTER 1	2
Physical, chemical and biological characteristics of chemical photosensitizers	2
Introduction:.....	2
Photosensitizer overview:	3
Bacteria:	7
Viruses:	10
Carbon nanomaterials:	11
Photosensitizers and complex water systems:	16
CHAPTER 2	19
Relevant aspects of disinfection in complex water systems	19
Introduction:.....	19
Common disinfection methods:	22
The disinfection challenge of protected microorganisms:	28
Particles and disinfection kinetics:.....	36
PART II: EXPERIMENTAL.....	42
CHAPTER 3	43
Microbial survival with <i>in vitro</i> treatment of fullerol and ultraviolet irradiation	43
Abstract	43
Introduction.....	44
Materials and Methods.....	45
Photosensitizer handling and analysis	45

Ultraviolet light source	47
Selected microorganisms and culture	48
Bacterial ultraviolet irradiation experiments	50
Viral ultraviolet irradiation experiments.....	53
Relative sensitivity of the test bacteria to ultraviolet irradiation	55
Results.....	56
Discussion.....	69
CHAPTER 4	76
Mechanistic studies of a microbial protective effect of fullerol	76
Abstract.....	76
Introduction.....	77
Materials and Methods.....	78
Results.....	81
Scanning electron microscopy analysis	81
Dynamic light scattering analysis	84
Absorption analysis.....	85
Discussion.....	103
PART III: MATHEMATICAL.....	111
CHAPTER 5	112
A deterministic dose-response model for microbial inactivation by ultraviolet irradiation in the presence of a protective concentrations of particles	112
Abstract.....	112
Introduction.....	113
Materials and Methods.....	117
Model derivation.....	117
Model simulations.....	129
Results.....	130

Discussion.....	139
PART IV: REFERENCES.....	143
REFERENCES	144
PART V: APPENDICES.....	157
APPENDIX A.....	158
Raw data for bacterial exposures	158
APPENDIX B.....	163
Raw data and Spearman-Kärber estimators of TCID50/mL for viral exposures.....	163
APPENDIX C.....	164
Raw data for SEM images of fullerol aggregate size and shape analysis.....	164
APPENDIX D.....	175
Raw data for fullerol aggregate size measurements	175
APPENDIX E.....	187
Raw data for UV-vis spectrophotometry of fullerol treatments	187
APPENDIX F.....	190
Statistical calculations of experimental data.....	190
APPENDIX G.....	209
MATLAB code for mathematical modeling.....	209
APPENDIX H.....	217
Visual Molecular Dynamics (VMD) code for Figure 1-2 and Figure 3-1	217

LIST OF TABLES

Table 3-1: Components and quantities for bacterial and viral experiments. Quantities are given in microliters. Each dose was run twice, one each for irradiated and non-irradiated groups.....	51
Table 3-2: Median survival ratios (N/N_0) of test microorganisms by fullerol dose. Bs = <i>Bacillus subtilis</i> ; Ec = <i>Escherichia coli</i> ; Se = <i>Salmonella enterica</i> serotype Newport; Vp = <i>Vibrio parahaemolyticus</i> ; SVCV = Spring Viremia of Carp Virus.....	59
Table 3-3: Bacterial sensitivities at 0 mg/L fullerol to ultraviolet irradiation for 15 seconds. Bs = <i>Bacillus subtilis</i> ; Ec = <i>Escherichia coli</i> ; Se = <i>Salmonella enterica</i> serotype Newport; Vp = <i>Vibrio parahaemolyticus</i>	60
Table 3-4: Approximate minimum ultraviolet irradiation dose required to inactivate greater than 99% of certain microorganisms	71
Table 3-5: Characteristics of several virus families of interest to aquaculture. Adapted from Virus Taxonomy, 7 th edition (van Regenmortel, 2000)	71
Table 4-1: Median area, perimeter, circularity and equivalent circular diameter (ECD) for fullerol SEM image analysis by treatment groups. (U=untreated; S=sonicated; 31, 62, 125 and 250 indicate fullerol concentration in mg/L).	83
Table 4-2: Summary table of dynamic light scattering (DLS) data for the four major treatment groups.....	84
Table 5-1: Approximate minimum ultraviolet irradiation dose required to inactivate greater than 99% of certain microorganisms	125
Table 5-2: Best-fit curve calculations for tested microorganisms and fullerol concentrations.	133
Table 5-3: Assumptions of EC50 dose-response model.....	139
Table A-1: Raw data for <i>Bacillus subtilis</i> viability versus fullerol concentration.....	158
Table A-2: Raw data for <i>Escherichia coli</i> (K12) viability versus fullerol concentration....	159

Table A-3: Raw data for <i>Salmonella enterica</i> serotype Newport viability versus fullerol concentration.....	160
Table A-4: Raw data for <i>Vibrio parahaemolyticus</i> viability versus fullerol concentration.	161
Table A-5: Raw data for relative bacterial sensitivity to ultraviolet irradiation.....	162
Table B-1: Raw data and statistics for Spring Viremia of Carp Virus (SVCV) TCID50 assay.	163
Table C-1: Quantitative SEM size and shape analysis data.....	164
Table D-1: Zetasizer data for fullerol aggregate sizes.....	175
Table E-1: UV-vis data.....	187
Table F-1: Statistics for bacterial ultraviolet irradiation studies.....	190
Table F-2: Statistics for relative bacterial sensitivity to ultraviolet irradiation.....	195
Table F-3: Statistics for SEM image analysis.....	196
Table F-4: Statistics for Zetasizer analysis.....	198
Table F-5: Statistics for UV-vis absorbance data.....	208
Table G-1: MATLAB code.....	209
Table H-1: VMD code for C ₆₀ fullerene for Figure 1-2.....	217
Table H-2: VMD code for derivatized C ₆₀ fullerene (fullerol) for Figure 3-1.....	218

LIST OF FIGURES

Figure 1-1: Pathways of photoinactivation of microorganisms by chemical a photosensitizer.	5
Figure 1-2: Structure of fullerene (C ₆₀). Image generated by author with Visual Molecular Dynamics (VMD) version 1.8.6 (Humphrey, Dalke, & Schulten, 1996). PDB code file provided in Appendix H.....	12
Figure 2-1: The intensity of light that reaches a microorganism partially depends upon the concentration of suspended matter. More photons reach microbes in low concentrations (a), while less photons reach microbes when the particulate concentration is relatively high (b).36	
Figure 2-2: Inactivation of microorganisms exhibits tailing when particulate matter interferes with efficacy of disinfection. Modified from (Emerick, et al., 1999).....	40
Figure 3-1: Fullerol is a polyhydroxylated C ₆₀ fullerene. In this representative image, the red spheres represent oxygen atoms. Hydrogen atoms are not shown. Image generated by author with Visual Molecular Dynamics (VMD) version 1.8.6 (Humphrey, et al., 1996). PDB code file provided in Appendix H.....	45
Figure 3-2: Above-view diagram of the physical setup for irradiation experiments.....	48
Figure 3-3: TCID50 assay experimental layout of the 96-well plate.....	54
Figure 3-4: Nuclear Magnetic Resonance (NMR) spectroscopy results for fullerol analysis. The peaks that in the range of about 1-2 ppm is the fullerol and the peak around 3.5 ppm is D ₂ O. The minor peaks are contaminants or noise. The section above and to the left is a 50x magnification of the lower right section.	57
Figure 3-5: <i>Bacillus subtilis</i> viability versus fullerol concentration for irradiated and non-irradiated groups. Boxes indicate 95% confidence interval for the median.	61
Figure 3-6: <i>Escherichia coli</i> (K12) viability versus fullerol concentration for irradiated and non-irradiated groups. Boxes indicate 95% confidence interval for the median.....	62

Figure 3-7: *Salmonella enterica* serotype Newport viability versus fullerol concentration for irradiated and non-irradiated groups. Boxes indicate 95% confidence interval for the median. 63

Figure 3-8: *Vibrio parahaemolyticus* viability versus fullerol concentration for irradiated and non-irradiated groups. Boxes indicate 95% confidence interval for the median. 64

Figure 3-9: Spring Viremia of Carp Virus (SVCV) viability versus fullerol concentration for irradiated and non-irradiated groups. Boxes indicate 95% confidence interval for the median. 65

Figure 3-10: Median survival ($\text{Log}_{10} N/N_0$) of test microorganisms by fullerol concentration for 60 seconds ultraviolet irradiation. Bs = *Bacillus subtilis*; Ec = *Escherichia coli*; Se = *Salmonella enterica* serotype Newport; Vp = *Vibrio parahaemolyticus*; SVCV = Spring Viremia of Carp Virus. 66

Figure 3-11: Median survival (N/N_0) of test microorganisms by fullerol concentration for 60 seconds ultraviolet irradiation. Bs = *Bacillus subtilis*; Ec = *Escherichia coli*; Se = *Salmonella enterica* serotype Newport; Vp = *Vibrio parahaemolyticus*; SVCV = Spring Viremia of Carp Virus. 67

Figure 3-12: Comparison of test bacteria sensitivities to ultraviolet irradiation at 0 mg/L fullerol with the experimental setup. Bs = *Bacillus subtilis*; Ec = *Escherichia coli*; Se = *Salmonella enterica* serotype Newport; Vp = *Vibrio parahaemolyticus*. 68

Figure 4-1: Scanning electron microscopy image of 31 mg/L fullerol in ddH₂O (850x magnification). 86

Figure 4-2: Scanning electron microscopy image of 31 mg/L fullerol in ddH₂O solution (9,900x magnification). 87

Figure 4-3: Scanning electron microscopy image of 62 mg/L fullerol in 0.9% saline solution (12,900x magnification). 88

Figure 4-4: Scanning electron microscopy image of 250 mg/L fullerol in 0.9% saline solution (1,400x magnification). 89

Figure 4-5: Scanning electron microscopy image of 125 mg/L fullerol in 0.9% saline solution 42,500x magnification). 90

Figure 4-6: Scanning electron microscopy image of 62 mg/L fullerol in ddH ₂ O (70,800x magnification).	91
Figure 4-7: Scanning electron microscopy image of 31 mg/L fullerol in ddH ₂ O sonicated solution (12,800x magnification).	92
Figure 4-8: Histogram of untreated fullerol solution at 31 mg/L after SEM image analysis for area, perimeter, circularity, and equivalent circular diameter (ECD).	93
Figure 4-9: Histogram of untreated fullerol solution at 62 mg/L after SEM image analysis for area, perimeter, circularity, and equivalent circular diameter (ECD).	94
Figure 4-10: Histogram of untreated fullerol solution at 125 mg/L after SEM image analysis for area, perimeter, circularity, and equivalent circular diameter (ECD).	95
Figure 4-11: Histogram of untreated fullerol solution at 250 mg/L after SEM image analysis for area, perimeter, circularity, and equivalent circular diameter (ECD).	96
Figure 4-12: Histogram of sonicated fullerol solution at 31 mg/L after SEM image analysis for area, perimeter, circularity, and equivalent circular diameter (ECD).	97
Figure 4-13: Interval plot of SEM image analysis results. Bars indicate 95% confidence interval for the mean.	98
Figure 4-14: Zetasizer Nano ZS fullerol aggregate mean Z-average diameters plotted against concentration.	99
Figure 4-15: Zetasizer Nano ZS fullerol aggregate mean Peak 1 diameters plotted against concentration.	100
Figure 4-16: The 254 nm UV-vis absorbance across a 1.0 mm pathlength of fullerol solutions for untreated, sonicated, filtered and centrifuged treatment groups. This wavelength was output from the experimental UV lamp.	101
Figure 4-17: The 300 nm UV-vis absorbance across a 1.0 mm pathlength of fullerol solutions for untreated, sonicated, filtered and centrifuged treatment groups. This wavelength was output from the experimental UV lamp.	102
Figure 5-1: Median survival (N/N ₀) of test microorganisms by fullerol concentration for 60 seconds ultraviolet irradiation. Bs = <i>Bacillus subtilis</i> ; Ec = <i>Escherichia coli</i> ; Se = <i>Salmonella</i>	

enterica serotype Newport; Vp = *Vibrio parahaemolyticus*; SVCV = Spring Viremia of Carp Virus..... 114

Figure 5-2: Inactivation of microorganisms exhibits tailing when particulate matter interferes with efficacy of disinfection. Y-axis is logarithmic. Modified from (Emerick, et al., 1999).
..... 116

Figure 5-3: Dose-Response curves for tested microorganisms. Solid line is the best-fit curve for the data, while the dashed lines indicate the 95% confidence band for the best-fit curve.
..... 132

Figure 5-4: Results of MATLAB simulation at $\pm 5\%$ change in fullerol EC50..... 134

Figure 5-5: Results of MATLAB simulation at $\pm 5\%$ change in fullerol dose..... 135

Figure 5-6: Results of MATLAB simulation at $\pm 50\%$ change in fullerol EC50..... 136

Figure 5-7: Results of MATLAB simulation at $\pm 50\%$ change in fullerol dose..... 137

Figure 5-8: Plot of maximum sensitivities when EC50 is changed by 10 mg/L. 138

Figure 5-9: Plot of maximum sensitivities when dose is changed by 10 mg/L. 138

PART I: LITERATURE REVIEW

CHAPTER 1

Physical, chemical and biological characteristics of chemical photosensitizers

Introduction: Throughout the past few centuries, knowledge of biology, chemistry and physics progressed to improve the health of humans and other species. Scientists were confident that with the discovery of antibiotics like penicillin, microbial diseases would become problems of the past. This eradication was never realized despite the development of stronger and more specific antimicrobial drugs and disinfection methods. Today, significant amounts of time and other resources are spent to investigate novel or improved antimicrobial drugs and disinfection technologies.

Disinfection is an important aspect of drinking water, wastewater and aquacultural water treatment. The intent of disinfection is to reduce overall numbers of viable microorganisms, which could include possible disease-causing agents, to below minimal infective doses. Water can be a complex medium and has a large range of purity and clarity. Particularly, wastewater of all origins, from human to agricultural, presents challenges to disinfection. This is due to the effects of organic and inorganic matter that is dissolved or suspended within the water. This material can make it difficult to inactivate microorganisms, can cause the dose of disinfection to be miscalculated, and can impair the ability to predict efficacy of disinfection using standard models. Disinfection efforts are also challenged by

the survival of microorganisms in biofilms, crevices, substrates, and other system areas that allow avoidance of disinfection. New investigations into methods of disinfection must address these challenges to be successful.

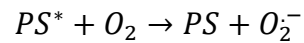
A current focus in the area of novel disinfection methods is the use of photosensitizing compounds. Among several prospects, photosensitizing agents like porphyrins, phthalocyanines, phenothiazines and carbon nanomaterials like C₆₀ fullerenes and nanotubules are currently investigated as alternatives or supplemental disinfection methods in certain applications.

Photosensitizer overview: Much of the prior research into photosensitizing compounds involved their use for medical purposes. Photodynamic antimicrobial chemotherapy (PACT) uses these types of compounds to combat infectious diseases and to disinfect media like blood and hospital water. Photosensitizers (PS) received much attention for a number of reasons. Their efficacy has been considered generally independent of antibiotic resistance, and they do not seem to select for photoresistant strains. Also, many photosensitizers have a broad spectrum of action. Yet, photosensitizers cause limited damage to normal host tissues and they do not seem to be mutagenic. Compared to other agents used for similar purposes, photosensitizers are relatively inexpensive to purchase (Jori, et al., 2006).

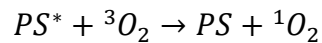
The disinfection capability of photosensitizers is achieved through the requirements of light energy and molecular oxygen. Photosensitization can be described by one of two pathways (Foote, 1991). A type I photosensitization pathway involves the formation of

radicals like superoxide, while a type II pathway forms singlet oxygen, both pathways of which require light energy ($\lambda\nu$). These reaction pathways are depicted below (asterisks indicate activated molecule).

Type I pathway:



Type II pathway:



In the presence of light and oxygen, the photosensitizer acts as a catalyst and can be regenerated to cause multiple reactions and resultant microbial damage (Jori & Brown, 2004). The exact mechanism by which this oxidative damage occurs is complex and is not fully understood. Likely, however, there is not a single mechanism that is valid across all photosensitizing compounds or organic targets. Figure 1-1 depicts the possible primary steps in photoinactivation of different microorganisms by a cationic (positively-charged) photosensitizer (Jori, et al., 2006).

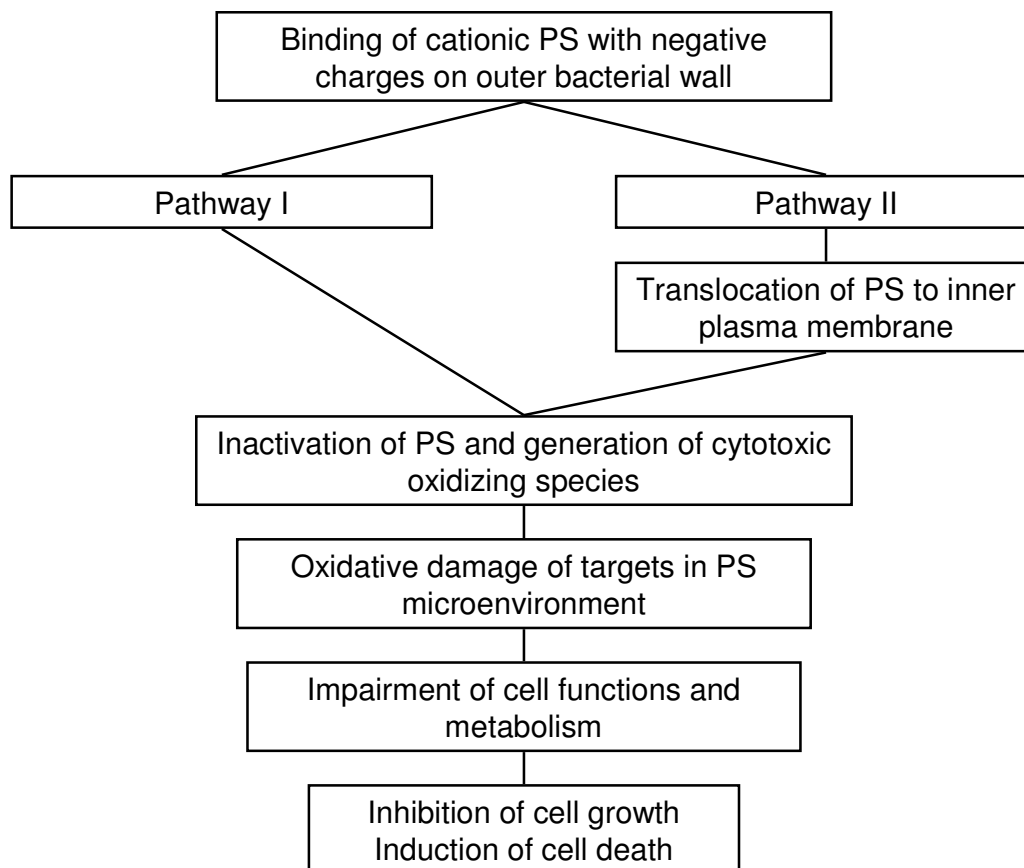


Figure 1-1: Pathways of photoinactivation of microorganisms by chemical a photosensitizer.

As clarification, the pathways in this diagram are not the type I or type II pathways of photosensitization. Pathway I shows the probable scenario for Gram-positive bacteria, viruses and protozoa in the trophozoitic stage. Pathway II shows the steps for inactivation of Gram-negative bacteria, yeasts and protozoa in the cystic stage. In either case, the end result is the same and likely involves an electrostatic interaction between the cationic photosensitizer and the negatively charged functional groups on the cell surface (Jori, et al., 2006).

Inactivation of microorganisms likely occurs through a number of mechanisms dependent on microbial, photosensitizer and environmental properties. Some damage has been found to be intracellular. Many of these data are derived from studies of eukaryotic cells and the responses of tumor cells to photodynamic therapy (PDT). Prokaryotic and eukaryotic cells differ greatly in structure. Prokaryotes lack a nucleus and mitochondria, which leaves the entire genome free within the cytosol. Many photosensitizers do not accumulate in the nucleus (Dougherty, et al., 1998; Moan, 1986). If the intracellular target is DNA, then prokaryotic DNA could be exposed to greater damage by intracellular photosensitizers than eukaryotic DNA that is more protected by the nuclear envelope.

Some photosensitizers are known to localize in the mitochondria or participate in the natural porphyrin biosynthesis pathway within the mitochondria. These photosensitizers are reported to induce apoptosis. The commercially available porphyrin-derived mixture Photofrin® (Axcan Pharma) is an example of these compounds (Dougherty, et al., 1998). This drug has been used with success against esophageal, bladder, lung, head, neck and several other types of cancers. Newer generations of photosensitizers have been investigated and continue to make their way into the pharmaceutical market (Dougherty, et al., 1998).

Some photosensitizers can aggregate at the cell membrane. These compounds can be either hydrophilic or hydrophobic in nature. These aggregated molecules and also the hydrophilic free-floating photosensitizers are often taken up by endocytosis, pinocytosis or both into the cells, and are found associated with lysosomes and endosomes (Berg & Moan, 1994; Dougherty, et al., 1998). When these photosensitizers are exposed to light they can

disrupt the lysosomal membranes and cause the release of destructive enzymes into the cytosol. Within the cytosol, photosensitizers can also cause damage to tubulin (Berg & Moan, 1997).

Prokaryotic inactivation by photosensitizers can occur through damage to the microbial cell envelope and cause an influx of photosensitizer into the cell (Jori, et al., 2006). Within the cytoplasmic space, a variety of subcellular targets like DNA and organelle membranes can be damaged by the reactive species that are generated from the photodynamic processes. Ultimately, these can cause cellular inactivation or death. These damaged endoplasmic components, however, are considered secondary to the primary disruptive damage at the cell membrane (Jori, et al., 2006).

Bacteria: Much of the knowledge of photoinactivation in microbes comes from the studies of bacteria. Chemical photosensitizers, by way of the photooxidative process, can cause significant cellular damage, which can result in bacterial inactivation. *In vitro* studies have demonstrated a 5-6 log₁₀ reduction in bacterial viability after incubation with micromolar concentrations of photosensitizers and exposure to mild light intensities and durations (Jori, et al., 2006; Merchat, Spikes, Bertoloni, & Jori, 1996; Minnock, et al., 1996). These types of investigations reveal that the efficacy of photoinactivation of a given photosensitizer can vary with the Gram-positive versus Gram-negative nature of bacteria. Structural differences in the cell envelopes of Gram-positive and Gram-negative bacteria are at least partially responsible for this variation (Bertoloni, et al., 1992; Malik, Hanania, &

Nitzan, 1990). Gram-positive bacteria are largely susceptible to inactivation by a broad range of photosensitizers, while some Gram-negative organisms are inactivated only after treatment with membrane-disrupting agents such as CaCl₂, Tris-EDTA or polymyxin nonapeptide (Bertoloni, Rossi, Valduga, Jori, & van Lier, 1990; Malik, Ladan, & Nitzan, 1992; Nitzan, Gutterman, Malik, & Ehrenberg, 1992).

Not unexpectedly, a photosensitizer effective against both Gram-positive and Gram-negative bacteria would be desirable. Several cationic agents were investigated, and this led to the discovery of agents that inactivate Gram-positive and Gram-negative bacteria without the use of membrane-disrupting pre-treatment (Merchat, Bertolini, Giacomini, Villanueva, & Jori, 1996; Minnock, et al., 1996; Villanueva, 1993). Cationic photosensitizers include substituted porphyrins and phthalocyanines. The side-chains of these substituted compounds determine the net positive charge of the molecule. The number and length of cationic substituents on the amino nitrogen groups of core photosensitizer molecules influence the hydrophobicity of compounds and alter target inactivating capacity (Hamblin, et al., 2002). For example, Gram-positive bacteria are greatly photoinactivated by amphiphilic porphyrins with two positively charged substitutions bound to two adjacent pyrrole rings. Conversely, Gram-negative bacteria are inactivated well by tetracationic photosensitizers (Jori, et al., 2006).

Some of the differences noted in inactivation among various photosensitizers are attributed to interactions among the substituted groups on the photosensitizers and components of cell membranes. Long-chain hydrocarbon moieties interfere with the three-

dimensional membrane structure and can reduce membrane stability (Merchat, Spikes, et al., 1996). Improvements in photoinactivation are made by longer hydrocarbon chains of up to 18-22 carbon atoms and supports the hypothesis that hydrophobic interactions are important in membrane disruption (Reddi, et al., 2002).

Membrane components are susceptible to damage by reactive oxygen species (Gutteridge, 1995; Vroegop, Decker, & Buxser, 1995). Cell membranes contain large amounts of oxidizable compounds, principally carbohydrates, amino acid side chains and unsaturated fatty acids. Additionally, microbial cell membranes frequently have net negative surface charge. These negative charges arise from the membrane polysaccharides, proteins, and phospholipids (Alberts, et al., 2002; Rijnaarts, Norde, Lyklema, & Zehnder, 1995). Side chain charges are important to interactions between photosensitizers and cell membranes. Negative charges can help bring the positively charged side chains on cationic photosensitizers into close proximity to the cell membranes by electrostatic attraction. The cell membrane, therefore, is a primary location for generated reactive species to come into contact with cellular components. Singlet oxygen diffuses less than 0.02 μm in up to 0.04 μs . after generation by the interaction of a photosensitizer and light (Moan & Berg, 1991). Singlet oxygen decay occurs within $3.5 \mu\text{s} \pm 0.5 \mu\text{s}$ in water and $14 \mu\text{s} \pm 2 \mu\text{s}$ in bacterial membrane phospholipids (Maisch, et al., 2007). For this reason, some investigators think of cellular damage as a marker for the locality where photosensitizers accumulate within or onto a cell (Dougherty, et al., 1998; Moan, et al., 1989).

The thought that bacterial photoinactivation occurs through plasma membrane interactions is supported by several lines of evidence. Fluorescence microscopy conducted on bacteria and protozoa show that photosensitizer localizes at the plasma membrane before irradiation and diffuses into the cell only after several minutes of irradiation. This transition strongly correlates with decreased microbial viability (Jori, et al., 2006). Freeze-fracture electron microscopy of cells after photosensitizer treatment localizes these compounds at the cell membrane (Lambrechts, Aalders, & Van Marle, 2005). The plasma membrane interactions seem to be important to bacterial inactivation by a number of photosensitizing agents.

Viruses: Photoinactivation of viruses was first reported in 1928 (Schultz & Krueger, 1928) and was studied since then in a number of mammalian and plant viruses and bacteriophages with moderate to good success (Alexander, 1935; Birkeland, 1934; Helprin & Hiatt, 1959; Perdrau & Todd, 1933; Wallis & Melnick, 1963; Welsh & Adams, 1954; Yamamoto, 1958). The novelty of the success dampened in the early 1970s when the photosensitizer neutral red was used clinically to treat infections of Herpes Simplex Virus (HSV)(Felber, Smith, & Knox, 1973). Several patients developed Bowen's disease, a form of squamous cell carcinoma that does not invade the dermal layer of the skin. This correlation raised questions about the carefree and inconsistent use of agents such as neutral red to treat patients with HSV or other viruses (Wainwright, 2003).

Viruses can be divided into two major types based upon their membrane structure: enveloped and non-enveloped. Enveloped viruses are enclosed within a lipid membrane derived from the host cell. Examples of enveloped viruses include herpesviruses, rhabdoviruses and retroviruses like Human Immunodeficiency Virus (HIV) (van Regenmortel, 2000). Human Papilloma Virus (HPV) and adenoviruses are examples of non-enveloped viruses that are devoid of a cell-derived packaging (van Regenmortel, 2000; Wainwright, 2004). A number of photosensitizers are effective against both enveloped and non-enveloped viruses, but generally their efficacy of kill is greater for enveloped viruses (Wainwright, 2004). As noted above, cell membranes are composed of easily oxidized compounds like fatty acids or other constituents. The membranes of enveloped viruses are susceptible to damage by the same interactions that impact cell membranes, because they are derived from host cell membranes. For example, enveloped viruses, like HIV and HSV, have much greater susceptibility to photoinactivation by phthalocyanine photosensitizers than non-enveloped viruses (Wainwright, 2004). These studies provide further support to the thought that the cell membrane is a primary target of a large number of photosensitizers.

Carbon nanomaterials: Many fullerenes and carbon nanotubes offer opportunities for the microbial disinfection because they are able to generate reactive oxygen species with light irradiation. Carbon nanomaterials are a class of carbon allotropes in the form of hollow spheres, ellipsoids, or tubes. Fullerenes are sometimes referred to as “buckyballs”, especially the 60 carbon (C₆₀) molecule called “buckminsterfullerene”. This C₆₀ “buckyball”

form is one of the most common forms of investigated fullerenes, and is shaped as a hollow ball with carbon atoms outlining the points of pentagons and hexagons to form sides of the sphere (Ströck, 2006)(Figure 1-2).

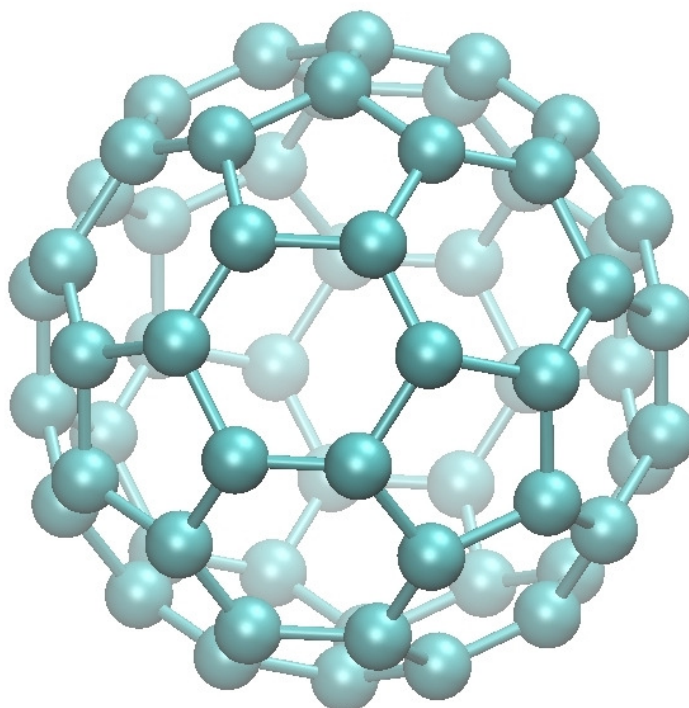


Figure 1-2: Structure of fullerene (C_{60}). Image generated by author with Visual Molecular Dynamics (VMD) version 1.8.6 (Humphrey, Dalke, & Schulten, 1996). PDB code file provided in Appendix H.

Fullerenes were named after Richard Buckminster Fuller, a twentieth century American architect who made popular geodesic domes similar in shape to these molecules. Fullerenes were actually discovered in 1985, two years after Fuller's death. Since then,

fullerene research has grown markedly due to its potential biological and pharmacological uses (Mroz, et al., 2007; Pradeep, 1997), among the many other applications for these compounds. C_{60} fullerenes can encapsulate other compounds, and the fullerene considered to be the “host”. The compound within the cavity of the fullerene is sometimes called the guest. These fullerenes are broadly called inclusion compounds, or more specifically, endohedral fullerenes, and can include atoms such as metals (Shinohara, 2000). Also, C_{60} fullerenes can be functionalized through covalent bonds with various molecular groups to the outer surface of the cage structure. These are commonly called derivatized fullerenes (dC_{60}). Differences in these moieties can change the antimicrobial efficacy of these fullerenes, but in general, increased derivatization is associated with decreased antimicrobial activity (Bosi, Da Ros, Castellano, Banfi, & Prato, 2000; Da Ros, Prato, Novello, Maggini, & Banfi, 1996; Mashino, Nishikawa, et al., 2003; Y. J. Tang, et al., 2007; Tegos, et al., 2005).

Fullerenes exhibit varied degrees of aggregation in solvents like water. The C_{60} molecules can exist in monomeric form (C_{60}) or in aggregates (nC_{60}) that are stably suspended or settled out of an aqueous solution. Several factors can contribute to aggregation of C_{60} fullerenes. Greater salt contents are found to increase C_{60} aggregation (Lyon, Fortner, Sayes, Colvin, & Hughe, 2005). The electrokinetic and charge properties of fullerenes (the dispersed phase) and water (the continuous medium) can also alter the degree of aggregation (Brant, Lecoanet, & Wiesner, 2005; Chen & Elimelech, 2009; Pu, Shuang, & Guo, 2008). This can depend upon the pH, surface charges, or the van der Waals forces between the solvent and the fullerene structures. The preparation method of the fullerene

solution also plays a role in fullerene solubility and aggregation behavior. For example, increased concentration of fullerenes in solution has been shown to result in less solubility and greater aggregating behavior (Liu, Guan, & Cheng, 2007; Murthy & Geckeler, 2001).

Research into the use of fullerenes for microbial inactivation continues and shows some promise. Fullerenes absorb strongly in the ultraviolet and moderately in the visible light spectra (Markovic & Trajkovic, 2008). These compounds were found to act through Type I and II photooxidation reactions (DeRosa & Crutchley, 2002; Guldi & Prato, 2000; Hotze, Labille, Alvarez, & Wiesner, 2008; Vilen, et al., 2006). This reactive oxygen species can then interact with microorganism structures and cause possible inactivation.

Cationic fullerenes, like a number of non-fullerene cationic photosensitizers, can display greater microbial inactivation compared to anionic or neutral compounds (Lee, et al., 2009). Because C_{60} fullerene is near completely insoluble in a polar solvent like water, covalent modification to create charged moieties (i.e. derivatized fullerenes) often results in greater solubility and photoactive capacity. This has been demonstrated with fulleropyrrolidines to create cationic C_{60} nanomaterials with covalently attached moieties (Da Ros, et al., 1996). Several variations of these covalently-modified fullerenes were later incubated with cultures of three *Mycobacterium* species for prolonged periods (3 weeks inhibited mycobacterial growth)(Bosi, et al., 2000). Carboxyfullerene [$C_{63}(\text{COOH})_6$], a water-soluble trimalonic acid derivative, is reported to be effective against both Gram-positive and Gram-negative bacteria (Tsao, et al., 2002). Carboxyfullerene action on at least Gram-positive bacteria is thought to be due to insertion and destruction of the cell membrane

as could be the case for other cationic photosensitizers (Tsao, et al., 2002). Similarly, C₆₀-bis(N,N-dimethylpyrrolidinium iodide, a cationic fullerene derivative, inhibits *Escherichia coli* replication in conditions where an anionic regio-isomer does not (Mashino, Nishikawa, et al., 2003). While many of the properties for other photosensitizers seem applicable to fullerene-based agents, the issue of the site of antimicrobial action for cationic fullerenes is not yet resolved. Some researchers suspect inhibition of the bacterial respiratory chain while others favor membrane disruption as the primary mechanism of bacterial inactivation (Mashino, Usui, Okuda, Hirota, & Mochizuki, 2003; Y. J. Tang, et al., 2007).

Viruses also are inactivated by fullerenes. A C₆₀-derived fullerene has a 50% effective concentration (EC50) of about 3 μM with virus inactivation assays conducted *in vitro* against enveloped HIV-1 (Schinazi, Sijbesma, Srdanov, Hill, & Wudl, 1993). A more recent study found enveloped viruses reduced infectivity by greater than 7 log₁₀ (TCID50) when buffered solutions of viruses and C₆₀ are created and then subjected to visible light irradiation (Kasermann & Kempf, 1997). This viral inactivation is light and oxygen dependent, but protein and other organic content independent.

Several fullerenes like fullerol have antioxidant properties (Chiang, Lu, & Lin, 1995; Dugan, Gabrielsen, Yu, Lin, & Choi, 1996). Although this seems contradictory to the production of ROS and singlet oxygen with conditions of visible and UV irradiation, fullerol has superoxide and hydroxyl radical scavenging ability in non-irradiative conditions (Chiang, et al., 1995; Jeng, et al., 2001; Lu, et al., 1998). That is, ROS quenching occurs in dark conditions (Markovic & Trajkovic, 2008). Increased numbers and types of covalent side-

chains, also known as functionalization, on C₆₀ fullerene molecules (for example, higher numbers of covalently-attached hydroxyl (-OH) functional groups on fullerols), can also result in greater ability of fullerenes to deactivate singlet oxygen (Markovic & Trajkovic, 2008). This scavenging ability of fullerol is complicated by aggregation of molecules in aqueous solution. Despite the relatively high water solubility of fullerols, these compounds cluster into supramolecular structures with increasing concentration, starting at low (micromolar) concentrations (Vileno, et al., 2006). It is proposed that increased radical scavenging could be attributed to concurrent increases in aggregation behavior (Jeng, et al., 2001).

Photosensitizers and complex water systems: Photosensitizing compounds can cause microbial inactivation in a variety of environmental circumstances in which traditional disinfection methods fail. Photosensitizers can have efficacy in a wide range of physical, chemical and biological environments, have shown toxicity toward microorganisms and abnormal eukaryotic cells, and have lesser toxicity to normal eukaryotic cells and organisms (Bonnett, 1995; Mroz, et al., 2007; Wainwright, 1998, 2004).

The primary direction of the series of studies that comprise this dissertation is to further investigate the antimicrobial ability of fullerenes on a bench-scale setup intended to simulate ultraviolet light exposures that could be used in wastewater or aquacultural disinfection. Nanomaterials like fullerenes have potential water disinfection applications (Li, et al., 2008). In complex water systems, like those found in recirculating aquaculture

systems, water quality parameters, microbial diversity, and other environmental conditions can complicate disinfection efforts. For disinfection efficacy, a prospective photosensitizer would need to address these challenges. Fullerenes have several attractive characteristics related to water disinfection. Fullerenes are not destroyed by the photooxidation reaction because they act as a catalyst in the transfer of photonic energy to microbial components. Also, fullerenes have a wide range of absorbance from near-infrared to greater absorbance in the ultraviolet spectrum (Arbogast, et al., 1991; Guldi & Prato, 2000). This includes the same wavelength range (250-270 nm) that optimally inactivates microbial DNA and RNA. This target inactivation wavelength is why ultraviolet disinfection units in aquaculture are designed to emit wavelengths at 253.7 nm (Liltved, 2002) and is true also of wastewater treatment facilities. The basis drawn upon in our studies is that ultraviolet disinfection methods currently in use could be combined with antimicrobial properties of photosensitized fullerenes. If basic research and proof of concept studies demonstrated effective inactivation with simulated conditions, then more applied studies and products could be engineered into a combined system that used fullerenes and ultraviolet light. This could result in less energy consumption, greater microbial inactivation, or both. Fullerenes could prove to be an environmentally safe alternative to traditional chemical disinfectants if they could be effectively and efficiently removed from the water. Greater knowledge of fullerene properties and the steps required for their cost-effective removal from treated water is necessary to determine their role in an engineered disinfection system. This work was oriented toward freshwater fish aquaculture and recirculating systems because of personal

interest and available resources. Certain aspects could be relevant to other types of farmed species, aquaculture systems, or wastewater applications.

CHAPTER 2

Relevant aspects of disinfection in complex water systems

Introduction: Wastewater treatment and recirculating aquaculture systems use a wide range of technologies at various stages for solids removal and disinfection. Disinfection efforts can often be hampered in these complex water systems due to factors associated with water quality. Because of some of the similarities in the processes and components of water quality between human wastewater and aquaculture wastewater routinely found in an intensive recirculating aquaculture system, knowledge is drawn from both fields and related to the current research.

Reduction of solids can greatly enhance the efficacy of disinfection. Recirculating aquaculture systems are designed to remove settleable, suspended, fine or dissolved solids waste in the water (Losordo, Masser, & Rakocy, 1999). Settling methods remove particulates that are large enough to fall to the bottom of the water column by gravity. These solids are most easily removed. Particles too small to settle can often be removed by mechanical filtration and depends on the size restriction design of the filter unit. Mechanical filtration methods include screen filters and expandable granular media filters (Losordo, et al., 1999). There are limits to efficiency with mechanical filtration because very fine solids require such a fine mesh to exclude them that the pump pressure needed to provide flow

through the filters becomes impractical. Very fine solids and dissolved waste are commonly removed by methods like foam fractionation, biological filtration, ozonation, aeration and a number of other technologies that rely on principles other than size exclusion.

Particulate and dissolved waste in aquaculture consist of uneaten food, fish feces, aggregates of bacteria, algae or other organic or inorganic matter (Timmons, Ebeling, Wheaton, Summerfelt, & Vinci, 2002). The organic waste material within aquaculture water can provide nutrients to microorganisms and enable them to flourish, not only as planktonic (“free floating”) entities, but also associated with particulate matter and biofilms within the system (Liltved & Cripps, 1999). In well-designed and properly-operated aquaculture reuse systems, most of these microorganisms do not cause disease to fish or other cultured species (Timmons, et al., 2002). Outbreaks of infectious diseases in recirculating aquaculture systems can be related to overcrowded environments or suboptimal water quality, which in turn can be a consequence of poor system design or management. When stressful conditions are present, fish can become more susceptible to opportunistic and primary pathogens, which can lead to disease outbreaks (El-Sayed, 2006; Sharrer & Summerfelt, 2007).

As is the case for filtration, water disinfection methods also have physical, chemical and biological limitations. The problem is more evident when system design is complex and this complexity increases as the number of components and types of materials used also increases. Despite efforts to eliminate microbes from an aquaculture system by way of solids removal and disinfection, the environments provided within biofilms and residual particulates can afford enough protection to potential pathogens to prevent their extirpation

from the system. Various new technologies are currently being investigated to improve the ability to eliminate potential pathogens from complex water systems. Of interest to this research is the use of photosensitizing compounds. As discussed in Chapter 1, much of the research on photosensitizing compounds focuses on pathogens and eukaryotic cells of concern to human health. Fewer studies are published that pertain to pathogens of aquacultural importance or the use of photosensitizers in complex water systems.

Science builds upon a foundation of previous knowledge. To investigate new ideas, knowledge of the old systems in place is important. The strengths and weaknesses of these previous technologies help build a framework for what is included in the new design and what is discarded. Where photosensitizers fit into disinfection strategies depends upon a number of factors related to the current disinfection methods and the intended purpose of disinfection. The presence of various surface types, biofilms that seed microorganisms into a system, and cavities and crevices where microbes avoid disinfection can all serve to provide complexity to a disinfection effort. The physical, chemical and biological characteristics of the system are critical to the success of any disinfection method. The potential success of photosensitizers, therefore, is not solely dependent on technologic innovation and the ability of these efforts to provide greater photosensitizer-based disinfection at a low cost. Success is dependent upon a systems approach to disinfection.

Common methods of disinfection for large systems of water currently include the use of heat, chlorination, ozonation, ultraviolet radiation, and other less common physical,

chemical or biological methods. A short review of some of these disinfection technologies is necessary and is oriented toward aquaculture.

Common disinfection methods: Heat has long been used for disinfection. Dairy processing facilities routinely use regenerative heat pasteurizing units to achieve adequate bacterial inactivation by a combination of holding time, temperature, and pressure. Use of heat in wastewater and aquaculture is often not practical due to the greater costs required to treat large volumes of aqueous liquids in this manner. Water has a high specific heat capacity (the amount of heat per unit mass needed to raise the temperature by one degree Celsius). About 4.18 J/(g·K) is required to reach temperatures to achieve at least a 3 log₁₀ microbial inactivation. A 3 log₁₀ reduction is equivalent to one microbe of an original 1,000 before disinfection that survives (equivalent to 99.9% inactivation). Even greater temperatures or longer heat contact times are necessary for more complete inactivation of microorganisms. After water is heated within an aquacultural system, it must also be cooled before it is inhabitable by aquaculture organisms like fish, a challenge that can possibly incur greater costs per unit volume disinfected. Because profit margins are slim in many of the aquaculture industries, use of heat, even with regenerative systems, is often cost-prohibitive on a large scale (Wheaton, 1993).

Chlorination is a common disinfection method used for public drinking water, wastewater treatment, and disinfection of tanks and equipment in aquaculture (Tree, Adams, & Lees, 2003; Wedemeyer, 1996; White, 1999). There are risks associated with the use of

chlorine where fish are present because exposure to it causes oxidation of red blood cells and hemoglobin, which can cause methemoglobinemia and death (Grothe & Eaton, 1975).

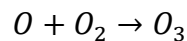
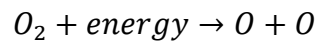
Equipment and tank components disinfected with chlorine must be thoroughly rinsed or given time for chlorine to dissipate (24-48 hours). If a municipal water source is used for aquaculture, chlorine can be removed by methods like activated charcoal filtration, sulfur dioxide neutralization, and aeration and off-gassing before release of the water into the tank containing fish (Wedemeyer, 1996; Wheaton, 1993). The risk of contamination and possible death is great to fish or other cultured organisms if chlorine dissipation methods fail.

Ozone is often used to improve water quality and supplement other disinfection methods like ultraviolet irradiation in a recirculating aquaculture system (Sharrer & Summerfelt, 2007; Summerfelt & Hochheimer, 1997; Summerfelt, Sharrer, Tsukuda, & Gearheart, 2009). Ozone, much like chlorine and other oxidative chemical disinfectants, causes damage to microorganisms through metabolic interference or cell membrane disruption (Blatchley, Dumoutier, Halaby, Levi, & Laine, 2001). Like other disinfection methods, effective ozonation requires sufficient contact time for microbial inactivation or oxidation of organic matter. The ozone residual must be inactivated or off-gassed (usually through aeration) to eliminate toxic risk to cultured animals (Summerfelt & Hochheimer, 1997).

Ozone interacts with inorganic and organic matter within the water. It has the ability to enhance fine solids removal by altering particle surface properties, which results in microflocculation (Krumins, Ebeling, & Wheaton, 2001; Summerfelt, Hankins, Weber, &

Durant, 1997). This aggregating behavior could be due to decreased electrostatic repulsion that is seen in response to some oxidizing compounds (Rav-Acha 1995). Aggregated material settles or floats, and is larger after ozonation, which augments its removal by mechanical means (Tobiason, Edzwald, Reckhow, & Switzenbaum, 1993). Because ozone can clarify water through flocculation and also because UV light at 254 nm destroys ozone, the ozone contactors are routinely placed upstream from ultraviolet irradiation in a recirculating aquaculture system. This allows for greater UV disinfection efficiency as a result of the greater water clarity. This is one example of a combined system that enhances disinfection efficacy or efficiency

Ozone is generated at the location of use through feeding air or oxygen through an electrical corona discharge. The general reaction is



where O_3 is the formula for ozone. Ozone must then be transferred into the water for it to interact oxidatively with microbes and organic matter. This transfer depends on the water temperature, the concentration and type of organic and inorganic materials contained within the water, and the efficiency of the contacting system used (Summerfelt, 2003; Summerfelt & Hochheimer, 1997).

Ozone has the advantages of rapid oxidative reaction rate, few harmful by-products produced in freshwater, less affected by water pH, and oxygen is produced as an end-product (Summerfelt, 2003; Wedemeyer, 1996). Disadvantages include that it currently must be generated on site, the toxicity and hazards to humans and cultured organisms, and the greater cost compared to UV, especially if production and transfer into water is not efficient (Summerfelt & Hochheimer, 1997; Summerfelt, et al., 2009).

Ultraviolet radiation (UVR) can be an effective means of disinfection if properly applied and is probably the most common method in current use within recirculating aquaculture systems. Ultraviolet radiation does not produce known toxic residuals, it can be less complex and more safe than ozonation, and it is often less costly compared to methods like heat and ozonation (Summerfelt, 2003). Ultraviolet dose is sometimes referred to as fluence and is expressed in microwatt seconds per square centimeter ($\mu\text{Ws}/\text{cm}^2$) and is the product of the intensity and the time of exposure. Effective microbial inactivation depends on a number of factors and include the dose and wavelength of the ultraviolet radiation (Summerfelt, 2003). Inactivation, as used here, implies either the loss of ability to replicate or actual cell death. Viability is the ability to replicate. Microorganisms can be inactivated by light in the ultraviolet wavelength range of 100 to 400 nanometers (nm). Ultraviolet light exposure denatures DNA and RNA (Cadet, Anselmino, Douki, & Voituriez, 1992). A wavelength of 260-270 nm is particularly well absorbed by pyrimidine and purine nucleobases and can cause the formation of dimers (Pfeifer, You, & Besaratinia, 2005).

Because low pressure ultraviolet lamps produce radiation at 254 nm and this is close to the optimal nucleic acid absorption, this wavelength is commonly used in ultraviolet reactors.

Dose and wavelength are not the only important considerations in ultraviolet disinfection. Sufficient intensity of the proper wavelengths of ultraviolet radiation can effectively inactivate bacteria, viruses, protozoa, and fungi (Hoffman, 1975; Liltved, 2001; Liltved, Hektoen, & Efraimsen, 1995; Oye & Rimstad, 2001; Wedemeyer, 1996). All microorganisms respond differently, however, to ultraviolet irradiation in terms of behavior and sensitivity (Blatchley, et al., 2001; Liltved, Vogelsang, Modahl, & Dannevig, 2006). The physical and biochemical characteristics of the target organism can affect the ability of UV light to achieve a kill or otherwise inactivate (Summerfelt, 2003). For example, viruses exhibit a differential sensitivity to UV exposure that depends on the type of nucleic acid organization. Double stranded genomes afford more protection against damage compared to single stranded viruses (Liltved, et al., 2006).

Ultraviolet irradiation has other limitations aside from the impact variability on various microorganisms. Ultraviolet light transmission is severely limited by turbidity and dissolved mineral salts (Wedemeyer, 1996). Particle sizes and concentration can affect UV transmission in water. Particulate loads and iron and alkali salts can interfere with UV light transmission and reduce microbial inactivation at a given UV dose (Wheaton, 1993).

Another important consideration in ultraviolet disinfection is the ability of a number of bacteria to repair damaged nucleic acids. This occurs by way of dark repair, photoreactivation, or both. Dark repair is also known as liquid holding recovery. This

potentially makes ultraviolet inactivation only a transient condition (Liltved & Landfald, 1996). Many bacteria are not outright killed by ultraviolet radiation and as many as 10% or more retain cellular respiratory function (Blatchley, et al., 2001). Dark repair processes allow survival of microorganisms in the absence of electromagnetic radiation by excision of UV-damaged nucleic acid base pairs and replication of the complementary bases. This process is slow and can take up to about 48 hours. Photoreactivation is more rapid and can occur in a few hours. When microbes are allowed contact with visible light in the range of 330-480 nm for as little as 20 minutes (Liltved & Landfald, 2000), nucleic acid repair is completed by light-activated enzymes. This repair occurs when the enzymes split thymine dimers formed from UV damage (Wedemeyer, 1996). The photoreactivation rate is positively correlated with visible light intensity (Liltved & Landfald, 1996). Not all microorganisms have repair mechanisms, even among bacteria. Also, it is likely that because viruses lack repair enzymes, photoreactivation has not been observed or is possible (Liltved, et al., 2006).

Ultraviolet disinfection efficacy is generally diminished by anything that reduces electromagnetic radiation transmission such as increased particle loads. Prefiltration, ozonation and other methods of solids flocculation or removal can optimize ultraviolet disinfection. Unfortunately, it is not feasible to eliminate all particles within which microbes can avoid disinfection. Because of their direct toxicity to aquatic production species, neither UV exposure nor ozonation can be safely applied broadly in an occupied water space. Even if total removal of suspended particulate matter was attained from the filtration flow, the

existence of biofilms or the surfaces of system components could still provide avenues of protection to microbes and serve to re-establish populations in the water should ozone or UV disinfection fail. This failure is not limited to mechanical failure of the ultraviolet lamps or other components. Ultraviolet disinfection can also fail because of poor engineering design where the UV system is inadequate for the system it intends to disinfect. Mismanagement can also play a role. Errors in turbidity, flow rate or exposure measurements and calculations can also result in the underestimation or overestimation of applied ultraviolet dose in a complex water system. This can result in inadequate disinfection or the waste of energy.

The disinfection challenge of protected microorganisms: Despite the efforts to eliminate potential pathogens from complex water systems, seeding and regeneration of microorganisms still occurs. Within recirculating aquaculture systems, protection of pathogenic and opportunistic microorganisms is possible through the existence of biotic and abiotic particles, biofilms and fish reservoirs (Sharrer & Summerfelt, 2007). Rough areas in tank walls or crevices in concrete, the insides of pipes or other components, or particulate matter all can provide refuge to microorganisms (Sharrer, Summerfelt, Bullock, Gleason, & Taeuber, 2005).

Though it is dogma that free-living (planktonic) microorganisms are readily inactivated by common disinfection methods like ultraviolet irradiation and ozonation, in reality, “free” bacteria as single or paired cells, but also in aggregates, can have significant resistance to inactivation (Blatchley, et al., 2001; Bossier & Verstraete, 1996; Fletcher &

Marshall, 1982; Qualls, Flynn, & Johnson, 1983). A number of these exposure studies suggest that resistance can result because of the inability of light to penetrate deeply enough into aggregations to inactivate all bacteria.

Aggregates of bacteria can result from attempts to inactivate them. A substantial fraction of bacteria that survive ultraviolet irradiation are found in aggregates of 50-100 bacterial cells with diameters of about 10 micrometers (Blatchley, et al., 2001). Because less bacterial aggregation is observed in non-irradiated water compared to irradiated water, it is thought that exposure to ultraviolet light induces a cluster response. Bacteria deep inside aggregated clusters are protected functionally in the same way that microbes are protected by particle or biofilm association, because the disinfectant is unable to reach the target microbes.

When nutrients in the water increase, populations of bacteria can also increase. Greater feed ingestion by fish can result in greater numbers of fixed (particle- and biofilm-associated) and planktonic bacteria due to the availability of nutrients from uneaten fish food and feces (Leonard, Blancheton, & Guiraud, 2000). Another source of organic particles and bacteria in recirculating aquaculture systems is from the biofilms themselves. Biofilms can disperse microbes from physical filters or sheared release off component surfaces within the system (Mamane, Kohn, & Adin, 2008). Biofilms are known to release high numbers of bacteria into the water (Blancheton & Canaguier, 1995).

Within a properly designed and operated aquaculture system, fluctuations in microbial loads usually are not detrimental to fish from the perspective of mortality or reduced growth or feed conversion. When system design or operation fails, water parameters

can change in ways that favor the growth of pathogenic bacteria more than other species. For example, low numbers of *Vibrio* bacteria are observed among fixed bacterial populations on the pipes, the tank and the biofilter unless the biofilter clogs and leads to the production of anoxic areas within the system (Leonard, et al., 2000). Disruption of the balance of the microbial biodiversity in this scenario can lead to disease outbreaks.

Particles in water can cause health problems for fish and other aquaculture species. Particles can contain pathogens or they can irritate gills or other sensitive anatomy of fishes. Particles can release ammonia or consume oxygen on decomposition, which depends on their chemical composition (Krumins, et al., 2001). Not all particulate matter in water is the same. Particles in supply water can be vastly different from particles in wastewater or aquaculture reuse water (Wu, Clevenger, & Deng, 2005). Water intended for consumption generally contains smaller particles comprised of more minerals and clay, while wastewaters often contain larger, more organic particles (Mamane, Ducoste, & Linden, 2006). Organic particles are especially detrimental in terms of effective disinfection. Organic particles often afford the greatest protection to microorganisms in an aggregation (Qualls, et al., 1983; Sproul, 1979). Microorganisms become easily imbedded and protected within or adsorbed to this organic material. Protection can depend on the size, form, concentration, material, or time of attachment of particles (Wu, et al., 2005).

Particles can cause substantial interference to disinfection efforts. Radiometers are routinely used to estimate the dose (fluence) of ultraviolet radiation that reaches microorganisms. These instruments measure perpendicularly (normal) to the planar surface

of the detector (Mamane, et al., 2006). Radiometers do not accurately measure within ultraviolet light arrays (banks of multiple lamps that emit light in multiple directions), nor in water with significant loads of particulate matter. Significant error can be associated with measurements when particles that scatter light are present (Mamane & Linden, 2006). This can result in overestimation of the actual UV dose that reaches microbes, because scattered light is still able to inactivate microorganisms. Methods exist to minimize this error and obtain more accurate dose or absorbance measurements. These include the use of beam collimators or integrating sphere spectrophotometry. These technologies make incident light more parallel or more accurately measure multi-directional incident light. In wastewater treatment or recirculating aquaculture systems, the routine use of these laboratory methods is impractical and generally used for ultraviolet reactor validation purposes.

Shielding of microbes from ultraviolet light by particles or aggregates is well studied, but less well understood. Many studies have focused on particle shielding from UV light in wastewater and drinking water treatment facilities. Scattering and absorption of light is influenced by particle size, shape, chemical conditions or concentration (Bohren & Huffman, 1983; Mamane, et al., 2006).

Larger particles offer greater protection by physically shielding microbes from ultraviolet light (Mamane, et al., 2006; Oliver & Cosgrove, 1975). Particles larger than 8 – 10 micrometers are found to be more protective against ultraviolet inactivation than smaller suspended material (Qualls, et al., 1983). Greater inactivation of coliforms is achieved when particles larger than 7-8 micrometers are removed through physical pre-filtration (Darby,

Snider, & Tchobanoglous, 1993; Jolis, Lam, & Pitt, 2001; Qualls, et al., 1985). Fractions passed through only a 70 micrometer filter or no filtration have low disinfection rates even when the percent of these larger particles is low compared to smaller particle concentration (Qualls, et al., 1983).

When larger particles that hamper ultraviolet inactivation are present, greater doses are required for the same level of disinfection achieved as when particles are smaller. The greater UV doses penetrate more deeply into larger particles and reach target microorganisms (Jolis, et al., 2001). Studies like these suggest a shielding effect from ultraviolet inactivation by larger particles (Jolis, et al., 2001). They also indicate that when larger particles exist in decreased concentrations compared to smaller particles, these larger particles are what limits disinfection efficacy unless very high UV doses are used.

Particles larger than 5 micrometers in diameter are mostly associated with forward scatter, while smaller particles of about 0.05 micrometers scatter light in all directions equally (Huber & Frost, 1998). If particles greater than 7-8 micrometers limit inactivation, then this suggests that multi-directional scattering of light could be associated with greater disinfection efficacy compared to light that is scattered primarily in one direction. It is possible that ultraviolet radiation spreading multi-directionally would make it less likely that microorganisms would find refuge at any given location. This was previously noted when the addition of submicron particles to an aqueous solution enhanced disinfection by light dispersion (Mamane, et al., 2006). Added submicron particulates in a medium, however, does not necessitate greater disinfection efficacy. The behavior of incident light can depend

on the size, shape, chemistry or the concentration of the particles within the continuous medium.

Absorption of radiation and conversion to heat energy is also a possible consequence when light interacts with a particle (Mishchenko, Travis, & Lacis, 2002). This can be significant when the absorbance of a compound and the associated electrical changes of a particle or aggregate are great at the wavelength of the incident light. For chemical photosensitizers like fullerenes, this can be associated with the wavelength range of greatest photoactivation (Arbogast, et al., 1991; Guldi & Prato, 2000).

As mentioned, the shape of particles can affect how light behaves. Shapes of particulate matter depend on the chemical constituents of the particle, as well as the chemical and physical influences of the surrounding media (Adin, 1999; Mamane, et al., 2008). Wastewater particles vary widely in shape, but are commonly irregular or elongated and can be aggregations of smaller particles (Mamane, et al., 2008). Non-spherical particles can scatter light in many directions and make the analysis of light behavior in these sorts of particle fields more of a challenge (Mishchenko, et al., 2002). It is possible, however, that a more important aspect of particle shape is the ability of elongated microorganisms to be shielded from ultraviolet radiation (Mamane, et al., 2008).

Sizes and shapes are not the only considerations when particles are highly heterogeneous like those observed in wastewater (Mamane, et al., 2008). The chemical characteristics of the medium and the dispersed particles are also important. Water chemistry influences particle aggregation and turbidity (Adin, 1999). Wastewater, either from human

or aquacultural origin, is primarily a sol-type colloid where water is the continuous liquid medium and the particles are the dispersed solid phase. The suspended particles in wastewater generally carry a net negative charge (Adin, 1999; Grutsch, 1978). This charge is quantified in terms of the electrokinetic surface potential known as the zeta potential (ζ). The greater the negative values, the more electrostatically repulsive the interactions are among particles, while smaller zeta potentials can result in tendency for greater flocculation or aggregation. This surface potential of particles in wastewater ranges from about -10 to -18 mV (Adin, 1999). Coagulation or aggregation often occurs within this zeta potential range. Net surface charge can be important in disinfection. Some chemical oxidizers like ozone cause flocculation of particles and an associated decrease in zeta potential (Ravacha, Kummel, Salamon, & Adin, 1995). This right shift in the particle size distribution is a consequence of the decreased electrostatic repulsion among particles. As particles aggregate, the sizes and shapes naturally change. This alters the dynamics of light scattering and absorption and the amount of light available to inactivate microorganisms.

Particle concentration is another factor involved in light behavior within solutions of suspended particles (Mamane, et al., 2006; Teorell, 1931). As the concentration of suspended material increases, the inter-particulate space diminishes per unit volume. Incident light can strike a particle and be absorbed or scattered or it can pass through the particle field (Mamane, et al., 2006; Mishchenko, et al., 2002). The intensity of light that reaches the far side of a group of suspended particles is attenuated due to this scattering or absorption. If a microorganism lies on the far side of this particle field, then less ultraviolet

photons that passed through the field will reach the surface of the microbe (Figure 2-1).

Decreases in the inter-particulate space by increased concentration could result in greater frequency of interactions of photons and the suspended material. This could further attenuate the photonic energy on the far side and possibly less microbial interaction.

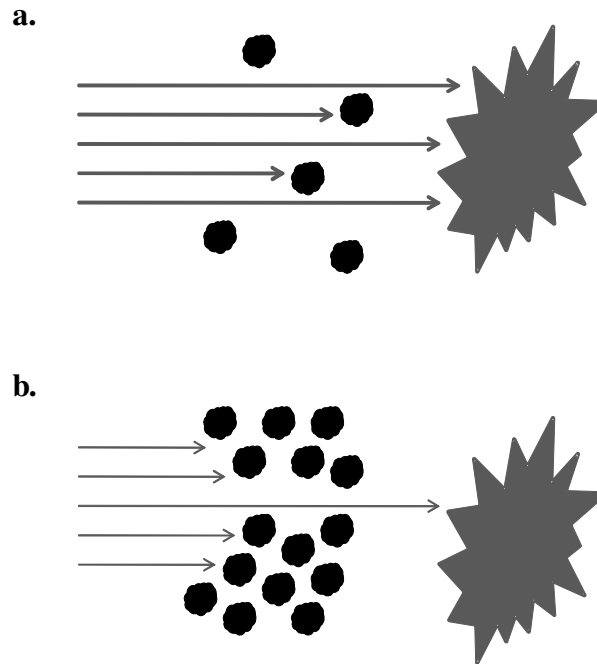


Figure 2-1: The intensity of light that reaches a microorganism partially depends upon the concentration of suspended matter. More photons reach microbes in low concentrations (a), while less photons reach microbes when the particulate concentration is relatively high (b).

Particles and disinfection kinetics: Many mathematical models for disinfection exist that describe microbial inactivation in various conditions and locations. Most are based on a simple model. For a given period of disinfection time (t), the number of viable microorganisms after disinfection (N) compared to the original number of microbes (N_0) before disinfection is known as survival (S) or the survival ratio (N/N_0). In 1908, the rate of disinfection was modeled in two papers by Chick and then Watson by first order inactivation kinetics (Chick, 1908; Watson, 1908). This model relates the rate (r) of inactivation of microbes to the concentration (C) of the disinfectant and contact time (t). The product of concentration and time ($C \cdot t$) is commonly called the dose of the disinfectant. The survival, as

shown in the Chick-Watson model, is a function of the dose. Mathematically, these are written as

$$r = -k \cdot C^n \cdot N$$

where k is the empirical rate constant of inactivation and n is the coefficient of dilution. This equation is more commonly written in the integrated form

$$\frac{N}{N_0} = e^{-k \cdot C \cdot t}$$

where N/N_0 is the survival ratio of microorganisms. The concentration of a chemical disinfectant is analogous to the intensity of light in ultraviolet disinfection kinetics.

Replacing C with I in the above equation gives

$$\frac{N}{N_0} = e^{-k \cdot I \cdot t}$$

or

$$N = N_0 \cdot e^{-k \cdot I \cdot t}$$

where the ultraviolet intensity (I) is traditionally given in microwatts per square centimeter ($\mu\text{W}/\text{cm}^2$) and time is in seconds (s). The dose of ultraviolet radiation is then the product $I \cdot t$ and the units are in microwatt seconds per square centimeter ($\mu\text{Ws}/\text{cm}^2$). Some papers use other units, so it is important to be aware how these units relate. The exponent of the natural logarithm is without units and so the kinetic inactivation rate constant (k) has units of $\text{cm}^2/\mu\text{Ws}$. This constant represents how fast and by how much a microorganism is inactivated at a given wavelength. This can vary dramatically by the type of bacteria and the experimental conditions.

Inactivation kinetics change when particles are present in the water that protects microorganisms. Several authors have attempted to model various systems where particles interfere with disinfection efforts (Emerick, Loge, Ginn, & Darby, 2000; Farnood, 2005; Loge, et al., 1996; Qualls & Johnson, 1985; Scheible, 1987). Protection of microbes can be illustrated by tailing curves (Figure 2-2). As the dose of disinfection increases, the numbers of viable microorganisms decreases. This theoretically could occur with any chemical, physical or biological method of disinfection when further increases in disinfectant dose are associated with little concurrent increases in inactivation. The left region of the curve represents exponential decreases in microbial numbers where protective substances have little influence on disinfection. This first order region is thought to be due to the rapid inactivation of free-swimming organisms (Loge, Bourgeois, Emerick, & Darby, 2001). When particulate matter is present, disinfection efficiency reaches a location on the graph

where the slope approaches zero (tailing region). This can occur well before 100% inactivation is achieved.

A number of theories attempt to explain tailing in microbial dose-response curves. These include association with particles, genetic and cultural variability and resistance induced by the disinfection processes themselves (Blatchley, et al., 2001). Microorganisms can survive inside or otherwise associate with aggregates of particulate matter and are partially protected from ultraviolet inactivation (Oliver & Cosgrove, 1975). Particle number has been found to directly correlate with residual bacterial concentration in wastewater treated with ultraviolet disinfection (Emerick, Loge, Thompson, & Darby, 1999). Also, when large particles are present that hamper ultraviolet inactivation, greater doses are required for the same efficacy as with smaller particles. Greater ultraviolet doses penetrate more deeply into the larger particles to reach the target microorganisms (Jolis, et al., 2001). In addition, greater ultraviolet dose allows for more photons to pass through a particle field and reach a microorganism, which was protected by a previously lesser ultraviolet dose, by particle size shielding, or by lesser particle concentrations.

Reduction of loads of particulate matter that provide safe havens and nutrients for microbes is supported by the proper operation and maintenance of particle pre-filtration systems or other clarification systems, by the routine reduction of biofilm accumulations and by controlled feed programs. Protected microorganisms also could potentially be made more accessible to disinfection by the use of methods like ultrasonication or agitation to break up aggregates into smaller particles.

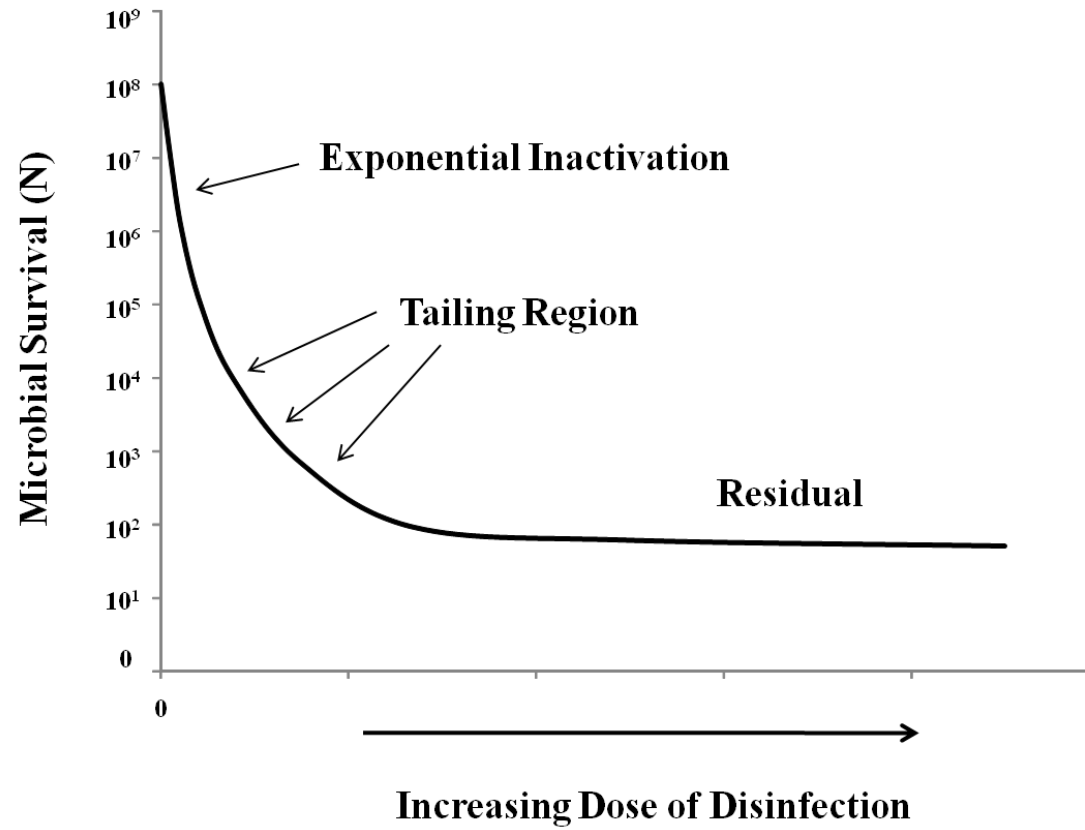


Figure 2-2: Inactivation of microorganisms exhibits tailing when particulate matter interferes with efficacy of disinfection. Modified from (Emerick, et al., 1999).

As mentioned in Chapter 1, photosensitizing compounds are candidates to supplement or replace disinfection methods in certain applications. The studies reported in this dissertation build upon current knowledge of the ability and mechanism of disinfection of fullerol, a derivatized fullerene shown to have antimicrobial properties against several surrogate and pathogenic test organisms. This information is needed to inform a mathematical model of disinfection in complex water systems that could use fullerenes.

PART II: EXPERIMENTAL

CHAPTER 3

Microbial survival with *in vitro* treatment of fullerol and ultraviolet irradiation

Abstract

Fullerenes have antimicrobial capacity in the presence of ultraviolet or visible light. Fullerol, a polyhydroxylated ultraviolet photoactive fullerene, was tested as a disinfectant against four bacterial species, *Bacillus subtilis*, *Escherichia coli* (K12), *Salmonella enterica* serotype Newport, and *Vibrio parahaemolyticus* and one virus, Spring Viremia of Carp Virus (SVCV). These microorganisms were exposed to fullerol concentrations and monochromatic ultraviolet light. The concentration of fullerol was varied from 0 to 250 mg/L, and the survival of microorganisms was calculated for conditions of exposure and non-exposure to ultraviolet irradiation. With the conditions of this study, fullerol was not found to have significant antimicrobial properties. Instead, this compound was protective in nature and microbial survival was greater with increased fullerol concentration. This study underscores the complexity of disinfection and the importance of experimental studies run under a variety of conditions.

Introduction

In their simplest form, fullerenes take on a variety of shapes and are comprised of primarily carbon atoms. The complexity of fullerenes is greater with the addition of side-chains and the degree of aggregation, which in turn can alter their physical and chemical properties, as well as their interactions with biological systems. Fullerenes have been shown to have antimicrobial properties against bacteria and viruses (Y. J. J. Tang, et al., 2007; Tsao, et al., 2002) and have been suggested as candidates for water disinfection applications (Li, et al., 2008). Monomeric C₆₀ fullerene presents a challenge for this type of application because it has low water solubility (Ruoff, Tse, Malhotra, & Lorents, 1993). One method used to counter this problem has been to synthesize derivatives of this fullerene with enhanced aqueous solubility (Li, et al., 2008; Nakamura & Isobe, 2003). Polyhydroxylated fullerene, a water soluble derivative of fullerene, also known as fullerol or fullerenol, produces reactive oxygen species (ROS), specifically, superoxide anion radicals (O₂⁻), and singlet oxygen (¹O₂) in aqueous solution after irradiation with ultraviolet or visible light (Pickering & Wiesner, 2005). Fullerol has been shown to inactivate several species of bacteria (Aoshima, et al., 2009; Lee, et al., 2009) and bacteriophages (Badireddy, Hotze, Chellam, Alvarez, & Wiesner, 2007), and suggests that this photoactive compound, or similar agents, could possibly be engineered into a combined system that uses ultraviolet irradiation for disinfection of aquatic systems. This study investigated the ability of fullerol to inactivate four microorganisms of empirical, biological or aquacultural importance.

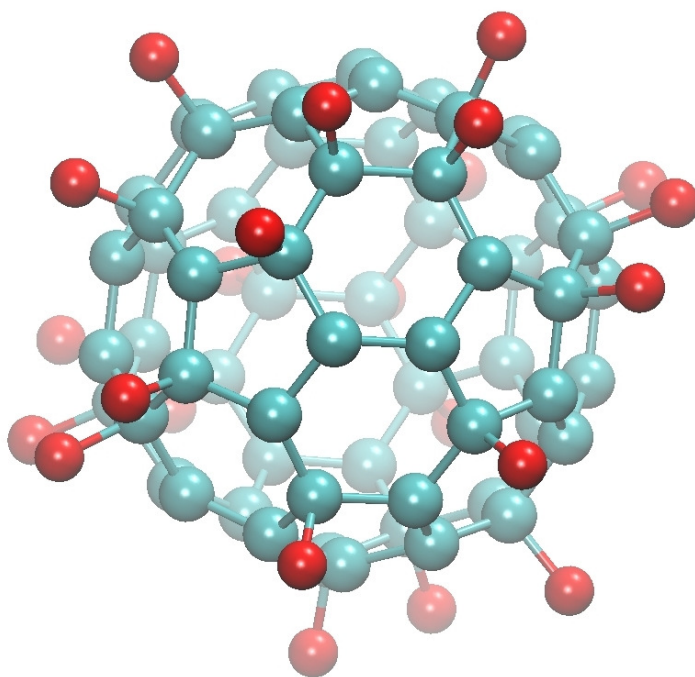


Figure 3-1: Fullerol is a polyhydroxylated C₆₀ fullerene. In this representative image, the red spheres represent oxygen atoms. Hydrogen atoms are not shown. Image generated by author with Visual Molecular Dynamics (VMD) version 1.8.6 (Humphrey, et al., 1996). PDB code file provided in Appendix H.

Materials and Methods

Photosensitizer handling and analysis

Polyhydroxylated fullerene was obtained as a fullerenol salt (C₆₀(OH)_x(ONa)_y; x+y≈24; y≈6-8) in dry powder from (MER Corporation, Tucson, Arizona, USA, Lot #TL6P15A). The fullerol salt had manufacturer-stated impurities of less than 1%. Nuclear magnetic resonance (NMR) spectroscopy was used to confirm fullerol purity. The fullerol (17.5 mg) of fullerol was dissolved in 0.6 mL of 99.8% D₂O in 5 mm PP-535 NMR tubes.

The concentration could not be calculated as the hydroxyl groups and sodium content were unknown. One hour NMR spectroscopy was conducted at 25°C with a Varian Unity Inova NMR instrument at 600 MHz with a 5 mm inverse gradient probe. Thirty-two scans were collected with standard pulse sequence, 2 second relaxation delay and 14 ppm spectral window. Residual water was suppressed using a preset pulse sequence. A 1.0 hertz line broadening parameter was used for data processing. The integration peaks were defined and reported normalized to 100 and the vertical scale of the inset was adjusted to 50,000 (10x) and vertical scale of the complete spectrum was 5,000 units. Baseline correction was done using standard spline algorithm.

Water used in the irradiation experiments was double-distilled water (ddH₂O) and vacuum-filtered through a 0.45 µm mean diameter pore size cellulose nitrate canister filter. Sodium chloride was added to this water to obtain a 0.9% physiological saline solution that was autoclaved for 15 minutes. A stock solution of fullerol was prepared with 22.9 mg of powdered fullerol dissolved in 22.9 mL of physiological saline for a final weight per volume (w/v) concentration of 1,000 mg/L. The solution was agitated for about 4 hours and then stored refrigerated at 8°C. A NanoDrop ND-1000 spectrophotometer (NanoDrop Technologies, LLC, Wilmington, Delaware, USA) was used to measure the ultraviolet absorption of various concentrations of fullerol used in the experiments and the optical density of bacteria concentrations for standard curve generation.

Ultraviolet light source

These studies used a T6 style, 50 watt, high output ultraviolet (UV) lamp with a high output UV power supply (Emperor Aquatics, Pottsville, Pennsylvania, USA). This lamp was effectively monochromatic with a manufacturer-stated peak output of 253.7 nm. Despite the bench-scale design of these studies, the purpose was to include the effects of light absorption and scattering. Also, our experiments were conducted on samples contained in UV-transparent cuvettes and irradiated simultaneously and horizontally. For these reasons, a beam collimator was not used. The uncollimated design was also an advantage because of the different culture and preparation methods required for the microorganisms, which allowed for some standardization between the bacterial and virus studies. The lamp manufacturer's intended kill radius for the specified lamp is about 7.5 centimeters (3 inches). Because the desired response was to inactivate microorganisms with photoactivated fullerol and not with ultraviolet light, the samples were irradiated at a distance of 15 cm as measured from the diametrical center of the lamp (Figure 3-2).

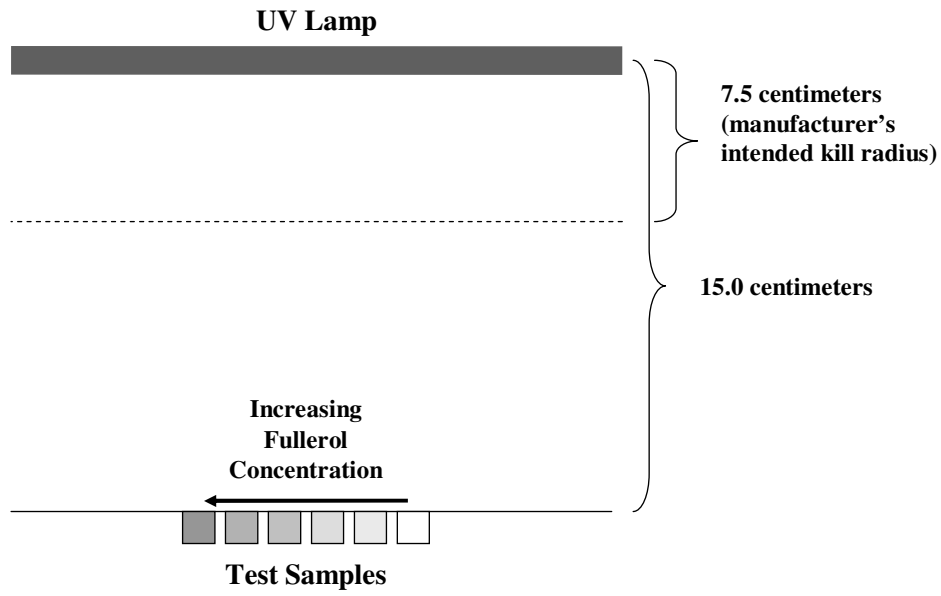


Figure 3-2: Above-view diagram of the physical setup for irradiation experiments.

Selected microorganisms and culture

Bacillus subtilis, *Escherichia coli* (K12), *Salmonella enterica* serotype Newport, and *Vibrio parahaemolyticus* were used in these experiments. *Bacillus subtilis* and *Escherichia coli* (K12) were chosen because they are common surrogates for endospore-forming and coliform bacteria in photosensitizing experiments and disinfection studies. A *Salmonella* species was used because they are common Gram-negative enterobacteria of many animal species to include aquatic invertebrates. The selected species can cause zoonotic infections (disease passed from animals to humans) and can persist outside the host for long periods (Brands, et al., 2005; You, et al., 2006). *Vibrio parahaemolyticus* was chosen as a representative Gram-negative organism. It also is zoonotic and is an aquatic microbe that thrives in brackish water to seawater conditions. All bacteria species were grown non-

selectively on LB broth or agar. *Vibrio* was cultured in LB broth or on LB agar supplemented with 3% sodium chloride. Cultures were incubated at 37°C until a desired liquid media concentration (by optical density determination) or colony forming unit (CFU) size on agar was obtained.

Spring Viremia of Carp Virus (SVCV), an enveloped negative-sense ssRNA fish rhabdovirus, was also used for this study. The virus was cultured on epithelioma papillosum cyprini (EPC) cell line supplied with L-15 (Leibovitz) medium without glutamine supplemented with 10% fetal bovine serum (FBS) and 1% penicillin-streptomycin (growth medium). The EPC cells were grown in T-25 treated tissue culture flasks containing 7-9 mL of medium for about two days at 20°C to about 95%-100% confluence, and then either split or infected.

If split, the medium that overlaid the cells was removed and 2.0 mL of versene-trypsin solution was added and incubated for about five minutes until cells detached from the flask. The cell suspension was then added to about twice the volume of growth medium to stop the proteolytic action of trypsin. The suspension was then centrifuged at 3,000 revolutions per minute (RPM) for five minutes. The supernatant was decanted and the cells resuspended in growth medium and placed with appropriate medium volumes in new flasks. Cell cultures were generally split at a 2:1 to 3:1 ratio.

For infection, the medium was removed and the monolayer was rinsed twice with Hank's Balanced Salt Solution (HBSS). The cells were then inoculated with 100 µL of virus suspension and 1.0 mL of L-15 without FBS or antibiotic to avoid interaction of virus with serum proteins. The flask was then gently rocked for one hour to allow viral infection of the

EPC cells. After this incubation, the cells were overlaid with 7 mL of L-15 medium supplemented with 2% FBS and 1% penicillin-streptomycin for cell maintenance during virus replication. Infected cells were incubated at 20°C for 2-3 days until cytopathic effects (CPE) were seen (usually evidence of apoptosis and detachment from the flask). Virus was harvested by medium removal from the cells and centrifugation at 3,000 RPM for 5 minutes. The virus-containing supernatant was removed from the pellet of cellular debris and either used for infection or stored short-term at -20°C.

Cells were grown on treated 96-well plates for the TCID₅₀ assays. After the cell monolayer was trypsinized and centrifuged, the cellular pellet was resuspended in about 20 mL of growth medium. From this suspension, each well of the 96-well plate was filled with 200 µL. The plate was covered and incubated at 20°C for about two days until monolayers formed in each well.

Bacterial ultraviolet irradiation experiments

A bacterial colony was removed from a Petri dish containing LB agar and transferred to 5.0 mL of liquid LB medium and incubated at 37°C for 3-7 hours, which depended on the bacterial species (*Bacillus subtilis* culture times were generally greater in duration). Subsequently, 100 µL of bacterial suspension was transferred to 5.0 mL of liquid media and incubated for another 3-7 hours, after which optical density (OD₆₀₀) readings were taken using the NanoDrop ND-1000 spectrophotometer. Suspensions were used experimentally once they reached about 10⁷ to 10⁹ CFU/mL.

A 1.0 mL aliquot of bacterial solution was 10-fold serially diluted to about 10^4 to 10^6 CFU/mL, which depended on species. All serial dilutions used in these experiments were made in 0.9% saline except for those for *Vibrio parahaemolyticus*, which were made in 3% saline. This concentration was used for the treatment and control groups. Amounts of culture (always 0.5 mL of the end concentration), fullerol (1,000 mg/L) and 0.9% saline (to make up a total volume of 1.0 mL) were mixed together for the “irradiated” treatment group and the “non-irradiated” control group (Table 3-1). The fullerol doses for the irradiated and non-irradiated groups were 0, 50, 100, 200 and 250 mg/L. These concentrations were chosen because they produced a good range of results in several test runs.

Table 3-1: Components and quantities for bacterial and viral experiments. Quantities are given in microliters. Each dose was run twice, one each for irradiated and non-irradiated groups.

Fullerol Dose	Culture	Fullerol	Saline
0 mg/L	500	0	500
50 mg/L	500	50	450
100 mg/L	500	100	400
200 mg/L	500	200	300
250 mg/L	500	250	250

After the experimental samples were mixed, the five aliquots to be irradiated were transferred to 1.5 mL UV-transparent (220–900 nm) plastic cuvettes. These aliquots were irradiated for 60 seconds at 15 centimeters distance from the center of the ultraviolet lamp. This time was chosen from test runs that revealed longer exposure durations killed nearly all bacteria, and did not allow for us to see an effect of the fullerol.

After irradiation, the samples for both irradiated and non-irradiated groups were each 10-fold serially diluted and then 100 μ L of dilution was added to an LB agar Petri dish. A range of 3 to 5 \log_{10} of the dilutions was plated in triplicate. After an incubation time of about 8-10 hours at 37°C, the colony forming units on the plates were counted and recorded. Generally, the data represents plates that gave about 30-300 CFU/mL. If counts were not available within this range, lesser resolution counts or greater counts via quadrant counting and estimation were used. This occurred in only a few instances. From these colony counts, the titers were calculated by multiplication by the respective dilutions and enumerated in terms of \log_{10} CFU/mL of the original experimental concentration (i.e. about $10^5 - 10^6$ CFU/mL). Boxplots of the medians of the logarithmic values were constricted with 95% confidence intervals for the median microbial numbers and was called viability. Additionally, the median survival ratio (N/N_0) at each fullerol concentration was calculated for each microorganism and the median survival ratios were plotted against the fullerol concentration.

$$\text{Median Survival Ratio} = \frac{\text{median of CFU per mL with irradiation}}{\text{median of CFU per mL without irradiation}} = \frac{N}{N_0}$$

In the log survival plots, values of zero or negative four, which depended on the plot, were arbitrarily inserted when no viable bacteria were present and the \log_{10} value would be undefined. The non-parametric Kruskal-Wallis test was used to evaluate statistical

differences among the log-transformed data to evaluate differences among the concentrations of irradiated bacteria.

Viral ultraviolet irradiation experiments

The viral suspension was not diluted before irradiation because of the assay method used. Instead, all dilutions occurred as part of the TCID₅₀ assay to determine the original viral particle concentration. A 0.5 mL volume of virus-containing supernatant was used for the experimental irradiated and non-irradiated groups (Table 3-1). Unlike in the bacterial experiments where physiological saline was used for dilution, unmodified L-15 medium was used for viral dilutions so that proper media concentrations would be present for EPC cell culture. The UV treatment aliquots of 0, 50, 100, 200 and 250 mg/L were subjected to 60 seconds irradiation. Subsequently, all aliquots were 10-fold serially diluted to 10⁻⁸ with unmodified L-15 medium. A positive control was created using undiluted virus supernatant and a negative control consisted of unmodified L-15 medium.

To infect EPC cells on the 96-well plates, old media was removed from the wells and then 100 µL of the dilution aliquots was overlaid onto the cells. Positive and negative controls were placed in appropriate wells (Figure 3-3). Each dilution was replicated five times for irradiated and non-irradiated groups.

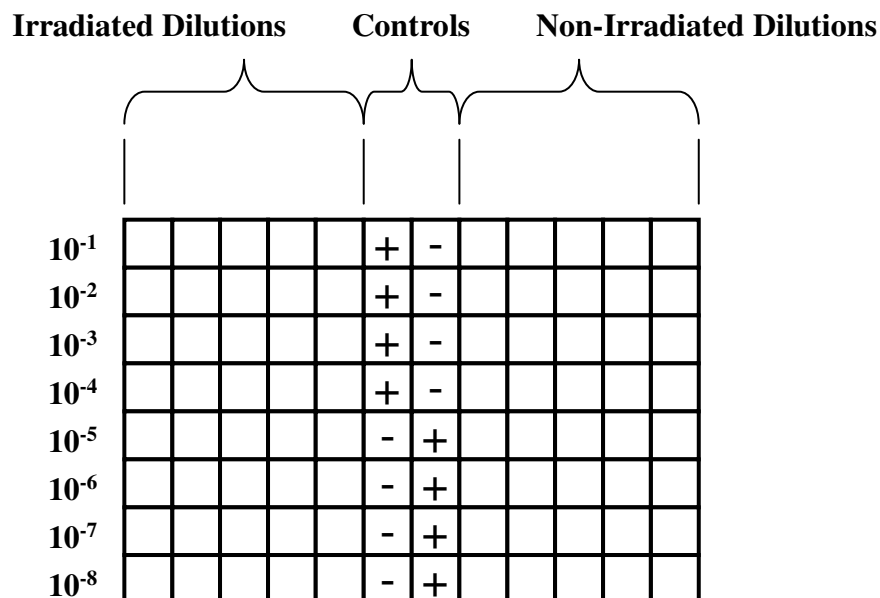


Figure 3-3: TCID50 assay experimental layout of the 96-well plate.

The virus and cells were allowed a one-hour infection period while the plates were gently rocked at 50 RPM at room temperature. The wells were then filled with proper maintenance media to achieve an overall 2% FBS and 1% penicillin-streptomycin concentration in L-15 media. The plates were incubated at 20°C for 2-3 days until cytopathic effects were noted. The plates were then read and each well was marked as CPE positive or negative. The TCID50 determinations and associated standard error calculations were based on the Spearman-Kärber estimator (Hubert, 1992). The calculations were completed with a software calculator created by the author. The median survival ratios were calculated in the same manner as were the bacterial calculations, except the ratio used was of the respective TCID50 values. Numerical and statistical analysis, as well as related graphs and figures, were made with Minitab Version 15.1.0.0 (Minitab, Inc., State College, Pennsylvania, USA),

Microsoft Excel 2003 (Microsoft Corporation, Redmond, Washington, USA), and Microsoft PowerPoint 2003 (Microsoft Corporation, Redmond, Washington, USA).

Relative sensitivity of the test bacteria to ultraviolet irradiation

The relative sensitivities of the bacteria species used to ultraviolet light were evaluated to help in cross-species comparisons of the disinfection effectiveness of combined ultraviolet and fullerol exposure. SVCV was not included in these tests, however, because the virus could not be handled identically to the tested bacteria. Test runs were conducted at various time lengths of UV exposure to determine bacterial sensitivity to UV light without fullerol. From these, an ultraviolet exposure of 15 seconds was selected for the interspecies comparisons. Sensitivity experiments were run with the same conditions described previously except for the shorter irradiation period (15 versus 60 seconds) and the absence of fullerol. Controls without irradiation were performed for each bacterial species to obtain the data needed to calculate median survival ratios as described previously.

Results

The purity of the fullerol used was 99.67% as determined by NMR (Figure 3-4). As seen in the figure there are broad peaks between 1-2 ppm, which can be attributed to hydroxyl groups. The four major peaks (including the broad peak) contribute to 99.67% of the total spectrum. Few peaks are seen at 8.36, 3.85, 3.0 and 2.01 ppm, which contribute to a total of 0.33%. The errors that result from other peaks are well within experimental errors of the instrument. An alternative scenario is that the peak at 1.8 ppm is due to solvent and in those circumstances the fullerol would be 98.15% pure.

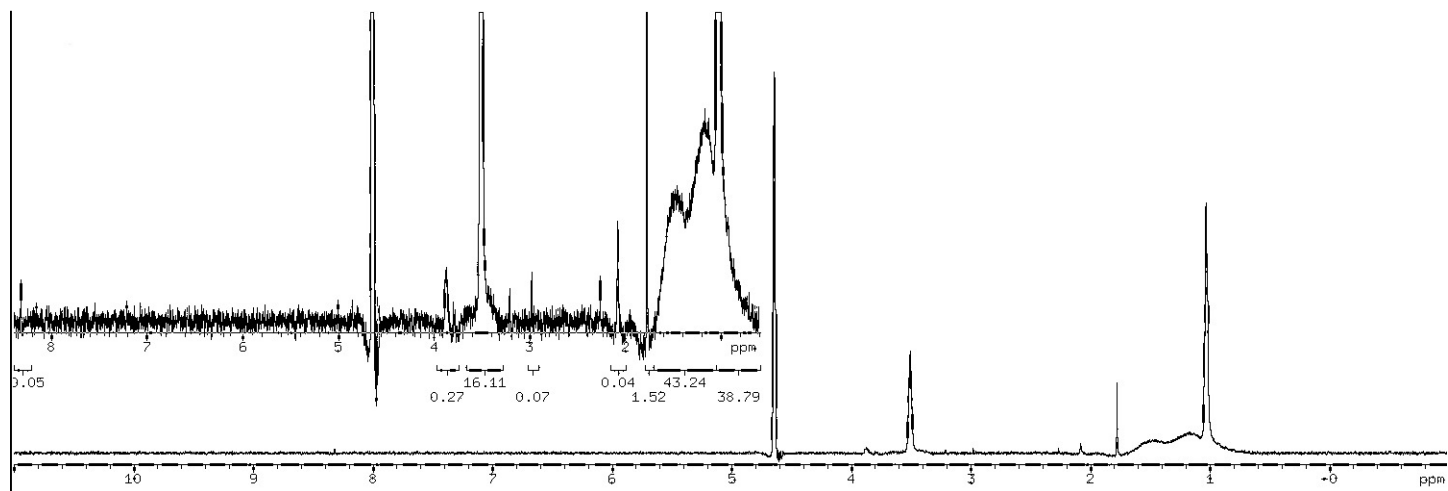


Figure 3-4: Nuclear Magnetic Resonance (NMR) spectroscopy results for fullerol analysis. The peaks that in the range of about 1-2 ppm is the fullerol and the peak around 3.5 ppm is D₂O. The minor peaks are contaminants or noise. The section above and to the left is a 50x magnification of the lower right section.

The peak ultraviolet absorption for an aqueous solution of fullerol at a concentration of 100 mg/L was between 223-226 nm. Absorbance was only about 15% lower for 254 nm wavelength light (APPENDIX E). At other concentrations the amplitude (absorbance) changed, but there was little shift in the wavelength of peak absorbance.

These studies revealed a protective effect of fullerol for all tested microorganisms (Figure 3-5, Figure 3-6, Figure 3-7, Figure 3-8, and Figure 3-9). No antimicrobial property was discernable in these studies with the specified experimental conditions. No significant statistical differences were observed in the median \log_{10} bacterial viability within the range of non-irradiated fullerol concentrations for any bacterial species tested (APPENDIX F). Likewise, SVCV viability was not significantly affected by the presence of fullerol in the non-irradiated samples. Statistically significant differences in viability were seen among the concentrations for the irradiated bacterial groups.

The data and plots of the median \log_{10} survival ratio revealed a protective effect or a decreased inactivation for all microbial species that increased with fullerol concentration (Figure 3-10). *Vibrio parahaemolyticus* was protected only at the greater test concentrations and to a lesser degree than the other microorganisms. Across the range of fullerol concentrations, a nearly 4 \log_{10} protective effect was observed for *Bacillus subtilis*, *Escherichia coli*, and *Salmonella enterica* serotype Newport, while only about 2 \log_{10} and 1 \log_{10} protection was seen with *Vibrio parahaemolyticus* and Spring Viremia of Carp Virus. When the logarithm transformation is dropped and the median survival ratio (N/N_0) for each dose is used, the protective effect is in terms of the proportion or percent of survived microorganisms (Table 3-2 and Figure 3-11). Again, *Vibrio parahaemolyticus* exhibited less

protection by fullerol compared to the other microorganisms. Survival of SVCV showed relatively little change at fullerol concentrations less than 200 mg/L and then increased sharply to nearly 70% survival at 250 mg/L. *Bacillus subtilis* and *Escherichia coli* curves are similar in shape and have survivals of about 50-60% for fullerol concentrations of 200-250 mg/L. *Salmonella enterica* serotype Newport showed 30-40% protection at these same concentrations.

Table 3-2: Median survival ratios (N/N₀) of test microorganisms by fullerol dose. Bs = *Bacillus subtilis*; Ec = *Escherichia coli*; Se = *Salmonella enterica* serotype Newport; Vp = *Vibrio parahaemolyticus*; SVCV = Spring Viremia of Carp Virus.

Microorganism	Median Survival Ratios (N/N ₀) Versus Fullerol Concentration (mg/L)				
	0	50	100	200	250
Bs	0	0	0.03	0.59	0.62
Ec	0	0.01	0.13	0.43	0.53
Se	0	0	0.02	0.32	0.39
Vp	0	0	0	0.01	0.02
SVCV	0.03	0.02	0.03	0.10	0.68

The test of relative bacterial sensitivity to ultraviolet irradiation with these experimental conditions showed that *Vibrio parahaemolyticus* was fully inactivated, while the other bacterial species that were tested simultaneously had about 2 log₁₀ inactivation (Table 3-3).

Table 3-3: Bacterial sensitivities at 0 mg/L fullerol to ultraviolet irradiation for 15 seconds. Bs = *Bacillus subtilis*; Ec = *Escherichia coli*; Se = *Salmonella enterica* serotype Newport; Vp = *Vibrio parahaemolyticus*.

Bacteria Species	Median Survival Percents (N/N₀ x 100)
Bs	1.56%
Ec	1.15%
Se	1.03%
Vp	0%

Microbial Viability versus Fullerol Concentration *Bacillus subtilis*

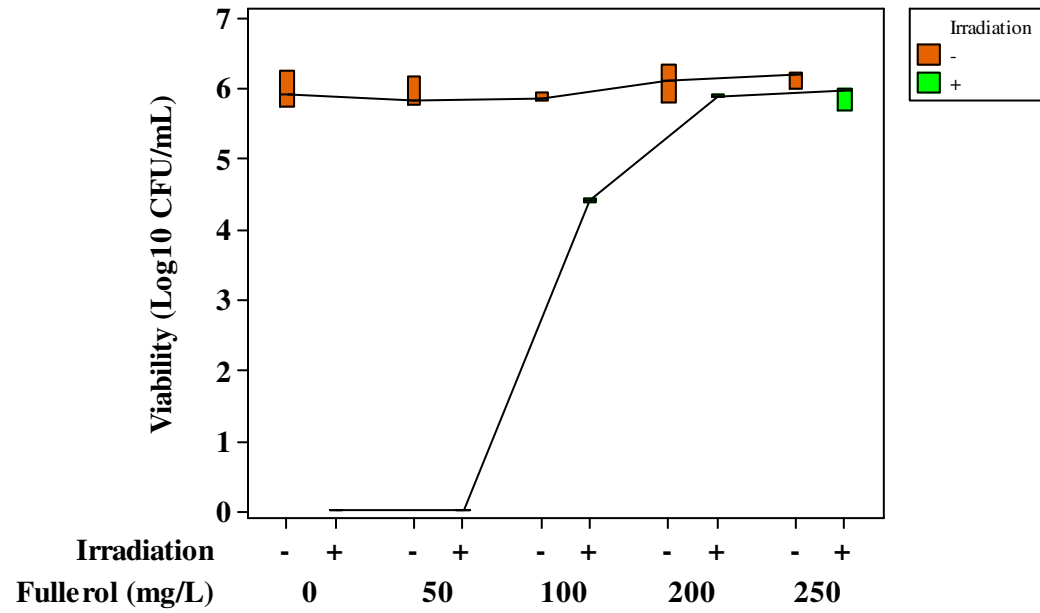


Figure 3-5: *Bacillus subtilis* viability versus fullerol concentration for irradiated and non-irradiated groups. Boxes indicate 95% confidence interval for the median.

Microbial Viability versus Fullerol Concentration *Escherichia coli*

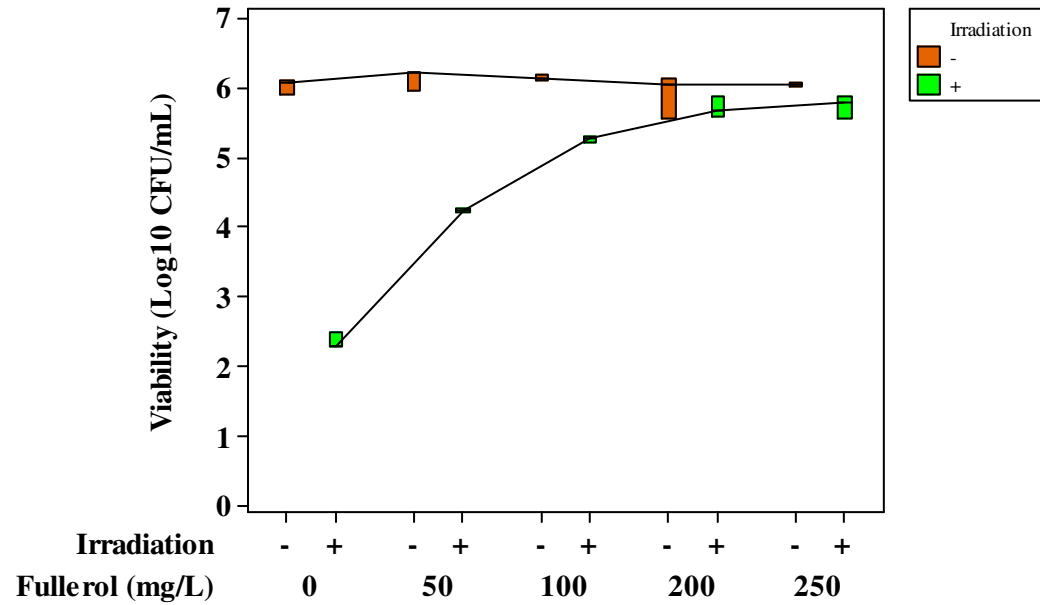


Figure 3-6: *Escherichia coli* (K12) viability versus fullerol concentration for irradiated and non-irradiated groups. Boxes indicate 95% confidence interval for the median.

Microbial Viability versus Fullerol Concentration *Salmonella enterica*

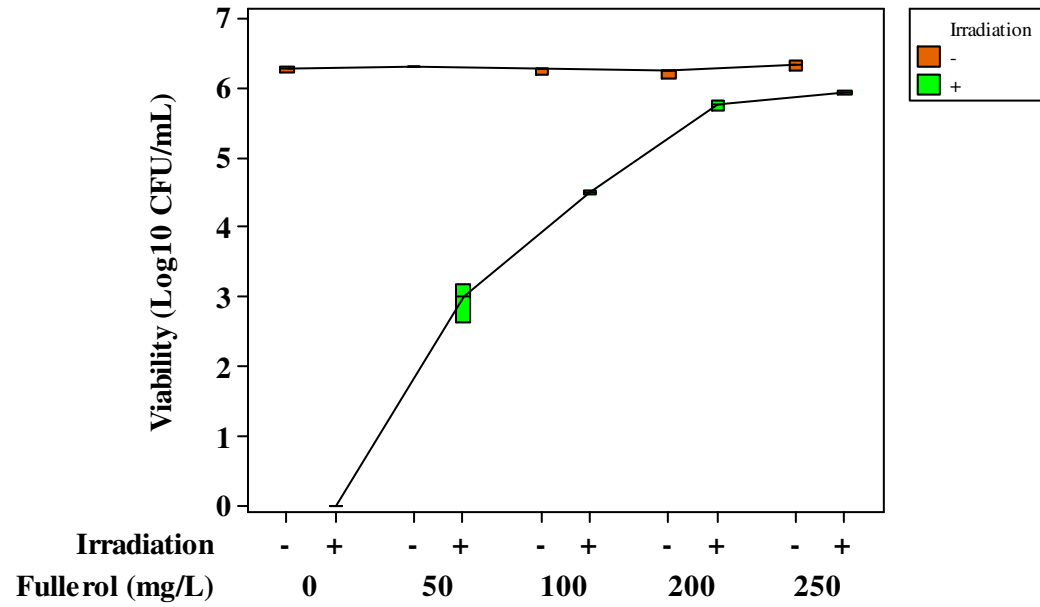


Figure 3-7: *Salmonella enterica* serotype Newport viability versus fullerol concentration for irradiated and non-irradiated groups. Boxes indicate 95% confidence interval for the median.

Microbial Viability versus Fullerol Concentration *Vibrio parahaemolyticus*

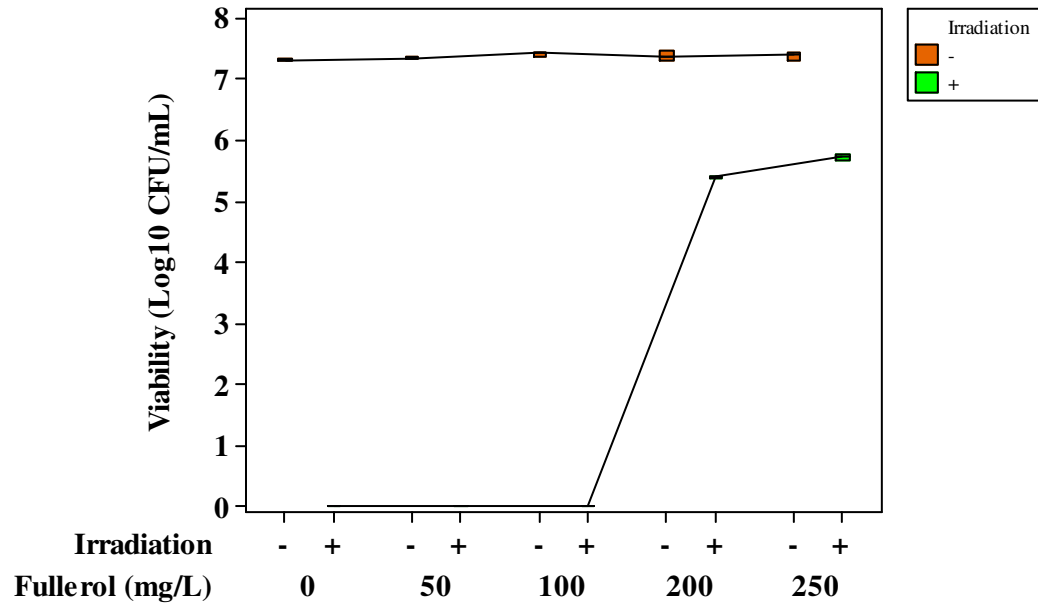


Figure 3-8: *Vibrio parahaemolyticus* viability versus fullerol concentration for irradiated and non-irradiated groups. Boxes indicate 95% confidence interval for the median.

Microbial Viability versus Fullerol Concentration Spring Viremia of Carp Virus

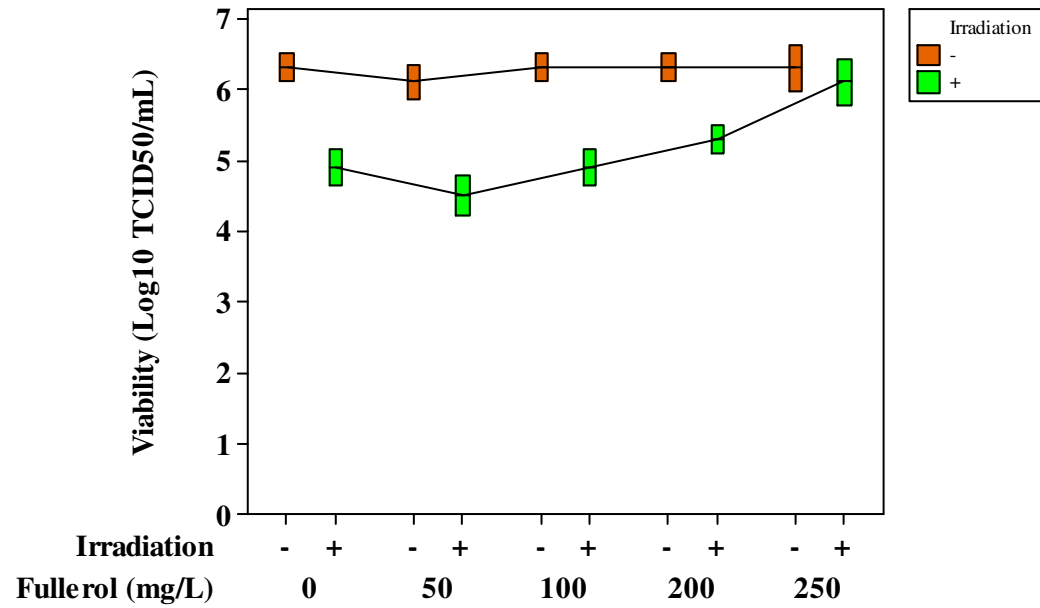


Figure 3-9: Spring Viremia of Carp Virus (SVCV) viability versus fullerol concentration for irradiated and non-irradiated groups. Boxes indicate 95% confidence interval for the median.

Log Median Survival versus Fullerol Concentration

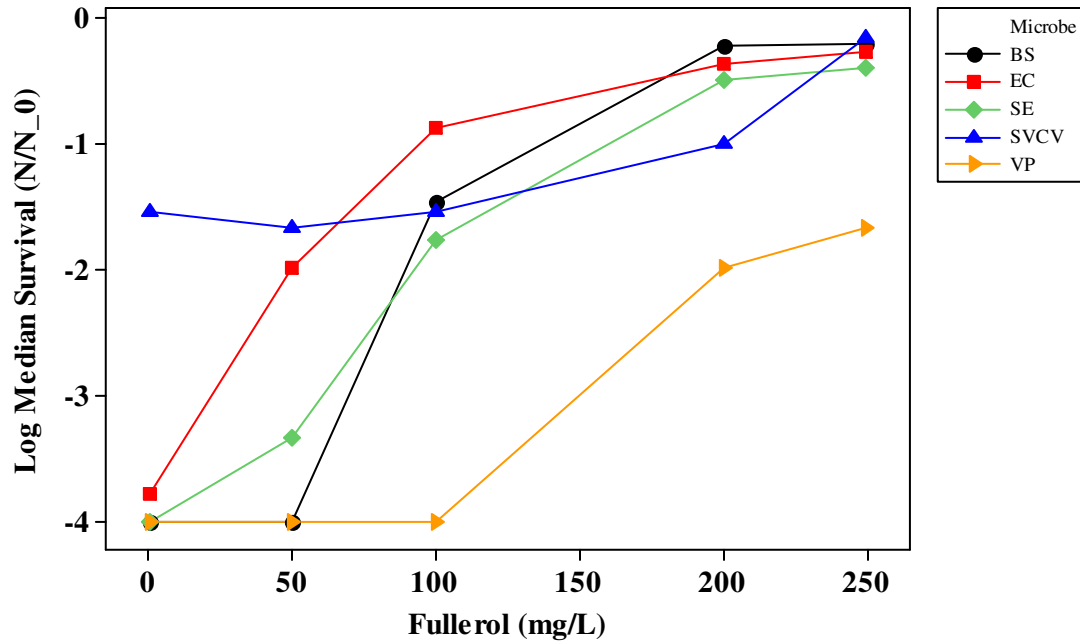


Figure 3-10: Median survival ($\text{Log}_{10} N/N_0$) of test microorganisms by fullerol concentration for 60 seconds ultraviolet irradiation. Bs = *Bacillus subtilis*; Ec = *Escherichia coli*; Se = *Salmonella enterica* serotype Newport; Vp = *Vibrio parahaemolyticus*; SVCV = Spring Viremia of Carp Virus.

Median Survival versus Fullerol Concentration

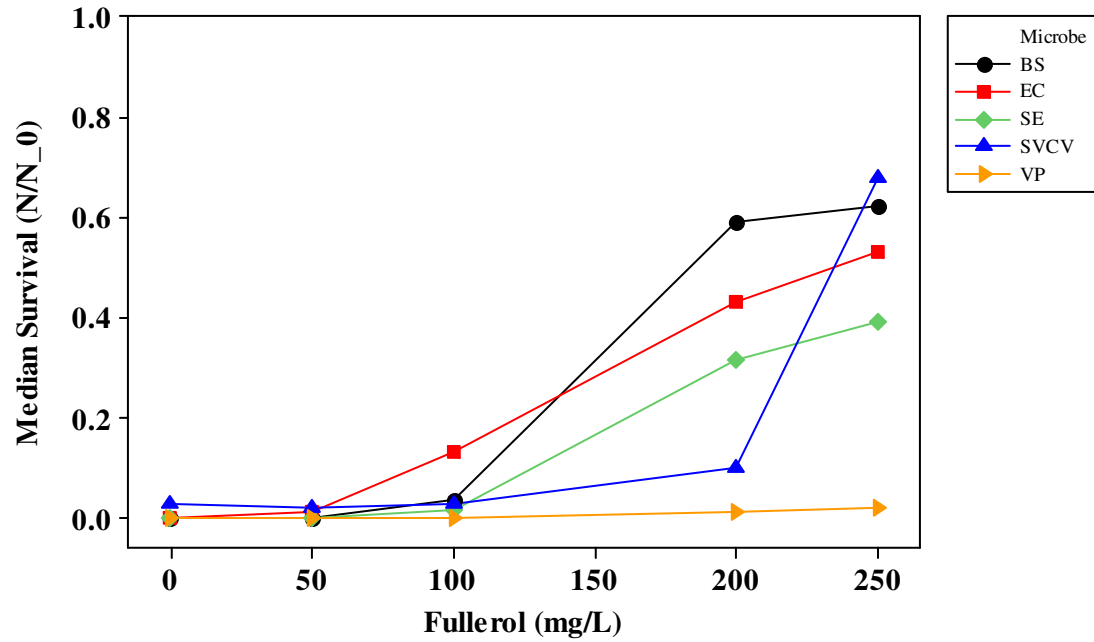


Figure 3-11: Median survival (N/N_0) of test microorganisms by fullerol concentration for 60 seconds ultraviolet irradiation. Bs = *Bacillus subtilis*; Ec = *Escherichia coli*; Se = *Salmonella enterica* serotype Newport; Vp = *Vibrio parahaemolyticus*; SVCV = Spring Viremia of Carp Virus.

Test Bacteria Sensitivity to Ultraviolet Irradiation

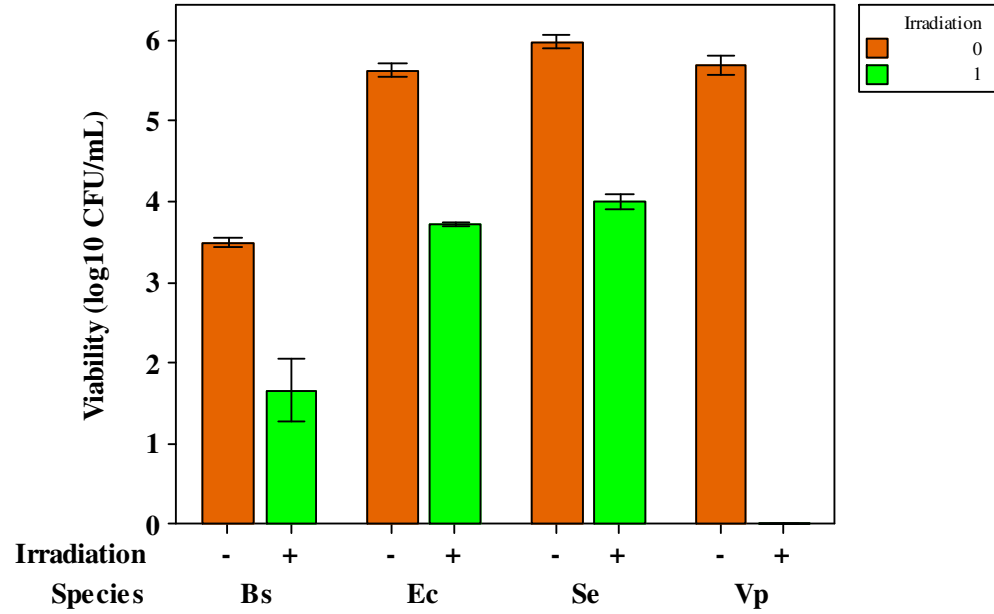


Figure 3-12: Comparison of test bacteria sensitivities to ultraviolet irradiation at 0 mg/L fullerol with the experimental setup. Bs = *Bacillus subtilis*; Ec = *Escherichia coli*; Se = *Salmonella enterica* serotype Newport; Vp = *Vibrio parahaemolyticus*.

Discussion

Escherichia coli and *Bacillus subtilis* are the standard bacterial species tested in inactivation studies. The *Salmonella* and *Vibrio* geneses are tested on occasion although we could not find specific reference to *Salmonella enterica* serotype Newport or *Vibrio parahaemolyticus* tests with fullerenes. No reports of SVCV tests with fullerenes exist to our knowledge.

With the conditions of these experiments, an apparent protective effect by fullerol was observed for all bacteria species and the virus examined. The effect was about the same for all bacteria, except for *Vibrio parahaemolyticus*, which showed the least protection by this compound. SVCV seemed to be less affected by fullerol changes in fullerol concentration except at the 250 mg/L dose. This could be partly a function of the lower innate susceptibility of some viruses to ultraviolet irradiation, but is also likely due to other factors. Viruses have a wide range of susceptibilities to ultraviolet radiation (Kasai, Yoshimizu, & Ezura, 2001; Timmons, et al., 2002). Fish rhabdoviruses like SVCV, along with fish herpesviruses and iridoviruses are inactivated at lower ultraviolet doses compared to fish birnaviruses, reoviruses and nodaviruses (Table 3-4). Of the first three virus families, all are double-stranded DNA with the exception of rhabdoviruses, which have a single-stranded RNA genome. Rhabdoviruses and herpesviruses are enveloped, while iridoviruses are not. The latter group that consists of birnaviruses, reoviruses and nodaviruses are not enveloped and all three have RNA as genomic material (Table 3-5). Viruses with larger genomes and with RNA as the genomic material can be more susceptible to inactivation with

ultraviolet radiation (Vonbrodorotti & Mahnel, 1982). Because SVCV contains a larger RNA genome (11,019 base pairs) (Ahne, et al., 2002) compared to some viruses, the roles genome size and type have in the results of these studies is unclear, but likely other factors are again at play. A future study that further investigates the protection or inactivation of viruses by fullerenes could consider the roles of genome size and type across a number of viruses.

Table 3-4: Approximate minimum ultraviolet irradiation dose required to inactivate greater than 99% of certain microorganisms

Microbe	k⁻¹ (μWs/ cm²)	Reference
<i>Bacillus subtilis</i> , spores	22,000	(Phillips & Hanel, 1960)
<i>Bacillus subtilis</i> , vegetative	11,000	(Phillips & Hanel, 1960)
<i>Escherichia coli</i>	7,000	(Kelly, 1974)
<i>Salmonella enteritidis</i>	7,600	(Phillips & Hanel, 1960)
<i>Vibrio anguilianon</i>	1000	(Kasai, et al., 2001)
Bacteriophage (<i>E. coli</i>)	6,600	(Kelly, 1974)
Fish rhabdoviruses (such as SVCV), herpesviruses and iridoviruses	1,000 – 10,000	(Kasai, et al., 2001)
Fish birnaviruses, reoviruses and nodaviruses	1.5 – 2.5 x 10 ⁵	(Kasai, et al., 2001)

Table 3-5: Characteristics of several virus families of interest to aquaculture. Adapted from Virus Taxonomy, 7th edition (van Regenmortel, 2000)

Virus	Morphology	Genome	Envelope	Size (nm)
Rhabdoviruses	bullet-shaped	ssRNA(-)	+	100 x 275
Herpesviruses	Isometric	dsDNA	+	200
Iridoviruses	Isometric	dsDNA	-	175
Birnaviruses	Isometric	dsRNA	-	50
Reoviruses	Isometric	dsRNA	-	100
Nodaviruses	Isometric	ssRNA(+)	-	45

With the exception of *Vibro parahaemolyticus*, the two other Gram-negative bacteria tested had similar survival to the survival previously recorded for *Bacillus subtilis*, the single Gram-positive bacteria species tested. This was true for the fullerol survival tests and the

relative bacterial sensitivity test. Endospores from spore-forming bacteria like *Bacillus subtilis* and Gram-positive bacteria often have greater resistance to ultraviolet light than Gram-negative bacteria (Jagger, 1967). *Escherichia coli* bacteria are generally more sensitive to ultraviolet light than are *Bacillus subtilis* endospores or vegetative cells (Table 3-4). This is thought to be a function of the thicker peptidoglycan cell walls and endospore structures of Gram-positive bacteria compared to the thinner outer structures of Gram-negative bacteria. *Bacillus subtilis* appeared to have greater survival in the presence of fullerol and also in the relative bacterial sensitivity test compared to the Gram-negative bacteria. This is consistent with the literature.

The bacteria species tested in our studies were protected by fullerol to different degrees. *Escherichia coli*, *Bacillus subtilis* and *Salmonella enterica* serotype Newport were protected at the lower test concentrations of fullerol (Figures 3-5 to 3-7). This protection generally increased with the concentration of fullerol. In contrast, *Vibrio parahaemolyticus* bacteria were protected by fullerol only at the greater fullerol concentrations and with steeper change in protection at the greater fullerol concentrations (Figure 3-8). The TCID₅₀ survival ratio of SVCV viral particles was similar to the median survival ratios of the bacterial species tested, except for a sharp increase in protection from 200 mg/L to 250 mg/L.

In the relative sensitivity experiment, *Vibrio parahaemolyticus* was much more sensitive to the ultraviolet irradiation. This organism showed the least protection from fullerol. Because of this we suspect some of the differences in protection shown in the survival curves could be attributed to the individual responses of the microorganisms to the combined effect of various doses of ultraviolet light and fullerol concentrations. Another

possibility is that the salt used with *Vibrio parahaemolyticus* culture caused greater inactivation of this species in the presence of fullerol. Some fullerenes are known to have lower solubility with greater salt contents (Fortner, et al., 2005). If this caused fullerol to become less stable and have greater tendency for precipitation out of solution, this would imply the protective effect could be due primarily to a shielding effect by fullerol molecules suspended in solution.

The protective effect was statistically significant across all microorganisms and was especially evident at greater fullerol concentrations. This protection is contradictory to the expected antimicrobial effect previously described in the literature for fullerenes. Several differences exist between our experiments and the studies found in the literature. First, we increased the concentration of fullerol as opposed to time of irradiation as was common to most other experiments. If we had observed the results over time, an antimicrobial effect could have been more evident. As was noted previously, however, we wanted to run our experiments under conditions that would be closer to those used in an actual disinfection scenario. This means that irradiation periods of 30 or more minutes that were common to previous fullerene photosensitization studies are not practical in a disinfection design. Instead, an increase in fullerene dose as opposed to time would provide more realistic information in this regard.

Second, we did not use a collimated design, which is used to make incident light more parallel when it strikes bacteria and reduce effects of scattering. If we did have more scattering in our experiments, then this scatter would be expected to cause greater inactivation of bacteria than if a collimated apparatus was used to reduce this scatter. This is

because scattered ultraviolet light is still able to inactivate microorganisms. Although we have no collimated-design inactivation results to compare with our data, the greater microbial survival in our data could indicate light scattering did not play a large role.

These antioxidant effects of fullerol or other fullerenes are described in the literature with *in vitro* conditions or with eukaryotic cells. From the literature, it appears only one other study found a protective effect for fullerol to *Escherichia coli* (Brunet, Lyon, Hotze, Alvarez, & Wiesner, 2009). This study described an overall protective effect after white incandescent light irradiation for 6 hours. The conclusion with respect to this part of the study was that the fullerol seemed to encourage bacterial growth in visible light irradiation and that the warmth of the lamp or surface roughness of the substrate could account for this result. In contrast, our study irradiated with monochromatic ultraviolet light for only 60 seconds. The warmth of the light in our setup would not be expected within this short exposure time to contribute to increased bacterial growth. Additionally, our samples demonstrated a protective effect in aqueous solutions rather than on the rougher surfaces of that experiment where this cause of protection was hypothesized.

There are several possible mechanisms for the protective effect observed in our studies. Protection could be due to physical shielding of microbes from ultraviolet irradiation by the fullerol molecules. Fewer UV photons reach the microorganisms either by the scattering of photons or through absorption by fullerol particles. Because fullerol has peak absorbance within the UV range the latter is a distinct possibility. If fullerol aggregation occurred to create supramolecular structures or if aggregation was greater with increased concentration as noted in the literature (Mohan, et al., 1998), then it is also possible that

greater physical shielding of microbes from irradiation existed due to this agglomeration effect. Greater microbial survival by way of shielding could also occur independently of aggregation. Specifically, greater concentrations of fullerol in suspension could block, scatter or attenuate more ultraviolet photons and result in fewer destructive effects on the microbes. Additionally, we do not expect the negatively charged fullerol molecule to coat the microorganisms used in this study. The negatively-charged nature of bacterial cell walls and membranes of both Gram-positive and Gram-negative bacteria would likely preclude this occurrence by way of electrostatic repulsions.

The results of these inactivation studies imply that the protective effect observed by fullerol is possibly due to multiple factors. It is important to note, however, that differences in experimental design, like those in our experiments compared to other studies related to inactivation with fullerenes or other disinfectants, can result in differences in outcome. There is no reason to question the validity of these previously-conducted and standardized disinfection experiments. We do not challenge that fullerol has some, albeit perhaps minimal, antimicrobial capability. This effect, however, was at least overpowered by the protective effect of fullerol in these studies. We found that changes in experimental design to move beyond basic science toward applied science can possibly change the outcome and projections of how well a technology would work in a realistic environment.

CHAPTER 4

Mechanistic studies of a microbial protective effect of fullerol

Abstract

Fullerol has a protective effect on *Bacillus subtilis*, *Escherichia coli* (K12), *Salmonella enterica* serotype Newport, *Vibrio parahaemolyticus* and Spring Viremia of Carp Virus (SVCV) exposed to ultraviolet radiation. In this investigation, the role of fullerol size, shape, concentration and absorption were examined with electron microscopy and image analysis, dynamic light scattering (DLS), and ultraviolet spectrophotometry. Fullerol shape and absorption contribution did not appear to be associated with fullerol-based protection from ultraviolet radiation. No appreciable size change was found after sonication, filtration or ultracentrifugation of fullerol solutions. These studies confirm previous reports that fullerol aggregate size can increase with concentration and suggest a concentration-related shielding effect that could explain the observed microbial protection.

Introduction

Fullerol, also known as fullerenol or polyhydroxylated fullerene, is a water soluble derivatized fullerene (dC₆₀) found to have antimicrobial action (Aoshima, et al., 2009; Badireddy, et al., 2007; Lee, et al., 2009). Inactivation by fullerol occurs through photosensitization reactions with ultraviolet or visible light irradiation. Based on the literature fullerol can also be protective through its antioxidant activity (Chiang, et al., 1995; Dugan, et al., 1996; Jeng, et al., 2001; Lu, et al., 1998). This occurs by way of superoxide and singlet oxygen scavenging in non-irradiative conditions. One report described a protective effect to a microorganism with light (Brunet, et al., 2009), but no studies examined the mechanism of protection. Previously, we reported a protective effect for several bacteria and virus agents with monochromatic ultraviolet light (Chapter 3). This protection increased to various degrees, which depended on the organism and the concentration of fullerol. Some of the possible mechanisms of the protection include shielding through changes in aggregate size and shape, attenuation of radiation by concentration-related effects and chemical dynamics such as charge interactions. The aim of this investigation was to determine a possible mechanism for the protective effect of fullerol to microorganisms in the presence of ultraviolet irradiation.

Materials and Methods

All fullerol aliquots and solutions were made with 0.9% physiological saline as described in Chapter 3 and double-distilled water at concentrations of 31.25, 62.5, 125 and 250 mg/L fullerol (referenced as 31, 62, 125 and 250 mg/L for simplicity). The 1,000 mg/L stock solution used previously was diluted to a small aliquot of 250 mg/L, the highest concentration used in our previous study. This was then serially diluted in half three times to achieve the range of solutions that were viewed with the electron microscope. To examine the solutions by scanning electron microscopy (SEM) (Hitachi S4000, cold field emission SEM), 2 μ L droplets were vacuum-evaporated onto a gold-coated thin glass, and viewed at several magnifications. Sections of carbon were attached to the glass to reduce charging, an effect in electron microscopy that results in sample and signal degradation.

Scanning electron micrographs were taken of areas that appeared uniform in distribution within the microscopic views and that had separateness of particle space that could be analyzed effectively with image analysis software. The scanning electron micrographs were selected on the basis of the ability to analyze the images with software. All images that could be analyzed were used for analysis. These images were gamma corrected and converted to 8-bit grayscale images (Photoshop CS2 v. 9.0, Adobe Systems, Inc., San Jose, California, USA). The intensity and noise thresholds of the images were set and then the images were converted to binaries for final aggregate count and size measurements (ImageJ v. 1.42q, National Institutes of Health, Bethesda, Maryland, USA). Scanning electron micrograph image analysis helped to measure the aggregate two

dimensional areas and perimeters. The circularity and the equivalent circular diameter (ECD) were calculated from these parameters using the following equations.

$$Circularity = \frac{4\pi \cdot Area}{Perimeter^2}$$

$$Equivalent\ Circular\ Diameter = \sqrt{\frac{4 \cdot Area}{\pi}}$$

Circularity is a dimensionless parameter ranging from 0 to 1, where 1.0 is a perfect circle and a value that approaches zero is associated with increased elongation. Equivalent circular diameter is the diameter of a circle of the same area as the polygonal aggregate.

A fresh solution of 1,000 mg/L fullerol was made and processed in the same manner as previously with the exception we did not add sodium chloride to the solution. This was done because we did not feel it was a necessary component for the SEM analysis and could interfere with our results through crystal formation or influence aggregate sizes. A protective effect of this new solution was also confirmed for *Escherichia coli* and *Bacillus subtilis*. The stock solution of fullerol was divided into four smaller aliquots. One did not receive any treatment while another was ultrasonicated for 30 minutes to attempt size reduction of the aggregates (Sonic Dismembrator, Model 150, 275 Watts, Artek Systems Corporation, Farmingdale, NY). Two other treatment groups were created by filtration through a 0.22 μm mean diameter pore size cellulose nitrate canister filter or by centrifugation at 18,500 times

gravity for two hours. These four treatment groups were labeled untreated, sonicated, filtered and centrifuged.

Aggregate size determination was made by dynamic light scattering (DLS) method with a Zetasizer Nano ZS (Red Badge), Model ZEN3600 (Malvern Instruments, LTD, Worcestershire, United Kingdom). The limits of detection of this instrument were 0.6 nm to 6.0 μm . Samples were run for fullerol concentrations of 50, 100, 200, 250, 500, 750 and 1,000 mg/L at 13 repetitions each. All concentrations were run for the following treatment groups: untreated, sonicated, filtered and centrifuged. The results were plotted and analyzed for statistical differences in aggregate size distribution among the four treatment groups and within each treatment group among the fullerol concentrations. Z-average intensity (mean of all detected intensities of light reflected from particles) and peak mean intensity (peaks are localized intensities that represent particles of similar size) were generated by instrument conversions that used a combination of internal constants and measured parameters (Malvern, 2005). These diameter conversions are in units of nanometers. The Z-average has greater validity for similar treatments, spherical particles, monomodal samples (one peak), and monodisperse samples (no width to distribution of size intensities). Multiple observations were made because different reported peaks can vary dramatically for unknown reasons.

UV-visible (UV-vis) light absorbance measurements were made for each of the fullerol concentrations in the four treatment groups with a spectrophotometer (NanoDrop ND-1000, NanoDrop Technologies, LLC, Wilmington, Delaware, USA). The results were plotted and analyzed to determine if changes in absorption patterns among the treatment

groups and concentrations could help explain the protective effect. If there were differences in absorption patterns among the treatment groups, the variation could be due to size and shape changes. Changes in absorption with concentrations could be interpreted as concentration-dependent effects.

Results

Scanning electron microscopy analysis

Image analysis of the fullerol solutions visually confirmed aggregation of the fullerol. All scanning electron micrographs showed this aggregation behavior. The structures varied widely in size and shape. Figure 4-1 and Figure 4-2 are SEM photos of aggregates in untreated fullerol dissolved in double distilled water at a concentration of 31 mg/L. The aggregate sizes ranged from submicronic to nearly 100 micrometers. Aggregate shapes varied from tight clusters to elongated, near filamentous elements.

The concentration of the fullerol solution also seemed to affect the nature of the aggregates. At lower concentration, aggregates were more dense and similar in shape; most were submicronic in size (Figure 4-3 and Figure 4-4, scanning electron micrographs taken of solutions of 62 mg/L and 250 mg/L fullerol in 0.9% saline). This uniformity is replaced by a mix of crystalline-like structures and aggregates when a concentration of 250 mg/L is

examined. These crystalline-like structures do not appear to be sodium chloride crystals based on crystal morphology.

Images of aggregates taken at 125 mg/L and 62 mg/L fullerol in saline solutions at higher magnification (Figure 4-5 and Figure 4-6) appeared to be comprised of smaller aggregates in a lobular-like structure (Figure 4-5). At the higher magnification (Figure 4-6) a speckled appearance to the lobe-like areas was vaguely present and could approach the scale of fullerol molecules themselves, which was also present in the unprocessed image.

After sonication of the fullerene solutions (Figure 4-7, a scanning electron micrograph taken of 31 mg/L fullerol in ddH₂O solution), the aggregates had a rough appearance. Large, smaller, and a background of fine aggregates were present. The larger aggregates were about 600-800 nm in diameter. The smaller aggregates were about 100-300 nm in diameter. The larger aggregates appeared to be comprised of lobes of a dimension similar to the smaller aggregates and suggested sonication resulted in the fracture of larger aggregates into smaller ones.

Quantitative analysis of the scanning electron micrographs confirmed the wide variability of aggregate size and shape. Not all images lent themselves well to image analysis, mostly due to an inadvertent loss of reference scale due to aggregate superimposition. An image of 31 mg/L sonicated (labeled as S31) fullerol and of 31, 62, 125 and 250 mg/L (labeled as U31, U62, U125, and U250) untreated fullerol were analyzed.

Descriptive statistics (Table 4-1 and Table 2), histograms (Figure 4-8, Figure 4-9, Figure 4-10, Figure 4-11, and Figure 4-12) and a combined interval plot (Figure 4-13) were made from the SEM image size and shape analyses. There was no consistent pattern to the

distribution of aggregates in terms of area, perimeter, circularity and equivalent circular diameter (ECD). Some of the histograms revealed a normal distribution to the data, while others were right skewed (Figure 4-8, Figure 4-9, Figure 4-10, and Figure 4-11). The one image of sonicated fullerol solution (31 mg/L) is skewed and could have a slight bimodal distribution (Figure 4-12) representative of the larger and smaller aggregates observed in the scanning electron micrograph. The image shows a much finer particle group that could not be easily analyzed because of resolution limitations for the analytical software and the prior treatment of the data to remove particles and noise of 1-2 pixels before analysis.

Table 4-1: Median area, perimeter, circularity and equivalent circular diameter (ECD) for fullerol SEM image analysis by treatment groups. (U=untreated; S=sonicated; 31, 62, 125 and 250 indicate fullerol concentration in mg/L).

Treatment Group	Number of aggregates in image	Area (μm^2)	Perimeter (μm)	Circularity (0-1)	ECD (μm)
U31	62	0.046	1.127	0.430	0.242
U62	72	0.075	1.357	0.437	0.309
U125	54	0.060	1.430	0.338	0.276
U250	87	6.860	15.460	0.353	2.955
S31	176	0.003	0.994	0.406	0.195

The non-parametric Kruskal-Wallis test was used to compare across treatment groups due to the large differences among the numbers of particles for each treatment group, as well as the consistent inability to assume either normal distributions or small variances for any of the parameters of interest. Statistically, the area, perimeter and ECD of the aggregates were equal among the different treatment concentrations of fullerol, with the exception of the untreated 250 mg/L group ($p < 0.001$) (Figure 4-13 and Table 4-2). This U250 treatment

group also exhibited greater variance for area, perimeter and ECD. All aggregates had low and similar circularity (medians ranged 0.338 – 0.437) and indicates elongation of aggregate shapes compared to a circle.

Dynamic light scattering analysis

The Zetasizer Nano ZS instrument allowed for multiple runs of all four treatment groups and more concentrations of fullerol. Aggregate size data of most importance was reported as Z-average and Peak 1 diameters in nanometers (Table 4-2).

Table 4-2: Summary table of dynamic light scattering (DLS) data for the four major treatment groups.

Treatment	Total Count	Mean Diameter (nm)	SE Mean
<u>Z-average Diameter</u>			
Centrifuged	91	42.34	1.75
Filtered	91	124.36	1.93
Sonicated	91	149.61	0.34
Untreated	91	440.31	4.38
<u>Peak 1 Diameter</u>			
Centrifuged	91	131.38	4.74
Filtered	91	167.40	3.67
Sonicated	91	175.43	0.81
Untreated	91	382.39	5.53

These data were also plotted by treatment group (Figure 4-14 and Figure 4-15) and indicated little of the variation in the size of aggregates was a result of changes in fullerol

concentration, with the exception of the untreated group Peak 1 values ($R^2 = 0.54$). The values for diameter obtained by DLS were generally within the larger range of error for the image analysis data.

Absorption analysis

Measurements of absorbance showed the fullerol solutions strongly absorbed ultraviolet radiation at 254 nm (Figure 4-16). The variability was greater as the dose increased. This is in comparison to absorbance measurements taken at 300 nm (Figure 4-17). The peak absorption for these fullerol solutions occurred at about 223 – 226 nm. Absorbance was statistically insignificant among the four treatment groups.

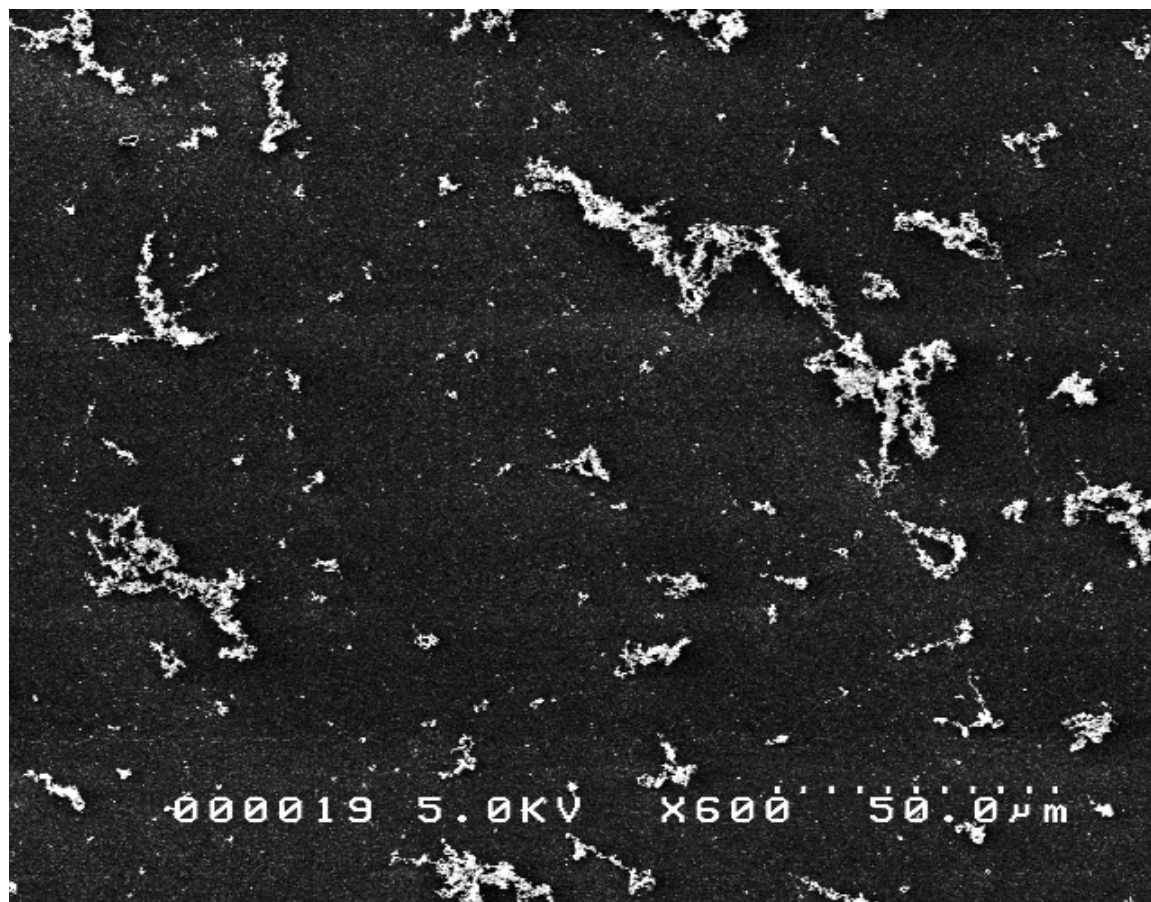


Figure 4-1: Scanning electron microscopy image of 31 mg/L fullerol in ddH₂O (850x magnification).

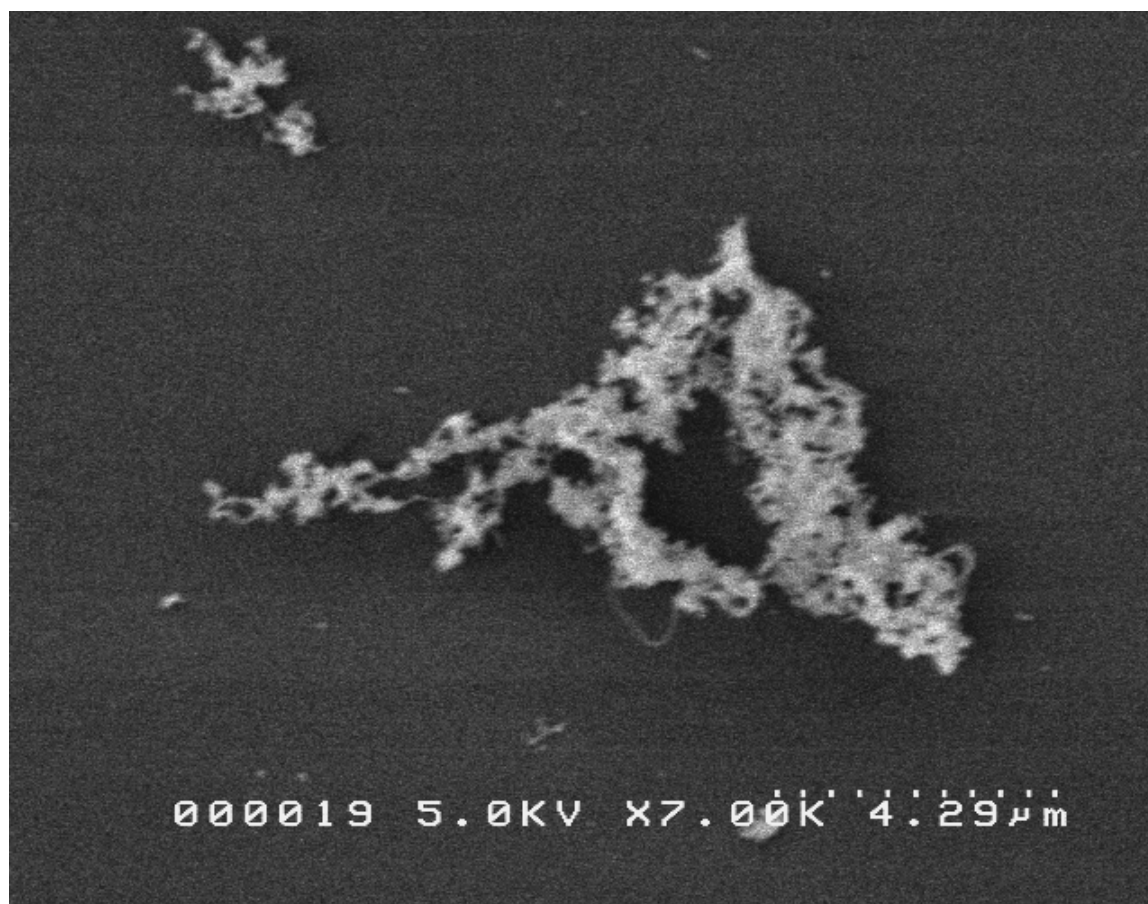


Figure 4-2: Scanning electron microscopy image of 31 mg/L fullerol in ddH₂O solution (9,900x magnification).

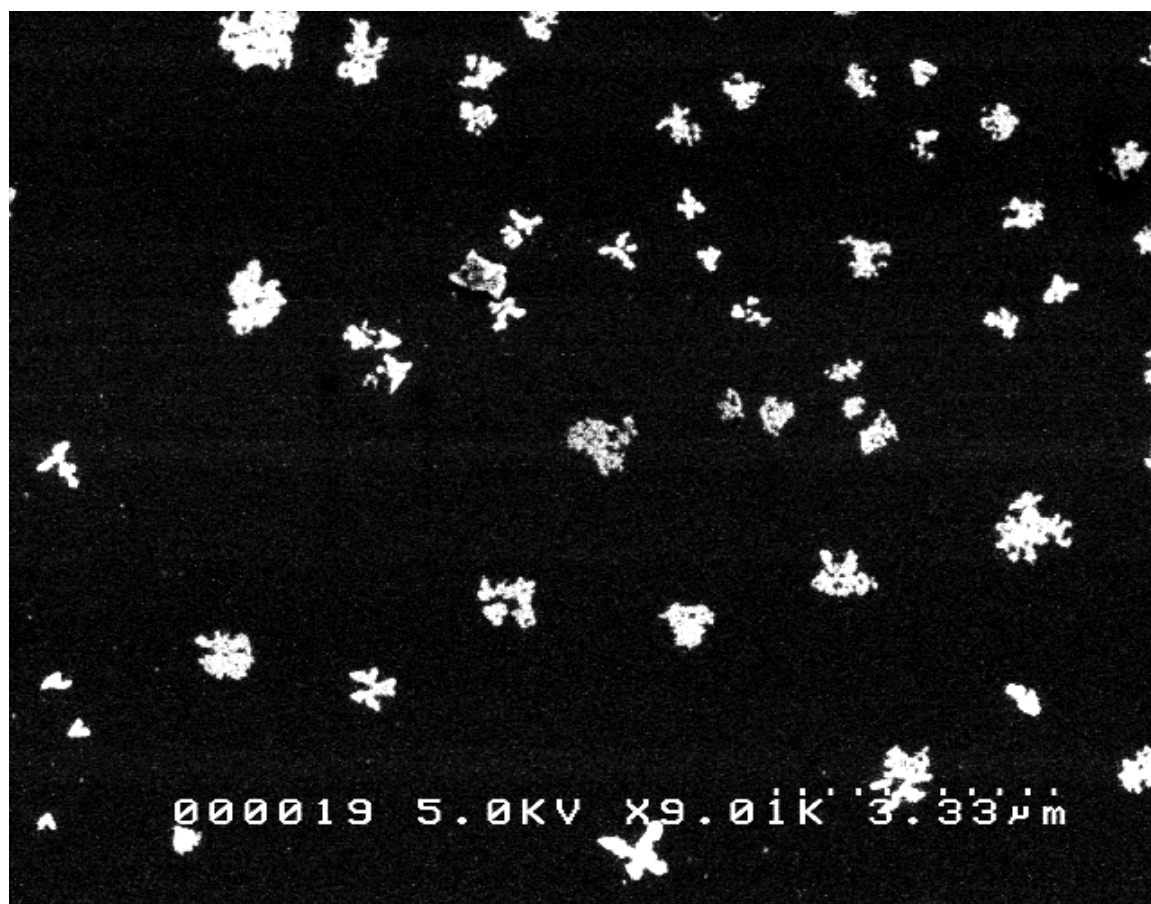


Figure 4-3: Scanning electron microscopy image of 62 mg/L fullerol in 0.9% saline solution (12,900x magnification).



Figure 4-4: Scanning electron microscopy image of 250 mg/L fullerol in 0.9% saline solution (1,400x magnification).

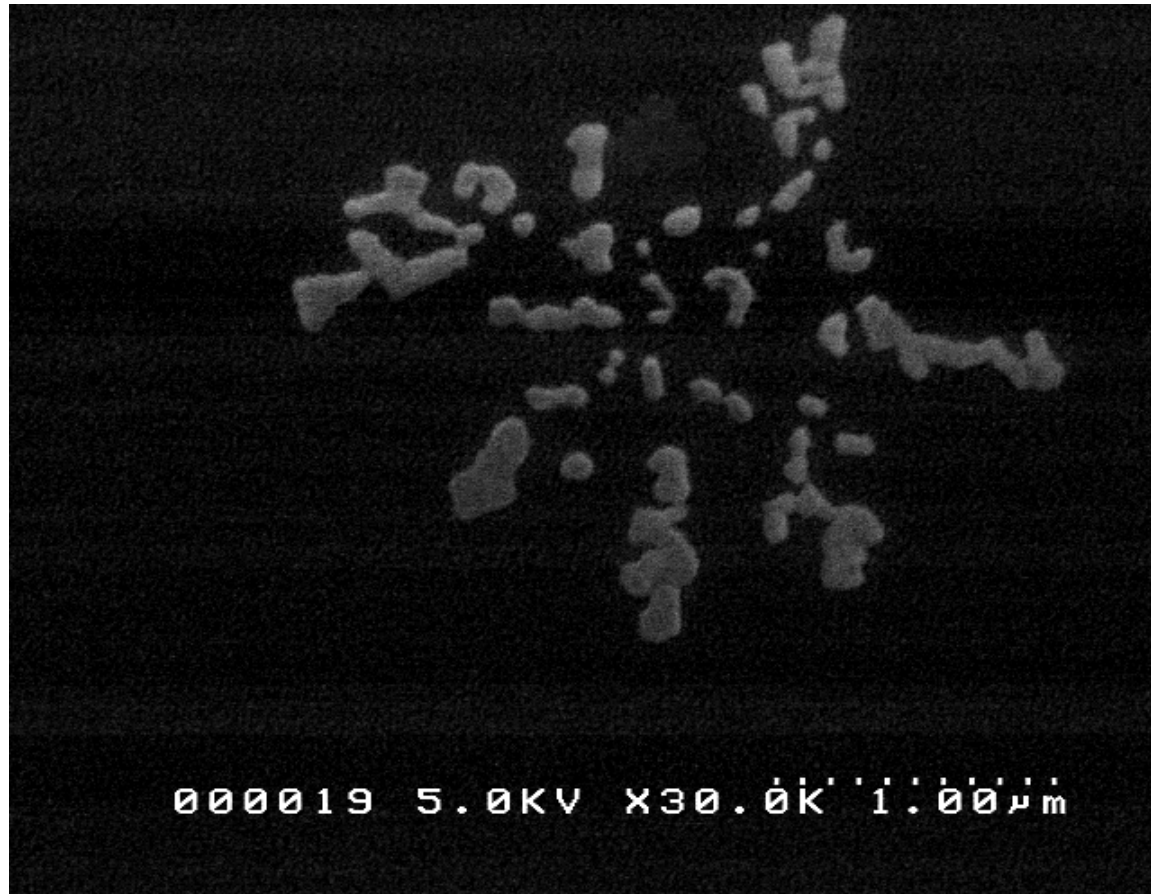


Figure 4-5: Scanning electron microscopy image of 125 mg/L fullerol in 0.9% saline solution 42,500x magnification).



Figure 4-6: Scanning electron microscopy image of 62 mg/L fullerol in ddH₂O (70,800x magnification).

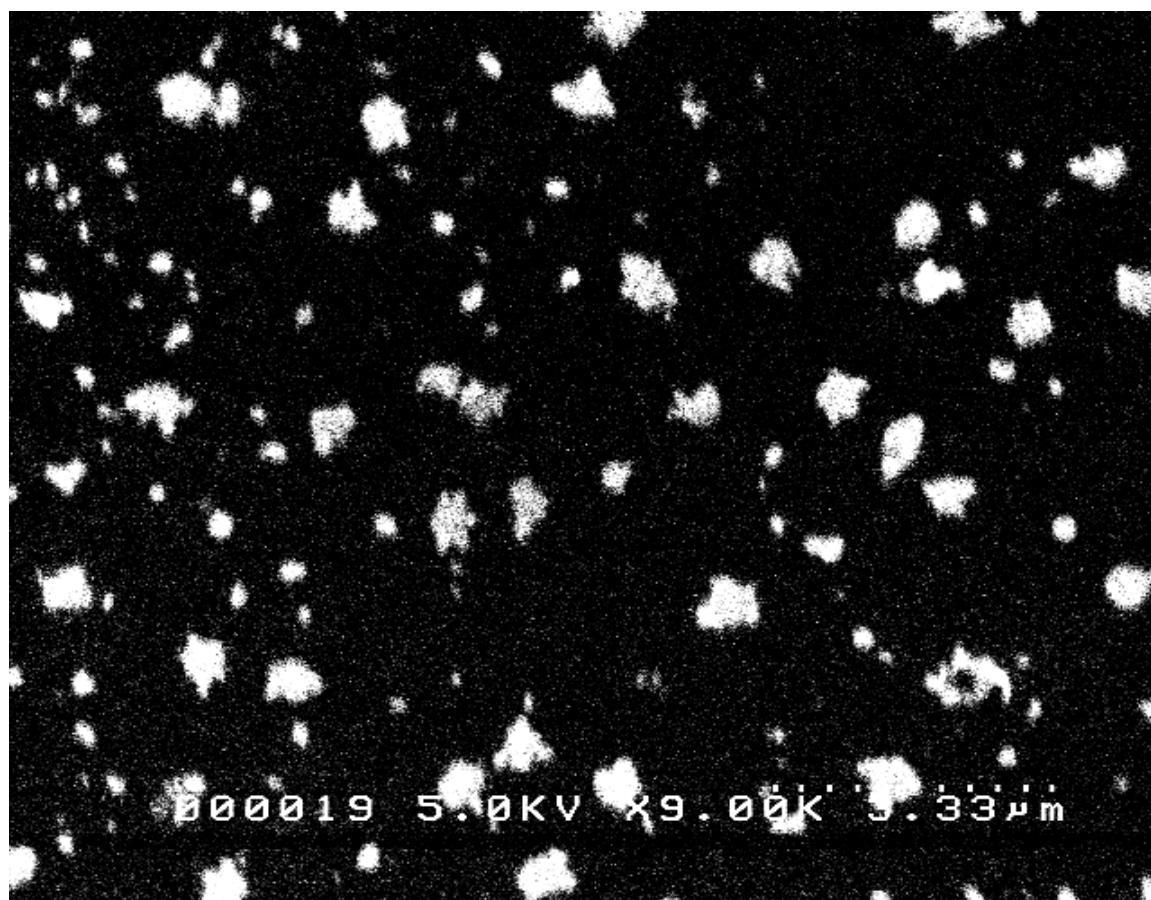


Figure 4-7: Scanning electron microscopy image of 31 mg/L fullerol in ddH₂O sonicated solution (12,800x magnification).

Histogram of U31 Area, Perimeter, Circularity, and ECD

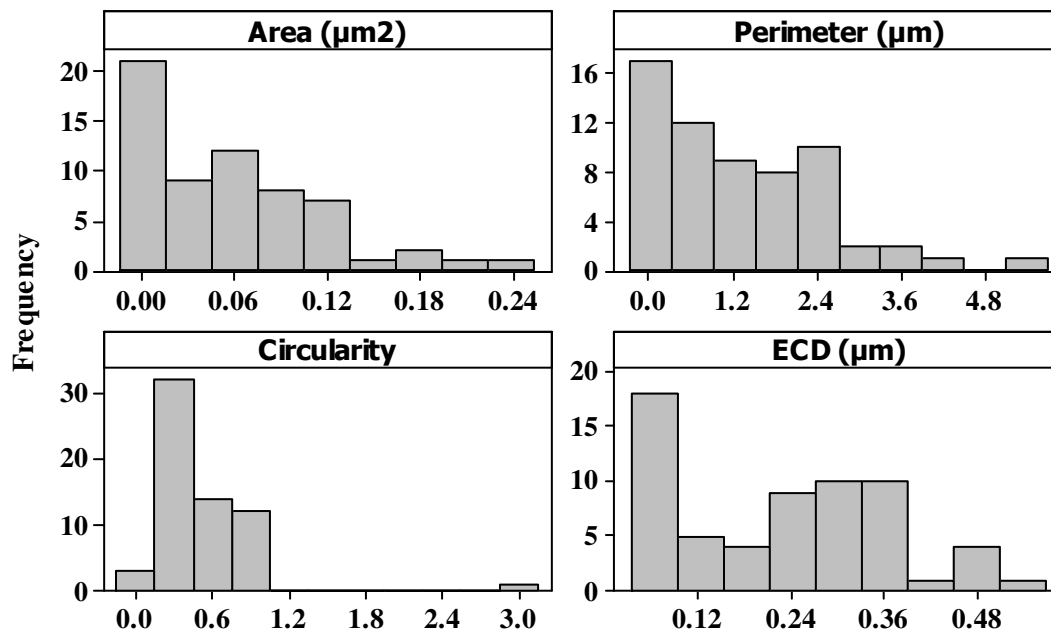


Figure 4-8: Histogram of untreated fullerol solution at 31 mg/L after SEM image analysis for area, perimeter, circularity, and equivalent circular diameter (ECD).

Histogram of U62 Area, Perimeter, Circularity, and ECD

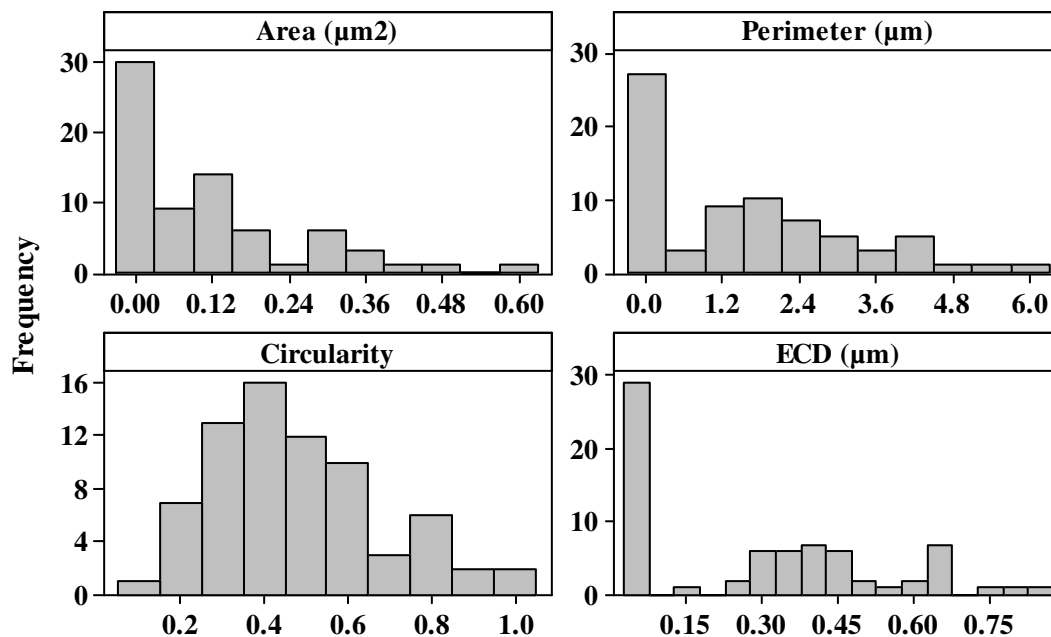


Figure 4-9: Histogram of untreated fullerol solution at 62 mg/L after SEM image analysis for area, perimeter, circularity, and equivalent circular diameter (ECD).

Histogram of 125 Area, Perimeter, Circularity, and ECD

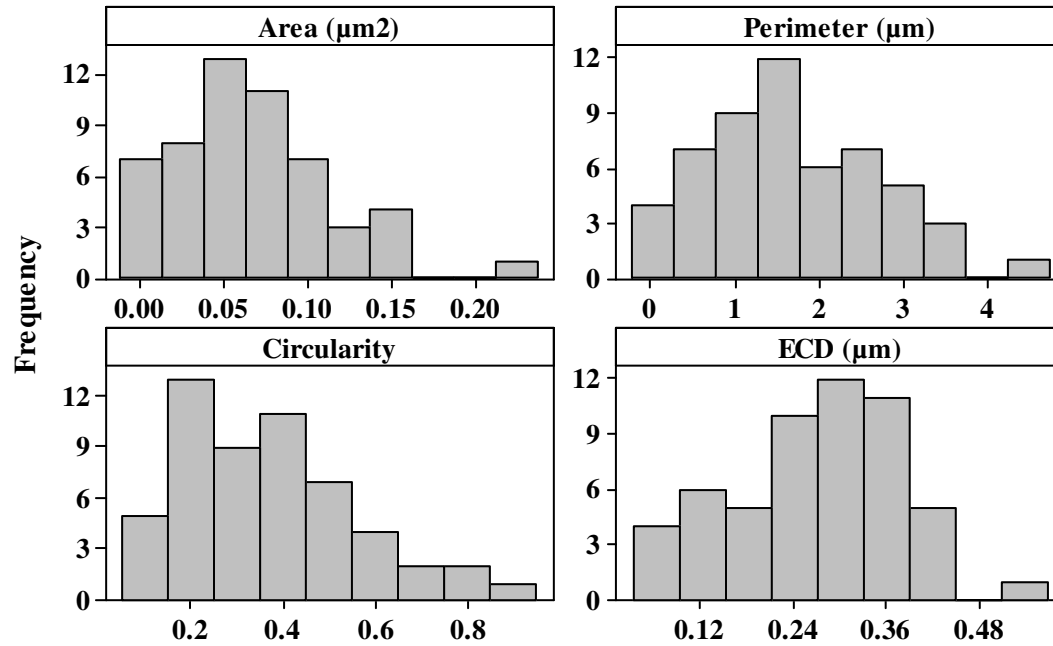


Figure 4-10: Histogram of untreated fullerol solution at 125 mg/L after SEM image analysis for area, perimeter, circularity, and equivalent circular diameter (ECD).

Histogram of U250 Area, Perimeter, Circularity, and ECD

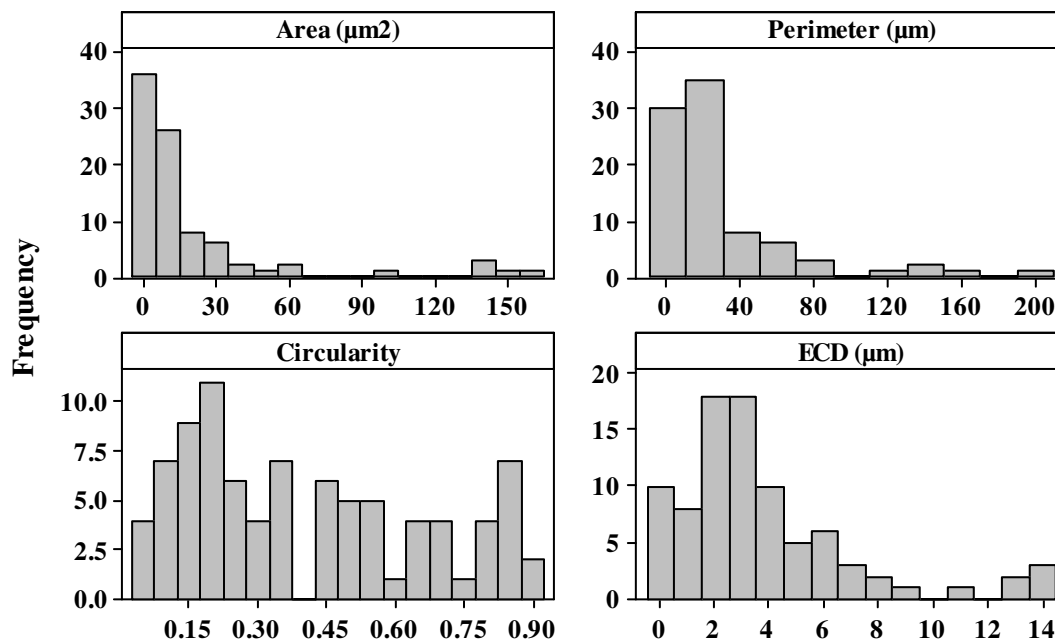


Figure 4-11: Histogram of untreated fullerol solution at 250 mg/L after SEM image analysis for area, perimeter, circularity, and equivalent circular diameter (ECD).

Histogram of S31 Area, Perimeter, Circularity, and ECD

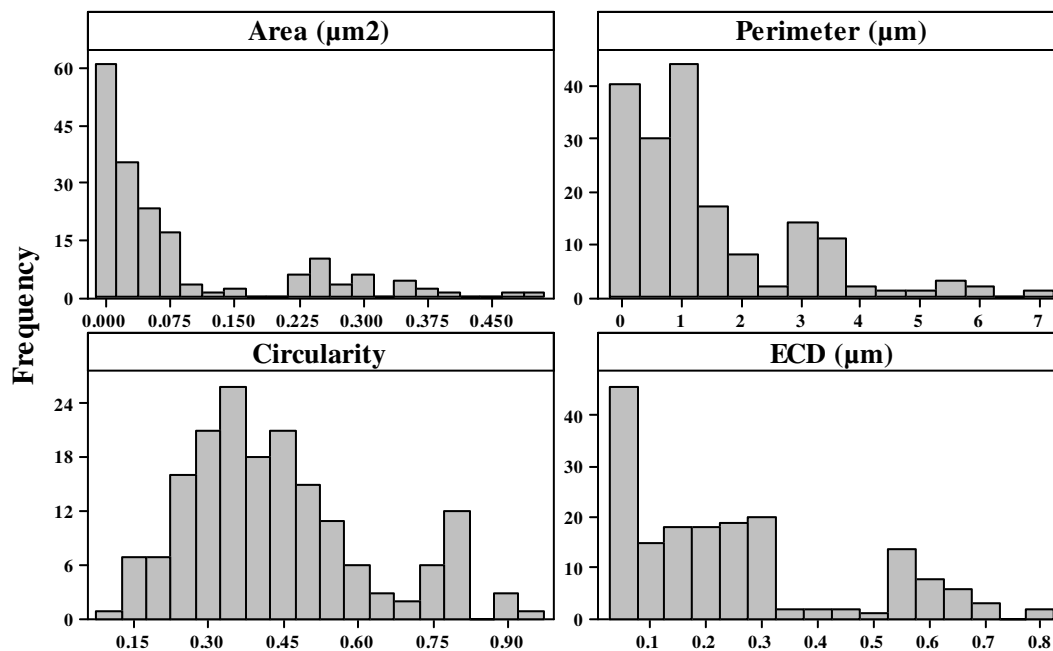


Figure 4-12: Histogram of sonicated fullerol solution at 31 mg/L after SEM image analysis for area, perimeter, circularity, and equivalent circular diameter (ECD).

Interval Plot of Area, Perimeter, Circularity, and ECD 95% CI for the Mean

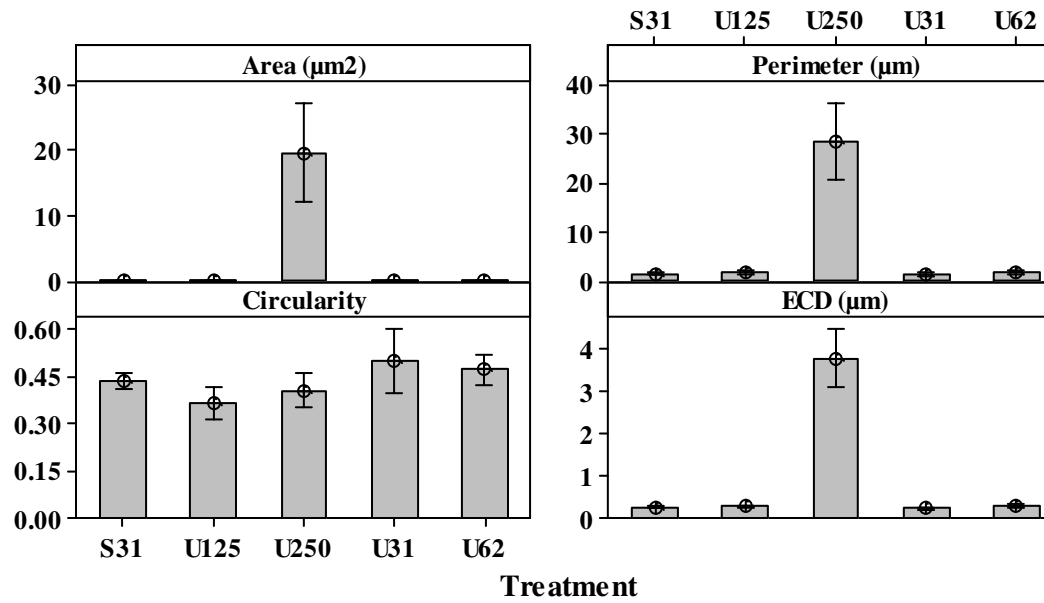


Figure 4-13: Interval plot of SEM image analysis results. Bars indicate 95% confidence interval for the mean.

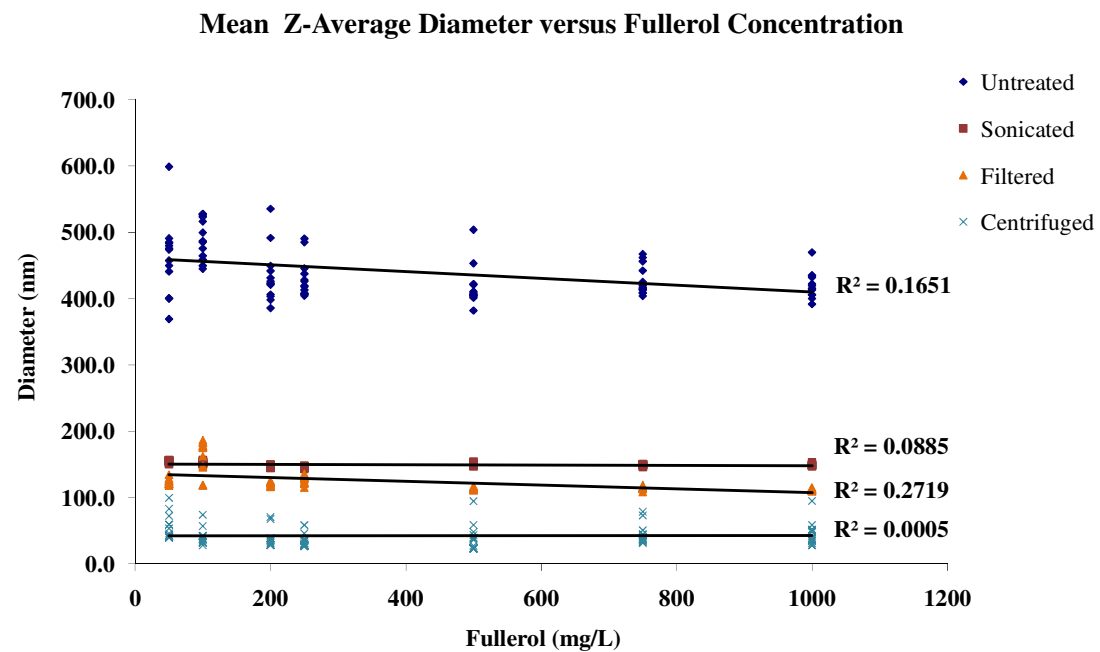


Figure 4-14: Zetasizer Nano ZS fullerol aggregate mean Z-average diameters plotted against concentration.

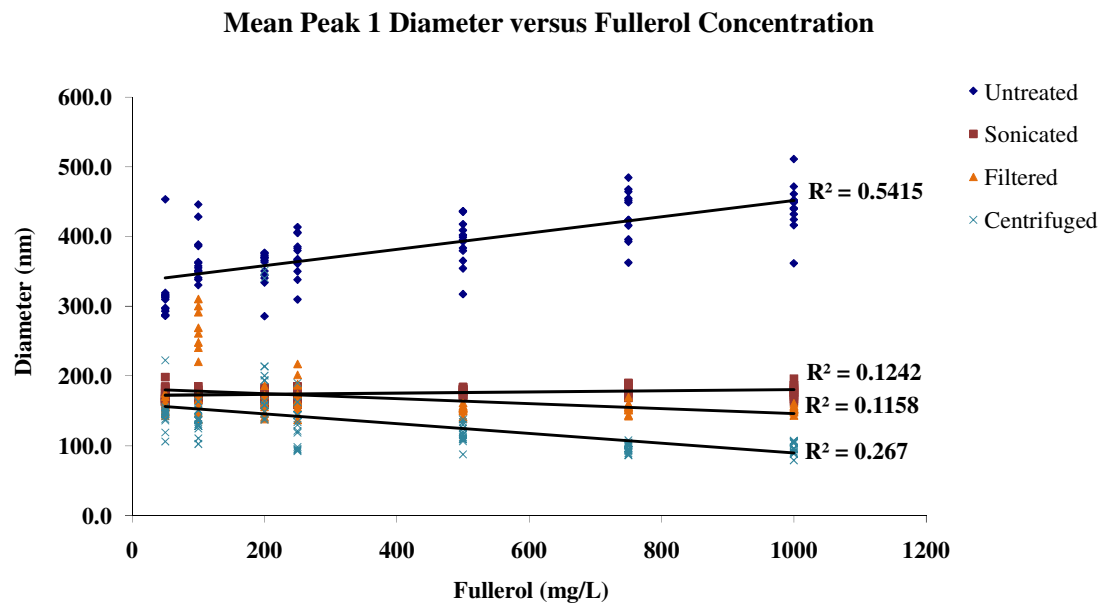


Figure 4-15: Zetasizer Nano ZS fullerol aggregate mean Peak 1 diameters plotted against concentration.

Fullerol Absorbance at 254 nm for Treatment Groups

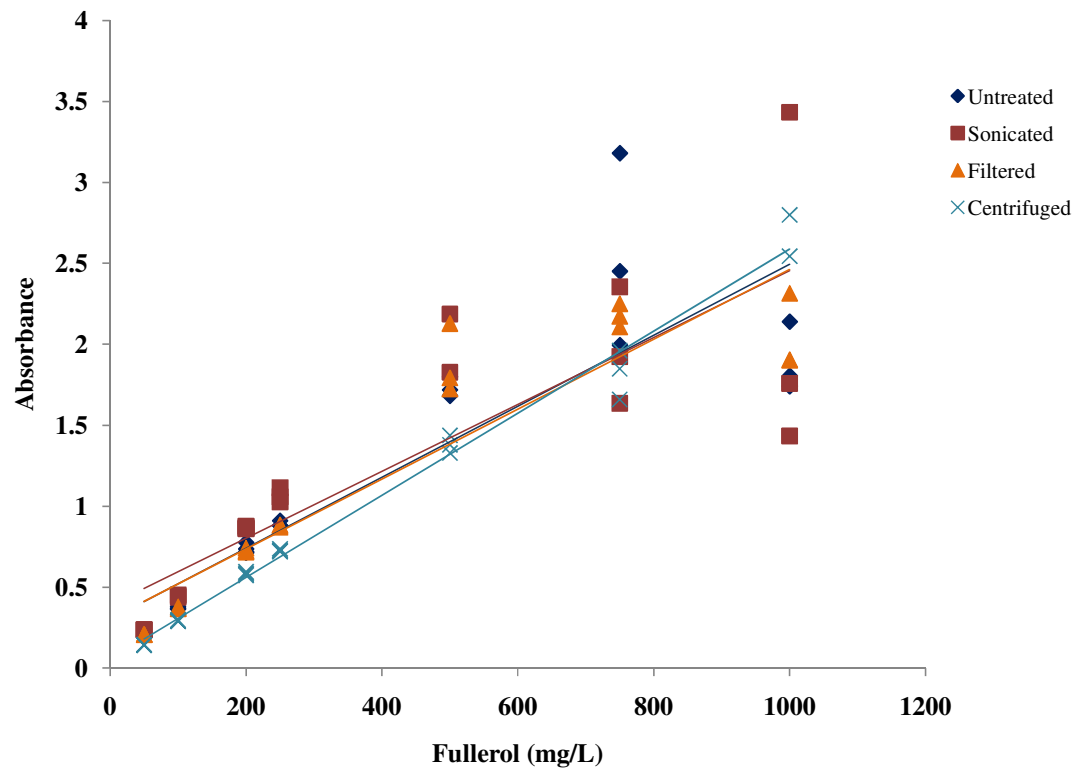


Figure 4-16: The 254 nm UV-vis absorbance across a 1.0 mm pathlength of fullerol solutions for untreated, sonicated, filtered and centrifuged treatment groups. This wavelength was output from the experimental UV lamp.

Fullerol Absorbance at 300 nm for Treatment Groups

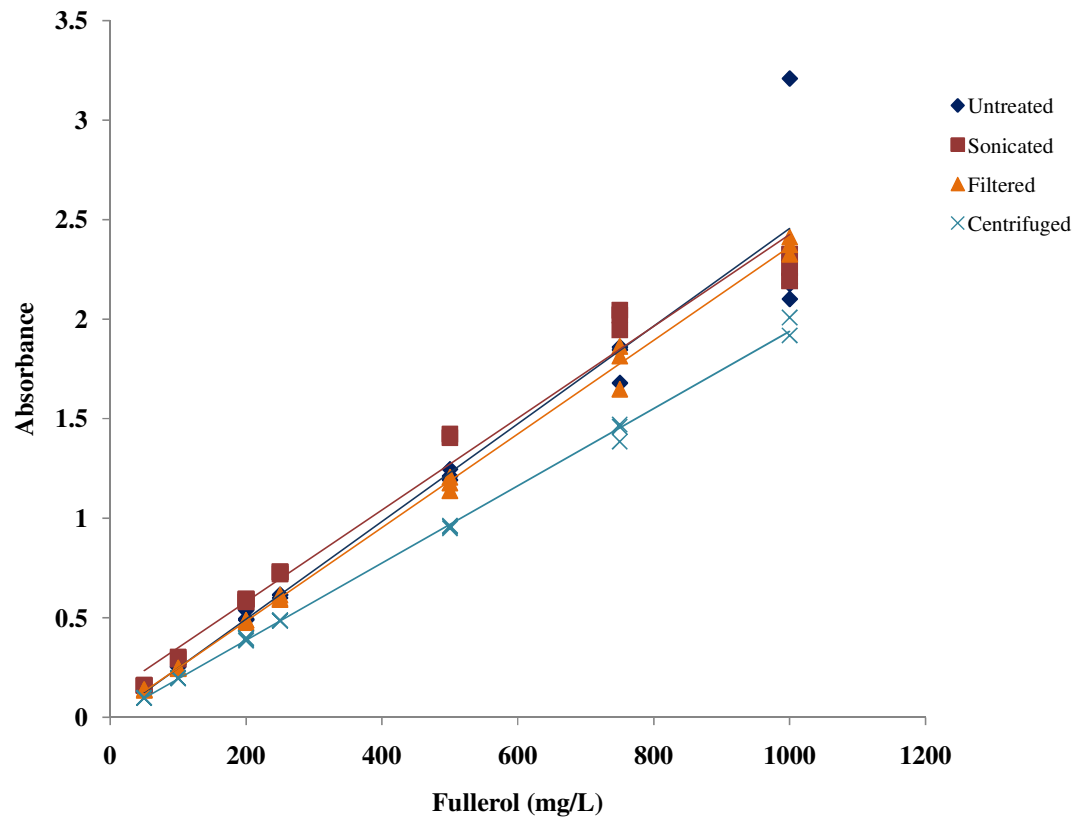


Figure 4-17: The 300 nm UV-vis absorbance across a 1.0 mm pathlength of fullerol solutions for untreated, sonicated, filtered and centrifuged treatment groups. This wavelength was output from the experimental UV lamp.

Discussion

Scattering and absorption of light is influenced by the physical and chemical attributes of particle size, shape, chemical conditions and concentration (Bohren & Huffman, 1983; Mamane, et al., 2006). Many studies have been conducted on how particulate matter interferes with ultraviolet disinfection efforts in complex water systems like those found in wastewater treatment. The results of these wastewater studies are drawn upon because of their relevance to the current investigations in recirculating aquaculture system.

A major assumption of this work is that aggregates of fullerol behave physically and chemically in many of the same ways that particles and aggregates of organic material do in wastewater. There are reasons to assume this is valid. First, both systems are colloidal in nature with water as the continuous liquid medium and the particulates or aggregates as the dispersed solid phase. Second, wastewater is a complex system due to its large variability in water chemistry, microbial diversity, and particulates. These factors can influence the efficacy of disinfection and are important to the current research in terms of protection of microorganisms. In particular, the large variation in shape and size of particles applies also to fullerol aggregates. Generally, the particle size distributions (PSDs), areas and perimeters of particles in wastewater are not normally distributed, but are right skewed with the majority of particles in the smaller size range (Aguilar, Saez, Llorens, Soler, & Ortuno, 2003; Droppo & Ongley, 1992; Mamane, et al., 2008). Right skewness was also noted in a number of the fullerol PSDs, areas and perimeters in these studies. The majority of the fullerol aggregates were smaller than 10 micrometers and a fraction consisted of aggregates larger than 10

micrometers. The fullerol used in these experiments had an approximate molecular weight of 1,129 g/mol, with an individual fullerol molecule about one nanometer in size. As some of the scanning electron micrographs reveal, fullerol aggregates range in size from less than 10 nanometers to nearly 100 micrometers. Finally, fullerenes are organic compounds like many wastewater particles. Fullerol has a net negative surface potential (zeta potential), like that of many wastewater particles (Husebo, Sitharaman, Furukawa, Kato, & Wilson, 2004), which could also play a role in aggregate dynamics.

Despite the similarities there are several differences between wastewater particles and fullerol aggregates. Fullerol is able to generate reactive oxygen species (ROS) mainly in the form of superoxide in the dark and singlet oxygen with exposure to UV and visible light. This can indirectly affect the amount of radiation that reaches microorganisms by way of changes in aggregate sizes and shapes. Second, the fullerol aggregates are assumed to be composed of smaller aggregates and individual fullerol molecules and so are considered homogenous. Wastewater particles, in contrast, are comprised of a multitude of organic and inorganic entities that are constituents of the waste within the system. Also, wastewater particles, unlike fullerol aggregates, can provide nutrients to bacteria.

Scanning electron microscopy is somewhat limited in this study, because the analyses depended on computer processing of scanning electron micrographs, which could be associated with a loss of actual aggregate size and shape data and lead to error. The particle sizes and shapes for most of the concentrations and treatments, other than the 250 mg/L sample, are not significantly different from others. It is unclear why the 250 mg/L sample is different, but it could be that a concentration as great as this results in disproportionate

aggregation. Further analyses at fullerol concentrations at least as great as 250 mg/L would need to be completed to confirm this thought. More crystalline-like and elongated structures are seen at greater fullerol concentrations. Aggregates are disrupted to some extent by ultrasonication and the fragments were on the size order of the lobes of the parent aggregates. The limits of aggregate size in the scanning electron micrographs are less than 10 micrometers to nearly 100 micrometers diameter at the longest dimension with most about 100-800 nm in diameter.

Aggregate sizes determined by dynamic light scattering (DLS) are less variable and easier to interpret than those obtained from scanning electron microscopy. For the untreated group, lesser concentrations are associated with smaller aggregates in untreated fullerol solutions. The Z-average has greater validity for similar treatments, spherical particles, monomodal samples (one size intensity distribution peak), and monodisperse samples (no width to the distributions of size intensities). There is a statistical difference between all treatment groups, regardless of whether Z-average or Peak 1 data are used. Compared to the untreated group, aggregate sizes were reduced the most by centrifugation, followed by 0.22 micron filtration and then sonication. Comparison of mean Z-average and Peak 1 diameters for each treatment group reveals similarity in size with the exception of the centrifuged and untreated groups (Table 4-2). The Z-average mean diameter for the centrifuged group is 42.34 nm, while that of Peak 1 is 131.38 nm. The untreated group Z-average diameter is 440.31 nm and Peak 1 diameter is 382.39 nm. Peak 1 was greatest amplitude (intensity) and width (distribution of intensities) for all samples tested.

An assumption with respect to our samples is that the majority of fullerol aggregates are represented by Peak 1. Smaller peaks would represent larger or smaller aggregates. Because the SEM data was right skewed with respect to size, large aggregates would likely have a greater effect on Z-average values. Peak 1 mean diameter would be less influenced by larger or smaller aggregate populations. Because four treatment groups were used, the circularity of the aggregates was low, and multiple peaks were observed in the data, Peak 1 data could have greater validity.

Aside from the untreated group in the Peak 1 results it is difficult to justify size change within treatment groups that could be due to differences in concentrations. Within the range of 50 mg/L to 1,000 mg/L, there is an upward trend in Peak 1 mean aggregate diameters for the untreated group as measured by DLS. SEM image analysis shows a significant difference only for the 250 mg/L untreated group. Other concentrations of untreated or sonicated groups in the SEM images are not statistically different. This compares to the DLS diameters within treated groups.

The shapes of fullerol aggregates could also play a role in the protective effect previously observed. Particle shape can be described by circularity (Mamane, et al., 2008). As mentioned previously, the closer the circularity value to 0, the more elongated the shape while values closer to 1 indicate more rounded forms. SEM image analysis showed that the fullerol aggregates had circularity values less than 0.5, which indicates more elongated polygonal structures on average. Irregularly-shaped particles could more scatter of light at various angles. Elongated structures could block UV photons from reaching similarly elongated microbes (Mamane, et al., 2008), and could offer more protection than more

circular particles. This could be a factor in these experiments because all test bacteria have elongated shapes. The SEM analysis, however, did not reveal differences in circularity among any concentration or treatment group analyzed.

Challenges arise when sizes and shapes of particles or aggregates are compared. Some researchers feel it is difficult to compare particle sizes and shapes with different analysis techniques (Mamane, et al., 2008). In our experiments, electron microscopy and dynamic light scattering were the two techniques used for shape and size analyses. Image analysis is sometimes not statistically representative, can be subjective and subject to greater error. There was more error associated with the SEM data in our study compared to the DLS data. Dynamic light scattering techniques are more accurate, but require multiple repetitions to reduce variability, which was done in our studies. It could also be difficult to compare results of SEM where fullerene solutions were vacuum-evaporated onto gold-coated silica versus in DLS where a fluid medium was used. That is, differences in processing between the two techniques could cause differences when results are compared. During SEM analysis, areas that appeared more uniformly distributed and representative of the entire field were selected for the scanning electron micrographs. Greatly precise comparison is not possible, because of the differences in measurement between the techniques and the greater error associated with a computer-based analysis of the SEM images. Although limited conclusions can be made outside of sizes and shapes for the SEM image analyses data, these data are consistent with those of DLS and indicate the data loss of image analysis is reasonable.

Absorption of ultraviolet radiation could also be important in the protective effect. Peak ultraviolet absorbance of the untreated fullerol solution in these experiments is about 223 – 226 nm. The solutions of fullerol absorbed greatly throughout the ultraviolet spectrum to include the experimental lamp output wavelength of 254 nm. There is, however, no significant difference in UV absorbance pattern among the four treatment groups of sonicated, filtered, centrifuged or untreated. It does not appear, therefore, that any change in the size of the particles attempted by the various treatments had an effect upon the absorbance of the fullerol solutions. Comparatively, this is also observed in wastewater where filtration had little change on spectrophotometric UV absorbance of suspended particles (Qualls, et al., 1983).

The increase in aggregate size could result in a decrease in negative surface charge on the aggregates and allow closer association with microbes. Determination of surface charge changes with concentration was not conducted and this would need to be investigated further to access its impact.

Concentration can affect free radical scavenging and singlet oxygen production. Fullerol can act as free radical scavenger of superoxide and singlet oxygen in the dark, and when the fullerol concentration is increased, less reactive oxygen species are found in solution (Chiang, et al., 1995; Lu, et al., 1998; Markovic & Trajkovic, 2008). The antioxidant ability of fullerol does not increase linearly with concentration (Jeng, et al., 2001). This is consistent with greater aggregate formation with increases in concentration. Photosensitization of fullerol causes the production of both superoxide and singlet oxygen (Pickering & Wiesner, 2005). The singlet oxygen yield is strongly correlated to the

concentration of fullerol (Vileno, et al., 2006). Little data exist for concentration related protection by fullerol to microorganisms. Radioprotection by fullerol to the protozoan *Stylonychia mytilus* exposed to gamma-rays depends on the concentration of fullerol and gamma ray dose (Zhao, Li, Xu, Liu, & Li, 2005). The concentration range in that study was 60 – 250 mg/L with irradiation held constant.

Given the overall results of our studies, changes in concentration seem to play the primary role in the observed protective effect of fullerol on the test organisms and with the conditions of our experiments. Fullerol is known to form fractal aggregates with increased concentration (Jeng, et al., 2001). The increase in mean fullerol aggregate size with increased concentration in the untreated group is consistent with the hypothesis that protection is by way of microbial shielding by aggregates. This shielding could protect microorganisms from ultraviolet light and enhance their survival. The observed protection seen in the untreated group could result from decreased inter-particle spacing that results from increased aggregate sizes or from higher density of aggregates. An increase in fullerol concentration could cause less light to reach microbes by signal attenuation via scattering or absorption. SEM image analysis and dynamic light scattering show that the aggregate diameters range from less than 10 nm to about 800 nm. Peak 1 diameters from the DLS data are about 400 nm for the untreated group. The untreated fullerol solution was used in the experiments where microbial protection was observed. The 400 nm mean diameter of aggregates in this solution is much less than the 7-8 micrometer threshold mentioned in the wastewater literature. Wastewater particles below this size do not affect the ultraviolet kinetic activation rate. Because of this, a direct protective effect as a result of increased

aggregate size is less likely than that of shielding by way of decreased inter-aggregate spacing due to increased concentration. It is likely that increased concentrations causes decreased inter-aggregate spaces, which physically blocks more ultraviolet photons from reaching microorganisms. This, in turn, resulted in the observed protective effect of fullerol.

We feel that although we did not observe the expected antimicrobial action of fullerol, the differences in our data contribute to the understanding of fullerol and how aggregates of this compound interact in an *in vitro* biological system. Contribution is also made to the knowledge base of disinfection in complex water systems like wastewater and recirculating aquaculture systems in how molecules comprised primarily of carbon could behave and protect microorganisms from ultraviolet irradiation.

PART III: MATHEMATICAL

CHAPTER 5

A deterministic dose-response model for microbial inactivation by ultraviolet irradiation in the presence of a protective concentrations of particles

Abstract

Fullerol has routinely demonstrated antimicrobial activity *in vitro*. Recently, we showed this derivatized C₆₀ fullerene can also impart a protective effect in a concentration-dependent manner. A sigmoidal dose-response model was selected to fit the data. This fitted model was subsequently placed within the traditional kinetic inactivation model commonly used in disinfection. Simulations and sensitivity were run using MATLAB. Dose (concentration of fullerol) was the most influential variable. The derived model could be used in other situations where a dose-response curve could be generated. These situations could include similar laboratory experiments that use fullerenes, colloidal applications that involve ultraviolet light penetration and microbial survival, and certain water disinfection scenarios where carbon-based particulate matter interferes with disinfection.

Introduction

Fullerol, a polyhydroxylated fullerene, has been shown to inactivate several species of microorganisms when exposed to ultraviolet (UV) or visible light (Aoshima, et al., 2009; Badireddy, et al., 2007; Lee, et al., 2009). This compound likely accomplishes this through the generation of reactive the oxygen species of singlet oxygen and superoxide radicals (Pickering & Wiesner, 2005). Fullerol is reported to have protective effects in the dark by quenching of singlet oxygen and various radicals (Chiang, et al., 1995; Dugan, et al., 1996; Jeng, et al., 2001; Lu, et al., 1998). A protective ability of fullerol was mentioned in the literature for *Escherichia coli*, but the mechanism of the protection was not investigated (Brunet, et al., 2009).

Our previous studies showed a protective effect for fullerol when irradiated by monochromatic (253.7 nm) ultraviolet light (Chapter 3). The four bacterial species and the virus used in those experiments were *Bacillus subtilis*, *Escherichia coli* (K12), *Salmonella enterica* serotype Newport, *Vibrio parahaemolyticus* and Spring Viremia of Carp Virus (SVCV). The survival of the microorganisms was tested at various fullerol concentrations (0-250 mg/L) with a constant exposure time of 60 seconds to ultraviolet light. The test microorganisms were protected from ultraviolet irradiation by fullerol aggregates, although the response varied with microbe and dose (Figure 5-1).

Median Survival versus Fullerol Concentration

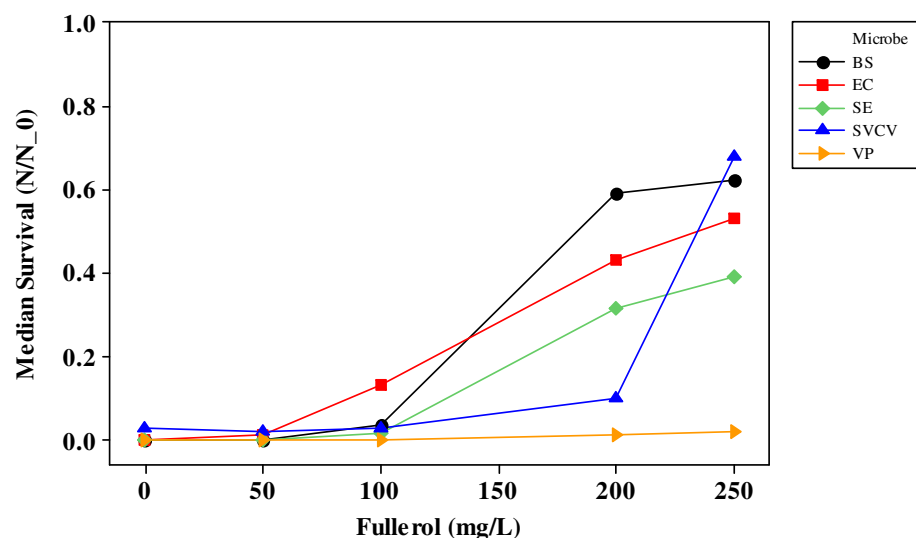


Figure 5-1: Median survival (N/N_0) of test microorganisms by fullerol concentration for 60 seconds ultraviolet irradiation. Bs = *Bacillus subtilis*; Ec = *Escherichia coli*; Se = *Salmonella enterica* serotype Newport; Vp = *Vibrio parahaemolyticus*; SVCV = Spring Viremia of Carp Virus.

The mechanism of protection of the UV-irradiated fullerol was investigated (Chapter 4). Fullerol solutions were sonicated, filtered and ultracentrifuged and compared to the untreated solution in an attempt to remove larger particles. Dynamic Light Scattering (DLS) was used to estimate the mean aggregate diameters of the four treatment groups. As the concentration of fullerol increased, the mean diameters of the aggregates increased with this group. Aggregate size did not increase for the other groups with fullerol concentration. No statistical difference was found in UV absorbance patterns among the four treatment groups. UV absorbance was found to increase with fullerol concentration for all groups. Consequently, greater concentrations appeared to block more incident UV photons from microorganisms that could result in inactivation.

Efficacy of ultraviolet disinfection is highly dependent on the degree of light penetration due to absorbance or scattering by particles and the medium (Mamane, et al., 2006). Inactivation of dispersed microorganisms that are not protected by particles by way of shielding or physical association follow the first order model for ultraviolet disinfection kinetics.

$$\frac{N}{N_0} = e^{-k \cdot I \cdot t}$$

Equation 5.1

where N = number of surviving microbes after a time period t

N_0 = number of bacteria at t=0

k = kinetic inactivation rate constant

I = intensity of ultraviolet radiation in microwatt seconds (μ Ws)

t = time period of irradiation in seconds

Tailing can be seen in ultraviolet log-linear dose-response curves for water disinfection when suspended particulate matter is present. There are several regions of a tailing curve (Figure 5-2). The first order region is explained by a rapid inactivation of dispersed organisms (Loge, et al., 2001). Disinfection efficiency tails and approaches zero when protective aggregates of bacteria or particulates are present. This routinely occurs before 100% inactivation. Microorganisms can also survive inside or otherwise physically

associate with particles or aggregates and can be protected from UV inactivation (Oliver & Cosgrove, 1975).

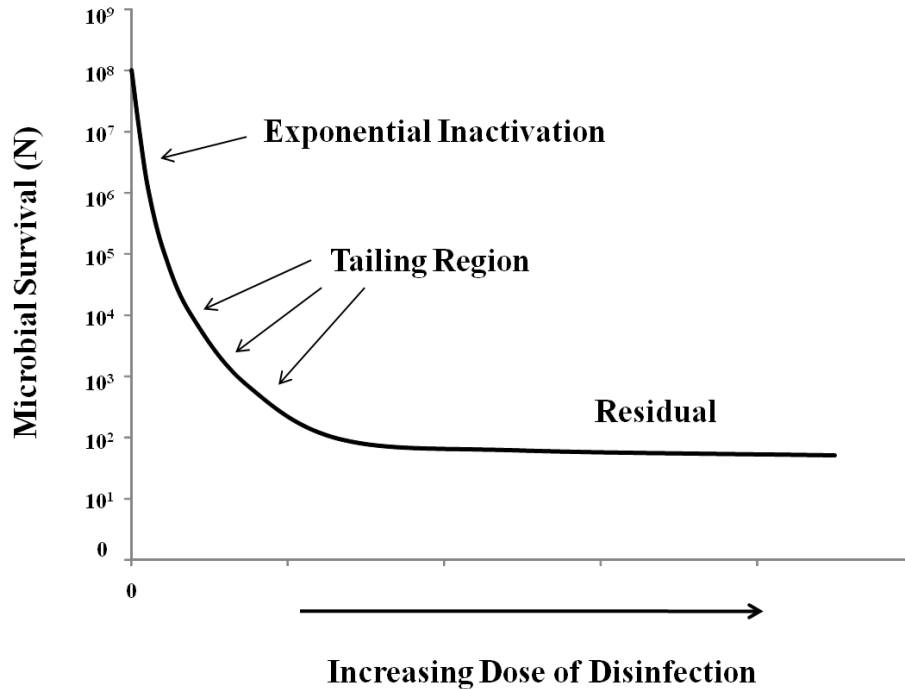


Figure 5-2: Inactivation of microorganisms exhibits tailing when particulate matter interferes with efficacy of disinfection. Y-axis is logarithmic. Modified from (Emerick, et al., 1999).

There are models that consider the protective effect of suspended material on disinfection efficacy. Many of these models used to determine the effect of particles on disinfection efficacy are complicated or require knowledge or calculation of associated kinetic rate or other model constants, numbers or ratios of particle-associated or UV-resistant bacteria, and ultraviolet intensities (Emerick, et al., 2000; Farnood, 2005; Loge, et al., 1996; Qualls & Johnson, 1985; Scheible, 1987). A model that does not rely on these factors would

be desirable in some situations where the concentrations of particles or aggregates of material could be measured and associated microbial survivals could be determined.

Our previous data indicated a protective effect of fullerol that varied with dose and was likely due to a concentration effect. The percent protection of microorganisms terms of disinfection is 100% minus the percent of inactivated microbes. Protected microorganisms can be viewed as simply the population that is able to resist or avoid disinfection efforts for any reason. These could include genetic resistance, association with other microbes or protecting particles or shielding from ultraviolet radiation. Protection and inactivation, therefore, are related. The aim of this mathematical analysis is to develop a model to simplify the system from which we collected data and relate it to the fundamental equation for ultraviolet disinfection (Equation 5.1).

Materials and Methods

Model derivation

Prism (Version 4.03, GraphPad Software, Inc., La Jolla, California, USA) was used to initially model the data obtained previously. Because the data were non-linear as shown in Figure 5-1 and because the survival ratio was the desired response to changes in fullerol concentration, a sigmoidal dose-response model was used to fit the data. The response was constrained from 0 to 1 for the survival ratio and the dose was given on a \log_{10} scale. A fit of

the measured data allowed estimation of the EC50, which is the concentration of fullerol in mg/L that protects 50% of the microorganisms.

The irradiation time used in our experiments was 60 seconds. For a fixed 60 second treatment at an assumed constant ultraviolet light intensity, the ratio of survived microbes (N) to the original number of microbes (N₀) is given by

$$y = \text{survival ratio} = \frac{\text{Number alive at end of irradiation time } (t)}{\text{Number alive at beginning of irradiation time } (t)} = \frac{N}{N_0}$$

$$\text{survival ratio} = \frac{1}{(1 + 10^{(\text{Log}_{10}\{EC50\} - \text{Log}_{10}\{Dose\})})}$$

Equation 5.2

$$\text{survival ratio} = \frac{1}{\left(1 + 10^{\text{Log}_{10}\left\{\frac{EC50}{Dose}\right\}}\right)} = \frac{1}{\left(1 + \frac{EC50}{Dose}\right)}$$

Simplifying,

$$\text{survival ratio} = \frac{N}{N_0} = \frac{Dose}{(EC50 + Dose)}$$

Equation 5.3

Equation 5.2 is the general sigmoidal dose-response equation. The EC50 is the concentration that has an effect on 50% of the study population. The dose is the applied

concentration of fullerol. Equation 5.3 represents the survival ratio of the populations of microorganisms after a population is treated with a given dose of a compound with a specified EC50. Because the effect of our experiments with fullerol is protective in nature, the sigmoidal dose-response curve associated with Equation 5.2 represents a protective effect. That is, if the concentration of fullerol is zero, then no protective effect would be observed. With increased doses of fullerol, greater survival at a given dose would be observed.

Protection can be viewed as the population of microorganisms that survive as disinfection event for any reason. If the survived microbe numbers are subtracted from the starting population number, the number of inactivated microbes is obtained. That is, one minus the survival ratio due a protective effect gives the ratio of microorganisms that were inactivated. To put Equation 5.3 in terms of inactivation so that it can be compared to current kinetic equations for disinfection, the survival ratio associated with protection needs to be subtracted from one.

$$1 - \frac{N}{N_0} = \frac{Dose}{(EC50 + Dose)}$$

$$-\frac{N}{N_0} = \frac{Dose}{(EC50 + Dose)} - 1$$

$$\frac{N}{N_0} = 1 - \frac{Dose}{(EC50 + Dose)}$$

$$\frac{N}{N_0} = \left(\frac{(EC50 + Dose)}{(EC50 + Dose)} - \frac{Dose}{(EC50 + Dose)} \right)$$

$$\frac{N}{N_0} = \frac{EC50}{(EC50 + Dose)}$$

This equation is now in terms of EC50-based dose-response inactivation. Multiplication by the number of microorganisms at the start of an ultraviolet irradiation treatment (N_0) gives

$$N = N_0 \frac{EC50}{(EC50 + Dose)}$$

Equation 5.4

The rate at which microorganisms are inactivated at any instant by ultraviolet irradiation is assumed to be proportional to the number of live cells at that time (N_t). This is expressed mathematically by the ordinary differential equation

$$\frac{dN_t}{dt} = A \cdot N_t$$

Equation 5.5

where A is a constant of proportionality. This differential equation has a general solution given by

$$N_t = C \cdot e^{A \cdot t}$$

Equation 5.6

where C is an integration constant.

To test the validity of this general solution, we first take its derivative.

$$\frac{dN_t}{dt} = A \cdot C \cdot e^{A \cdot t}$$

If the Equation 5.5 is rearranged,

$$\frac{dN_t}{dt} - A \cdot N_t = 0$$

and the derivative and the solution (Equation 5.6) into this differential equation, then the test demonstrates the validity of the start and end equations through zero equivalence.

$$A \cdot C \cdot e^{A \cdot t} - A \cdot C \cdot e^{A \cdot t} = 0$$

$$0 = 0$$

Two instances when the number of microorganisms must be identified to evaluate the constants C and A in Equation 5.6. Experimental data provide us with the number of microorganisms at the start of irradiation and the number after the 60 second time period. So, for zero seconds,

$$N_{at\ 0\ seconds} = N_0 = C \cdot e^{A \cdot (0\ seconds)}$$

The constant A cancels out at zero seconds.

$$C \cdot e^0 = C \cdot 1 = C$$

Therefore,

$$C = N_0$$

At the end of the 60 second irradiation period,

$$N_{at\ 60\ seconds} = N = N_0 \cdot e^{A \cdot (60\ seconds)}$$

We divide both sides by N_0 and take the natural logarithm to obtain

$$\text{Log}_e \left(\frac{N}{N_0} \right) = A \cdot 60 \text{ seconds}$$

Solving for A gives

$$A = \frac{\text{Log}_e \left(\frac{N}{N_0} \right)}{60 \text{ seconds}}$$

Finally, this equation and $C=N_0$ are inserted into Equation 5.6,

$$N = N_0 \cdot e^{\left(\frac{\text{Log}_e \left(\frac{N}{N_0} \right)}{60 \text{ seconds}} \right) \cdot t}$$

Equation 5.7

We know from Equation 5.4 that

$$\frac{N}{N_0} = \frac{EC50}{(EC50 + Dose)}$$

This is substituted into Equation 5.7 and this gives a final solution of

$$N = N_0 \cdot e^{\left(\frac{\text{Log}_e\left(\frac{EC50}{(EC50+Dose)}\right)}{60 \text{ seconds}} \right) \cdot t}$$

Equation 5.8

The general solution of Equation 5.8 is related to the general form of Equation 5.6. The derivative related to Equation 5.5 that denotes the change in N with respect to time and is used in the modeling software is

$$\frac{dN}{dt} = N_0 \cdot \frac{\left(\frac{EC50}{(EC50 + Dose)} \right) \cdot t}{60 \text{ seconds}}$$

Equation 5.8 is similar in form to the general ultraviolet kinetic inactivation model for disinfection by ultraviolet light.

$$N = N_0 \cdot e^{-k \cdot I \cdot t}$$

Equation 5.9

where k is the kinetic inactivation rate constant and I is ultraviolet radiation intensity. This constant indicates the rate at which a target microorganism is inactivated and varies dramatically by the type of bacteria and the experimental conditions. Some values of 1/k for some microorganisms are provided in Table 5-1.

Table 5-1: Approximate minimum ultraviolet irradiation dose required to inactivate greater than 99% of certain microorganisms

Microbe	k⁻¹ (μWs/ cm²)	Reference
<i>Bacillus subtilis</i> , spores	22,000	(Phillips & Hanel, 1960)
<i>Bacillus subtilis</i> , vegetative	11,000	(Phillips & Hanel, 1960)
<i>Escherichia coli</i>	7,000	(Kelly, 1974)
<i>Salmonella enteritidis</i>	7,600	(Phillips & Hanel, 1960)
<i>Vibrio anguilianon</i>	1,000	(Kasai, et al., 2001)
Bacteriophage (<i>E. coli</i>)	6,600	(Kelly, 1974)
Fish rhabdoviruses (such as SVCV), herpesviruses and iridoviruses	1,000 – 10,000	(Kasai, et al., 2001)
Fish birnaviruses, reoviruses and nodaviruses	1.5 – 2.5 x 10 ⁵	(Kasai, et al., 2001)

The traditional ultraviolet inactivation kinetic model (Equation 5.9) has the same form as the EC50 dose-response model (Equation 5.8). This leads to the equivalency of

$$N = N_0 \cdot e^{-k \cdot I \cdot t} = N_0 \cdot e^{\left(\frac{\text{Log}_e \left(\frac{EC50}{(EC50 + Dose)} \right)}{60 \text{ seconds}} \right) \cdot t}$$

This sequentially reduces to

$$e^{-k \cdot I \cdot t} = e^{\left(\frac{\text{Log}_e \left(\frac{EC50}{(EC50 + Dose)} \right)}{60 \text{ seconds}} \right) \cdot t}$$

$$-k \cdot I \cdot t = \left(\frac{\text{Log}_e \left(\frac{EC50}{(EC50 + Dose)} \right)}{60 \text{ seconds}} \right) \cdot t$$

$$k \cdot I = \frac{-\text{Log}_e \left(\frac{EC50}{(EC50 + Dose)} \right)}{60 \text{ seconds}}$$

Equation 5.10

This equation demonstrates mathematically that the product of k and I can be replaced by dose and EC50 values if known.

Sensitivity calculations for EC50 and dose were also completed to determine the relative interactions of these parameters and provide a standardized measurement of change in the survival ratio to change in the EC50 or dose. The sensitivity (S) of the curves to a given dose can be easily computed and is defined as the percentage change in output (microbial survival) divided by the percentage change in input (dose or concentration of fullerol). For this derivation, the unchanged dose is increased and decreased by 5%.

$$S = \frac{\frac{\text{change in output}}{\text{output}}}{\frac{\text{change in input}}{\text{input}}}$$

$$S = \frac{\frac{N_0 \text{ at 5\% increase in dose} - N_0 \text{ at 5\% decrease dose}}{N_0 \text{ at unchanged dose}}}{\frac{5\% \text{ increased Dose} - 5\% \text{ decreased Dose}}{\text{unchanged Dose}}}$$

To use the equations from the previous derivation gives

$$S = \frac{N_0 \cdot \left(\frac{1.05 \cdot EC50}{(EC50 + 1.05 \cdot Dose)} \right)^{\frac{t}{60 \text{ secs}}} - N_0 \cdot \left(\frac{0.95 \cdot EC50}{(EC50 + 0.95 \cdot Dose)} \right)^{\frac{t}{60 \text{ secs}}}}{N_0 \cdot \left(\frac{EC50}{(EC50 + Dose)} \right)^{\frac{t}{60 \text{ secs}}}} \cdot \frac{1.05 \text{ Dose} - 0.95 \text{ Dose}}{\text{Dose}}$$

$$S = \frac{\left(\frac{1.05 \cdot EC50}{(EC50 + 1.05 \cdot Dose)} \right)^{\frac{t}{60 \text{ secs}}} - \left(\frac{0.95 \cdot EC50}{(EC50 + 0.95 \cdot Dose)} \right)^{\frac{t}{60 \text{ secs}}}}{\left(\frac{EC50}{(EC50 + Dose)} \right)^{\frac{t}{60 \text{ secs}}}} \cdot 0.1$$

$$S = \frac{\left(\frac{(EC50 + Dose)}{EC50} \cdot \frac{1.05 \cdot EC50}{(EC50 + 1.05 \cdot Dose)}\right)^{\frac{t}{60 \text{ secs}}} - \left(\frac{(EC50 + Dose)}{EC50} \cdot \frac{0.95 \cdot EC50}{(EC50 + 0.95 \cdot Dose)}\right)^{\frac{t}{60 \text{ secs}}}}{0.1}$$

$$S = \frac{\left(\frac{1.05 \cdot (EC50 + Dose)}{(EC50 + 1.05 \cdot Dose)}\right)^{\frac{t}{60 \text{ secs}}} - \left(\frac{0.95 \cdot (EC50 + Dose)}{(EC50 + 0.95 \cdot Dose)}\right)^{\frac{t}{60 \text{ secs}}}}{0.1}$$

Model simulations

The EC50 dose-response inactivation model (Equation 5.8) and the traditional $k \cdot I$ inactivation model (Equation 5.1) were simulated in MATLAB (Version 7.1, The MathWorks, Inc., Natick, Massachusetts, USA). The code written for these simulations is provided in APPENDIX G. The survival ratios (N/N_0) versus time in seconds were plotted. The differential equations related to both models can be considered stiff in that rapid variation in the solution could exist. For this reason, the multistep ordinary differential equation (ODE) solver chosen in MATLAB was ODE15s. The value of k^{-1} was set at 10,000 $\mu\text{Ws}/\text{cm}^2$ and the ultraviolet intensity (I) was estimated from Equation 5.10. The base values for EC50 and dose were set at 250 mg/L because these values were a general approximation of the microbial EC50 values for fullerol and because 250 mg/L was an actual experimental dose. The time (x -axis) ranged from zero to 600 seconds (10 minutes). Sensitivity calculations were conducted at $\pm 5\%$ and $\pm 50\%$ for each time step for EC50 and dose variables. Sensitivity was not calculated for the $k \cdot I$ model. The sensitivity for each time step was also plotted and the overall maximum sensitivity for the time period of the simulation was recorded. In addition, the simulations were repeated 300 times at serial increase of 10 mg/L EC50 and then dose. The maximum sensitivities were recorded and plotted for each of the 300 iterations to observe the trend in maximum sensitivity with changes in EC50 or dose.

Results

The data were successfully fitted to the sigmoidal dose-response model, most of which fell as expected within the 95% confidence band for the best-fit curve (Figure 5-3). The estimated protective fullerol EC50 values for *Escherichia coli* and *Bacillus subtilis* were about the same at 269.2 mg/L and 277.3 mg/L (Table 5-2). *Salmonella enterica* serotype Newport and Spring Viremia of Carp Virus had greater and more similar EC50 values of 502.6 mg/L and 449.6 mg/L than the previous microbes. The EC50 for *Vibrio parahaemolyticus* was much greater at 16,255. The standard error was greatest for SVCV and resulted in the widest 95% confidence interval. The goodness of fit as indicated by the coefficient of determination (R^2) was about 0.70 – 0.80 and indicates the proportion of variability in the data that is explained by the sigmoidal dose-response model. The R^2 value for SVCV, however, is only about 0.46 with this model.

The MATLAB simulation of the two models showed comparable results and is depicted in various parameter settings in Figure 5-4, Figure 5-5, Figure 5-6, and Figure 5-7. The EC50 dose-response model decreased exponentially as expected and was similar in survival ratio response to that of the traditional k·I inactivation model. For all simulations examined, the sensitivity increased monotonically throughout the irradiation period of zero to 600 seconds. That is, the values for the maximum sensitivities were taken at 600 seconds. Figures 5-4 and 5-5 show the results of a $\pm 5\%$ change in EC50 and dose. There is little observable difference between the original (zero-change) inactivation curve and those calculated from the $\pm 5\%$ sensitivity change. The maximum sensitivity, however, is much

greater for dose than for EC50. Figures 5-6 and 5-7 use $\pm 50\%$ allow an easier view of the direction of changes in EC50 and dose. Specifically, a $\pm 50\%$ change in EC50 and dose values of 250 mg/L equate to 125 mg/L and 375 mg/L. As illustrated in Figure 5-6, when the EC50 is decreased to 125 mg/L the survival is extended for a longer time period, while an EC50 increase to 375 mg/L causes more rapid inactivation. As expected, therefore, a greater EC50 indicates a greater concentration of fullerol is required to protect with the given set of conditions. Likewise, lesser EC50 values are associated with more protection given by fullerol with the particular set of conditions. When EC50 is held constant and the sensitivity of the survival ratio to $\pm 50\%$ change in dose is evaluated, a larger dose of 375 mg/L results in slower inactivation and is consistent with the observed protective effect of fullerol or perhaps other particles that attenuate ultraviolet light intensity (Figure 5-7). The lesser dose of 125 mg/L results in more rapid inactivation. The dose of light-interfering material, therefore, is confirmed to be protective in this model.

When the simulations were repeated 300 times and the maximum sensitivities for EC50 and dose were plotted against concentration for all iterations, changes in EC50 sensitivity showed little change with increase (Figure 5-8 and Figure 5-9). In contrast, dose showed a large initial increase in maximum sensitivity followed by a decrease with increased concentration.

Dose-Response Curves for Tested Microorganisms and Fullerol Concentrations

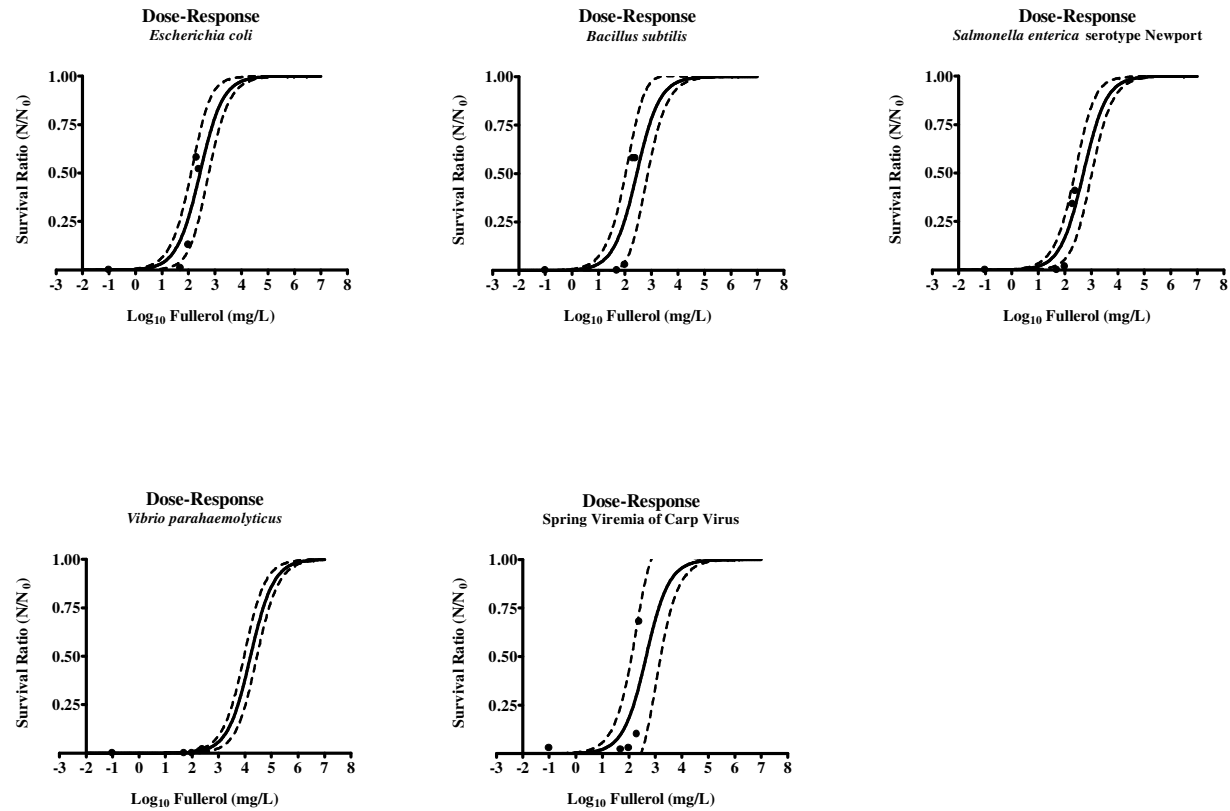


Figure 5-3: Dose-Response curves for tested microorganisms. Solid line is the best-fit curve for the data, while the dashed lines indicate the 95% confidence band for the best-fit curve.

Table 5-2: Best-fit curve calculations for tested microorganisms and fullerol concentrations.

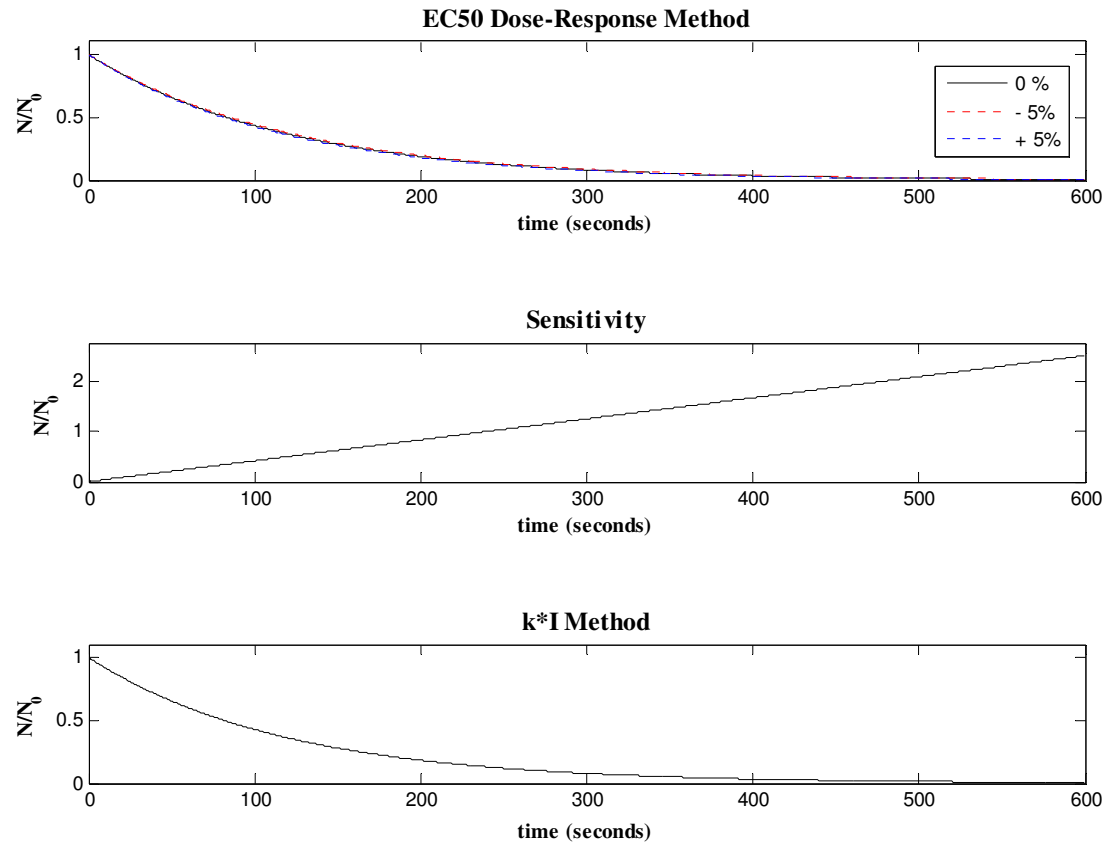
	Ec	Bs	Se	Vp	SVCV
Sigmoidal dose-response					
Best-fit values					
Bottom	0	0	0	0	0
Top	1.0	1.0	1.0	1.0	1.0
Log₁₀EC50 (mg/L)	2.43	2.443	2.701	4.211	2.653
EC50 (mg/L)	269.2	277.3	502.6	16255	449.6
Std. Error					
Log₁₀EC50 (mg/L)	0.1325	0.176	0.1254	0.09253	0.2557
95% Confidence Intervals					
Log₁₀EC50 (mg/L)	2.062 to 2.798	1.954 to 2.931	2.353 to 3.049	3.954 to 4.468	1.943 to 3.363
EC50 (mg/L)	115.4 to 627.7	90.03 to 853.9	225.4 to 1121	8998 to 29366	87.72 to 2305
Goodness of Fit					
Degrees of Freedom	4	4	4	4	4
R²	0.7899	0.7037	0.7639	0.7657	0.4562
Absolute Sum of Squares	0.06646	0.1157	0.03892	7.50E-05	0.178
Root Mean Square	0.1289	0.1701	0.09864	0.00433	0.2109
Constraints					
Bottom	0	0	0	0	0
Top	1.0	1.0	1.0	1.0	1.0

Equation: $Y = \text{Bottom} + (\text{Top} - \text{Bottom}) / (1 + 10^{((\text{Log}_{10}\text{EC50} - X)))}$

X is the base 10 logarithm of concentration. Y is the survival ratio (N/N₀)

Y starts at Bottom (0) and goes to Top (1.0) with a sigmoid shape.

Survival Ratio Response and Sensitivity Plots

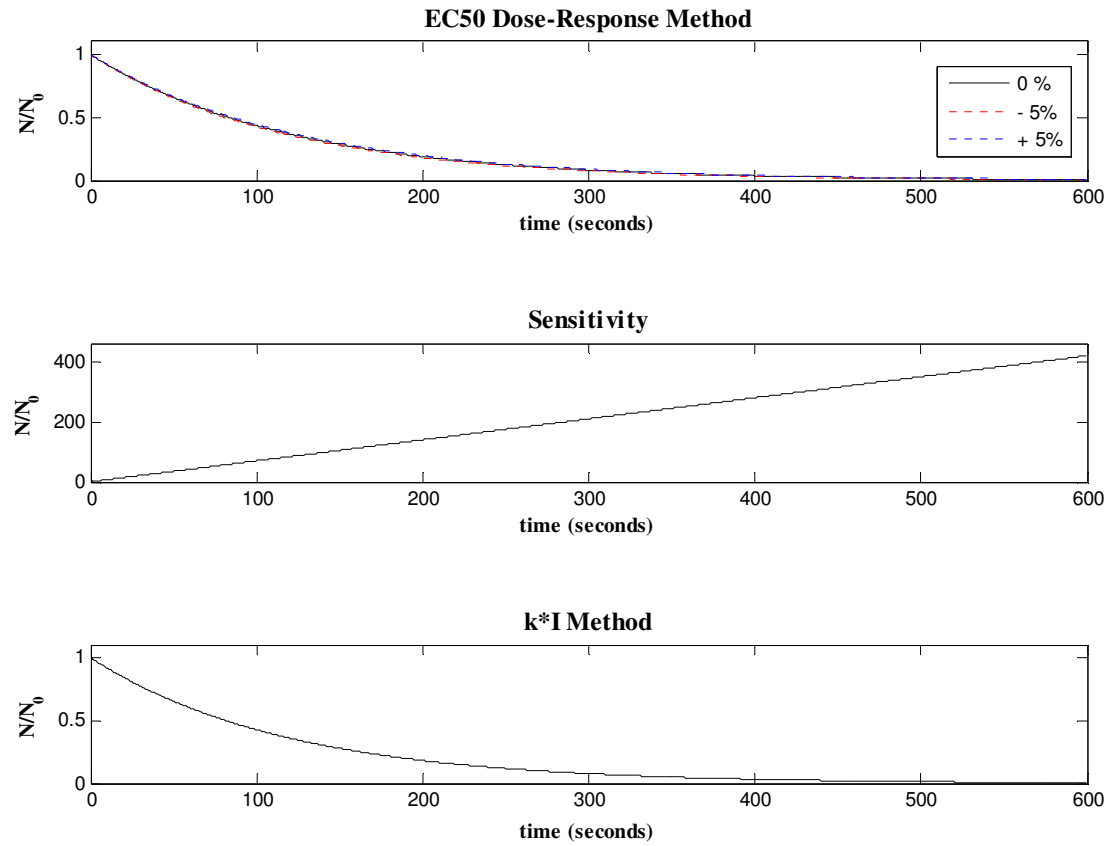


EC50 = 250 mg/L; Dose = 250 mg/L; $k = 0.0001 \text{ cm}^2/\mu\text{Ws}$; Intensity = $85 \mu\text{W}/\text{cm}^2$

Effect on survival ratio by +/- 5% change in EC50 of fullerol (mg/L). Maximum Sensitivity = 2.5142

Figure 5-4: Results of MATLAB simulation at $\pm 5\%$ change in fullerol EC50.

Survival Ratio Response and Sensitivity Plots

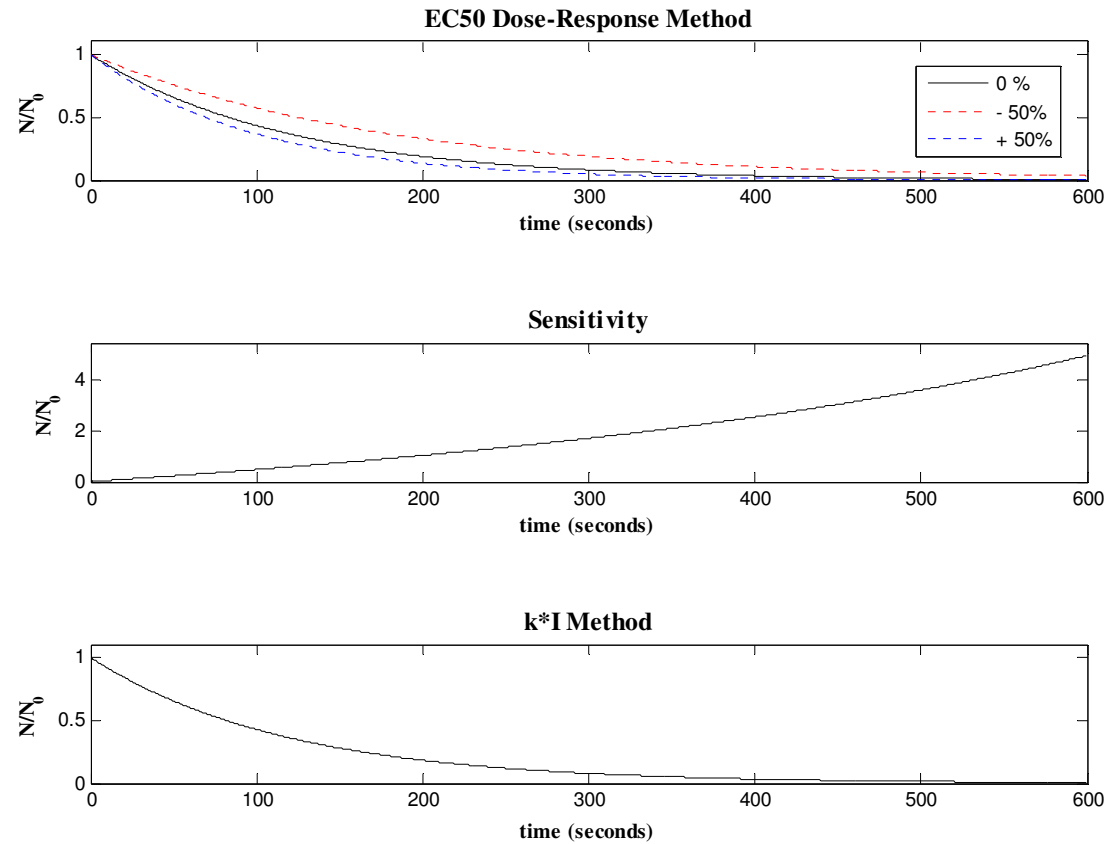


EC50 = 250 mg/L; Dose = 250 mg/L; $k = 0.0001 \text{ cm}^2/\mu\text{Ws}$; Intensity = $85 \mu\text{W}/\text{cm}^2$

Effect on survival ratio by +/- 5% change in dose of fullerol (mg/L). Maximum Sensitivity = 418.3242

Figure 5-5: Results of MATLAB simulation at $\pm 5\%$ change in fullerol dose.

Survival Ratio Response and Sensitivity Plots

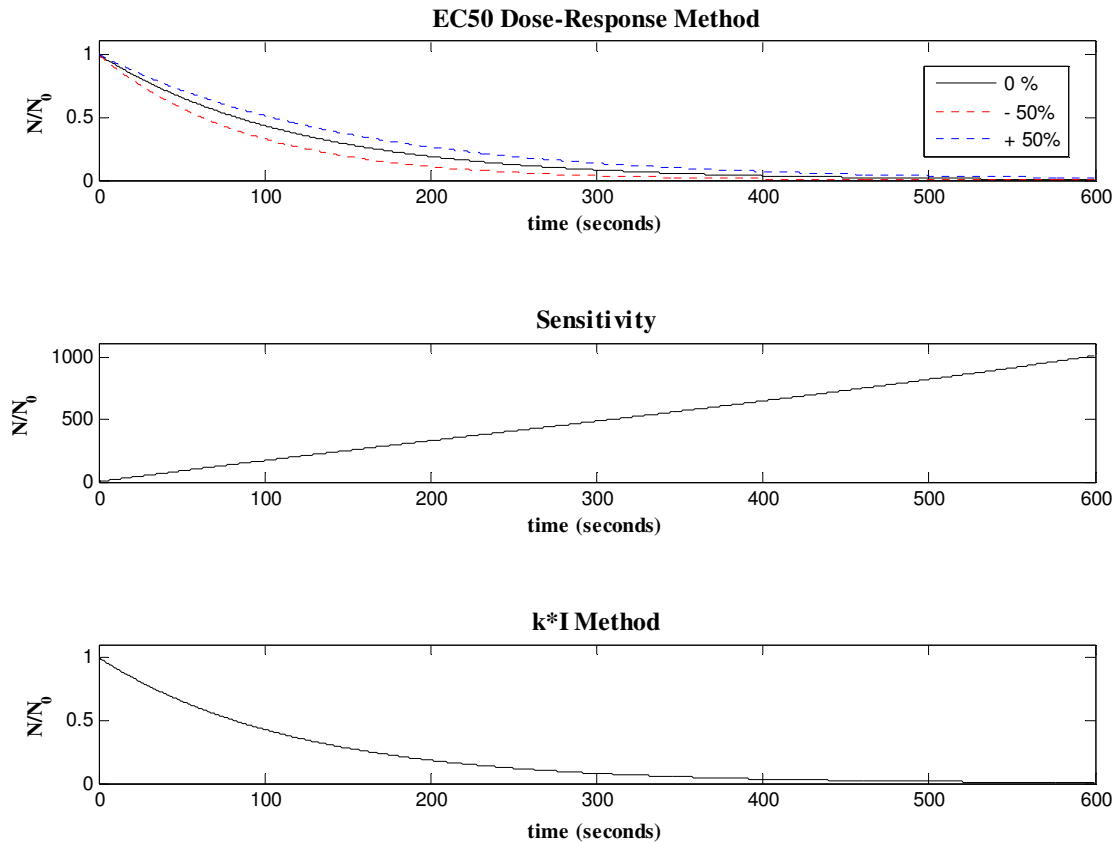


EC50 = 250 mg/L; Dose = 250 mg/L; $k = 0.0001 \text{ cm}^2/\mu\text{Ws}$; Intensity = $85 \mu\text{W}/\text{cm}^2$

Effect on survival ratio by +/- 50% change in EC50 of fullerol (mg/L). Maximum Sensitivity = 4.921

Figure 5-6: Results of MATLAB simulation at $\pm 50\%$ change in fullerol EC50.

Survival Ratio Response and Sensitivity Plots



EC50 = 250 mg/L; Dose = 250 mg/L; $k = 0.0001 \text{ cm}^2/\mu\text{Ws}$; Intensity = $85 \mu\text{W}/\text{cm}^2$

Effect on survival ratio by +/- 50% change in dose of fullerol (mg/L). Maximum Sensitivity = 1017.6848

Figure 5-7: Results of MATLAB simulation at $\pm 50\%$ change in fullerol dose.

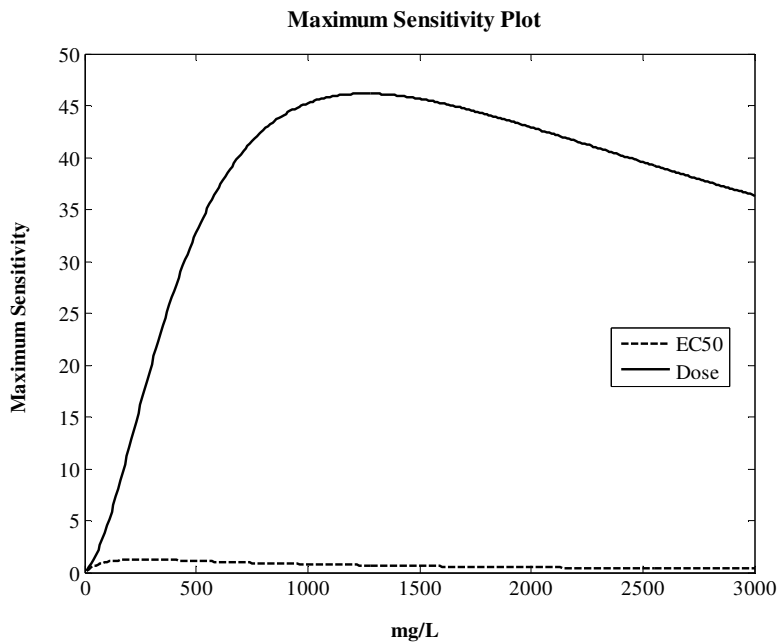


Figure 5-8: Plot of maximum sensitivities when EC50 is changed by 10 mg/L.

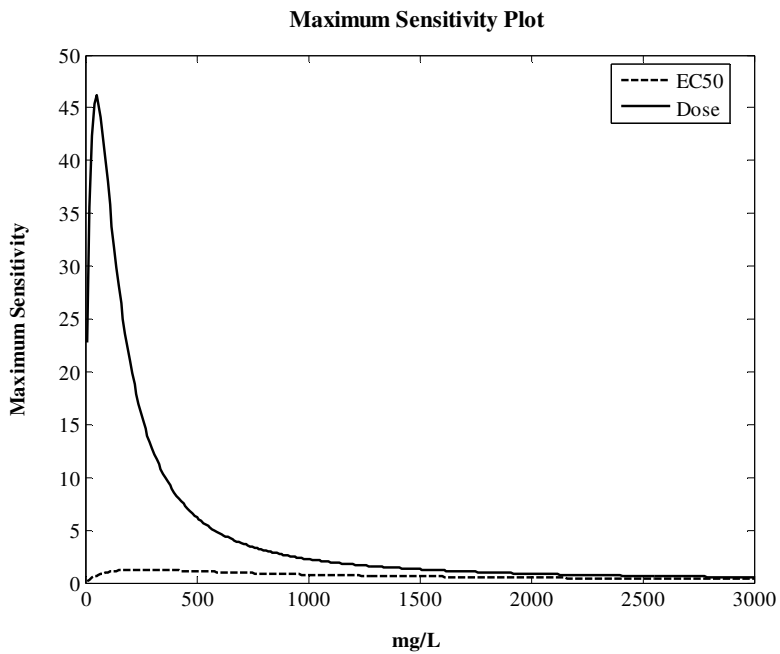


Figure 5-9: Plot of maximum sensitivities when dose is changed by 10 mg/L.

Discussion

As with any model, the objective of this EC50 dose-response model is to simplify the experimental system. The validity of a mathematical model depends on how well a dataset is explained by the model. The usefulness of a model will be determined by how well it will predict future situations and could be used within the environment for which it was designed. As a result of the simplification, a number of assumptions are made (Table 5-3).

Table 5-3: Assumptions of EC50 dose-response model.

Assumptions
1. The intensity (I) of ultraviolet radiation is constant during the modeled time period.
2. The kinetic inactivation rate (k) is constant during the modeled time period
3. The dose and EC50 do not change for each time period (iteration) that is modeled
4. Data points at greater doses follow the sigmoidal dose-response trajectory

Although the EC50 dose-response model does not use intensity (I) as a variable, it is implied though Equation 5.10. This is also the case for the first order kinetic inactivation rate (k). In reality, ultraviolet light intensity changes throughout time in longer and shorter timeframes. Throughout the life of the ultraviolet lamp, ultraviolet intensity can diminish and require their replacement. In a time period of irradiation as short as 60 seconds, the intensity of the lamp decreases from startup as the lamp equilibrates. The intensity in our experimental system was observed to change in this manner. This intensity decrease is likely

not significant to the results of microbial survival during the period of 60 seconds and can be viewed as an average intensity for the irradiation time. Likewise, the kinetic inactivation rate, which represents the inverse of the ultraviolet radiation dose required for a given kill of a certain organism, is considered to remain constant in the first order model for ultraviolet disinfection kinetics (Equation 5.1). It is reasonable, therefore, to assume that ultraviolet intensity and the first order rate constant are unchanged for a given calculation using the EC50 dose-response model.

Although the EC50 and dose were changed incrementally in the simulations for each iteration the EC50 and dose were constant. The EC50 represents the concentration of a compound or particles that has a specified effect on 50% of the population. This number is generally inherent to the compound with respect to the population and test environment. It can be considered to remain constant for those conditions. The concentration or dose of a compound or ultraviolet light-attenuating particles can change throughout time. For example, in our experimental system, the dose of fullerol was changed to observe different responses in microbial survival. Similarly, in wastewater treatment system or recirculating aquaculture system environments, the concentration of particles can change throughout time as the wastewater system receives more waste or fish produce varied amounts of waste at certain times of the day. Measurements of the dose and the microbial response to ultraviolet irradiation can be taken at various times throughout a change to create a sigmoidal dose-response curve in the same manner as we did with fullerol. To make the assumption that dose is constant throughout time means for the purposes of the model the dose remains constant for the time period of the calculation or iteration.

The most far-reaching assumption is that data points in response to greater doses follow the sigmoidal dose-response trajectory. We did not test at fullerol doses greater than 250 mg/L because we did not feel practical use of the compound could occur at greater concentrations. The intent of the original investigation was to look at several compounds that could be engineered for use in an aquaculture setting to augment disinfection. Instead, a protective nature of fullerol was observed and investigated in the course of our studies. A budget for analyses at greater concentrations than 250 mg/L was not available.

As a result, our use of the data in a model, like the sigmoidal dose-response model, is limited because the upper end of the curve reflects doses of fullerol that are greater than 1,000 mg/L. To gather data in this region for further model validation probably would not change the results much other than to increase the coefficient of determination (R^2). Between 70-80% of the variability in the survival ratios from our experimental data is explained by the sigmoidal dose-response model. Nearly any set of data can be fit to a model with enough parameters. While it is possible that more complex models with a greater number of parameters could have achieved R^2 values of more than 0.90, the simplicity of the model allows it to work well with minimal data and with only the knowledge of survival ratios at several doses.

In terms of microorganism survival ratio prediction, the environment for which this model is designed to be useful is one where a compound incompletely dissolves or aggregates to form an aqueous colloidal suspension. If it is suspected that this suspension attenuates ultraviolet light and possibly shields microorganisms, information on two data variables would need to be collected to generate a standard sigmoidal dose-response curve to

estimate the EC50. These are the concentration of the particles in the suspension and the survival of microbes at that concentration. This model, therefore, would work best when the concentration of a compound could be changed as was done in our previous fullerol experiments or if the concentration of particulate matter fluctuates naturally in diurnal or seasonal cycles like what can be observed in wastewater treatment operations or recirculating aquaculture systems.

In terms of the sensitivity of the model, it is clear from the simulations that changes in dose have the greatest effect on the survival ratio. It is critical to take accurate measurements of dose when the sigmoidal dose-response model is constructed for EC50 estimation. The fact that dose is the more sensitive variable is not unexpected given that dose is present in the numerator and the denominator of the basic ratio equation (Equation 5.3). At very large doses of fullerol, the sensitivity of the survival ratio to EC50 or dose alteration is reduced. In the case of our experiments, however, large concentrations of fullerol are not reasonable to pursue.

The EC50 dose-response model is able to replace the product $k \cdot I$ of the traditional ultraviolet first order inactivation model (Equation 5.1 & Equation 5.10). The significance of this is that these factors do not need to be measured or calculated. Instead, a simple collection of data could occur in a system where the concentration of ultraviolet light-attenuating particles or aggregates and the associated survival of microorganisms can be measured.

PART IV: REFERENCES

REFERENCES

- Adin, A. (1999). *Particle characteristics: A key factor in effluent treatment and reuse*.
- Aguilar, M. I., Saez, J., Llorens, M., Soler, A., & Ortuno, J. F. (2003). Microscopic observation of particle reduction in slaughterhouse wastewater by coagulation-flocculation using ferric sulphate as coagulant and different coagulant aids. *Water Research*, 37(9), 2233-2241.
- Ahne, W., Bjorklund, H. V., Essbauer, S., Fijan, N., Kurath, G., & Winton, J. R. (2002). Spring viremia of carp (SVC). *Diseases of Aquatic Organisms*, 52(3), 261-272.
- Alberts, B., Johnson, A., Lewis, J., Raff, M., Roberts, K., & Walter, P. (2002). *Molecular Biology of the Cell* (4th ed.). New York, NY: Garland Science.
- Alexander, R. A. (1935). Studies on the neurotropic virus of horse-sickness. *Onderstepoort Jour Vet Sci and Animal Indust*, 4((2)), 291-388.
- Aoshima, H., Kokubo, K., Shirakawa, S., Ito, M., Yamana, S., & Oshima, T. (2009). Antimicrobial Activity of Fullerenes and Their Hydroxylated Derivatives. [Article]. *Biocontrol Science*, 14(2), 69-72.
- Arbogast, J. W., Darmany, A. P., Foote, C. S., Rubin, Y., Diederich, F. N., Alvarez, M. M., et al. (1991). Photophysical properties of C60. [Letter]. *Journal of Physical Chemistry*, 95(1), 11-12.
- Badireddy, A. R., Hotze, E. M., Chellam, S., Alvarez, P., & Wiesner, M. R. (2007). Inactivation of bacteriophages via photosensitization of fullerol nanoparticles. *Environ Sci Technol*, 41(18), 6627-6632.
- Berg, K., & Moan, J. (1994). Lysosomes as photochemical targets. *Int J Cancer*, 59(6), 814-822.
- Berg, K., & Moan, J. (1997). Lysosomes and microtubules as targets for photochemotherapy of cancer. *Photochem Photobiol*, 65(3), 403-409.
- Bertoloni, G., Rossi, F., Valduga, G., Jori, G., Ali, H., & van Lier, J. E. (1992). Photosensitizing activity of water- and lipid-soluble phthalocyanines on prokaryotic and eukaryotic microbial cells. *Microbios*, 71(286), 33-46.
- Bertoloni, G., Rossi, F., Valduga, G., Jori, G., & van Lier, J. (1990). Photosensitizing activity of water- and lipid-soluble phthalocyanines on Escherichia coli. *FEMS Microbiol Lett*, 59(1-2), 149-155.

- Birkeland, J. M. (1934). Photodynamic action of methylene blue on plant viruses. *Science*, 80((2077)), 357-358.
- Blancheton, J. P., & Canaguier, B. (1995). Bacteria and Particulate Materials in Recirculating Sea-Bass (*Dicentrarchus-Labrax*) Production System. *Aquaculture*, 133(3-4), 215-224.
- Blatchley, E. R., Dumoutier, N., Halaby, T. N., Levi, Y., & Laine, J. M. (2001). Bacterial responses to ultraviolet irradiation. *Water Science and Technology*, 43(10), 179-186.
- Bohren, C., & Huffman, D. (1983). *Absorption and Scattering of Light by Small Particles*: Wiley-Interscience.
- Bonnett, R. (1995). Photosensitizers of the porphyrin and phthalocyanine series for photodynamic therapy. [Review]. *Chemical Society Reviews*, 24(1), 19-33.
- Bosi, S., Da Ros, T., Castellano, S., Banfi, E., & Prato, M. (2000). Antimycobacterial activity of ionic fullerene derivatives. *Bioorg Med Chem Lett*, 10(10), 1043-1045.
- Bossier, P., & Verstraete, W. (1996). Triggers for microbial aggregation in activated sludge? *Applied Microbiology and Biotechnology*, 45(1-2), 1-6.
- Brands, D. A., Inman, A. E., Gerba, C. P., Mare, C. J., Billington, S. J., Saif, L. A., et al. (2005). Prevalence of *Salmonella* spp. in oysters in the United States. [Article]. *Applied and Environmental Microbiology*, 71(2), 893-897.
- Brant, J., Lecoanet, H., & Wiesner, M. R. (2005). Aggregation and deposition characteristics of fullerene nanoparticles in aqueous systems. *Journal of Nanoparticle Research*, 7(4-5), 545-553.
- Brunet, L., Lyon, D. Y., Hotze, E. M., Alvarez, P. J. J., & Wiesner, M. R. (2009). Comparative Photoactivity and Antibacterial Properties of C-60 Fullerenes and Titanium Dioxide Nanoparticles. *Environmental Science & Technology*, 43(12), 4355-4360.
- Cadet, J., Anselmino, C., Douki, T., & Voituriez, L. (1992). Photochemistry of Nucleic-Acids in Cells. *Journal of Photochemistry and Photobiology B-Biology*, 15(4), 277-298.
- Chen, K. L., & Elimelech, M. (2009). Relating Colloidal Stability of Fullerene (C-60) Nanoparticles to Nanoparticle Charge and Electrokinetic Properties. *Environmental Science & Technology*, 43(19), 7270-7276.

- Chiang, L., Lu, F., & Lin, J. (1995). Free radical scavenging activity of water-soluble fullerenols. *Journal of the Chemical Society, Chemical Communications*(12).
- Chick, H. (1908). An Investigation of the Laws of Disinfection. *The Journal of Hygiene*, 8(1), 92-158.
- Da Ros, T., Prato, M., Novello, F., Maggini, M., & Banfi, E. (1996). Easy Access to Water-Soluble Fullerene Derivatives via 1,3-Dipolar Cycloadditions of Azomethine Ylides to C(60). *J Org Chem*, 61(25), 9070-9072.
- Darby, J. L., Snider, K. E., & Tchobanoglous, G. (1993). Ultraviolet Disinfection for Waste-Water Reclamation and Reuse Subject to Restrictive Standards. *Water Environment Research*, 65(2), 169-180.
- DeRosa, M. C., & Crutchley, R. J. (2002). Photosensitized singlet oxygen and its applications. *Coordination Chemistry Reviews*, 233, 351-371.
- Dougherty, T. J., Gomer, C. J., Henderson, B. W., Jori, G., Kessel, D., Korbelik, M., et al. (1998). Photodynamic therapy. *J Natl Cancer Inst*, 90(12), 889-905.
- Droppo, I. G., & Ongley, E. D. (1992). The state of suspended sediment in the fresh-water fluvial environment - a method of analysis. *Water Research*, 26(1), 65-72.
- Dugan, L. L., Gabrielsen, J. K., Yu, S. P., Lin, T. S., & Choi, D. W. (1996). Buckminsterfullerenol free radical scavengers reduce excitotoxic and apoptotic death of cultured cortical neurons. *Neurobiology of Disease*, 3(2), 129-135.
- El-Sayed, A. (2006). *Tilapia Culture*. Oxfordshire, UK: CABI Publishing.
- Emerick, R. W., Loge, F. J., Ginn, T., & Darby, J. L. (2000). Modeling the inactivation of particle-associated coliform bacteria. *Water Environment Research*, 72(4), 432-438.
- Emerick, R. W., Loge, F. J., Thompson, D., & Darby, J. L. (1999). Factors influencing ultraviolet disinfection performance part II: Association of coliform bacteria with wastewater particles. *Water Environment Research*, 71(6), 1178-1187.
- Farnood, R. (Ed.). (2005). *Flocs and Ultraviolet Disinfection*. Boca Raton, FL: CRC Press.
- Felber, T., Smith, E., & Knox, J. (1973). Photodynamic inactivation of herpes simplex: report of a clinical trial. *J Am Med Assoc*, 223, 289-292.
- Fletcher, M., & Marshall, K. C. (1982). Are Solid-Surfaces of Ecological Significance to Aquatic Bacteria. [Review]. *Advances in Microbial Ecology*, 6, 199-230.

- Foote, C. S. (1991). Definition of type-I and type-II photosensitized oxidation. *Photochemical & Photobiological Sciences*, 54, 659.
- Fortner, J. D., Lyon, D. Y., Sayes, C. M., Boyd, A. M., Falkner, J. C., Hotze, E. M., et al. (2005). C-60 in water: Nanocrystal formation and microbial response. *Environmental Science & Technology*, 39(11), 4307-4316.
- Grothe, D. R., & Eaton, J. W. (1975). Chlorine-induced mortality in fish. [Article]. *Transactions of the American Fisheries Society*, 104(4), 800-802.
- Grutsch, J. F. (1978). Wastewater-Treatment - Electrical Connection. *Environmental Science & Technology*, 12(9), 1022-1027.
- Guldi, D. M., & Prato, M. (2000). Excited-state properties of C-60 fullerene derivatives. [Review]. *Accounts of Chemical Research*, 33(10), 695-703.
- Gutteridge, J. M. C. (1995). Lipid-peroxidation and antioxidants as biomarkers of tissue-damage. [Proceedings Paper]. *Clinical Chemistry*, 41(12B), 1819-1828.
- Hamblin, M. R., O'Donnell, D. A., Murthy, N., Rajagopalan, K., Michaud, N., Sherwood, M. E., et al. (2002). Polycationic photosensitizer conjugates: effects of chain length and Gram classification on the photodynamic inactivation of bacteria. *J Antimicrob Chemother*, 49(6), 941-951.
- Helprin, J. J., & Hiatt, C. W. (1959). Photosensitization of coliphage-T2 with toluidine blue. *Journal of Bacteriology*, 77(4), 502-505.
- Hoffman, G. L. (1975). Whirling Disease Myxosoma-Cerebralis Control with Uv Irradiation and Effect on Fish. [Article]. *Journal of Wildlife Diseases*, 11(4), 505-507.
- Hotze, E. M., Labille, J., Alvarez, P., & Wiesner, M. R. (2008). Mechanisms of photochemistry and reactive oxygen production by fullerene suspensions in water. *Environmental Science & Technology*, 42(11), 4175-4180.
- Huber, E., & Frost, M. (1998). Light scattering by small particles. *Journal of Water Services Research and Technology-Aqua*, 47(2), 87-94.
- Hubert, J. (1992). *Bioassay* (Third ed.). Dubuque: Kendall/Hunt Publishing Company.
- Humphrey, W., Dalke, A., & Schulten, K. (1996). VMD: Visual molecular dynamics. [doi: DOI: 10.1016/0263-7855(96)00018-5]. *Journal of Molecular Graphics*, 14(1), 33-38.

- Husebo, L. O., Sitharaman, B., Furukawa, K., Kato, T., & Wilson, L. J. (2004). Fullerenols revisited as stable radical anions. *Journal of the American Chemical Society*, 126(38), 12055-12064.
- Jagger, J. (1967). *Introduction to Research in Ultraviolet Photobiology*. Englewood Cliffs, NJ: Prentice-Hall, Inc.
- Jeng, U., Lin, T., Chang, T., Lee, H., Hsu, C., Hsieh, Y., et al. (2001). Comparison of the aggregation behavior of water-soluble hexa(sulfobutyl)fullerenes and polyhydroxylated fullerenes for their free-radical scavenging activity *Trends in Colloid and Interface Science XV* (pp. 232-237).
- Jolis, D., Lam, C., & Pitt, P. (2001). Particle effects on ultraviolet disinfection of coliform bacteria in recycled water. *Water Environment Research*, 73(2), 233-236.
- Jori, G., & Brown, S. B. (2004). Photosensitized inactivation of microorganisms. *Photochem Photobiol Sci*, 3(5), 403-405.
- Jori, G., Fabris, C., Soncin, M., Ferro, S., Coppellotti, O., Dei, D., et al. (2006). Photodynamic therapy in the treatment of microbial infections: basic principles and perspective applications. *Lasers Surg Med*, 38(5), 468-481.
- Kasai, H., Yoshimizu, M., & Ezura, Y. (2001). Disinfection of Water for Aquaculture. *Fisheries Science*, 68(Supplement I), 821-824.
- Kasermann, F., & Kempf, C. (1997). Photodynamic inactivation of enveloped viruses by buckminsterfullerene. *Antiviral Res*, 34(1), 65-70.
- Kelly, C. (1974). *The Toxicity of Chlorinated Waste Effluents to Fish and Considerations of Alternative Processes for the Disinfection of Waste Effluents*.
- Krumins, V., Ebeling, J. M., & Wheaton, F. (2001). Ozone's effects on power-law particle size distribution in recirculating aquaculture systems. *Aquacultural Engineering*, 25(1), 13-24.
- Lambrechts, S. A., Aalders, M. C., & Van Marle, J. (2005). Mechanistic study of the photodynamic inactivation of *Candida albicans* by a cationic porphyrin. *Antimicrob Agents Chemother*, 49(5), 2026-2034.
- Lee, J., Mackeyev, Y., Cho, M., Li, D., Kim, J. H., Wilson, L. J., et al. (2009). Photochemical and Antimicrobial Properties of Novel C-60 Derivatives in Aqueous Systems. *Environmental Science & Technology*, 43(17), 6604-6610.

- Leonard, N., Blancheton, J. P., & Guiraud, J. P. (2000). Populations of heterotrophic bacteria in an experimental recirculating aquaculture system. *Aquacultural Engineering*, 22(1-2), 109-120.
- Li, Q., Mahendra, S., Lyon, D. Y., Brunet, L., Liga, M. V., Li, D., et al. (2008). Antimicrobial nanomaterials for water disinfection and microbial control: potential applications and implications. *Water Res*, 42(18), 4591-4602.
- Liltved, H. (2001). Ozonation and UV-Irradiation. In M. Timmons, J. Ebeling, F. Wheaton, S. Summerfelt & B. Vinci (Eds.), *Recirculating Aquaculture Systems* (pp. 351-382). North Dartmouth, MA: Northeast Regional Aquaculture Center.
- Liltved, H. (2002). *Recirculating Aquaculture Systems* (2nd ed.). Ithaca, NY: Cayuga Aqua Ventures.
- Liltved, H., & Cripps, S. J. (1999). Removal of particle-associated bacteria by prefiltration and ultraviolet irradiation. *Aquaculture Research*, 30(6), 445-450.
- Liltved, H., Hektoen, H., & Efraimsen, H. (1995). Inactivation of Bacterial and Viral Fish Pathogens by Ozonation or Uv Irradiation in Water of Different Salinity. *Aquacultural Engineering*, 14(2), 107-122.
- Liltved, H., & Landfald, B. (1996). Influence of liquid holding recovery and photoreactivation on survival of ultraviolet-irradiated fish pathogenic bacteria. *Water Research*, 30(5), 1109-1114.
- Liltved, H., & Landfald, B. (2000). Effects of high intensity light on ultraviolet-irradiated and non-irradiated fish pathogenic bacteria. *Water Research*, 34(2), 481-486.
- Liltved, H., Vogelsang, C., Modahl, I., & Dannevig, B. H. (2006). High resistance of fish pathogenic viruses to UV irradiation and ozonated seawater. *Aquacultural Engineering*, 34(2), 72-82.
- Liu, X. F., Guan, W. C., & Cheng, Z. X. (2007). Synthesis of fulleropyrrolidine carboxylic acids and their aggregation behavior in aqueous solution. *Acta Chimica Sinica*, 65(5), 430-436.
- Loge, F. J., Bourgeois, K., Emerick, R. W., & Darby, J. L. (2001). Variations in wastewater quality parameters influencing UV disinfection performance: Relative impact of filtration. *Journal of Environmental Engineering-Asce*, 127(9), 832-837.
- Loge, F. J., Emerick, R. W., Heath, M., Jacangelo, J., Tchobanoglous, G., & Darby, J. L. (1996). Ultraviolet disinfection of secondary wastewater effluents: Prediction

- of performance and design. [Article]. *Water Environment Research*, 68(5), 900-916.
- Losordo, T., Masser, M., & Rakocy, J. (1999). Recirculating Aquaculture Tank Production Systems: A Review of Component Options. *Southern Regional Aquaculture Center, Publication No. 453*.
- Lu, C.-Y., Yao, S.-D., Lin, W.-Z., Wang, W.-F., Lin, N.-Y., Tong, Y.-P., et al. (1998). Studies on the fullerol of C60 in aqueous solution with laser photolysis and pulse radiolysis. *Radiation Physics and Chemistry*, 53(2), 137-143.
- Lyon, D. Y., Fortner, J. D., Sayes, C. M., Colvin, V. L., & Hughe, J. B. (2005). Bacterial cell association and antimicrobial activity of a C60 water suspension. *Environ Toxicol Chem*, 24(11), 2757-2762.
- Maisch, T., Baier, J., Franz, B., Maier, M., Landthaler, M., Szeimies, R. M., et al. (2007). The role of singlet oxygen and oxygen concentration in photodynamic inactivation of bacteria. [Article]. *Proceedings of the National Academy of Sciences of the United States of America*, 104(17), 7223-7228.
- Malik, Z., Hanania, J., & Nitzan, Y. (1990). Bactericidal effects of photoactivated porphyrins--an alternative approach to antimicrobial drugs. *J Photochem Photobiol B*, 5(3-4), 281-293.
- Malik, Z., Ladan, H., & Nitzan, Y. (1992). Photodynamic inactivation of Gram-negative bacteria: problems and possible solutions. *J Photochem Photobiol B*, 14(3), 262-266.
- Malvern. (2005). Zetasizer Nano User Manual, MAN0317, Issue 2.2: Malvern Instruments Ltd.
- Mamane, H., Ducoste, J. J., & Linden, K. G. (2006). Effect of particles on ultraviolet light penetration in natural and engineered systems. *Applied Optics*, 45(8), 1844-1856.
- Mamane, H., Kohn, C., & Adin, A. (2008). *Characterizing shape of effluent particles by image analysis*.
- Mamane, H., & Linden, K. G. (2006). Impact of particle aggregated microbes un UV disinfection. II: Proper absorbance measurement for UV fluence. *Journal of Environmental Engineering-Asce*, 132(6), 607-615.
- Markovic, Z., & Trajkovic, V. (2008). Biomedical potential of the reactive oxygen species generation and quenching by fullerenes (C60). *Biomaterials*, 29(26), 3561-3573.

- Mashino, T., Nishikawa, D., Takahashi, K., Usui, N., Yamori, T., Seki, M., et al. (2003). Antibacterial and antiproliferative activity of cationic fullerene derivatives. *Bioorg Med Chem Lett*, 13(24), 4395-4397.
- Mashino, T., Usui, N., Okuda, K., Hirota, T., & Mochizuki, M. (2003). Respiratory chain inhibition by fullerene derivatives: hydrogen peroxide production caused by fullerene derivatives and a respiratory chain system. *Bioorg Med Chem*, 11(7), 1433-1438.
- Merchat, M., Bertolini, G., Giacomini, P., Villanueva, A., & Jori, G. (1996). Meso-substituted cationic porphyrins as efficient photosensitizers of gram-positive and gram-negative bacteria. *J Photochem Photobiol B*, 32(3), 153-157.
- Merchat, M., Spikes, J. D., Bertolini, G., & Jori, G. (1996). Studies on the mechanism of bacteria photosensitization by meso-substituted cationic porphyrins. *J Photochem Photobiol B*, 35(3), 149-157.
- Minnock, A., Vernon, D. I., Schofield, J., Griffiths, J., Parish, J. H., & Brown, S. T. (1996). Photoinactivation of bacteria. Use of a cationic water-soluble zinc phthalocyanine to photoinactivate both gram-negative and gram-positive bacteria. *J Photochem Photobiol B*, 32(3), 159-164.
- Mishchenko, M., Travis, L., & Lacin, A. (2002). *Scattering, Absorption and Emission of Light by Small Particles*. Cambridge, UK: Cambridge University Press.
- Moan, J. (1986). Porphyrin photosensitization and phototherapy. *Photochem Photobiol*, 43(6), 681-690.
- Moan, J., & Berg, K. (1991). The photodegradation of porphyrins in cells can be used to estimate the lifetime of singlet oxygen. *Photochem Photobiol*, 53(4), 549-553.
- Moan, J., Berg, K., Kvam, E., Western, A., Malik, Z., Ruck, A., et al. (1989). Intracellular localization of photosensitizers. *Ciba Found Symp*, 146, 95-107; discussion 107-111.
- Mohan, H., Palit, D. K., Mittal, J. P., Chiang, L. Y., Asmus, K. D., & Guldi, D. M. (1998). Excited states and electron transfer reactions of C-60(OH)(18) in aqueous solution. [Article]. *Journal of the Chemical Society-Faraday Transactions*, 94(3), 359-363.
- Mroz, P., Tegos, G. P., Gali, H., Wharton, T., Sarna, T., & Hamblin, M. R. (2007). Photodynamic therapy with fullerenes. [Article]. *Photochemical & Photobiological Sciences*, 6(11), 1139-1149.

- Murthy, C. N., & Geckeler, K. E. (2001). Solubility correlation of 60 fullerene in different solvents. *Fullerene Science and Technology*, 9(4), 477-486.
- Nakamura, E., & Isobe, H. (2003). Functionalized fullerenes in water. The first 10 years of their chemistry, biology, and nanoscience. *Acc Chem Res*, 36(11), 807-815.
- Nitzan, Y., Gutterman, M., Malik, Z., & Ehrenberg, B. (1992). Inactivation of gram-negative bacteria by photosensitized porphyrins. *Photochem Photobiol*, 55(1), 89-96.
- Oliver, B. G., & Cosgrove, E. G. (1975). Disinfection of Sewage-Treatment Plant Effluents Using Ultraviolet-Light. *Canadian Journal of Chemical Engineering*, 53(2), 170-174.
- Oye, A. K., & Rimstad, E. (2001). Inactivation of infectious salmon anaemia virus, viral haemorrhagic septicaemia virus and infectious pancreatic necrosis virus in water using UVC irradiation. *Diseases of Aquatic Organisms*, 48(1), 1-5.
- Perdrau, J. R., & Todd, C. (1933). Canine distemper: The high antigenic value of the virus after photodynamic inactivation by methylene blue. *Jour Comp Path and Therap*, 46((2)), 78-89.
- Pfeifer, G. P., You, Y. H., & Besaratinia, A. (2005). Mutations induced by ultraviolet light. *Mutation Research-Fundamental and Molecular Mechanisms of Mutagenesis*, 571(1-2), 19-31.
- Phillips, G., & Hanel, E. (1960). *Use of Ultraviolet Radiation in Microbiological Laboratories*. US Army Chemical Corps, Biological Laboratories, Fort Detrick, MD.
- Pickering, K. D., & Wiesner, M. R. (2005). Fullerol-sensitized production of reactive oxygen species in aqueous solution. *Environ Sci Technol*, 39(5), 1359-1365.
- Pradeep, T. (1997). A glimpse into the fascinating world of fullerenes. [Review]. *Current Science*, 72(2), 124-136.
- Pu, Z., Shuang, L., & Guo, Z. X. (2008). Aggregation behavior of amphiphilic C-60 derivatives in aqueous solution. *Progress in Chemistry*, 20(4), 548-557.
- Qualls, R. G., Flynn, M. P., & Johnson, J. D. (1983). The Role of Suspended Particles in Ultraviolet Disinfection. *Journal Water Pollution Control Federation*, 55(10), 1280-1285.
- Qualls, R. G., & Johnson, J. D. (1985). Modeling and efficiency of ultraviolet disinfection systems. [Article]. *Water Research*, 19(8), 1039-1046.

- Qualls, R. G., Ossoff, S. F., Chang, J. C. H., Dorfman, M. H., Dumais, C. M., Lobe, D. C., et al. (1985). Factors Controlling Sensitivity in Ultraviolet Disinfection of Secondary Effluents. *Journal Water Pollution Control Federation*, 57(10), 1006-1011.
- Ravacha, C., Kummel, M., Salamon, I., & Adin, A. (1995). The Effect of Chemical Oxidants on Effluent Constituents for Drip Irrigation. *Water Research*, 29(1), 119-129.
- Reddi, E., Ceccon, M., Valduga, G., Jori, G., Bommer, J. C., Elisei, F., et al. (2002). Photophysical properties and antibacterial activity of meso-substituted cationic porphyrins. *Photochem Photobiol*, 75(5), 462-470.
- Rijnaarts, H. H. M., Norde, W., Lyklema, J., & Zehnder, A. J. B. (1995). The isoelectric point of bacteria as an indicator for the presence of cell-surface polymers that inhibit adhesion. *Colloids and Surfaces B-Biointerfaces*, 4(4), 191-197.
- Ruoff, R. S., Tse, D. S., Malhotra, R., & Lorents, D. C. (1993). Solubility of fullerene (C60) in a variety of solvents (Vol. 97, pp. 3379-3383).
- Scheible, O. K. (1987). Development of a rationally based design protocol for the ultraviolet-light disinfection process. [Article]. *Journal Water Pollution Control Federation*, 59(1), 25-31.
- Schinazi, R. F., Sijbesma, R., Srdanov, G., Hill, C. L., & Wudl, F. (1993). Synthesis and virucidal activity of a water-soluble, configurationally stable, derivatized C60 fullerene. *Antimicrob Agents Chemother*, 37(8), 1707-1710.
- Schultz, E., & Krueger, A. (1928). Inactivation of Staphylococcus bacteriophage by methylene blue. *Proc Soc Exp Biol Med*, 26, 100-101.
- Sharrer, M. J., & Summerfelt, S. T. (2007). Ozonation followed by ultraviolet irradiation provides effective bacteria inactivation in a freshwater recirculating system. [Article]. *Aquacultural Engineering*, 37(2), 180-191.
- Sharrer, M. J., Summerfelt, S. T., Bullock, G. L., Gleason, L. E., & Taeuber, J. (2005). Inactivation of bacteria using ultraviolet irradiation in a recirculating salmonid culture system. *Aquacultural Engineering*, 33(2), 135-149.
- Shinohara, H. (2000). Endohedral metallofullerenes. [Review]. *Reports on Progress in Physics*, 63(6), 843-892.
- Sproul, O. (1979). *Effect of Particulates on Ozone Disinfection of Bacteria and Viruses in Water*.

- Ströck, M. (2006). 3D model of a C60 molecule, *iMol for Mac OS X and Photoshop CS2*: Wikipedia.
- Summerfelt, S. T. (2003). Ozonation and UV irradiation - an introduction and examples of current applications. *Aquacultural Engineering*, 28(1-2), 21-36.
- Summerfelt, S. T., Hankins, J. A., Weber, A. L., & Durant, M. D. (1997). Ozonation of a recirculating rainbow trout culture system - II. Effects on microscreen filtration and water quality. *Aquaculture*, 158(1-2), 57-67.
- Summerfelt, S. T., & Hochheimer, J. N. (1997). Review of ozone processes and applications as an oxidizing agent in aquaculture. *Progressive Fish-Culturist*, 59(2), 94-105.
- Summerfelt, S. T., Sharrer, M. J., Tsukuda, S. M., & Gearheart, M. (2009). Process requirements for achieving full-flow disinfection of recirculating water using ozonation and UV irradiation. *Aquacultural Engineering*, 40(1), 17-27.
- Tang, Y. J., Ashcroft, J. M., Chen, D., Min, G., Kim, C. H., Murkhejee, B., et al. (2007). Charge-associated effects of fullerene derivatives on microbial structural integrity and central metabolism. *Nano Lett*, 7(3), 754-760.
- Tang, Y. J. J., Ashcroft, J. M., Chen, D., Min, G. W., Kim, C. H., Murkhejee, B., et al. (2007). Charge-associated effects of fullerene derivatives on microbial structural integrity and central metabolism. *Nano Letters*, 7(3), 754-760.
- Tegos, G. P., Demidova, T. N., Arcila-Lopez, D., Lee, H., Wharton, T., Gali, H., et al. (2005). Cationic fullerenes are effective and selective antimicrobial photosensitizers. *Chem Biol*, 12(10), 1127-1135.
- Teorell, T. (1931). Photometric measurement on the concentration and dispersity in colloid solutions III. [Article]. *Kolloid-Zeitschrift*, 54(2), 150-156.
- Timmons, M., Ebeling, J., Wheaton, F., Summerfelt, S., & Vinci, B. (2002). *Recirculating Aquaculture Systems* (2nd ed.). Ithaca, NY: Cayuga Aqua Ventures.
- Tobiason, J. E., Edzwald, J. K., Reckhow, D. A., & Switzenbaum, M. S. (1993). Effect of Pre-Ozonation on Organics Removal by in-Line Direct-Filtration. *Water Science and Technology*, 27(11), 81-90.
- Tree, J. A., Adams, M. R., & Lees, D. N. (2003). Chlorination of indicator bacteria and viruses in primary sewage effluent. *Applied and Environmental Microbiology*, 69(4), 2038-2043.

- Tsao, N., Luh, T. Y., Chou, C. K., Chang, T. Y., Wu, J. J., Liu, C. C., et al. (2002). In vitro action of carboxyfullerene. *J Antimicrob Chemother*, 49(4), 641-649.
- van Regenmortel, M. (Ed.). (2000). *Virus Taxonomy* (7 ed.). San Diego, CA: Academic Press.
- Vileno, B., Marcoux, P., Lekka, M., Sienkiewicz, A., Fehér, T., & Forró, L. (2006). Spectroscopic and Photophysical Properties of a Highly Derivatized C60 Fullerol (Vol. 16, pp. 120-128).
- Villanueva, A. (1993). The cationic meso-substituted porphyrins: an interesting group of photosensitizers. *J Photochem Photobiol B*, 18(2-3), 295-296.
- Vonbrodorotti, H. S., & Mahnel, H. (1982). Comparative studies on susceptibility of viruses to ultraviolet rays. [Article]. *Zentralblatt Fur Veterinarmedizin Reihe B- Journal of Veterinary Medicine Series B-Infectious Diseases Immunology Food Hygiene Veterinary Public Health*, 29(2), 129-136.
- Vroegop, S. M., Decker, D. E., & Buxser, S. E. (1995). Localization of damage-induced by reactive oxygen species in cultured-cells. *Free Radical Biology and Medicine*, 18(2), 141-151.
- Wainwright, M. (1998). Photodynamic antimicrobial chemotherapy (PACT). *J Antimicrob Chemother*, 42(1), 13-28.
- Wainwright, M. (2003). Local treatment of viral disease using photodynamic therapy. *Int J Antimicrob Agents*, 21(6), 510-520.
- Wainwright, M. (2004). Photoinactivation of viruses. *Photochem Photobiol Sci*, 3(5), 406-411.
- Wallis, C., & Melnick, J. L. (1963). Photodynamic inactivation of poliovirus. *Virology*, 21(3), 332-&.
- Watson, H. (1908). A Note on the Variation of the Rate of Disinfection with Change in the Concentration of the Disinfectant. *The Journal of Hygiene*, 8(4), 536-542.
- Wedemeyer, G. (1996). *Physiology of Fish in Intensive Culture Systems*. New York, NY: International Thompson Publishing.
- Welsh, J. N., & Adams, M. H. (1954). Photodynamic inactivation of bacteriophage. *Journal of Bacteriology*, 68(1), 122-127.
- Wheaton, F. W. (1993). *Aquacultural Engineering*. New York: Wiley.

- White, G. (1999).** *Handbook of chlorination and alternative disinfectants*. New York, NY: John Wiley & Sons, Inc.
- Wu, Y. X., Clevenger, T., & Deng, B. (2005).** Impacts of goethite particles on UV disinfection of drinking water. *Applied and Environmental Microbiology*, 71(7), 4140-4143.
- Yamamoto, N. (1958).** Photodynamic inactivation of bacteriophage and its inhibition. *Journal of Bacteriology*, 75(4), 443-448.
- You, Y. W., Rankin, S. C., Aceto, H. W., Benson, C. E., Toth, J. D., & Dou, Z. X. (2006).** Survival of *Salmonella enterica* serovar Newport in manure and manure-amended soils. [Article]. *Applied and Environmental Microbiology*, 72(9), 5777-5783.
- Zhao, Q., Li, Y., Xu, J., Liu, R., & Li, W. (2005).** Radioprotection by fullerenols of *Stylynychia mytilus* exposed to gamma-rays. *International Journal of Radiation Biology*, 81(2), 169-175.

PART V: APPENDICES

APPENDIX A

Raw data for bacterial exposures

Table A-1: Raw data for *Bacillus subtilis* viability versus fullerol concentration.

Fullerol (mg/L)	Irradiation	CFU Count	Dilution (10^x)	CFU/mL	Log₁₀ CFU/mL
0	-	54	-3	5.40E+05	5.73
0	-	179	-3	1.79E+06	6.25
0	-	82	-3	8.20E+05	5.91
0	+	0	0	0.00E+00	.
0	+	0	0	0.00E+00	.
0	+	0	0	0.00E+00	.
50	-	65	-3	6.50E+05	5.81
50	-	58	-3	5.80E+05	5.76
50	-	144	-3	1.44E+06	6.16
50	+	0	0	0.00E+00	.
50	+	0	0	0.00E+00	.
50	+	0	0	0.00E+00	.
100	-	73	-3	7.30E+05	5.86
100	-	66	-3	6.60E+05	5.82
100	-	89	-3	8.90E+05	5.95
100	+	241	-1	2.41E+04	4.38
100	+	279	-1	2.79E+04	4.45
100	+	251	-1	2.51E+04	4.40
200	-	61	-3	6.10E+05	5.79
200	-	132	-3	1.32E+06	6.12
200	-	212	-3	2.12E+06	6.33
200	+	78	-3	7.80E+05	5.89
200	+	80	-3	8.00E+05	5.90
200	+	77	-3	7.70E+05	5.89
250	-	97	-3	9.70E+05	5.99
250	-	151	-3	1.51E+06	6.18
250	-	170	-3	1.70E+06	6.23
250	+	102	-3	1.02E+06	6.01
250	+	48	-3	4.80E+05	5.68
250	+	94	-3	9.40E+05	5.97

Table A-2: Raw data for *Escherichia coli* (K12) viability versus fullerol concentration.

Fullerol (mg/L)	Irradiation	CFU Count	Dilution		Log ₁₀ CFU/mL
			(10 ^x)	CFU/mL	
0	-	83	-3	8.30E+05	5.92
0	-	121	-3	1.21E+06	6.08
0	-	129	-3	1.29E+06	6.11
0	+	2	-1	2.00E+02	2.30
0	+	2	-1	2.00E+02	2.30
0	+	3	-1	3.00E+02	2.48
50	-	92	-3	9.20E+05	5.96
50	-	171	-3	1.71E+06	6.23
50	-	166	-3	1.66E+06	6.22
50	+	172	-1	1.72E+04	4.24
50	+	193	-1	1.93E+04	4.29
50	+	167	-1	1.67E+04	4.22
100	-	134	-3	1.34E+06	6.13
100	-	143	-3	1.43E+06	6.16
100	-	164	-3	1.64E+06	6.21
100	+	170	-2	1.70E+05	5.23
100	+	203	-2	2.03E+05	5.31
100	+	187	-2	1.87E+05	5.27
200	-	38	-3	3.80E+05	5.58
200	-	114	-3	1.14E+06	6.06
200	-	136	-3	1.36E+06	6.13
200	+	492	-2	4.92E+05	5.69
200	+	696	-2	6.96E+05	5.84
200	+	39	-3	3.90E+05	5.59
200	+	46	-3	4.60E+05	5.66
200	+	75	-3	7.50E+05	5.88
250	-	107	-3	1.07E+06	6.03
250	-	118	-3	1.18E+06	6.07
250	-	121	-3	1.21E+06	6.08
250	+	38	-3	3.80E+05	5.58
250	+	78	-3	7.80E+05	5.89
250	+	63	-3	6.30E+05	5.80

Table A-3: Raw data for *Salmonella enterica* serotype Newport viability versus fullerol concentration.

Fullerol (mg/L)	Irradiation	CFU Count	Dilution (10^x)	CFU/mL	Log₁₀ CFU/mL
0	-	191	-3	1.91E+06	6.28
0	-	177	-3	1.77E+06	6.25
0	-	207	-3	2.07E+06	6.32
0	+	0	0	0.00E+00	.
0	+	0	0	0.00E+00	.
0	+	0	0	0.00E+00	.
50	-	217	-3	2.17E+06	6.34
50	+	10	-1	1.00E+03	3.00
50	+	4	-1	4.00E+02	2.60
50	+	5	-1	5.00E+02	2.70
50	+	1	-2	1.00E+03	3.00
50	+	2	-2	2.00E+03	3.30
50	+	1	-2	1.00E+03	3.00
100	-	198	-3	1.98E+06	6.30
100	-	195	-3	1.95E+06	6.29
100	-	166	-3	1.66E+06	6.22
100	+	33	-2	3.30E+04	4.52
100	+	30	-2	3.00E+04	4.48
100	+	34	-2	3.40E+04	4.53
200	-	137	-3	1.37E+06	6.14
200	-	183	-3	1.83E+06	6.26
200	-	189	-3	1.89E+06	6.28
200	+	58	-3	5.80E+05	5.76
200	+	49	-3	4.90E+05	5.69
200	+	66	-3	6.60E+05	5.82
250	-	226	-3	2.26E+06	6.35
250	-	182	-3	1.82E+06	6.26
250	-	252	-3	2.52E+06	6.40
250	+	82	-3	8.20E+05	5.91
250	+	89	-3	8.90E+05	5.95
250	+	98	-3	9.80E+05	5.99

Table A-4: Raw data for *Vibrio parahaemolyticus* viability versus fullerol concentration.

Fullerol (mg/L)	Irradiation	CFU Count	Dilution (10^x)	CFU/mL	Log₁₀ CFU/mL
0	-	217	-4	2.17E+07	7.34
0	-	196	-4	1.96E+07	7.29
0	-	207	-4	2.07E+07	7.32
0	+	0	0	0.00E+00	.
0	+	0	0	0.00E+00	.
0	+	0	0	0.00E+00	.
50	-	215	-4	2.15E+07	7.33
50	-	218	-4	2.18E+07	7.34
50	-	237	-4	2.37E+07	7.37
50	+	0	0	0.00E+00	.
50	+	0	0	0.00E+00	.
50	+	0	0	0.00E+00	.
100	-	236	-4	2.36E+07	7.37
100	-	272	-4	2.72E+07	7.43
100	-	272	-4	2.72E+07	7.43
100	+	0	0	0.00E+00	.
100	+	0	0	0.00E+00	.
100	+	0	0	0.00E+00	.
200	-	235	-4	2.35E+07	7.37
200	-	202	-4	2.02E+07	7.31
200	-	283	-4	2.83E+07	7.45
200	+	244	-2	2.44E+05	5.39
200	+	227	-2	2.27E+05	5.36
200	+	251	-2	2.51E+05	5.40
250	-	200	-4	2.00E+07	7.30
250	-	268	-4	2.68E+07	7.43
250	-	245	-4	2.45E+07	7.39
250	+	520	-2	5.20E+05	5.72
250	+	560	-2	5.60E+05	5.75
250	+	452	-2	4.52E+05	5.66

Table A-5: Raw data for relative bacterial sensitivity to ultraviolet irradiation

Fullerol (mg/L)	Irradiation	CFU Count	Dilution (10^x)	CFU/mL	Log₁₀ CFU/mL
Bs	-	296	0	2.96E+03	3.47
Bs	-	320	0	3.20E+03	3.51
Bs	-	328	0	3.28E+03	3.52
Bs	+	6	0	6.00E+01	1.78
Bs	+	5	0	5.00E+01	1.70
Bs	+	3	0	3.00E+01	1.48
Ec	-	456	-2	4.56E+05	5.66
Ec	-	452	-2	4.52E+05	5.66
Ec	-	400	-2	4.00E+05	5.60
Ec	+	520	0	5.20E+03	3.72
Ec	+	518	0	5.18E+03	3.71
Ec	+	540	0	5.40E+03	3.73
Se	-	924	-2	9.24E+05	5.97
Se	-	964	-2	9.64E+05	5.98
Se	-	1060	-2	1.06E+06	6.03
Se	+	99	-1	9.90E+03	4.00
Se	+	91	-1	9.10E+03	3.96
Se	+	108	-1	1.08E+04	4.03
Vp	-	460	-2	4.60E+05	5.66
Vp	-	568	-2	5.68E+05	5.75
Vp	-	472	-2	4.72E+05	5.67
Vp	+	0	0	0	0
Vp	+	0	0	0	0
Vp	+	0	0	0	0

APPENDIX B

Raw data and Spearman-Kärber estimators of TCID50/mL for viral exposures

Table B-1: Raw data and statistics for Spring Viremia of Carp Virus (SVCV) TCID50 assay.

Fullerol (mg/L)	Irradiation	Log10 TCID50/mL	Log ₁₀ SE	95% LCL Log ₁₀ TCID50/mL	95% UCL Log ₁₀ TCID50/mL	Counts of Wells Per Dilution Containing Cytopathic Effects							
						10 ⁻¹	10 ⁻²	10 ⁻³	10 ⁻⁴	10 ⁻⁵	10 ⁻⁶	10 ⁻⁷	10 ⁻⁸
0	+	4.9000	0.2449	4.6551	5.1449	5	5	5	2	0	0	0	0
50	+	4.5000	0.2828	4.2172	4.7828	5	5	4	1	0	0	0	0
100	+	4.9000	0.2449	4.6551	5.1449	5	5	5	2	0	0	0	0
200	+	5.3000	0.2000	5.1000	5.5000	5	5	5	4	0	0	0	0
250	+	6.1000	0.3162	5.7838	6.4162	5	5	5	5	2	1	0	0
0	-	6.3000	0.2000	6.1000	6.5000	5	5	5	5	4	0	0	0
50	-	6.1000	0.2449	5.8551	6.3449	5	5	5	5	3	0	0	0
100	-	6.3000	0.2000	6.1000	6.5000	5	5	5	5	4	0	0	0
200	-	6.3000	0.2000	6.1000	6.5000	5	5	5	5	4	0	0	0
250	-	6.3000	0.3162	5.9838	6.6162	5	5	5	5	3	1	0	0

LCL = Lower Confidence Limit **UCL = Upper Confidence Limit**

APPENDIX C

Raw data for SEM images of fullerol aggregate size and shape analysis

Table C-1: Quantitative SEM size and shape analysis data.

Treatment	Area (μm^2)	Perimeter (μm)	Circularity	Equivalent Circular Diameter (μm)
S31	0.015	0.565	0.590	0.138
S31	0.231	3.527	0.233	0.542
S31	0.238	3.040	0.324	0.550
S31	0.029	0.795	0.577	0.192
S31	0.070	1.590	0.348	0.299
S31	0.059	1.453	0.351	0.274
S31	0.062	1.174	0.565	0.281
S31	0.065	1.180	0.587	0.288
S31	0.001	0.124	0.817	0.036
S31	0.010	0.397	0.797	0.113
S31	0.002	0.199	0.635	0.050
S31	0.012	0.578	0.451	0.124
S31	0.056	2.148	0.153	0.267
S31	0.079	2.137	0.217	0.317
S31	0.303	3.061	0.406	0.621
S31	0.001	0.186	0.363	0.036
S31	0.060	1.466	0.351	0.276
S31	0.015	0.857	0.257	0.138
S31	0.252	3.105	0.328	0.566
S31	0.032	1.105	0.329	0.202
S31	0.045	1.471	0.261	0.239
S31	0.046	1.112	0.467	0.242
S31	0.001	0.155	0.523	0.036
S31	0.027	1.043	0.312	0.185
S31	0.025	0.950	0.348	0.178
S31	0.030	0.901	0.464	0.195
S31	0.003	0.317	0.375	0.062
S31	0.055	1.559	0.284	0.265
S31	0.259	3.038	0.353	0.574
S31	0.017	0.875	0.279	0.147
S31	0.075	1.719	0.319	0.309
S31	0.032	0.839	0.571	0.202

S31	0.020	0.968	0.268	0.160
S31	0.019	0.578	0.715	0.156
S31	0.261	2.751	0.433	0.576
S31	0.054	1.384	0.354	0.262
S31	0.064	1.280	0.491	0.285
S31	0.012	0.707	0.302	0.124
S31	0.026	0.932	0.376	0.182
S31	0.009	0.459	0.537	0.107
S31	0.003	0.268	0.525	0.062
S31	0.001	0.150	0.559	0.036
S31	0.065	1.241	0.530	0.288
S31	0.012	0.596	0.425	0.124
S31	0.018	0.689	0.476	0.151
S31	0.044	1.156	0.414	0.237
S31	0.251	3.105	0.327	0.565
S31	0.050	1.156	0.470	0.252
S31	0.001	0.124	0.817	0.036
S31	0.020	0.906	0.306	0.160
S31	0.073	1.763	0.295	0.305
S31	0.002	0.261	0.369	0.050
S31	0.221	2.955	0.318	0.530
S31	0.002	0.168	0.890	0.050
S31	0.013	0.516	0.614	0.129
S31	0.022	0.694	0.574	0.167
S31	0.002	0.186	0.726	0.050
S31	0.239	2.932	0.349	0.552
S31	0.041	1.211	0.351	0.228
S31	0.001	0.168	0.445	0.036
S31	0.075	1.789	0.294	0.309
S31	0.013	0.534	0.573	0.129
S31	0.075	1.455	0.445	0.309
S31	0.357	5.486	0.149	0.674
S31	0.052	1.211	0.446	0.257
S31	0.279	2.957	0.401	0.596
S31	0.029	0.707	0.729	0.192
S31	0.375	5.809	0.140	0.691
S31	0.215	3.502	0.220	0.523
S31	0.030	1.068	0.331	0.195
S31	0.001	0.168	0.445	0.036
S31	0.308	3.399	0.335	0.626
S31	0.001	0.124	0.817	0.036
S31	0.001	0.155	0.523	0.036
S31	0.067	1.615	0.323	0.292
S31	0.049	1.138	0.475	0.250
S31	0.146	2.312	0.343	0.431

S31	0.001	0.124	0.817	0.036
S31	0.106	1.814	0.405	0.367
S31	0.001	0.124	0.817	0.036
S31	0.232	2.986	0.327	0.543
S31	0.010	0.632	0.315	0.113
S31	0.036	0.957	0.494	0.214
S31	0.020	0.777	0.416	0.160
S31	0.001	0.124	0.817	0.036
S31	0.284	3.843	0.242	0.601
S31	0.071	1.752	0.291	0.301
S31	0.037	1.074	0.403	0.217
S31	0.080	1.156	0.752	0.319
S31	0.130	2.173	0.346	0.407
S31	0.074	1.440	0.448	0.307
S31	0.001	0.168	0.445	0.036
S31	0.259	2.976	0.367	0.574
S31	0.002	0.168	0.890	0.050
S31	0.054	1.303	0.400	0.262
S31	0.005	0.354	0.501	0.080
S31	0.001	0.137	0.670	0.036
S31	0.031	1.081	0.333	0.199
S31	0.001	0.155	0.523	0.036
S31	0.062	1.223	0.521	0.281
S31	0.302	3.740	0.271	0.620
S31	0.001	0.168	0.445	0.036
S31	0.026	1.068	0.286	0.182
S31	0.294	3.298	0.340	0.612
S31	0.075	1.520	0.408	0.309
S31	0.039	0.970	0.521	0.223
S31	0.016	0.689	0.424	0.143
S31	0.001	0.168	0.445	0.036
S31	0.023	0.733	0.538	0.171
S31	0.002	0.212	0.559	0.050
S31	0.030	1.019	0.363	0.195
S31	0.001	0.155	0.523	0.036
S31	0.041	1.161	0.382	0.228
S31	0.064	1.223	0.538	0.285
S31	0.026	0.950	0.362	0.182
S31	0.002	0.230	0.475	0.050
S31	0.047	0.877	0.768	0.245
S31	0.001	0.168	0.445	0.036
S31	0.006	0.540	0.259	0.087
S31	0.012	0.596	0.425	0.124
S31	0.048	1.130	0.472	0.247
S31	0.001	0.168	0.445	0.036

S31	0.007	0.397	0.558	0.094
S31	0.019	1.180	0.171	0.156
S31	0.001	0.124	0.817	0.036
S31	0.002	0.168	0.890	0.050
S31	0.003	0.217	0.801	0.062
S31	0.001	0.124	0.817	0.036
S31	0.003	0.199	0.952	0.062
S31	0.006	0.335	0.672	0.087
S31	0.011	0.534	0.485	0.118
S31	0.152	2.108	0.430	0.440
S31	0.082	1.605	0.400	0.323
S31	0.003	0.305	0.405	0.062
S31	0.270	3.344	0.303	0.586
S31	0.001	0.168	0.445	0.036
S31	0.001	0.186	0.363	0.036
S31	0.006	0.428	0.412	0.087
S31	0.001	0.124	0.817	0.036
S31	0.065	1.293	0.489	0.288
S31	0.001	0.168	0.445	0.036
S31	0.046	1.200	0.401	0.242
S31	0.040	0.926	0.586	0.226
S31	0.002	0.243	0.426	0.050
S31	0.007	0.627	0.224	0.094
S31	0.002	0.186	0.726	0.050
S31	0.035	0.779	0.725	0.211
S31	0.001	0.124	0.817	0.036
S31	0.002	0.186	0.726	0.050
S31	0.016	0.802	0.313	0.143
S31	0.001	0.168	0.445	0.036
S31	0.004	0.292	0.590	0.071
S31	0.487	5.578	0.197	0.787
S31	0.004	0.403	0.309	0.071
S31	0.025	1.180	0.226	0.178
S31	0.023	1.105	0.237	0.171
S31	0.346	4.858	0.184	0.664
S31	0.309	3.409	0.334	0.627
S31	0.258	3.234	0.310	0.573
S31	0.247	3.678	0.229	0.561
S31	0.252	3.229	0.304	0.566
S31	0.376	5.933	0.134	0.692
S31	0.021	1.082	0.225	0.164
S31	0.236	3.409	0.255	0.548
S31	0.102	2.292	0.244	0.360
S31	0.013	0.888	0.207	0.129
S31	0.007	0.552	0.289	0.094

S31	0.224	3.510	0.228	0.534
S31	0.395	4.467	0.249	0.709
S31	0.494	6.925	0.129	0.793
S31	0.112	3.492	0.115	0.378
S31	0.343	5.428	0.146	0.661
S31	0.298	3.231	0.359	0.616
S31	0.056	1.652	0.258	0.267
S31	0.049	1.678	0.219	0.250
S31	0.349	3.818	0.301	0.667
U125	0.126	2.918	0.186	0.401
U125	0.017	0.640	0.522	0.147
U125	0.097	1.989	0.308	0.351
U125	0.015	0.467	0.864	0.138
U125	0.153	3.705	0.140	0.441
U125	0.147	2.823	0.232	0.433
U125	0.056	1.295	0.420	0.267
U125	0.076	1.430	0.467	0.311
U125	0.018	0.883	0.290	0.151
U125	0.148	3.115	0.192	0.434
U125	0.001	0.124	0.817	0.036
U125	0.042	1.138	0.408	0.231
U125	0.001	0.150	0.559	0.036
U125	0.045	1.437	0.274	0.239
U125	0.059	1.814	0.225	0.274
U125	0.043	1.174	0.392	0.234
U125	0.024	0.764	0.517	0.175
U125	0.038	0.926	0.557	0.220
U125	0.023	0.635	0.717	0.171
U125	0.010	0.503	0.497	0.113
U125	0.063	1.559	0.326	0.283
U125	0.108	2.361	0.243	0.371
U125	0.076	1.373	0.507	0.311
U125	0.071	1.778	0.282	0.301
U125	0.061	1.218	0.517	0.279
U125	0.011	0.459	0.656	0.118
U125	0.001	0.124	0.817	0.036
U125	0.001	0.150	0.559	0.036
U125	0.034	0.813	0.646	0.208
U125	0.039	1.311	0.285	0.223
U125	0.097	2.175	0.258	0.351
U125	0.119	2.367	0.267	0.389
U125	0.052	1.130	0.512	0.257
U125	0.075	1.504	0.417	0.309
U125	0.057	1.368	0.383	0.269
U125	0.220	4.493	0.137	0.529

U125	0.115	2.609	0.212	0.383
U125	0.143	3.558	0.142	0.427
U125	0.102	3.654	0.096	0.360
U125	0.106	2.658	0.189	0.367
U125	0.078	2.217	0.199	0.315
U125	0.087	2.571	0.165	0.333
U125	0.058	1.430	0.356	0.272
U125	0.071	2.320	0.166	0.301
U125	0.034	1.274	0.263	0.208
U125	0.086	3.126	0.111	0.331
U125	0.015	0.648	0.449	0.138
U125	0.103	2.859	0.158	0.362
U125	0.069	2.212	0.177	0.296
U125	0.100	2.498	0.201	0.357
U125	0.044	1.255	0.351	0.237
U125	0.067	1.531	0.359	0.292
U125	0.043	1.194	0.379	0.234
U125	0.007	0.467	0.403	0.094
U250	10.011	14.227	0.622	3.570
U250	30.034	40.245	0.233	6.184
U250	17.841	19.945	0.564	4.766
U250	4.012	9.462	0.563	2.260
U250	26.606	51.258	0.127	5.820
U250	4.012	8.673	0.670	2.260
U250	0.312	2.069	0.916	0.630
U250	58.782	61.848	0.193	8.651
U250	15.465	42.286	0.109	4.437
U250	8.414	19.040	0.292	3.273
U250	19.516	28.378	0.305	4.985
U250	0.234	2.069	0.687	0.546
U250	5.454	11.484	0.520	2.635
U250	4.363	7.903	0.878	2.357
U250	4.791	16.412	0.224	2.470
U250	6.350	9.972	0.802	2.843
U250	1.714	5.092	0.831	1.477
U250	6.311	10.531	0.715	2.835
U250	0.195	1.675	0.873	0.498
U250	5.570	12.668	0.436	2.663
U250	0.156	1.511	0.859	0.446
U250	38.682	44.096	0.250	7.018
U250	2.649	6.228	0.858	1.837
U250	3.779	7.508	0.842	2.194
U250	14.335	16.595	0.654	4.272
U250	4.363	13.206	0.314	2.357
U250	144.754	123.884	0.119	13.576

U250	1.208	6.440	0.366	1.240
U250	9.076	24.295	0.193	3.399
U250	19.711	30.938	0.259	5.010
U250	7.051	13.322	0.499	2.996
U250	0.390	3.369	0.432	0.705
U250	11.102	14.343	0.678	3.760
U250	5.415	9.019	0.837	2.626
U250	46.862	57.514	0.178	7.724
U250	0.935	4.976	0.475	1.091
U250	4.441	12.552	0.354	2.378
U250	6.934	15.718	0.353	2.971
U250	9.271	24.507	0.194	3.436
U250	0.117	1.348	0.809	0.386
U250	4.168	10.232	0.500	2.304
U250	0.117	1.348	0.809	0.386
U250	13.673	29.570	0.197	4.172
U250	0.312	2.464	0.646	0.630
U250	7.518	19.646	0.245	3.094
U250	6.700	13.158	0.486	2.921
U250	0.195	2.233	0.491	0.498
U250	0.156	1.675	0.699	0.446
U250	31.163	38.781	0.260	6.299
U250	0.156	1.906	0.540	0.446
U250	0.117	1.396	0.754	0.386
U250	0.117	1.348	0.809	0.386
U250	2.337	7.277	0.555	1.725
U250	23.762	29.850	0.335	5.500
U250	5.609	20.204	0.173	2.672
U250	96.957	85.015	0.169	11.111
U250	30.696	43.797	0.201	6.252
U250	3.116	10.252	0.373	1.992
U250	1.324	6.208	0.432	1.298
U250	2.104	7.835	0.431	1.637
U250	0.195	2.069	0.572	0.498
U250	11.530	14.997	0.644	3.832
U250	6.856	20.204	0.211	2.955
U250	8.025	26.548	0.143	3.197
U250	2.571	6.161	0.851	1.809
U250	7.869	25.479	0.152	3.165
U250	3.155	9.183	0.470	2.004
U250	162.947	148.401	0.093	14.404
U250	34.279	59.950	0.120	6.606
U250	23.412	70.054	0.060	5.460
U250	2.181	9.068	0.333	1.666
U250	15.543	23.035	0.368	4.449

U250	139.262	161.540	0.067	13.316
U250	55.666	80.018	0.109	8.419
U250	154.103	199.146	0.049	14.007
U250	11.453	26.875	0.199	3.819
U250	4.831	20.041	0.151	2.480
U250	4.675	15.459	0.246	2.440
U250	40.162	56.983	0.155	7.151
U250	25.788	32.545	0.306	5.730
U250	142.768	132.305	0.102	13.483
U250	3.194	13.812	0.210	2.017
U250	10.283	26.316	0.187	3.618
U250	9.271	31.158	0.120	3.436
U250	8.726	25.739	0.166	3.333
U250	10.011	29.387	0.146	3.570
U250	18.970	62.730	0.061	4.915
U31	0.002	0.168	0.890	0.050
U31	0.001	0.137	0.670	0.036
U31	0.104	2.113	0.293	0.364
U31	0.001	0.168	0.445	0.036
U31	0.017	0.480	0.927	0.147
U31	0.169	3.558	0.168	0.464
U31	0.001	0.124	0.817	0.036
U31	0.001	0.168	0.445	0.036
U31	0.021	0.870	0.349	0.164
U31	0.166	3.094	0.218	0.460
U31	0.002	0.186	0.726	0.050
U31	0.001	0.124	0.817	0.036
U31	0.006	0.485	0.321	0.087
U31	0.119	2.305	0.281	0.389
U31	0.046	1.182	0.414	0.242
U31	0.001	0.150	0.559	0.036
U31	0.049	1.517	0.268	0.250
U31	0.064	1.946	0.212	0.285
U31	0.001	0.124	0.817	0.036
U31	0.043	0.939	0.613	0.234
U31	0.001	0.124	0.817	0.036
U31	0.001	0.124	0.817	0.036
U31	0.025	0.635	0.779	0.178
U31	0.014	0.478	0.770	0.134
U31	0.001	0.155	0.523	0.036
U31	0.022	0.864	0.370	0.167
U31	0.071	1.399	0.456	0.301
U31	0.115	2.237	0.289	0.383
U31	0.098	2.379	0.218	0.353
U31	0.001	0.168	0.445	0.036

U31	0.078	1.920	0.266	0.315
U31	0.087	1.969	0.282	0.333
U31	0.066	1.081	0.710	0.290
U31	0.024	0.740	0.551	0.175
U31	0.012	0.472	0.677	0.124
U31	0.001	0.124	0.817	0.036
U31	0.001	0.150	0.559	0.036
U31	0.036	0.826	0.663	0.214
U31	0.064	1.318	0.463	0.285
U31	0.105	2.230	0.265	0.366
U31	0.132	2.586	0.248	0.410
U31	0.055	1.174	0.501	0.265
U31	0.001	0.168	0.445	0.036
U31	0.009	0.354	0.902	0.107
U31	0.079	1.585	0.395	0.317
U31	0.062	1.391	0.403	0.281
U31	0.001	0.124	0.817	0.036
U31	0.244	5.149	0.116	0.557
U31	0.162	3.246	0.193	0.454
U31	0.111	3.827	0.095	0.376
U31	0.195	4.083	0.147	0.498
U31	0.083	2.049	0.248	0.325
U31	0.060	0.499	3.028	0.276
U31	0.096	2.465	0.199	0.350
U31	0.107	2.554	0.206	0.369
U31	0.044	1.572	0.224	0.237
U31	0.017	0.648	0.509	0.147
U31	0.078	2.518	0.155	0.315
U31	0.108	2.500	0.217	0.371
U31	0.049	1.293	0.368	0.250
U31	0.046	1.647	0.213	0.242
U31	0.046	1.275	0.356	0.242
U62	0.307	3.535	0.309	0.625
U62	0.083	1.280	0.637	0.325
U62	0.138	2.121	0.385	0.419
U62	0.129	1.783	0.510	0.405
U62	0.145	2.462	0.301	0.430
U62	0.073	1.822	0.276	0.305
U62	0.077	1.360	0.523	0.313
U62	0.142	2.237	0.357	0.425
U62	0.111	2.163	0.298	0.376
U62	0.188	2.934	0.274	0.489
U62	0.064	1.130	0.630	0.285
U62	0.331	4.258	0.229	0.649
U62	0.002	0.230	0.475	0.050

U62	0.445	3.693	0.410	0.753
U62	0.098	1.468	0.571	0.353
U62	0.002	0.168	0.890	0.050
U62	0.002	0.186	0.726	0.050
U62	0.093	2.088	0.268	0.344
U62	0.110	1.721	0.467	0.374
U62	0.001	0.137	0.670	0.036
U62	0.001	0.150	0.559	0.036
U62	0.091	1.634	0.428	0.340
U62	0.080	1.473	0.463	0.319
U62	0.069	1.244	0.560	0.296
U62	0.150	2.148	0.409	0.437
U62	0.159	2.049	0.476	0.450
U62	0.001	0.150	0.559	0.036
U62	0.167	3.127	0.215	0.461
U62	0.001	0.124	0.817	0.036
U62	0.002	0.212	0.559	0.050
U62	0.001	0.155	0.523	0.036
U62	0.001	0.124	0.817	0.036
U62	0.001	0.124	0.817	0.036
U62	0.474	5.275	0.214	0.777
U62	0.003	0.199	0.952	0.062
U62	0.001	0.124	0.817	0.036
U62	0.301	3.448	0.318	0.619
U62	0.305	4.785	0.167	0.623
U62	0.321	3.285	0.374	0.639
U62	0.189	2.947	0.273	0.491
U62	0.002	0.168	0.890	0.050
U62	0.069	1.355	0.472	0.296
U62	0.119	1.869	0.428	0.389
U62	0.001	0.186	0.363	0.036
U62	0.054	1.056	0.609	0.262
U62	0.001	0.155	0.523	0.036
U62	0.001	0.186	0.363	0.036
U62	0.001	0.168	0.445	0.036
U62	0.002	0.230	0.475	0.050
U62	0.001	0.124	0.817	0.036
U62	0.001	0.150	0.559	0.036
U62	0.002	0.186	0.726	0.050
U62	0.001	0.150	0.559	0.036
U62	0.003	0.199	0.952	0.062
U62	0.001	0.124	0.817	0.036
U62	0.043	1.068	0.474	0.234
U62	0.312	3.928	0.254	0.630
U62	0.002	0.248	0.409	0.050

U62	0.582	4.309	0.394	0.861
U62	0.163	2.292	0.390	0.456
U62	0.108	2.013	0.335	0.371
U62	0.141	1.941	0.470	0.424
U62	0.123	2.039	0.372	0.396
U62	0.134	2.540	0.261	0.413
U62	0.319	5.859	0.117	0.637
U62	0.333	4.426	0.214	0.651
U62	0.002	0.287	0.305	0.050
U62	0.353	4.214	0.250	0.670
U62	0.248	2.816	0.393	0.562
U62	0.003	0.336	0.334	0.062
U62	0.004	0.354	0.401	0.071
U62	0.014	0.854	0.241	0.134

APPENDIX D

Raw data for fullerol aggregate size measurements

Table D-1: Zetasizer data for fullerol aggregate sizes.

Treatment	Fullerol (mg/L)	T (°C)	Z-Ave (d.nm)	PdI	Peak 1 Mean Intensity (d.nm)	Peak 2 Mean Intensity (d.nm)	Peak 3 Mean Intensity (d.nm)	Peak 1 Area Intensity %	Peak 2 Area Intensity %	Peak 3 Area Intensity %	Scattering Angle
Untreated	50	21.9	599.2	0.565	286.0	0.0	0.00	100.0	0.0	0.0	173
Untreated	50	21.9	491.0	0.497	315.4	0.0	0.00	100.0	0.0	0.0	173
Untreated	50	21.9	480.0	0.544	309.6	0.0	0.00	100.0	0.0	0.0	173
Untreated	50	22.0	450.0	0.531	317.3	0.0	0.00	100.0	0.0	0.0	173
Untreated	50	22.0	485.3	0.542	287.5	0.0	0.00	100.0	0.0	0.0	173
Untreated	50	22.0	474.2	0.653	296.4	0.0	0.00	100.0	0.0	0.0	173
Untreated	50	22.0	457.5	0.562	313.8	0.0	0.00	100.0	0.0	0.0	173
Untreated	50	22.0	400.6	0.534	292.9	0.0	0.00	100.0	0.0	0.0	173
Untreated	50	22.0	483.9	0.539	453.6	206.9	0.00	51.2	48.8	0.0	173
Untreated	50	22.0	369.4	0.512	312.1	5560.0	0.00	98.0	2.0	0.0	173
Untreated	50	22.0	475.7	0.633	319.4	0.0	0.00	100.0	0.0	0.0	173
Untreated	50	22.0	400.2	0.524	287.1	0.0	0.00	100.0	0.0	0.0	173
Untreated	50	22.0	441.0	0.551	297.5	0.0	0.00	100.0	0.0	0.0	173
Untreated	100	22.0	475.8	0.483	330.3	0.0	0.00	100.0	0.0	0.0	173
Untreated	100	22.0	464.7	0.471	351.3	0.0	0.00	100.0	0.0	0.0	173
Untreated	100	22.0	445.2	0.535	363.5	0.0	0.00	100.0	0.0	0.0	173
Untreated	100	22.0	516.5	0.456	386.5	0.0	0.00	100.0	0.0	0.0	173
Untreated	100	22.0	499.8	0.478	446.0	124.9	5560.00	87.1	10.8	2.1	173

Untreated	100	22.0	486.8	0.527	361.9	0.0	0.00	100.0	0.0	0.0	173
Untreated	100	22.0	527.9	0.542	349.3	0.0	0.00	100.0	0.0	0.0	173
Untreated	100	22.0	523.5	0.499	428.4	100.5	5560.00	91.4	7.6	1.0	173
Untreated	100	22.0	526.3	0.523	388.5	85.3	0.00	93.6	6.4	0.0	173
Untreated	100	22.0	449.8	0.491	341.0	0.0	0.00	100.0	0.0	0.0	173
Untreated	100	22.0	485.1	0.498	338.4	0.0	0.00	100.0	0.0	0.0	173
Untreated	100	22.0	458.8	0.517	355.1	5560.0	0.00	98.8	1.2	0.0	173
Untreated	100	22.0	527.8	0.579	357.8	0.0	0.00	100.0	0.0	0.0	173
Untreated	200	21.9	535.6	0.500	285.6	0.0	0.00	100.0	0.0	0.0	173
Untreated	200	21.9	449.6	0.495	340.5	0.0	0.00	100.0	0.0	0.0	173
Untreated	200	21.9	491.7	0.442	369.4	0.0	0.00	100.0	0.0	0.0	173
Untreated	200	22.0	431.4	0.481	363.5	118.0	0.00	95.5	4.5	0.0	173
Untreated	200	22.0	398.2	0.399	350.6	0.0	0.00	100.0	0.0	0.0	173
Untreated	200	22.0	422.4	0.469	372.9	0.0	0.00	100.0	0.0	0.0	173
Untreated	200	22.0	423.6	0.457	370.6	110.4	0.00	95.8	4.2	0.0	173
Untreated	200	22.0	406.3	0.427	376.9	87.4	0.00	96.5	3.5	0.0	173
Untreated	200	22.0	426.3	0.487	334.0	0.0	0.00	100.0	0.0	0.0	173
Untreated	200	22.0	385.9	0.398	344.5	5560.0	0.00	98.5	1.5	0.0	173
Untreated	200	22.0	441.9	0.442	365.9	0.0	0.00	100.0	0.0	0.0	173
Untreated	200	22.0	421.1	0.475	369.5	0.0	0.00	100.0	0.0	0.0	173
Untreated	200	22.0	403.7	0.454	375.5	87.0	5560.00	96.4	2.3	1.2	173
Untreated	250	22.0	485.1	0.435	309.8	0.0	0.00	100.0	0.0	0.0	173
Untreated	250	22.0	490.7	0.418	350.1	0.0	0.00	100.0	0.0	0.0	173
Untreated	250	22.0	426.3	0.479	367.4	5560.0	0.00	98.3	1.7	0.0	173
Untreated	250	22.0	445.5	0.439	361.3	0.0	0.00	100.0	0.0	0.0	173
Untreated	250	22.0	437.6	0.475	338.1	0.0	0.00	100.0	0.0	0.0	173
Untreated	250	22.0	408.2	0.430	406.1	114.6	0.00	95.2	4.8	0.0	173
Untreated	250	22.0	428.2	0.471	405.3	96.9	5544.00	94.6	3.4	1.9	173
Untreated	250	22.0	419.6	0.452	379.9	5560.0	0.00	98.6	1.4	0.0	173
Untreated	250	22.0	404.6	0.453	366.4	0.0	0.00	100.0	0.0	0.0	173
Untreated	250	22.0	413.1	0.438	385.5	5083.0	0.00	91.1	8.9	0.0	173
Untreated	250	22.0	418.3	0.436	383.2	5465.0	0.00	97.4	2.6	0.0	173

Untreated	250	22.0	406.8	0.418	364.2	5213.0	0.00	93.4	6.6	0.0	173
Untreated	250	22.0	407.3	0.452	413.6	121.7	0.00	91.3	8.7	0.0	173
Untreated	500	22.0	504.0	0.446	317.3	0.0	0.00	100.0	0.0	0.0	173
Untreated	500	22.0	453.2	0.450	354.4	0.0	0.00	100.0	0.0	0.0	173
Untreated	500	22.0	420.9	0.418	436.6	109.5	0.00	93.8	6.2	0.0	173
Untreated	500	22.0	408.7	0.316	393.0	5341.0	0.00	96.2	3.8	0.0	173
Untreated	500	22.0	405.1	0.398	417.8	98.8	5560.00	94.7	4.2	1.1	173
Untreated	500	22.0	406.8	0.397	395.5	5448.0	0.00	97.7	2.3	0.0	173
Untreated	500	22.0	405.3	0.389	402.1	5560.0	0.00	98.8	1.2	0.0	173
Untreated	500	22.0	382.1	0.396	365.1	5381.0	0.00	96.5	3.5	0.0	173
Untreated	500	22.0	403.4	0.318	399.3	5209.0	0.00	95.7	4.3	0.0	173
Untreated	500	22.0	422.2	0.412	379.7	5418.0	0.00	96.8	3.2	0.0	173
Untreated	500	22.0	401.5	0.308	409.0	107.0	5395.00	93.5	4.0	2.4	173
Untreated	500	22.0	405.6	0.346	383.6	5183.0	0.00	93.9	6.1	0.0	173
Untreated	500	22.0	410.9	0.338	435.7	111.7	5366.00	92.5	4.7	2.8	173
Untreated	750	21.9	462.0	0.422	362.6	0.0	0.00	100.0	0.0	0.0	173
Untreated	750	21.9	467.4	0.397	392.8	0.0	0.00	100.0	0.0	0.0	173
Untreated	750	21.9	425.4	0.401	415.9	0.0	0.00	100.0	0.0	0.0	173
Untreated	750	22.0	442.4	0.414	395.8	100.4	0.00	96.3	3.7	0.0	173
Untreated	750	22.0	456.4	0.325	464.5	5434.0	0.00	97.9	2.1	0.0	173
Untreated	750	22.0	419.8	0.300	454.6	97.6	5405.00	93.5	4.7	1.8	173
Untreated	750	22.0	414.2	0.359	484.5	5207.0	0.00	96.6	3.4	0.0	173
Untreated	750	22.0	404.1	0.339	467.8	4782.0	85.26	92.4	5.8	1.8	173
Untreated	750	22.0	412.8	0.320	424.1	5313.0	0.00	96.9	3.1	0.0	173
Untreated	750	22.0	408.3	0.302	422.5	5411.0	0.00	97.9	2.1	0.0	173
Untreated	750	22.0	408.8	0.327	423.6	5425.0	0.00	98.1	1.9	0.0	173
Untreated	750	22.0	416.4	0.342	449.1	5405.0	0.00	97.9	2.1	0.0	173
Untreated	750	22.0	414.5	0.314	452.1	110.8	5387.00	92.8	5.1	2.1	173
Untreated	1000	22.0	469.9	0.416	361.7	0.0	0.00	100.0	0.0	0.0	173
Untreated	1000	22.0	435.3	0.367	416.4	0.0	0.00	100.0	0.0	0.0	173
Untreated	1000	22.0	434.4	0.396	461.2	98.3	0.00	94.8	5.2	0.0	173
Untreated	1000	22.0	432.0	0.310	450.0	0.0	0.00	100.0	0.0	0.0	173

Untreated	1000	22.0	415.6	0.386	451.4	5205.0	0.00	95.9	4.1	0.0	173
Untreated	1000	22.0	419.8	0.314	452.5	111.6	5403.00	92.3	5.7	2.0	173
Untreated	1000	22.0	391.8	0.320	439.7	4986.0	0.00	95.5	4.5	0.0	173
Untreated	1000	22.0	422.3	0.392	448.7	5294.0	0.00	96.3	3.7	0.0	173
Untreated	1000	22.0	400.1	0.279	511.3	113.9	5276.00	93.0	5.9	1.1	173
Untreated	1000	22.0	405.8	0.349	471.7	4714.0	0.00	92.7	7.3	0.0	173
Untreated	1000	22.0	414.6	0.312	432.1	5435.0	0.00	98.3	1.7	0.0	173
Untreated	1000	22.0	413.4	0.325	424.6	5382.0	0.00	97.3	2.7	0.0	173
Untreated	1000	22.0	406.0	0.336	440.7	103.9	5482.00	93.6	5.1	1.3	173
Sonicated	50	22.1	154.8	0.270	162.3	4577.0	0.00	94.0	6.0	0.0	173
Sonicated	50	22.1	150.4	0.216	167.6	5020.0	0.00	98.0	2.0	0.0	173
Sonicated	50	22.1	156.2	0.272	171.9	4494.0	0.00	94.6	5.4	0.0	173
Sonicated	50	22.1	154.0	0.242	163.6	5225.0	0.00	98.0	2.0	0.0	173
Sonicated	50	22.1	155.7	0.222	176.4	4975.0	0.00	97.9	2.1	0.0	173
Sonicated	50	22.1	156.0	0.248	168.1	5114.0	0.00	97.4	2.6	0.0	173
Sonicated	50	22.1	153.0	0.228	163.4	5342.0	0.00	98.6	1.4	0.0	173
Sonicated	50	22.1	156.1	0.234	185.0	4642.0	0.00	97.2	2.8	0.0	173
Sonicated	50	22.1	156.6	0.246	162.7	4975.0	0.00	96.1	3.9	0.0	173
Sonicated	50	22.1	156.3	0.234	171.2	4920.0	0.00	97.1	2.9	0.0	173
Sonicated	50	22.1	154.5	0.204	198.5	0.0	0.00	100.0	0.0	0.0	173
Sonicated	50	22.1	154.5	0.192	182.5	0.0	0.00	100.0	0.0	0.0	173
Sonicated	50	22.1	154.8	0.235	166.5	5113.0	0.00	97.6	2.4	0.0	173
Sonicated	100	22.0	151.6	0.193	175.6	4991.0	0.00	98.9	1.1	0.0	173
Sonicated	100	22.0	149.4	0.198	185.3	0.0	0.00	100.0	0.0	0.0	173
Sonicated	100	22.0	153.0	0.242	164.8	5140.0	0.00	97.5	2.5	0.0	173
Sonicated	100	21.9	156.6	0.224	169.8	5389.0	0.00	98.9	1.1	0.0	173
Sonicated	100	21.9	152.4	0.210	169.2	5038.0	0.00	98.2	1.8	0.0	173
Sonicated	100	21.9	154.8	0.222	170.3	5168.0	0.00	98.1	1.9	0.0	173
Sonicated	100	21.9	152.8	0.214	172.7	4654.0	0.00	97.4	2.6	0.0	173
Sonicated	100	21.9	153.6	0.210	169.6	5246.0	0.00	98.7	1.3	0.0	173
Sonicated	100	21.9	153.2	0.237	172.7	5044.0	0.00	97.7	2.3	0.0	173
Sonicated	100	21.9	151.5	0.212	180.4	5061.0	0.00	99.0	1.0	0.0	173

Sonicated	100	21.9	153.3	0.209	175.5	4806.0	0.00	98.0	2.0	0.0	173
Sonicated	100	21.9	151.4	0.209	169.5	4814.0	0.00	97.6	2.4	0.0	173
Sonicated	100	21.9	150.4	0.199	171.1	5109.0	0.00	98.7	1.3	0.0	173
Sonicated	200	22.0	146.0	0.174	170.6	0.0	0.00	100.0	0.0	0.0	173
Sonicated	200	22.0	149.7	0.217	160.8	5389.0	0.00	99.0	1.0	0.0	173
Sonicated	200	22.0	147.2	0.188	183.3	0.0	0.00	100.0	0.0	0.0	173
Sonicated	200	22.0	147.6	0.170	177.9	0.0	0.00	100.0	0.0	0.0	173
Sonicated	200	22.0	144.5	0.188	171.6	0.0	0.00	100.0	0.0	0.0	173
Sonicated	200	22.0	149.4	0.163	173.5	0.0	0.00	100.0	0.0	0.0	173
Sonicated	200	22.0	146.6	0.189	181.9	0.0	0.00	100.0	0.0	0.0	173
Sonicated	200	22.0	145.5	0.187	166.5	0.0	0.00	100.0	0.0	0.0	173
Sonicated	200	22.0	145.8	0.200	171.7	4790.0	0.00	98.7	1.3	0.0	173
Sonicated	200	22.0	144.8	0.188	178.3	0.0	0.00	100.0	0.0	0.0	173
Sonicated	200	22.0	144.8	0.196	170.4	4785.0	0.00	98.8	1.2	0.0	173
Sonicated	200	22.0	148.2	0.166	178.7	0.0	0.00	100.0	0.0	0.0	173
Sonicated	200	22.0	146.7	0.180	167.5	0.0	0.00	100.0	0.0	0.0	173
Sonicated	250	22.0	145.6	0.174	177.1	0.0	0.00	100.0	0.0	0.0	173
Sonicated	250	22.0	147.3	0.183	175.0	0.0	0.00	100.0	0.0	0.0	173
Sonicated	250	22.0	145.7	0.166	173.5	0.0	0.00	100.0	0.0	0.0	173
Sonicated	250	22.0	147.5	0.201	185.3	0.0	0.00	100.0	0.0	0.0	173
Sonicated	250	22.0	144.9	0.162	168.2	0.0	0.00	100.0	0.0	0.0	173
Sonicated	250	22.0	147.8	0.165	177.0	0.0	0.00	100.0	0.0	0.0	173
Sonicated	250	22.0	146.5	0.179	179.6	0.0	0.00	100.0	0.0	0.0	173
Sonicated	250	22.0	146.1	0.200	164.4	0.0	0.00	100.0	0.0	0.0	173
Sonicated	250	22.0	143.2	0.192	158.6	4964.0	0.00	98.3	1.7	0.0	173
Sonicated	250	22.0	145.9	0.183	179.7	0.0	0.00	100.0	0.0	0.0	173
Sonicated	250	22.0	146.6	0.204	173.6	0.0	0.00	100.0	0.0	0.0	173
Sonicated	250	22.0	146.7	0.165	175.3	0.0	0.00	100.0	0.0	0.0	173
Sonicated	250	22.0	145.8	0.168	166.1	0.0	0.00	100.0	0.0	0.0	173
Sonicated	500	21.9	148.3	0.194	168.9	0.0	0.00	100.0	0.0	0.0	173
Sonicated	500	21.9	149.8	0.173	181.4	0.0	0.00	100.0	0.0	0.0	173
Sonicated	500	21.9	147.2	0.189	180.4	0.0	0.00	100.0	0.0	0.0	173

Sonicated	500	21.9	154.0	0.248	172.5	4989.0	0.00	97.1	2.9	0.0	173
Sonicated	500	21.9	148.5	0.195	180.1	0.0	0.00	100.0	0.0	0.0	173
Sonicated	500	21.9	149.8	0.199	173.0	4944.0	0.00	98.7	1.3	0.0	173
Sonicated	500	21.9	147.5	0.209	170.8	5005.0	0.00	98.5	1.5	0.0	173
Sonicated	500	21.9	149.0	0.205	183.9	0.0	0.00	100.0	0.0	0.0	173
Sonicated	500	21.9	148.6	0.165	177.6	0.0	0.00	100.0	0.0	0.0	173
Sonicated	500	21.9	148.1	0.198	176.8	0.0	0.00	100.0	0.0	0.0	173
Sonicated	500	21.9	148.1	0.185	183.9	0.0	0.00	100.0	0.0	0.0	173
Sonicated	500	21.9	147.9	0.188	182.0	0.0	0.00	100.0	0.0	0.0	173
Sonicated	500	21.9	149.1	0.196	180.6	0.0	0.00	100.0	0.0	0.0	173
Sonicated	750	22.0	150.4	0.174	178.9	0.0	0.00	100.0	0.0	0.0	173
Sonicated	750	22.0	148.6	0.164	177.3	0.0	0.00	100.0	0.0	0.0	173
Sonicated	750	22.0	148.6	0.178	177.1	0.0	0.00	100.0	0.0	0.0	173
Sonicated	750	22.0	149.2	0.187	168.9	0.0	0.00	100.0	0.0	0.0	173
Sonicated	750	22.0	146.0	0.196	183.1	0.0	0.00	100.0	0.0	0.0	173
Sonicated	750	22.0	150.0	0.175	182.3	0.0	0.00	100.0	0.0	0.0	173
Sonicated	750	22.0	150.1	0.191	175.1	0.0	0.00	100.0	0.0	0.0	173
Sonicated	750	22.0	149.5	0.188	183.2	0.0	0.00	100.0	0.0	0.0	173
Sonicated	750	22.0	147.7	0.170	178.8	0.0	0.00	100.0	0.0	0.0	173
Sonicated	750	22.0	150.2	0.205	188.9	0.0	0.00	100.0	0.0	0.0	173
Sonicated	750	22.0	150.2	0.198	190.0	29.1	0.00	98.7	1.3	0.0	173
Sonicated	750	22.0	149.7	0.197	178.3	0.0	0.00	100.0	0.0	0.0	173
Sonicated	750	22.0	148.3	0.197	180.2	0.0	0.00	100.0	0.0	0.0	173
Sonicated	1000	22.0	147.2	0.210	163.2	5061.0	0.00	98.2	1.8	0.0	173
Sonicated	1000	22.0	148.8	0.242	167.0	4873.0	0.00	96.9	3.1	0.0	173
Sonicated	1000	22.0	149.9	0.213	184.1	0.0	0.00	100.0	0.0	0.0	173
Sonicated	1000	21.9	149.6	0.203	182.2	0.0	0.00	100.0	0.0	0.0	173
Sonicated	1000	21.9	152.9	0.212	196.2	0.0	0.00	100.0	0.0	0.0	173
Sonicated	1000	21.9	150.3	0.207	175.9	4947.0	0.00	98.8	1.2	0.0	173
Sonicated	1000	21.9	148.2	0.188	170.6	0.0	0.00	100.0	0.0	0.0	173
Sonicated	1000	21.9	147.7	0.196	173.2	0.0	0.00	100.0	0.0	0.0	173
Sonicated	1000	21.9	148.6	0.203	176.8	0.0	0.00	100.0	0.0	0.0	173

Sonicated	1000	21.9	148.5	0.193	186.7	0.0	0.00	100.0	0.0	0.0	173
Sonicated	1000	21.9	147.7	0.205	175.4	4968.0	0.00	98.8	1.2	0.0	173
Sonicated	1000	21.9	149.7	0.226	187.1	0.0	0.00	100.0	0.0	0.0	173
Sonicated	1000	21.9	147.5	0.177	179.6	0.0	0.00	100.0	0.0	0.0	173
Filtered	50	22.0	120.2	0.349	143.4	5046.0	0.00	96.5	3.5	0.0	173
Filtered	50	22.0	117.9	0.389	158.8	4467.0	0.00	95.8	4.2	0.0	173
Filtered	50	22.0	125.2	0.348	148.3	4603.0	0.00	94.2	5.8	0.0	173
Filtered	50	22.0	134.4	0.356	175.2	4637.0	0.00	95.9	4.1	0.0	173
Filtered	50	22.0	120.3	0.360	151.2	4772.0	0.00	96.3	3.7	0.0	173
Filtered	50	22.0	121.0	0.363	154.4	4934.0	0.00	97.1	2.9	0.0	173
Filtered	50	22.0	127.0	0.293	163.5	5090.0	0.00	98.6	1.4	0.0	173
Filtered	50	22.0	128.6	0.343	158.7	4977.0	0.00	96.8	3.2	0.0	173
Filtered	50	22.0	120.5	0.349	170.6	0.0	0.00	100.0	0.0	0.0	173
Filtered	50	22.0	120.1	0.333	149.0	4823.0	0.00	96.5	3.5	0.0	173
Filtered	50	22.0	124.0	0.283	155.6	5012.0	0.00	98.2	1.8	0.0	173
Filtered	50	22.0	124.5	0.367	155.9	4821.0	0.00	96.3	3.7	0.0	173
Filtered	50	22.0	122.1	0.297	156.8	4595.0	0.00	97.0	3.0	0.0	173
Filtered	100	21.9	118.6	0.344	147.5	5159.0	0.00	98.0	2.0	0.0	173
Filtered	100	21.9	118.3	0.337	158.8	0.0	0.00	100.0	0.0	0.0	173
Filtered	100	21.9	118.9	0.337	166.1	4632.0	0.00	98.8	1.2	0.0	173
Filtered	100	22.0	147.8	0.223	137.5	0.0	0.00	100.0	0.0	0.0	173
Filtered	100	22.0	183.7	0.385	269.3	4654.0	0.00	97.7	2.3	0.0	173
Filtered	100	22.0	145.6	0.357	173.0	5374.0	0.00	98.2	1.8	0.0	173
Filtered	100	22.0	162.3	0.365	220.5	42.9	4884.00	92.0	4.9	3.1	173
Filtered	100	22.0	178.0	0.405	248.3	3210.0	0.00	90.1	9.9	0.0	173
Filtered	100	22.0	175.0	0.407	300.5	0.0	0.00	100.0	0.0	0.0	173
Filtered	100	22.0	186.7	0.354	261.2	4612.0	0.00	98.0	2.0	0.0	173
Filtered	100	22.0	178.0	0.419	291.5	0.0	0.00	100.0	0.0	0.0	173
Filtered	100	22.0	176.1	0.421	310.6	0.0	0.00	100.0	0.0	0.0	173
Filtered	100	22.0	182.4	0.384	240.6	4598.0	0.00	95.2	4.8	0.0	173
Filtered	200	22.0	117.5	0.284	138.4	0.0	0.00	100.0	0.0	0.0	173
Filtered	200	22.0	116.6	0.317	146.1	5324.0	0.00	98.9	1.1	0.0	173

Filtered	200	22.0	116.1	0.466	141.2	5167.0	0.00	96.8	3.2	0.0	173
Filtered	200	22.0	118.6	0.344	146.6	5367.0	0.00	98.9	1.1	0.0	173
Filtered	200	22.0	124.4	0.287	164.4	0.0	0.00	100.0	0.0	0.0	173
Filtered	200	22.0	122.1	0.355	159.1	5228.0	0.00	98.7	1.3	0.0	173
Filtered	200	22.0	122.1	0.341	158.9	0.0	0.00	100.0	0.0	0.0	173
Filtered	200	22.0	120.3	0.344	156.0	4851.0	0.00	97.7	2.3	0.0	173
Filtered	200	22.0	125.3	0.298	185.9	25.2	0.00	98.0	2.0	0.0	173
Filtered	200	22.0	122.8	0.285	159.7	4664.0	0.00	98.0	2.0	0.0	173
Filtered	200	22.0	121.3	0.279	172.6	0.0	0.00	100.0	0.0	0.0	173
Filtered	200	22.0	122.4	0.348	158.9	4783.0	0.00	97.4	2.6	0.0	173
Filtered	200	22.0	124.2	0.287	164.6	4565.0	0.00	98.0	2.0	0.0	173
Filtered	250	22.0	114.9	0.317	137.1	0.0	0.00	100.0	0.0	0.0	173
Filtered	250	22.0	120.9	0.284	154.6	0.0	0.00	100.0	0.0	0.0	173
Filtered	250	22.0	122.1	0.299	162.4	4578.0	0.00	97.4	2.6	0.0	173
Filtered	250	22.0	122.4	0.330	145.2	0.0	0.00	100.0	0.0	0.0	173
Filtered	250	22.0	129.3	0.382	188.5	4568.0	0.00	98.3	1.7	0.0	173
Filtered	250	22.0	123.4	0.367	159.5	4857.0	0.00	97.0	3.0	0.0	173
Filtered	250	22.0	129.2	0.386	187.2	4581.0	22.87	95.9	2.1	2.0	173
Filtered	250	22.0	136.1	0.315	217.5	0.0	0.00	100.0	0.0	0.0	173
Filtered	250	22.0	131.1	0.382	173.8	4550.0	0.00	96.1	3.9	0.0	173
Filtered	250	22.0	133.2	0.308	201.7	0.0	0.00	100.0	0.0	0.0	173
Filtered	250	22.0	130.0	0.376	164.3	4139.0	0.00	94.2	5.8	0.0	173
Filtered	250	22.0	131.5	0.317	186.8	3199.0	0.00	95.6	4.4	0.0	173
Filtered	250	22.0	127.0	0.387	164.6	3486.0	0.00	93.0	7.0	0.0	173
Filtered	500	22.1	113.3	0.269	139.1	0.0	0.00	100.0	0.0	0.0	173
Filtered	500	22.1	117.0	0.291	156.9	0.0	0.00	100.0	0.0	0.0	173
Filtered	500	22.1	115.3	0.287	161.4	0.0	0.00	100.0	0.0	0.0	173
Filtered	500	21.9	114.6	0.271	141.4	5188.0	0.00	98.8	1.2	0.0	173
Filtered	500	21.9	111.0	0.286	149.6	0.0	0.00	100.0	0.0	0.0	173
Filtered	500	21.9	113.9	0.275	154.2	0.0	0.00	100.0	0.0	0.0	173
Filtered	500	21.9	113.6	0.271	152.6	0.0	0.00	100.0	0.0	0.0	173
Filtered	500	21.9	113.0	0.276	152.2	0.0	0.00	100.0	0.0	0.0	173

Filtered	500	21.9	114.6	0.285	156.5	0.0	0.00	100.0	0.0	0.0	173
Filtered	500	21.9	111.2	0.293	154.2	0.0	0.00	100.0	0.0	0.0	173
Filtered	500	21.9	113.6	0.270	150.3	0.0	0.00	100.0	0.0	0.0	173
Filtered	500	21.9	112.1	0.282	155.1	0.0	0.00	100.0	0.0	0.0	173
Filtered	500	21.9	112.3	0.276	153.6	0.0	0.00	100.0	0.0	0.0	173
Filtered	750	21.9	108.4	0.361	142.7	0.0	0.00	100.0	0.0	0.0	173
Filtered	750	21.9	113.9	0.256	143.8	0.0	0.00	100.0	0.0	0.0	173
Filtered	750	21.9	112.8	0.261	151.5	0.0	0.00	100.0	0.0	0.0	173
Filtered	750	22.0	118.9	0.287	169.8	0.0	0.00	100.0	0.0	0.0	173
Filtered	750	22.0	113.5	0.272	151.0	0.0	0.00	100.0	0.0	0.0	173
Filtered	750	22.0	115.6	0.283	159.0	0.0	0.00	100.0	0.0	0.0	173
Filtered	750	22.0	114.2	0.281	155.2	0.0	0.00	100.0	0.0	0.0	173
Filtered	750	22.0	113.4	0.289	157.6	0.0	0.00	100.0	0.0	0.0	173
Filtered	750	22.0	113.7	0.290	159.9	0.0	0.00	100.0	0.0	0.0	173
Filtered	750	22.0	115.5	0.270	155.2	0.0	0.00	100.0	0.0	0.0	173
Filtered	750	22.0	114.7	0.270	152.1	0.0	0.00	100.0	0.0	0.0	173
Filtered	750	22.0	114.8	0.275	154.9	0.0	0.00	100.0	0.0	0.0	173
Filtered	750	22.0	115.6	0.288	160.1	0.0	0.00	100.0	0.0	0.0	173
Filtered	1000	22.0	110.5	0.286	143.5	0.0	0.00	100.0	0.0	0.0	173
Filtered	1000	22.0	113.6	0.272	155.4	0.0	0.00	100.0	0.0	0.0	173
Filtered	1000	22.0	115.1	0.285	157.2	0.0	0.00	100.0	0.0	0.0	173
Filtered	1000	21.9	111.5	0.280	153.4	0.0	0.00	100.0	0.0	0.0	173
Filtered	1000	21.9	110.4	0.296	151.3	0.0	0.00	100.0	0.0	0.0	173
Filtered	1000	21.9	113.7	0.275	153.0	0.0	0.00	100.0	0.0	0.0	173
Filtered	1000	21.9	112.4	0.282	153.8	0.0	0.00	100.0	0.0	0.0	173
Filtered	1000	21.9	113.3	0.292	161.0	0.0	0.00	100.0	0.0	0.0	173
Filtered	1000	21.9	110.7	0.277	147.9	0.0	0.00	100.0	0.0	0.0	173
Filtered	1000	21.9	109.3	0.292	152.8	0.0	0.00	100.0	0.0	0.0	173
Filtered	1000	21.9	112.8	0.276	149.1	0.0	0.00	100.0	0.0	0.0	173
Filtered	1000	21.9	110.1	0.281	150.7	0.0	0.00	100.0	0.0	0.0	173
Filtered	1000	21.9	110.7	0.290	152.0	0.0	0.00	100.0	0.0	0.0	173
Centrifuged	50	22.0	99.7	0.273	147.2	20.1	2.78	51.0	26.4	13.8	173

Centrifuged	50	22.0	42.0	0.772	149.7	7.5	3740.00	66.8	24.6	8.5	173
Centrifuged	50	22.0	39.2	0.712	138.3	8.2	4066.00	66.3	24.7	7.7	173
Centrifuged	50	22.0	39.9	0.739	155.7	7.8	3618.00	65.0	19.7	8.3	173
Centrifuged	50	22.0	59.2	0.334	136.3	8.4	3888.00	63.6	23.9	7.4	173
Centrifuged	50	22.0	72.2	0.178	106.0	7.6	3679.00	58.9	27.2	13.9	173
Centrifuged	50	22.0	83.1	0.233	119.0	6.6	3990.00	58.9	25.6	15.5	173
Centrifuged	50	22.0	41.2	0.620	222.5	32.1	3.35	51.2	27.5	16.4	173
Centrifuged	50	22.0	53.4	0.661	149.8	6.8	2978.00	59.0	21.2	19.8	173
Centrifuged	50	22.0	42.4	0.553	153.2	13.8	3.38	60.4	20.4	11.5	173
Centrifuged	50	22.0	45.8	0.426	145.1	11.4	1.21	59.5	26.0	9.8	173
Centrifuged	50	22.0	42.4	0.640	142.1	8.1	3726.00	62.3	27.6	9.9	173
Centrifuged	50	22.0	58.9	0.433	145.8	16.1	3.65	57.2	17.8	14.5	173
Centrifuged	100	22.0	57.1	0.418	110.7	4.7	4239.00	73.9	15.5	10.6	173
Centrifuged	100	22.0	32.1	0.847	136.7	6.6	2224.00	66.1	22.3	11.6	173
Centrifuged	100	22.0	41.5	0.736	150.5	7.6	3555.00	69.1	21.7	9.2	173
Centrifuged	100	22.0	37.1	0.810	163.3	11.1	3599.00	64.6	22.3	6.7	173
Centrifuged	100	22.0	42.4	0.629	151.9	7.6	3925.00	70.0	23.2	6.8	173
Centrifuged	100	22.0	36.1	0.669	131.0	7.5	3515.00	66.3	24.9	8.8	173
Centrifuged	100	22.0	41.8	0.628	136.2	6.8	2958.00	61.5	19.9	13.3	173
Centrifuged	100	22.0	33.2	0.737	128.3	10.9	3191.00	61.3	21.5	8.9	173
Centrifuged	100	22.0	31.8	0.815	139.7	8.3	3547.00	68.1	26.3	5.6	173
Centrifuged	100	22.0	32.4	0.848	128.3	7.1	2423.00	63.4	23.5	13.0	173
Centrifuged	100	22.0	74.1	0.432	102.5	10.4	485.00	47.2	18.3	17.4	173
Centrifuged	100	22.0	37.5	0.951	124.5	10.7	2143.00	55.8	19.5	18.4	173
Centrifuged	100	22.0	27.9	0.895	128.4	8.6	3604.00	64.6	27.6	6.9	173
Centrifuged	200	21.9	38.9	0.994	351.2	8.5	0.00	78.1	21.9	0.0	173
Centrifuged	200	22.0	36.3	1.000	340.3	11.6	3.33	75.7	16.7	7.6	173
Centrifuged	200	22.0	28.3	1.000	200.5	15.7	3.43	67.4	22.0	10.7	173
Centrifuged	200	22.0	33.8	1.000	213.9	5.3	0.00	84.6	15.4	0.0	173
Centrifuged	200	22.0	70.5	0.322	148.9	8.8	4696.00	68.3	25.7	6.0	173
Centrifuged	200	21.9	28.0	1.000	193.5	5.7	0.00	79.8	20.2	0.0	173
Centrifuged	200	22.0	35.5	0.771	139.4	12.1	2.70	63.3	22.1	8.4	173

Centrifuged	200	22.0	38.4	0.694	137.0	7.8	3655.00	68.4	23.8	7.8	173
Centrifuged	200	22.0	31.5	1.000	159.2	9.1	2538.00	64.4	22.0	9.0	173
Centrifuged	200	22.0	28.5	1.000	213.5	8.4	1.93	75.0	22.0	3.1	173
Centrifuged	200	22.0	28.8	1.000	194.0	18.2	5.20	68.5	16.4	15.1	173
Centrifuged	200	22.0	28.8	1.000	164.1	10.4	4459.00	68.7	27.6	3.7	173
Centrifuged	200	22.0	67.5	0.472	157.7	8.4	4353.00	66.3	23.3	10.5	173
Centrifuged	250	21.9	45.9	0.316	95.6	10.5	2.85	59.1	25.9	7.9	173
Centrifuged	250	21.9	26.5	1.000	143.5	11.5	3.39	60.7	20.7	9.3	173
Centrifuged	250	21.9	38.1	0.576	129.9	14.7	4.07	59.4	21.5	11.9	173
Centrifuged	250	21.9	58.5	0.365	121.4	7.7	4799.00	65.9	26.4	7.7	173
Centrifuged	250	21.9	35.3	0.777	94.1	8.6	549.60	52.0	20.7	16.1	173
Centrifuged	250	21.9	34.2	0.635	92.2	8.4	3052.00	56.9	23.8	14.4	173
Centrifuged	250	21.9	27.6	0.866	118.8	10.3	3710.00	62.4	24.7	6.6	173
Centrifuged	250	21.9	29.1	0.934	144.2	10.2	3207.00	62.5	23.7	8.2	173
Centrifuged	250	21.9	27.1	1.000	162.6	5.8	18.21	66.5	17.6	12.7	173
Centrifuged	250	21.9	31.0	0.986	98.3	999.2	7.00	53.7	23.7	22.7	173
Centrifuged	250	21.9	26.6	1.000	143.8	8.4	3515.00	68.2	24.3	4.4	173
Centrifuged	250	21.9	28.3	0.913	134.0	9.4	3530.00	63.0	25.9	7.1	173
Centrifuged	250	21.9	27.0	1.000	189.9	8.3	3015.00	71.4	23.9	4.7	173
Centrifuged	500	22.0	94.3	0.180	106.4	7.9	5193.00	67.4	26.9	5.8	173
Centrifuged	500	22.0	38.7	0.587	130.1	8.0	3543.00	65.8	23.8	10.5	173
Centrifuged	500	22.0	23.8	0.916	137.7	7.5	3061.00	69.2	24.3	3.7	173
Centrifuged	500	22.0	22.5	0.866	134.0	7.0	0.00	73.8	26.2	0.0	173
Centrifuged	500	22.0	43.4	0.404	112.5	8.8	4478.00	60.8	30.7	6.9	173
Centrifuged	500	22.0	58.7	0.273	115.8	7.4	4587.00	69.1	23.7	7.3	173
Centrifuged	500	22.0	39.6	0.439	87.6	6.7	2838.00	61.1	25.3	13.6	173
Centrifuged	500	22.0	36.2	0.551	110.0	15.2	4.31	60.5	15.8	15.7	173
Centrifuged	500	22.0	23.4	0.890	116.9	9.2	4064.00	64.7	31.9	3.4	173
Centrifuged	500	22.0	27.2	0.719	124.8	16.7	4.40	59.9	18.8	17.0	173
Centrifuged	500	22.0	23.6	0.893	109.1	8.1	3747.00	65.7	29.4	4.9	173
Centrifuged	500	22.0	47.9	0.374	109.5	7.7	4389.00	63.9	24.3	8.4	173
Centrifuged	500	22.0	22.7	0.882	120.1	8.1	3802.00	68.1	29.7	2.2	173

Centrifuged	750	22.0	73.0	0.134	87.1	8.0	2.00	66.8	26.1	4.8	173
Centrifuged	750	22.0	43.6	0.401	92.0	9.2	4271.00	59.9	22.4	9.7	173
Centrifuged	750	22.0	37.7	0.495	104.7	8.5	4344.00	62.8	29.5	7.6	173
Centrifuged	750	22.0	35.9	0.548	100.6	9.4	4266.00	61.3	24.6	7.8	173
Centrifuged	750	22.0	37.3	0.426	94.3	9.7	3.00	60.1	24.5	8.5	173
Centrifuged	750	22.0	78.8	0.146	89.4	9.3	2.71	62.9	26.8	7.1	173
Centrifuged	750	22.0	50.6	0.193	86.1	7.5	4976.00	65.3	29.9	4.9	173
Centrifuged	750	22.0	39.5	0.439	96.3	9.1	2.42	62.8	23.9	6.9	173
Centrifuged	750	22.0	36.9	0.483	93.9	8.8	4431.00	61.9	24.2	7.3	173
Centrifuged	750	22.0	34.8	0.535	103.7	8.5	4408.00	62.6	30.6	5.9	173
Centrifuged	750	22.0	33.2	0.611	102.3	7.4	4299.00	65.0	28.6	6.4	173
Centrifuged	750	22.0	44.8	0.412	108.0	6.8	4591.00	68.3	24.4	6.2	173
Centrifuged	750	22.0	31.4	0.592	100.3	8.7	4276.00	60.4	31.1	6.9	173
Centrifuged	1000	21.9	94.8	0.141	79.1	7.6	2.10	65.3	25.8	6.3	173
Centrifuged	1000	21.9	31.3	0.581	94.3	8.4	4595.00	64.4	30.2	5.3	173
Centrifuged	1000	21.9	48.5	0.305	96.2	8.5	2.32	64.7	26.1	5.0	173
Centrifuged	1000	21.9	48.0	0.326	96.0	8.0	4633.00	61.3	31.2	7.5	173
Centrifuged	1000	21.9	51.9	0.334	91.5	7.4	4986.00	63.9	29.0	7.0	173
Centrifuged	1000	21.9	50.9	0.202	89.7	8.5	1.85	63.8	26.5	5.5	173
Centrifuged	1000	21.9	58.7	0.141	88.2	9.0	2.42	62.5	25.2	7.3	173
Centrifuged	1000	21.9	50.9	0.245	96.1	8.5	4981.00	62.9	30.1	4.7	173
Centrifuged	1000	21.9	34.2	0.628	105.4	10.1	3.03	62.0	23.0	8.1	173
Centrifuged	1000	21.9	35.6	0.543	103.2	8.6	4791.00	64.8	30.5	4.7	173
Centrifuged	1000	21.9	27.9	0.732	107.5	8.9	2.20	65.5	25.0	5.5	173
Centrifuged	1000	21.9	28.2	0.738	106.2	9.0	4729.00	64.1	29.7	4.1	173
Centrifuged	1000	21.9	38.3	0.501	104.6	8.7	4513.00	61.6	28.4	6.8	173

APPENDIX E

Raw data for UV-vis spectrophotometry of fullerol treatments

Table E-1: UV-vis data.

Treatment	Fullerol (mg/L)	Cursor 1 Position (nm)	Cursor 1 Absolute	Cursor 2 Position (nm)	Cursor 2 Absolute
Blank	0	300	0.000	254	0.000
Untreated	50	300	0.133	254	0.192
Untreated	50	300	0.130	254	0.190
Untreated	50	300	0.137	254	0.195
Untreated	100	300	0.252	254	0.365
Untreated	100	300	0.253	254	0.367
Untreated	100	300	0.256	254	0.379
Untreated	200	300	0.490	254	0.736
Untreated	200	300	0.488	254	0.718
Untreated	200	300	0.537	254	0.776
Untreated	200	300	0.494	254	0.712
Untreated	250	300	0.615	254	0.910
Untreated	250	300	0.599	254	0.880
Untreated	250	300	0.614	254	0.880
Untreated	500	300	1.211	254	1.719
Untreated	500	300	1.246	254	1.800
Untreated	500	300	1.192	254	1.682
Untreated	750	300	1.846	254	2.451
Untreated	750	300	1.859	254	3.180
Untreated	750	300	1.679	254	1.994
Untreated	1000	300	2.101	254	1.741
Untreated	1000	300	2.177	254	1.805
Untreated	1000	300	3.209	254	2.140
Sonicated	50	300	0.160	254	0.237
Sonicated	50	300	0.159	254	0.238
Sonicated	50	300	0.160	254	0.236
Sonicated	100	300	0.292	254	0.439
Sonicated	100	300	0.301	254	0.447
Sonicated	100	300	0.302	254	0.453

Sonicated	200	300	0.595	254	0.876
Sonicated	200	300	0.592	254	0.860
Sonicated	200	300	0.580	254	0.867
Sonicated	250	300	0.720	254	1.027
Sonicated	250	300	0.731	254	1.114
Sonicated	250	300	0.729	254	1.058
Sonicated	500	300	1.405	254	1.827
Sonicated	500	300	1.423	254	2.187
Sonicated	750	300	2.045	254	1.924
Sonicated	750	300	2.021	254	2.355
Sonicated	750	300	1.945	254	1.636
Sonicated	1000	300	2.259	254	1.434
Sonicated	1000	300	2.192	254	1.758
Sonicated	1000	300	2.327	254	3.433
Filtered	50	300	0.136	254	0.206
Filtered	50	300	0.140	254	0.207
Filtered	50	300	0.137	254	0.207
Filtered	100	300	0.244	254	0.368
Filtered	100	300	0.247	254	0.367
Filtered	100	300	0.248	254	0.378
Filtered	200	300	0.488	254	0.741
Filtered	200	300	0.476	254	0.724
Filtered	200	300	0.488	254	0.717
Filtered	250	300	0.592	254	0.884
Filtered	250	300	0.614	254	0.871
Filtered	250	300	0.597	254	0.880
Filtered	500	300	1.177	254	2.129
Filtered	500	300	1.206	254	1.793
Filtered	500	300	1.138	254	1.725
Filtered	750	300	1.648	254	2.251
Filtered	750	300	1.863	254	2.174
Filtered	750	300	1.814	254	2.108
Filtered	1000	300	2.373	254	1.902
Filtered	1000	300	2.326	254	2.316
Filtered	1000	300	2.412	254	1.905
Centrifuged	50	300	0.098	254	0.142
Centrifuged	50	300	0.099	254	0.146
Centrifuged	50	300	0.096	254	0.141

Centrifuged	100	300	0.196	254	0.290
Centrifuged	100	300	0.195	254	0.289
Centrifuged	100	300	0.198	254	0.298
Centrifuged	200	300	0.398	254	0.595
Centrifuged	200	300	0.394	254	0.583
Centrifuged	200	300	0.385	254	0.574
Centrifuged	250	300	0.487	254	0.725
Centrifuged	250	300	0.484	254	0.720
Centrifuged	250	300	0.487	254	0.737
Centrifuged	500	300	0.957	254	1.379
Centrifuged	500	300	0.949	254	1.438
Centrifuged	500	300	0.963	254	1.329
Centrifuged	750	300	1.385	254	1.659
Centrifuged	750	300	1.471	254	1.849
Centrifuged	750	300	1.459	254	1.961
Centrifuged	1000	300	2.008	254	2.544
Centrifuged	1000	300	1.918	254	2.799
Centrifuged	1000	300	1.903	254	2.178

APPENDIX F

Statistical calculations of experimental data

Table F-1: Statistics for bacterial ultraviolet irradiation studies

Descriptive Statistics: Log10 (CFU/mL)

Results for Microbe = Bs, Concentration (mg/L) = 0

Variable	Irradiation	Total Count	Mean	StDev	Median	IQR
Log10 (CFU/mL)	-	3	5.966	0.264	5.914	0.520
	+	3	0.000000	0.000000	0.000000	0.000000

Results for Microbe = Bs, Concentration (mg/L) = 50

Variable	Irradiation	Total Count	Mean	StDev	Median	IQR
Log10 (CFU/mL)	-	3	5.912	0.215	5.813	0.395
	+	3	0.000000	0.000000	0.000000	0.000000

Results for Microbe = Bs, Concentration (mg/L) = 100

Variable	Irradiation	Total Count	Mean	StDev	Median	IQR
Log10 (CFU/mL)	-	3	5.8774	0.0661	5.8633	0.1298
	+	3	4.4091	0.0328	4.3997	0.0636

Results for Microbe = Bs, Concentration (mg/L) = 200

Variable	Irradiation	Total Count	Mean	StDev	Median	IQR
Log10 (CFU/mL)	-	3	6.077	0.273	6.121	0.541
	+	3	5.8939	0.00844	5.8921	0.0166

Results for Microbe = Bs, Concentration (mg/L) = 250

Variable	Irradiation	Total Count	Mean	StDev	Median	IQR
Log10 (CFU/mL)	-	3	6.1321	0.1284	6.1790	0.2437
	+	3	5.888	0.180	5.973	0.327

Results for Microbe = Ec, Concentration (mg/L) = 0

Variable	Irradiation	Total Count	Mean	StDev	Median	IQR
Log10 (CFU/mL)	-	3	6.0375	0.1035	6.0828	0.1915
	+	3	2.3597	0.1017	2.3010	0.1761

Results for Microbe = Ec, Concentration (mg/L) = 50

Variable	Irradiation	Total Count	Mean	StDev	Median	IQR
Log10 (CFU/mL)	-	3	6.1390	0.1518	6.2201	0.2692
	+	3	4.2479	0.0332	4.2355	0.0628

Results for Microbe = Ec, Concentration (mg/L) = 100

Variable	Irradiation	Total Count	Mean	StDev	Median	IQR
Log10 (CFU/mL)	-	3	6.1658	0.0448	6.1553	0.0877
	+	3	5.2699	0.0386	5.2718	0.0770

Results for Microbe = Ec, Concentration (mg/L) = 200

Variable	Irradiation	Total Count	Mean	StDev	Median	IQR
Log10 (CFU/mL)	-	3	5.923	0.300	6.057	0.554
	+	5	5.7327	0.1214	5.6920	0.2319

Results for Microbe = Ec, Concentration (mg/L) = 250

Variable	Irradiation	Total Count	Mean	StDev	Median	IQR
Log10 (CFU/mL)	-	3	6.0614	0.0282	6.0719	0.0534
	+	3	5.7571	0.1604	5.7993	0.3123

Results for Microbe = Se, Concentration (mg/L) = 0

Variable	Irradiation	Total Count	Mean	StDev	Median	IQR
Log10 (CFU/mL)	-	3	6.2817	0.0340	6.2810	0.0680
	+	3	0.000000	0.000000	0.000000	0.000000

Results for Microbe = Se, Concentration (mg/L) = 50

Variable	Irradiation	Total Count	Mean	StDev	Median	IQR
Log10 (CFU/mL)	-	1	6.3365	*	6.3365	*
	+	6	2.934	0.250	3.000	0.401

Results for Microbe = Se, Concentration (mg/L) = 100

Variable	Irradiation	Total Count	Mean	StDev	Median	IQR
Log10 (CFU/mL)	-	3	6.2689	0.0424	6.2900	0.0766
	+	3	4.5090	0.0284	4.5185	0.0544

Results for Microbe = Se, Concentration (mg/L) = 200

Variable	Irradiation	Total Count	Mean	StDev	Median	IQR
Log10 (CFU/mL)	-	3	6.2252	0.0770	6.2625	0.1397
	+	3	5.7577	0.0649	5.7634	0.1293

Results for Microbe = Se, Concentration (mg/L) = 250

Variable	Irradiation	Total Count	Mean	StDev	Median	IQR
Log10 (CFU/mL)	-	3	6.3385	0.0719	6.3541	0.1413
	+	3	5.9515	0.0387	5.9494	0.0774

Results for Microbe = Vp, Concentration (mg/L) = 0

Variable	Irradiation	Total Count	Mean	StDev	Median	IQR
Log10 (CFU/mL)	-	3	7.3149	0.0221	7.3160	0.0442
	+	3	0.000000	0.000000	0.000000	0.000000

Results for Microbe = Vp, Concentration (mg/L) = 50

Variable	Irradiation	Total Count	Mean	StDev	Median	IQR
Log10 (CFU/mL)	-	3	7.3485	0.0229	7.3385	0.0423
	+	3	0.000000	0.000000	0.000000	0.000000

Results for Microbe = Vp, Concentration (mg/L) = 100

Variable	Irradiation	Total Count	Mean	StDev	Median	IQR
Log10 (CFU/mL)	-	3	7.4140	0.0356	7.4346	0.0617
	+	3	0.000000	0.000000	0.000000	0.000000

Results for Microbe = Vp, Concentration (mg/L) = 200

Variable	Irradiation	Total Count	Mean	StDev	Median	IQR
Log10 (CFU/mL)	-	3	7.3761	0.0733	7.3711	0.1464
	+	3	5.3810	0.0225	5.3874	0.0436

Results for Microbe = Vp, Concentration (mg/L) = 250

Variable	Irradiation	Total Count	Mean	StDev	Median	IQR
Log10 (CFU/mL)	-	3	7.3728	0.0651	7.3892	0.1271
	+	3	5.7064	0.0473	5.7160	0.0930

Results for: (Irradiation = +)(Microbe = Bs)

Kruskal-Wallis Test: Log10 CFU/mL versus Dose (mg/L)

Kruskal-Wallis Test on Log10 CFU/mL

Dose (mg/L)	N	Median	Ave Rank	Z
0	3	0.000000000	3.5	-1.95
50	3	0.000000000	3.5	-1.95
100	3	4.399673721	8.0	0.00
200	3	5.892094603	12.0	1.73
250	3	5.973127854	13.0	2.17
Overall	15		8.0	

H = 12.23 DF = 4 P = 0.016
H = 13.04 DF = 4 P = 0.011 (adjusted for ties)

Results for: Worksheet 1(Irradiation = +)(Microbe = Ec)

Kruskal-Wallis Test: Log10 CFU/mL versus Dose (mg/L)

Kruskal-Wallis Test on Log10 CFU/mL

Dose (mg/L)	N	Median	Ave Rank	Z
0	3	2.301	2.0	-2.65
50	3	4.236	5.0	-1.51
100	3	5.272	8.0	-0.38
200	5	5.692	13.4	2.32
250	3	5.799	13.7	1.76
Overall	17		9.0	

H = 14.12 DF = 4 P = 0.007
H = 14.14 DF = 4 P = 0.007 (adjusted for ties)

Results for: Worksheet 1(Irradiation = +)(Microbe = Se)

Kruskal-Wallis Test: Log10 CFU/mL versus Dose (mg/L)

Kruskal-Wallis Test on Log10 CFU/mL

Dose (mg/L)	N	Median	Ave Rank	Z
0	3	0.000000000	2.0	-2.67
50	6	3.000000000	6.5	-1.69
100	3	4.518513940	11.0	0.53

200	3	5.763427994	14.0	1.60
250	3	5.949390007	17.0	2.67
Overall	18		9.5	

H = 16.11 DF = 4 P = 0.003
H = 16.24 DF = 4 P = 0.003 (adjusted for ties)

Results for: Worksheet 1(Irradiation = +)(Microbe = Vp)

Kruskal-Wallis Test: Log10 CFU/mL versus Dose (mg/L)

Kruskal-Wallis Test on Log10 CFU/mL

Dose (mg/L)	N	Median	Ave Rank	Z
0	3	0.000000000	5.0	-1.30
50	3	0.000000000	5.0	-1.30
100	3	0.000000000	5.0	-1.30
200	3	5.387389826	11.0	1.30
250	3	5.716003344	14.0	2.60
Overall	15		8.0	

H = 10.80 DF = 4 P = 0.029
H = 13.75 DF = 4 P = 0.008 (adjusted for ties)

Results for: Worksheet 1(Irradiation = -)(Microbe = Bs)

Kruskal-Wallis Test: Log10 CFU/mL versus Dose (mg/L)

Kruskal-Wallis Test on Log10 CFU/mL

Dose (mg/L)	N	Median	Ave Rank	Z
0	3	5.914	7.3	-0.29
50	3	5.813	5.7	-1.01
100	3	5.863	6.3	-0.72
200	3	6.121	9.3	0.58
250	3	6.179	11.3	1.44
Overall	15		8.0	

H = 3.23 DF = 4 P = 0.520

Results for: Worksheet 1(Irradiation = -)(Microbe = Ec)

Kruskal-Wallis Test: Log10 CFU/mL versus Dose (mg/L)

Kruskal-Wallis Test on Log10 CFU/mL

Dose (mg/L)	N	Median	Ave Rank	Z
0	3	6.083	6.2	-0.79
50	3	6.220	10.7	1.15
100	3	6.155	11.7	1.59
200	3	6.057	5.7	-1.01
250	3	6.072	5.8	-0.94

Overall 15 8.0
 H = 5.11 DF = 4 P = 0.276
 H = 5.12 DF = 4 P = 0.275 (adjusted for ties)

Results for: Worksheet 1(Irradiation = -)(Microbe = Se)

Kruskal-Wallis Test: Log10 CFU/mL versus Dose (mg/L)

Kruskal-Wallis Test on Log10 CFU/mL

Dose (mg/L)	N	Median	Ave Rank	Z
0	3	6.281	6.7	-0.17
50	1	6.336	11.0	1.07
100	3	6.290	6.3	-0.34
200	3	6.262	4.0	-1.52
250	3	6.354	9.7	1.35
Overall	13		7.0	

H = 4.35 DF = 4 P = 0.361

Results for: Worksheet 1(Irradiation = -)(Microbe = Vp)

Kruskal-Wallis Test: Log10 CFU/mL versus Dose (mg/L)

Kruskal-Wallis Test on Log10 CFU/mL

Dose (mg/L)	N	Median	Ave Rank	Z
0	3	7.316	3.7	-1.88
50	3	7.338	7.3	-0.29
100	3	7.435	12.0	1.73
200	3	7.371	8.7	0.29
250	3	7.389	8.3	0.14
Overall	15		8.0	

H = 5.37 DF = 4 P = 0.252
 H = 5.38 DF = 4 P = 0.251 (adjusted for ties)

Table F-2: Statistics for relative bacterial sensitivity to ultraviolet irradiation.

Descriptive Statistics: Log10 CFU/mL

Results for Species = Bs

Variable	Irradiation	Total Count	Mean	StDev	Median	IQR
Log10 CFU/mL	0	3	3.4974	0.0233	3.5051	0.0446
	1	3	1.6514	0.1560	1.6990	0.3010

Results for Species = Ec

Variable	Irradiation	Total Count	Mean	StDev	Median	IQR
Log10 CFU/mL	0	3	5.6387	0.0318	5.6551	0.0569
	1	3	3.7209	0.00998	3.7160	0.0181

Results for Species = Se

Variable	Irradiation	Total Count	Mean	StDev	Median	IQR
Log10 CFU/mL	0	3	5.9917	0.0305	5.9841	0.0596
	1	3	3.9960	0.0372	3.9956	0.0744

Results for Species = Vp

Variable	Irradiation	Total Count	Mean	StDev	Median	IQR
Log10 CFU/mL	0	3	5.6970	0.0500	5.6739	0.0916
	1	3	0.000000	0.000000	0.000000	0.000000

Table F-3: Statistics for SEM image analysis.

Descriptive Statistics: Area (μm^2), Perimeter (μm), Circularity, ECD (μm)

Variable	Treatment	Count	Mean	SE Mean	StDev	Variance	Total Minimum
Area (μm^2)	S31	176	0.08068	0.00854	0.11332	0.01284	0.00100
	U125	54	0.06578	0.00638	0.04687	0.00220	0.00100
	U250	87	19.65	3.82	35.67	1272.45	0.12
	U31	62	0.05521	0.00713	0.05613	0.00315	0.00100
	U62	72	0.1111	0.0158	0.1344	0.0181	0.0010
Perimeter (μm)	S31	176	1.399	0.105	1.388	1.926	0.124
	U125	54	1.670	0.141	1.038	1.078	0.124
	U250	87	28.39	3.95	36.80	1354.05	1.35
	U31	62	1.322	0.149	1.174	1.379	0.124
	U62	72	1.603	0.178	1.514	2.292	0.124
Circularity	S31	176	0.4379	0.0140	0.1863	0.0347	0.1154
	U125	54	0.3661	0.0261	0.1917	0.0368	0.0960
	U250	87	0.4078	0.0278	0.2593	0.0673	0.0488
	U31	62	0.4996	0.0514	0.4047	0.1638	0.0952
	U62	72	0.4741	0.0240	0.2035	0.0414	0.1168
ECD (μm)	S31	176	0.2479	0.0154	0.2037	0.0415	0.0357
	U125	54	0.2663	0.0156	0.1143	0.0131	0.0357
	U250	87	3.799	0.351	3.272	10.705	0.386

U31	62	0.2214	0.0187	0.1470	0.0216	0.0357
U62	72	0.2916	0.0282	0.2394	0.0573	0.0357

Variable	Treatment	Q1	Median	Q3	Maximum	Range
Area (μm^2)	S31	0.00325	0.03000	0.07500	0.49400	0.49300
	U125	0.03150	0.06000	0.09775	0.22000	0.21900
	U250	2.57	6.86	18.97	162.95	162.83
	U31	0.00175	0.04600	0.08925	0.24400	0.24300
	U62	0.0020	0.0750	0.1568	0.5820	0.5810
	Perimeter (μm)	S31	0.308	0.994	1.760	6.925
U125		0.865	1.430	2.400	4.493	4.369
U250		7.51	15.46	30.94	199.15	197.80
U31		0.168	1.127	2.142	5.149	5.025
U62		0.186	1.357	2.420	5.859	5.735
Circularity		S31	0.3096	0.4058	0.5290	0.9520
	U125	0.2009	0.3384	0.5079	0.8643	0.7683
	U250	0.1866	0.3527	0.6442	0.9159	0.8671
	U31	0.2483	0.4295	0.6851	3.0280	2.9328
	U62	0.3111	0.4368	0.5600	0.9520	0.8352
	ECD (μm)	S31	0.0642	0.1954	0.3090	0.7931
U125		0.1997	0.2764	0.3528	0.5293	0.4936
U250		1.809	2.955	4.915	14.404	14.018
U31		0.0468	0.2420	0.3370	0.5574	0.5217
U62		0.0505	0.3090	0.4467	0.8608	0.8251

Kruskal-Wallis Test: Area (μm^2) versus Treatment

Kruskal-Wallis Test on Area (μm^2)

Treatment	N	Median	Ave Rank	Z
S31	176	0.03000	177.0	-6.39
U125	54	0.06000	204.6	-1.28
U250	87	6.85600	399.7	13.84
U31	62	0.04600	171.0	-3.58
U62	72	0.07500	199.3	-1.90
Overall	451		226.0	

H = 195.01 DF = 4 P = 0.000

H = 195.57 DF = 4 P = 0.000 (adjusted for ties)

Kruskal-Wallis Test: Perimeter (μm) versus Treatment

Kruskal-Wallis Test on Perimeter (μm)

Treatment	N	Median	Ave Rank	Z
S31	176	0.9945	178.9	-6.14
U125	54	1.4300	219.7	-0.38
U250	87	15.4590	389.5	13.02

U31	62	1.1275	176.3	-3.23
U62	72	1.3575	191.1	-2.48
Overall	451		226.0	

H = 174.19 DF = 4 P = 0.000
H = 174.24 DF = 4 P = 0.000 (adjusted for ties)

Kruskal-Wallis Test: Circularity versus Treatment

Kruskal-Wallis Test on Circularity

Treatment	N	Median	Ave Rank	Z
S31	176	0.4058	234.3	1.09
U125	54	0.3384	184.6	-2.49
U250	87	0.3527	202.5	-1.87
U31	62	0.4295	237.4	0.74
U62	72	0.4368	255.2	2.07
Overall	451		226.0	

H = 13.08 DF = 4 P = 0.011
H = 13.09 DF = 4 P = 0.011 (adjusted for ties)

Kruskal-Wallis Test: ECD (μm) versus Treatment

Kruskal-Wallis Test on ECD (μm)

Treatment	N	Median	Ave Rank	Z
S31	176	0.1954	177.0	-6.39
U125	54	0.2764	204.6	-1.28
U250	87	2.9545	399.7	13.84
U31	62	0.2420	171.0	-3.58
U62	72	0.3090	199.3	-1.90
Overall	451		226.0	

H = 195.01 DF = 4 P = 0.000
H = 195.57 DF = 4 P = 0.000 (adjusted for ties)

Table F-4: Statistics for Zetasizer analysis.

Descriptive Statistics: Z-Ave Diameter (nm)

Variable	Treatment	Total Count	Mean	SE Mean	StDev	Variance
Z-Ave Diameter (nm)	Centrifuged	91	42.34	1.75	16.70	278.79
	Filtered	91	124.36	1.93	18.37	337.35
	Sonicated	91	149.61	0.344	3.28	10.77
	Untreated	91	440.31	4.38	41.79	1746.71

Variable	Treatment	Minimum	Q1	Median	Q3	Maximum
Z-Ave Diameter (nm)	Centrifuged	22.45	31.29	37.68	48.03	99.65
	Filtered	108.40	113.60	118.60	125.20	186.70
	Sonicated	143.20	147.30	149.00	151.60	156.60
	Untreated	369.40	408.20	425.40	467.40	599.20

Descriptive Statistics: Diameter Peak 1 (nm)

Variable	Treatment	Total				
		Count	Mean	SE Mean	StDev	Variance
Diameter Peak 1 (nm)	Centrifuged	91	131.38	4.74	45.21	2043.69
	Filtered	91	167.40	3.67	35.02	1226.45
	Sonicated	91	175.43	0.807	7.70	59.31
	Untreated	91	382.39	5.53	52.71	2778.73

Variable	Treatment	Minimum	Q1	Median	Q3	Maximum
Diameter Peak 1 (nm)	Centrifuged	79.07	102.30	124.50	145.80	351.20
	Filtered	137.10	151.20	156.00	164.60	310.60
	Sonicated	158.60	169.80	175.50	180.40	198.50
	Untreated	285.60	349.30	376.90	424.10	511.30

Descriptive Statistics: Z-Ave Diameter (nm), Diameter Peak 1 (nm)

Results for [dC60] (mg/L) = 50

Variable	Treatment	Total				
		Count	Mean	SE Mean	StDev	Variance
Z-Ave Diameter (nm)	Centrifuged	13	55.33	5.28	19.04	362.58
	Filtered	13	123.52	1.25	4.50	20.21
	Sonicated	13	154.84	0.472	1.70	2.90
	Untreated	13	462.2	15.6	56.4	3176.4

Diameter Peak 1 (nm)	Centrifuged	13	146.98	7.39	26.64	709.48
	Filtered	13	157.03	2.45	8.82	77.74
	Sonicated	13	172.28	2.99	10.76	115.86
	Untreated	13	314.5	12.1	43.6	1898.9

Variable	Treatment	Minimum	Q1	Median	Q3	Maximum
Z-Ave Diameter (nm)	Centrifuged	39.18	41.58	45.82	65.71	99.65
	Filtered	117.90	120.25	122.10	126.10	134.40
	Sonicated	150.40	154.25	154.80	156.15	156.60
	Untreated	369.4	420.8	474.2	484.6	599.2

Diameter Peak 1 (nm)	Centrifuged	106.00	137.30	145.80	151.50	222.50
	Filtered	143.40	150.10	155.90	161.15	175.20
	Sonicated	162.30	163.50	168.10	179.45	198.50
	Untreated	286.0	290.2	309.6	316.4	453.6

Variable	Treatment	Skewness
Z-Ave Diameter (nm)	Centrifuged	1.36
	Filtered	1.23
	Sonicated	-1.58
	Untreated	0.74
Diameter Peak 1 (nm)	Centrifuged	1.77
	Filtered	0.70
	Sonicated	1.39
	Untreated	3.10

Results for [dC60] (mg/L) = 100

Variable	Treatment	Total				
		Count	Mean	SE Mean	StDev	Variance
Z-Ave Diameter (nm)	Centrifuged	13	40.38	3.47	12.50	156.25
	Filtered	13	159.34	7.34	26.47	700.53
	Sonicated	13	152.62	0.517	1.86	3.47
	Untreated	13	491.38	8.60	31.03	962.59
Diameter Peak 1 (nm)	Centrifuged	13	133.23	4.54	16.38	268.23
	Filtered	13	225.0	17.1	61.7	3812.3
	Sonicated	13	172.81	1.49	5.36	28.78
	Untreated	13	369.08	9.63	34.72	1205.21

Variable	Treatment	Minimum	Q1	Median	Q3	Maximum
Z-Ave Diameter (nm)	Centrifuged	27.92	32.23	37.08	42.12	74.12
	Filtered	118.30	132.25	175.00	180.20	186.70
	Sonicated	149.40	151.45	152.80	153.45	156.60
	Untreated	445.20	461.75	486.80	524.90	527.90
Diameter Peak 1 (nm)	Centrifuged	102.50	126.40	131.00	145.10	163.30
	Filtered	137.5	162.4	240.6	280.4	310.6
	Sonicated	164.80	169.55	171.10	175.55	185.30
	Untreated	330.30	345.15	357.80	387.50	446.00

Variable	Treatment	Skewness
Z-Ave Diameter (nm)	Centrifuged	1.96
	Filtered	-0.73
	Sonicated	0.41
	Untreated	-0.13
Diameter Peak 1 (nm)	Centrifuged	-0.05
	Filtered	-0.11
	Sonicated	1.12
	Untreated	1.29

Results for [dC60] (mg/L) = 200

Variable	Treatment	Total				
		Count	Mean	SE Mean	StDev	Variance
Z-Ave Diameter (nm)	Centrifuged	13	38.05	3.96	14.29	204.20

	Filtered	13	121.05	0.839	3.03	9.15
	Sonicated	13	146.68	0.470	1.69	2.87
	Untreated	13	433.7	11.2	40.5	1642.7
Diameter Peak 1 (nm)	Centrifuged	13	201.0	19.3	69.5	4831.8
	Filtered	13	157.88	3.60	12.99	168.63
	Sonicated	13	173.28	1.80	6.50	42.22
	Untreated	13	355.34	7.01	25.28	639.00
Variable	Treatment	Minimum	Q1	Median	Q3	Maximum
Z-Ave Diameter (nm)	Centrifuged	27.99	28.64	33.77	38.64	70.47
	Filtered	116.10	118.05	122.10	123.50	125.30
	Sonicated	144.50	145.15	146.60	147.90	149.70
	Untreated	385.9	405.0	423.6	445.8	535.6
Diameter Peak 1 (nm)	Centrifuged	137.0	153.3	193.5	213.7	351.2
	Filtered	138.40	146.35	158.90	164.50	185.90
	Sonicated	160.80	168.95	171.70	178.50	183.30
	Untreated	285.60	342.50	365.90	371.75	376.90
Variable	Treatment	Skewness				
Z-Ave Diameter (nm)	Centrifuged	1.85				
	Filtered	-0.41				
	Sonicated	0.53				
	Untreated	1.56				
Diameter Peak 1 (nm)	Centrifuged	1.54				
	Filtered	0.48				
	Sonicated	-0.17				
	Untreated	-1.94				
Results for [dC60] (mg/L) = 250						
Variable	Treatment	Total				
Z-Ave Diameter (nm)	Centrifuged	Count	Mean	SE Mean	StDev	Variance
	Filtered	13	33.48	2.62	9.44	89.18
	Sonicated	13	127.01	1.64	5.91	34.93
	Untreated	13	146.12	0.334	1.21	1.45
	Untreated	13	430.10	7.90	28.49	811.66
Diameter Peak 1 (nm)	Centrifuged	13	128.33	8.13	29.31	859.36
	Filtered	13	172.55	6.34	22.87	522.95
	Sonicated	13	173.34	2.01	7.26	52.74
	Untreated	13	371.61	8.04	29.01	841.32
Variable	Treatment	Minimum	Q1	Median	Q3	Maximum
Z-Ave Diameter (nm)	Centrifuged	26.46	27.04	29.14	36.68	58.46
	Filtered	114.90	122.25	129.20	131.30	136.10
	Sonicated	143.20	145.65	146.10	147.00	147.80
	Untreated	404.60	407.75	419.60	441.55	490.70
Diameter Peak 1 (nm)	Centrifuged	92.21	96.95	129.90	144.00	189.90
	Filtered	137.10	157.05	164.60	187.85	217.50

	Sonicated	158.60	167.15	175.00	178.35	185.30
	Untreated	309.80	355.70	367.40	395.40	413.60
Variable	Treatment	Skewness				
Z-Ave Diameter (nm)	Centrifuged	1.87				
	Filtered	-0.51				
	Sonicated	-1.00				
	Untreated	1.42				
Diameter Peak 1 (nm)	Centrifuged	0.53				
	Filtered	0.42				
	Sonicated	-0.54				
	Untreated	-0.51				
Results for [dC60] (mg/L) = 500						
Variable	Treatment	Total	Mean	SE Mean	StDev	Variance
Z-Ave Diameter (nm)	Centrifuged	13	38.61	5.63	20.30	412.23
	Filtered	13	113.50	0.462	1.67	2.78
	Sonicated	13	148.92	0.476	1.72	2.95
	Untreated	13	417.67	8.46	30.52	931.47
Diameter Peak 1 (nm)	Centrifuged	13	116.50	3.69	13.29	176.67
	Filtered	13	152.08	1.68	6.07	36.85
	Sonicated	13	177.84	1.40	5.04	25.44
	Untreated	13	391.47	9.11	32.86	1079.81
Variable	Treatment	Minimum	Q1	Median	Q3	Maximum
Z-Ave Diameter (nm)	Centrifuged	22.45	23.48	36.20	45.64	94.34
	Filtered	111.00	112.20	113.60	114.60	117.00
	Sonicated	147.20	148.00	148.50	149.45	154.00
	Untreated	382.10	404.25	406.80	421.55	504.00
Diameter Peak 1 (nm)	Centrifuged	87.64	109.30	115.80	127.45	137.70
	Filtered	139.10	149.95	153.60	155.80	161.40
	Sonicated	168.90	172.75	180.10	181.70	183.90
	Untreated	317.30	372.40	395.50	413.40	436.60
Variable	Treatment	Skewness				
Z-Ave Diameter (nm)	Centrifuged	1.91				
	Filtered	0.41				
	Sonicated	2.38				
	Untreated	2.18				
Diameter Peak 1 (nm)	Centrifuged	-0.34				
	Filtered	-1.05				
	Sonicated	-0.55				
	Untreated	-0.76				

Results for [dC60] (mg/L) = 750

Variable	Treatment	Total Count	Mean	SE Mean	StDev	Variance
Z-Ave Diameter (nm)	Centrifuged	13	44.42	4.14	14.92	222.61
	Filtered	13	114.23	0.647	2.33	5.45
	Sonicated	13	149.12	0.350	1.26	1.60
	Untreated	13	427.12	6.12	22.08	487.69
Diameter Peak 1 (nm)	Centrifuged	13	96.83	1.95	7.03	49.45
	Filtered	13	154.83	1.97	7.10	50.41
	Sonicated	13	180.16	1.55	5.57	31.04
	Untreated	13	431.53	9.62	34.69	1203.69

Variable	Treatment	Minimum	Q1	Median	Q3	Maximum
Z-Ave Diameter (nm)	Centrifuged	31.44	35.35	37.68	47.73	78.77
	Filtered	108.40	113.45	114.20	115.55	118.90
	Sonicated	146.00	148.45	149.50	150.15	150.40
	Untreated	404.10	410.80	416.40	449.40	467.40
Diameter Peak 1 (nm)	Centrifuged	86.12	90.72	96.32	103.00	108.00
	Filtered	142.70	151.25	155.20	159.45	169.80
	Sonicated	168.90	177.20	178.90	183.15	190.00
	Untreated	362.60	405.85	424.10	459.55	484.50

Variable	Treatment	Skewness
Z-Ave Diameter (nm)	Centrifuged	1.71
	Filtered	-0.72
	Sonicated	-1.33
	Untreated	0.94

Diameter Peak 1 (nm)	Centrifuged	-0.07
	Filtered	0.13
	Sonicated	0.04
	Untreated	-0.42

Results for [dC60] (mg/L) = 1000

Variable	Treatment	Total Count	Mean	SE Mean	StDev	Variance
Z-Ave Diameter (nm)	Centrifuged	13	46.08	4.94	17.81	317.03
	Filtered	13	111.85	0.484	1.75	3.05
	Sonicated	13	148.97	0.427	1.54	2.38
	Untreated	13	420.08	5.52	19.92	396.81
Diameter Peak 1 (nm)	Centrifuged	13	96.76	2.34	8.43	71.08
	Filtered	13	152.39	1.20	4.32	18.67
	Sonicated	13	178.31	2.50	9.02	81.36
	Untreated	13	443.23	9.42	33.98	1154.35

Variable	Treatment	Minimum	Q1	Median	Q3	Maximum
Z-Ave Diameter (nm)	Centrifuged	27.93	32.72	48.03	51.39	94.82

250	13	419.6	42.0	-0.58
500	13	406.8	28.3	-2.61
750	13	416.4	40.7	-0.78
1000	13	415.6	34.6	-1.68
Overall	91		46.0	

H = 29.31 DF = 6 P = 0.000
H = 29.32 DF = 6 P = 0.000 (adjusted for ties)

Results for: Treatment = Sonicated

Kruskal-Wallis Test: Z-Ave Diameter (nm) versus [dC60] (mg/L)

Kruskal-Wallis Test on Z-Ave Diameter (nm)

[dC60] (mg/L)	N	Median	Ave Rank	Z
50	13	154.8	82.3	5.35
100	13	152.8	71.9	3.82
200	13	146.6	19.9	-3.84
250	13	146.1	14.2	-4.69
500	13	148.5	42.2	-0.56
750	13	149.5	48.0	0.29
1000	13	148.6	43.5	-0.37
Overall	91		46.0	

H = 68.98 DF = 6 P = 0.000
H = 69.00 DF = 6 P = 0.000 (adjusted for ties)

Results for: Treatment = Filtered

Kruskal-Wallis Test: Z-Ave Diameter (nm) versus [dC60] (mg/L)

Kruskal-Wallis Test on Z-Ave Diameter (nm)

[dC60] (mg/L)	N	Median	Ave Rank	Z
50	13	122.1	60.5	2.14
100	13	175.0	77.1	4.58
200	13	122.1	55.3	1.37
250	13	129.2	67.9	3.23
500	13	113.6	21.5	-3.62
750	13	114.2	27.3	-2.76
1000	13	111.5	12.5	-4.94
Overall	91		46.0	

H = 71.08 DF = 6 P = 0.000
H = 71.10 DF = 6 P = 0.000 (adjusted for ties)

Results for: Treatment = Centrifuged

Kruskal-Wallis Test: Z-Ave Diameter (nm) versus [dC60] (mg/L)

Kruskal-Wallis Test on Z-Ave Diameter (nm)

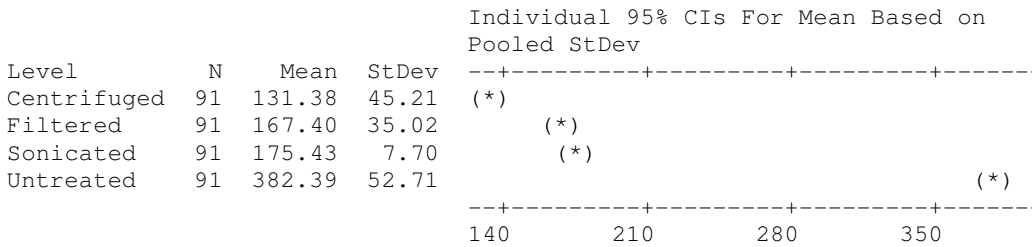
[dC60] (mg/L)	N	Median	Ave Rank	Z
50	13	45.82	69.9	3.53
100	13	37.08	45.2	-0.11
200	13	33.77	37.3	-1.28
250	13	29.14	27.7	-2.70
500	13	36.20	36.0	-1.47
750	13	37.68	52.5	0.95
1000	13	48.03	53.4	1.09
Overall	91		46.0	

H = 21.99 DF = 6 P = 0.001

One-way ANOVA: Diameter Peak 1 (nm) versus Treatment

Source	DF	SS	MS	F	P
Treatment	3	3534623	1178208	771.56	0.000
Error	360	549736	1527		
Total	363	4084359			

S = 39.08 R-Sq = 86.54% R-Sq(adj) = 86.43%



Pooled StDev = 39.08

Results for: Treatment = Untreated

Kruskal-Wallis Test: Diameter Peak 1 (nm) versus [dC60] (mg/L)

Kruskal-Wallis Test on Diameter Peak 1 (nm)

[dC60] (mg/L)	N	Median	Ave Rank	Z
50	13	309.6	13.9	-4.74
100	13	357.8	37.0	-1.32

200	13	365.9	32.2	-2.04
250	13	367.4	40.6	-0.79
500	13	395.5	52.1	0.90
750	13	424.1	71.0	3.69
1000	13	448.7	75.2	4.30
Overall	91		46.0	

H = 52.99 DF = 6 P = 0.000
H = 52.99 DF = 6 P = 0.000 (adjusted for ties)

Results for: Treatment = Sonicated

Kruskal-Wallis Test: Diameter Peak 1 (nm) versus [dC60] (mg/L)

Kruskal-Wallis Test on Diameter Peak 1 (nm)

[dC60] (mg/L)	N	Median	Ave Rank	Z
50	13	168.1	32.7	-1.97
100	13	171.1	35.8	-1.51
200	13	171.7	39.1	-1.02
250	13	175.0	40.1	-0.87
500	13	180.1	56.4	1.54
750	13	178.9	63.5	2.58
1000	13	176.8	54.5	1.25
Overall	91		46.0	

H = 15.89 DF = 6 P = 0.014
H = 15.89 DF = 6 P = 0.014 (adjusted for ties)

Results for: Treatment = Filtered

Kruskal-Wallis Test: Diameter Peak 1 (nm) versus [dC60] (mg/L)

Kruskal-Wallis Test on Diameter Peak 1 (nm)

[dC60] (mg/L)	N	Median	Ave Rank	Z
50	13	155.9	43.0	-0.44
100	13	240.6	70.4	3.60
200	13	158.9	46.0	-0.01
250	13	164.6	60.9	2.19
500	13	153.6	31.5	-2.13
750	13	155.2	39.7	-0.93
1000	13	152.8	30.5	-2.29
Overall	91		46.0	

H = 24.54 DF = 6 P = 0.000
H = 24.54 DF = 6 P = 0.000 (adjusted for ties)

Results for: Treatment = Centrifuged

Kruskal-Wallis Test: Diameter Peak 1 (nm) versus [dC60] (mg/L)

Kruskal-Wallis Test on Diameter Peak 1 (nm)

[dC60] (mg/L)	N	Median	Ave Rank	Z
50	13	145.80	65.3	2.85
100	13	131.00	55.0	1.33
200	13	193.50	80.2	5.04
250	13	129.90	47.0	0.14
500	13	115.80	40.1	-0.87
750	13	96.32	16.8	-4.31
1000	13	96.11	17.7	-4.17
Overall	91		46.0	

H = 61.71 DF = 6 P = 0.000

H = 61.71 DF = 6 P = 0.000 (adjusted for ties)

Table F-5: Statistics for UV-vis absorbance data.

Kruskal-Wallis Test: Standard Wavelength (300 nm) Absorbance versus Treatment

Kruskal-Wallis Test on Standard Wavelength Absorbance

Treatment	N	Median	Ave Rank	Z
Centrifuged	21	0.4870	36.5	-1.30
Filtered	21	0.5970	42.9	0.08
Sonicated	20	0.7245	47.2	0.99
Untreated	22	0.6065	43.5	0.23
Overall	84		42.5	

H = 2.06 DF = 3 P = 0.561

H = 2.06 DF = 3 P = 0.561 (adjusted for ties)

Kruskal-Wallis Test: Output Wavelength (254 nm) Absorbance versus Treatment

Kruskal-Wallis Test on Output Wavelength Absorbance

Treatment	N	Median	Ave Rank	Z
Centrifuged	21	0.7250	38.4	-0.89
Filtered	21	0.8800	44.3	0.38
Sonicated	20	1.0425	45.0	0.54
Untreated	22	0.8800	42.4	-0.02
Overall	84		42.5	

H = 0.93 DF = 3 P = 0.819

H = 0.93 DF = 3 P = 0.819 (adjusted for ties)

APPENDIX G

MATLAB code for mathematical modeling

Table G-1: MATLAB code

```
function scenarios

% Michael J. Berez April 2010
%
% This function is called by simply typing the name 'scenarios' at the command line.
%
% It calculates a set of preselected values for our experiments and creates plots of
the
% results.
%
% This program currently will not properly handle different values for ECN_0 and RIN_0

prog = 2; % There are two programs, 1 = calculates maximum sensitivities, 2 = does
only one iteration and gives sensitivity plot for one set of parameters

if (prog == 1)

    i = 300; % Number of iterations
    step = 10; % Step change in parameter
    stepmatrix = zeros(i,1);
    paramsens = zeros(1,5);
    sensmatrix = zeros(i,5);

    for j=step:step:i*step
        stepmatrix(j/step,1) = j;
```

```

        [paramsens] = sirdrive(prog, 300, 100000, 100000, 115.5245, 0, 10000, j, 250);
% Put j in 8th or 9th position. It will step through this parameter.
        sensmatrix(j/step,:)=paramsens;
        j/step
    end

    figure
    plot (stepmatrix,sensmatrix(:,4),'k--',stepmatrix,sensmatrix(:,5),'k-')
    title({'Maximum Sensitivity Plot'},'fontweight','bold','fontsize',12)
    axis([0 1.1*max(stepmatrix) 0 1.2*(max(sensmatrix(:,5)))]
    xlabel({'mg/L';' '},'fontweight','bold')
    ylabel ('Sensitivity','fontweight','bold')
    labelstring1 = ['EC50'];
    labelstring2 = ['Dose'];
    legend(labelstring1,labelstring2,'location','best')

else

        sirdrive(prog, 600, 100000, 100000, 85, 0, 10000, 250, 250); % This runs if prog =
2 and each parameter can be set individually.

end

% sirdrive(program, timesteps, ECN_0, RIN_0, LUV_init, abs, k^-1, EC50, Dose);
% Prog = program that is running
% timesteps is the final time step (starts at 0)
% ECN_0 = Initial bacterial number using EC50 equation
% RIN_0 = Residual bacterial number after absorptive effects, used by
%         traditional kinetic inactivation equation
% LUV_init = initial lamp UV intensity in mW/cm^2
% abs = absorption ratio (post-particle field intensity/emitted UV
%         intensity), used by traditional equation (range 0 to 1).
% k = kinetic inactivation rate constant. Higher number associated with
%         more resistant microbe. The value to enter here is the dose required to

```

```

%      inactivate a given microbe by >99% which is k^-1.  These values are given in
%      references such as Aquacultural Engineering (Fred Wheaton)
% EC50 = effective concentration to protect 50% of microbes in one minute
% dose = concentration of protecting particles

function paramsens=sirdrive(prog, timesteps, ECN_0, RIN_0, LUV_init, abs, k, EC50,
dose);

% SIRDRIVE is driver for sirode and is called by scenarios.m
%
% Function to solve a compartment-type model using input parameters and then plot
%      the results.
%
% Requires function sirode to solve differential equation
%
% THE PROGRAM
% setting some values
k=1/k; % The k entered is actually the dose needed to kill a given microbe.  k is 1
divided by that dose.  So inverting here.
name = {'intensity', 'absorption', 'kinetic inactivation rate constant (k)', 'EC50 of
fullerol (mg/L)', 'dose of fullerol (mg/L)'};
N_0=[ECN_0, RIN_0];
sensitivity = 0.05; % Sensitivity level for the parameters p (range 0-1)
paramsens = zeros(1,5); % For recording parameter sensitivities
p=[LUV_init, abs, k, EC50, dose]; % This vector used for sensitivity testing and is
the vector to which things are set back.

times=[]; % Initialize time vector
pops=[]; % Initialize population vector
times1=[]; % Initialize time vector for negative sensitivity testing
pops1=[]; % Initialize population vector for negative sensitivity testing
times2=[]; % Initialize time vector for positive sensitivity testing

```

```

pops2=[]; % Initialize population vector for positive sensitivity testing

for i = 4:5 % This program will properly calculate sensitivity for EC50 and Dose only.
These are p(4) and p(5).

    % Without sensitivity change
    p0 = p; % Reset all values back to original
    PUV_init = p0(1) - (p0(2) * p0(1));

    for j = 1:timesteps % Iterates through number of timesteps.
        [t,pop] = ode15s('sirode',[j-1 j],[ECN_0, p0(1), PUV_init, RIN_0 ],[], p0(3),
p0(4), p0(5));
        times = [times;t(1:length(t)-1)]; % Adds vector(s) from ode15s to previously
calculated vectors and subtracts duplicated number that resulted from ode for
timeframe j-1 to j
        pops = [pops;pop(1:length(t)-1,:)]; % Same here
        ECN_0 = pop(end,1); % Sets the last value as first value for next iteration in
the 'for' loop
        p0(1) = pop(end,2);
        PUV_init = pop(end,3);
        RIN_0 = pop(end,4);
    end

    % Sensitivity: This section repeats the above for negative and positive of the
various constants keeping others the same
    % Set one parameter at a time, sensitivity * 100% of initial value
    % Reset / hold others at initial values
    % Calculate effect survival ratio

    % Negative sensitivity
    ECN_0=N_0(1); % Reset to original bacterial numbers
    RIN_0=N_0(2);

    p1 = p; % Reset all values back to original

```

```

p1(i) = (1 - sensitivity) * p(i);
PUV_init = p1(1) - (p1(2) * p1(1));

for j = 1:timesteps % Iterates through number of timesteps.
    [t1,pop1] = ode15s('sirode',[j-1 j],[ECN_0, p1(1), PUV_init, RIN_0 ],[],
p1(3), p1(4), p1(5));
    times1 = [times1;t1(1:length(t1)-1)]; % Adds vector(s) from ode15s to
previously calculated vectors and subtracts duplicated number that resulted from ode
for timeframe j-1 to j
    pops1 = [pops1;pop1(1:length(t1)-1,:)]; % Same here
    ECN_0 = pop1(end,1); % Sets the last value as first value for next iteration
in the 'for' loop
    p1(1) = pop1(end,2);
    PUV_init = pop1(end,3);
    RIN_0 = pop1(end,4);
end

% Positive sensitivity
ECN_0=N_0(1); % Reset to original bacterial numbers
RIN_0=N_0(2);

p2 = p; % Reset all vaues back to original
p2(i) = (1 + sensitivity) * p(i);
PUV_init = p2(1) - (p2(2) * p2(1));

for j = 1:timesteps % Iterates through number of timesteps.
    [t2,pop2] = ode15s('sirode',[j-1 j],[ECN_0, p2(1), PUV_init, RIN_0 ],[],
p2(3), p2(4), p2(5));
    times2 = [times2;t2(1:length(t2)-1)]; % Adds vector(s) from ode15s to
previously calculated vectors and subtracts duplicated number that resulted from ode
for timeframe j-1 to j
    pops2 = [pops2;pop2(1:length(t2)-1,:)]; % Same here
    ECN_0 = pop2(end,1); % Sets the last value as first value for next iteration
in the 'for' loop
    p2(1) = pop2(end,2);

```

```

    PUV_init = pop2(end,3);
    RIN_0 = pop2(end,4);
end

% Calculates sensitivity vector
S = zeros(length(pops),1); % Initialize sensitivity vector
for z=1:length(pops)
    S(z,1) = (((pops2(z,1)-pops1(z,1))/pops(z,1))/((p2(i)-p1(i))/p(i))); % creates
vector of sensitivity values
end

S_abs=sqrt(real(S).^2 + imag(S).^2); % Creates new vector of absolute values in S
vector
S_index = find(S_abs == max(S_abs)); % Finds position of maximum sensitivity value

if (prog == 2)
    % Plot all on a single figure, but separate figures for each variable
    scrsz = get(0, 'ScreenSize');
    figure('Position',[20 scrsz(4)/16 scrsz(3)/1.5 scrsz(4)/1.2], 'Name', 'Survival
Ratio Responses', 'NumberTitle', 'off', 'color', 'white')

    subplot(3,1,1)
    plot (times, (pops(:,1)/pops(1,1)), 'k-
',times1, (pops1(:,1)/pops1(1,1)), 'r:',times2, (pops2(:,1)/pops2(1,1)), 'b:')
    title({'Survival Ratio Response and Sensitivity Plots';' ';'EC50 Dose-
Response Method'}, 'fontweight', 'bold', 'fontsize', 12, 'fontname', 'times')
    axis([0 timesteps 0 1.1])
    xlabel ({'time (seconds)';' '}, 'fontweight', 'bold', 'fontname', 'times')
    ylabel ('N/N_0', 'fontweight', 'bold', 'fontname', 'times')
    labelstring1 = ['- ', num2str(sensitivity*100), '%'];
    labelstring2 = ['+ ', num2str(sensitivity*100), '%'];
    legend('0 %', labelstring1, labelstring2, 'location', 'best')

    subplot(3,1,2)
    plot (times, S_abs(:,1), 'k-')

```

```

        title('Sensitivity','fontweight','bold','fontsize',12,'fontname','times')
        axis([0 timesteps 0 1.1*S_abs(S_index,1)])
        xlabel ({'time (seconds)';' '},'fontweight','bold','fontname','times')
        ylabel ('N/N_0','fontweight','bold','fontname','times')

        subplot(3,1,3)
        plot(times,(pops(:,4)/pops(1,4)), 'k-')
        title ('k*I Method','fontweight','bold','fontsize',12,'fontname','times')
        axis([0 timesteps 0 1.1])
        labelstring3 = ['          EC50 = ',num2str(EC50),' mg/L; Dose = ',num2str(dose),' mg/L; k = ',num2str(k),' cm^2/muWs; Intensity = ',num2str(pops(1,3)),' muW/cm^2'];
        labelstring4 = ['Effect on survival ratio by +/- ',num2str(sensitivity*100),'% change in ',name{i},'. Maximum Sensitivity = ',num2str(S_abs(S_index,1))];
        xlabel ({'time (seconds)';' ';labelstring3;'
;labelstring4;},'fontweight','bold','fontname','times')
        ylabel ('N/N_0','fontweight','bold','fontname','times')

        disp(' ')
        disp(['The maximum sensitivity of the survival ratio to ',name{i},' = ',num2str(S_abs(S_index,1)),' for EC50 method.'])
        disp(' ')
        disp(['End survival ratio = ',num2str(pops(length(pops(:,1)),1)/pops(1,1))])
        disp(' ')

        else
            paramsens(i) = S_abs(S_index,1); % Skips above plot if prog = 1 and sends
paramsens back to scenarios.m

        end

        % Reinitialize the vectors for next iteration of the i loop (next parameter for
sensitivity testing)

```

```
times=[]; % Initialize time vector
pops=[]; % Initialize population vector
times1=[]; % Initialize time vector for negative sensitivity testing
pops1=[]; % Initialize population vector for negative sensitivity testing
times2=[]; % Initialize time vector for positive sensitivity testing
pops2=[]; % Initialize population vector for positive sensitivity testing
```

```
end
```

```
function dpop = sirode(t, pop, flag, k, EC50, dose);
```

```
% SIRODE - odefile for the sirdrive.m file.
```

```
%
```

```
% flag is a placeholder variable for the ode solver options
```

```
dpop = zeros(4,1); %Initialize vector
```

```
dpop(1) = - pop(1) * EC50/(60*EC50+60*dose); % The change per time as determined by  
ODE solver for EC50 D-R Method.
```

```
dpop(2) = 0; % Keeping UV intensity emitted from lamp constant
```

```
dpop(3) = 0; % UV light left after particle interactions (scattering or absorption) if  
absorption greater than zero. Assumes particle interactions are constant and  
attenuate the light intensity only.
```

```
dpop(4) = - pop(4)*k*pop(3); % The change per time as determined by ODE solver for  
EC50 D-R Method.
```

APPENDIX H

Visual Molecular Dynamics (VMD) code for Figure 1-2 and Figure 3-1

Table H-1: VMD code for C₆₀ fullerene for Figure 1-2.

ATOM	1	C	MOL	1	3.451	0.685	0.000	inf	inf
ATOM	2	C1	MOL	1	3.451	-0.685	0.000	inf	inf
ATOM	3	C2	MOL	1	-3.451	0.685	0.000	inf	inf
ATOM	4	C3	MOL	1	-3.451	-0.685	0.000	inf	inf
ATOM	5	C4	MOL	1	0.685	0.000	3.451	inf	inf
ATOM	6	C5	MOL	1	-0.685	0.000	3.451	inf	inf
ATOM	7	C6	MOL	1	0.685	0.000	-3.451	inf	inf
ATOM	8	C7	MOL	1	-0.685	0.000	-3.451	inf	inf
ATOM	9	C8	MOL	1	0.000	3.451	0.685	inf	inf
ATOM	10	C9	MOL	1	0.000	3.451	-0.685	inf	inf
ATOM	11	C10	MOL	1	0.000	-3.451	0.685	inf	inf
ATOM	12	C11	MOL	1	0.000	-3.451	-0.685	inf	inf
ATOM	13	C12	MOL	1	3.004	1.409	1.172	inf	inf
ATOM	14	C13	MOL	1	3.004	1.409	-1.172	inf	inf
ATOM	15	C14	MOL	1	3.004	-1.409	1.172	inf	inf
ATOM	16	C15	MOL	1	3.004	-1.409	-1.172	inf	inf
ATOM	17	C16	MOL	1	-3.004	1.409	1.172	inf	inf
ATOM	18	C17	MOL	1	-3.004	1.409	-1.172	inf	inf
ATOM	19	C18	MOL	1	-3.004	-1.409	1.172	inf	inf
ATOM	20	C19	MOL	1	-3.004	-1.409	-1.172	inf	inf
ATOM	21	C20	MOL	1	1.409	1.172	3.004	inf	inf
ATOM	22	C21	MOL	1	1.409	-1.172	3.004	inf	inf
ATOM	23	C22	MOL	1	-1.409	1.172	3.004	inf	inf
ATOM	24	C23	MOL	1	-1.409	-1.172	3.004	inf	inf
ATOM	25	C24	MOL	1	1.409	1.172	-3.004	inf	inf
ATOM	26	C25	MOL	1	1.409	-1.172	-3.004	inf	inf
ATOM	27	C26	MOL	1	-1.409	1.172	-3.004	inf	inf
ATOM	28	C27	MOL	1	-1.409	-1.172	-3.004	inf	inf
ATOM	29	C28	MOL	1	1.172	3.004	1.409	inf	inf
ATOM	30	C29	MOL	1	-1.172	3.004	1.409	inf	inf
ATOM	31	C30	MOL	1	1.172	3.004	-1.409	inf	inf
ATOM	32	C31	MOL	1	-1.172	3.004	-1.409	inf	inf
ATOM	33	C32	MOL	1	1.172	-3.004	1.409	inf	inf
ATOM	34	C33	MOL	1	-1.172	-3.004	1.409	inf	inf
ATOM	35	C34	MOL	1	1.172	-3.004	-1.409	inf	inf
ATOM	36	C35	MOL	1	-1.172	-3.004	-1.409	inf	inf
ATOM	37	C36	MOL	1	2.581	0.724	2.280	inf	inf
ATOM	38	C37	MOL	1	2.581	0.724	-2.280	inf	inf
ATOM	39	C38	MOL	1	2.581	-0.724	2.280	inf	inf
ATOM	40	C39	MOL	1	2.581	-0.724	-2.280	inf	inf
ATOM	41	C40	MOL	1	-2.581	0.724	2.280	inf	inf

ATOM	42	C41	MOL	1	-2.581	0.724	-2.280	inf	inf
ATOM	43	C42	MOL	1	-2.581	-0.724	2.280	inf	inf
ATOM	44	C43	MOL	1	-2.581	-0.724	-2.280	inf	inf
ATOM	45	C44	MOL	1	0.724	2.280	2.581	inf	inf
ATOM	46	C45	MOL	1	0.724	-2.280	2.581	inf	inf
ATOM	47	C46	MOL	1	-0.724	2.280	2.581	inf	inf
ATOM	48	C47	MOL	1	-0.724	-2.280	2.581	inf	inf
ATOM	49	C48	MOL	1	0.724	2.280	-2.581	inf	inf
ATOM	50	C49	MOL	1	0.724	-2.280	-2.581	inf	inf
ATOM	51	C50	MOL	1	-0.724	2.280	-2.581	inf	inf
ATOM	52	C51	MOL	1	-0.724	-2.280	-2.581	inf	inf
ATOM	53	C52	MOL	1	2.280	2.581	0.724	inf	inf
ATOM	54	C53	MOL	1	-2.280	2.581	0.724	inf	inf
ATOM	55	C54	MOL	1	2.280	2.581	-0.724	inf	inf
ATOM	56	C55	MOL	1	-2.280	2.581	-0.724	inf	inf
ATOM	57	C56	MOL	1	2.280	-2.581	0.724	inf	inf
ATOM	58	C57	MOL	1	-2.280	-2.581	0.724	inf	inf
ATOM	59	C58	MOL	1	2.280	-2.581	-0.724	inf	inf
ATOM	60	C59	MOL	1	-2.280	-2.581	-0.724	inf	inf
TER									

Table H-2: VMD code for derivatized C₆₀ fullerene (fullerol) for Figure 3-1.

REMARK	This PDB file is created by CS Chem3D.								
SEQRES	1		1	MOL					
HETATM	1	C	MOL	1	3.669	0.747	-0.005		
C									
HETATM	2	H	MOL	1	-5.166	-1.690	1.892		
H									
HETATM	3	C19	MOL	1	-3.298	-1.685	-1.361		
C									
HETATM	4	O	MOL	1	1.129	-0.058	-5.344		
O									
HETATM	5	H	MOL	1	4.184	-1.932	1.517		
H									
HETATM	6	O	MOL	1	1.848	-4.544	-2.282		
O									
HETATM	7	H	MOL	1	3.565	-1.160	3.090		
H									
HETATM	8	C10	MOL	1	0.027	-3.779	0.637		
C									
HETATM	9	H	MOL	1	4.145	-1.907	-1.653		
H									

HETATM	10	C21	MOL	1	1.505	-1.369	3.207
C							
HETATM	11	C27	MOL	1	-1.547	-1.320	-3.413
C							
HETATM	12	C1	MOL	1	3.630	-0.764	-0.040
C							
HETATM	13	H	MOL	1	-4.172	1.807	-1.595
H							
HETATM	14	C45	MOL	1	0.764	-2.595	2.683
C							
HETATM	15	H	MOL	1	-3.055	-3.737	-1.069
H							
HETATM	16	C20	MOL	1	1.461	1.119	3.227
C							
HETATM	17	H	MOL	1	-4.838	-1.058	-0.107
H							
HETATM	18	H	MOL	1	3.606	-0.915	-3.140
H							
HETATM	19	C30	MOL	1	1.170	3.158	-1.469
C							
HETATM	20	C38	MOL	1	2.731	-0.859	2.429
C							
HETATM	21	H	MOL	1	4.765	0.894	-0.008
H							
HETATM	22	H	MOL	1	0.952	-3.161	-3.704
H							
HETATM	23	C36	MOL	1	2.764	0.685	2.518
C							
HETATM	24	O	MOL	1	-3.958	-0.945	-3.575
O							
HETATM	25	O	MOL	1	-4.686	1.803	1.694
O							
HETATM	26	H	MOL	1	-0.080	4.680	-0.898
H							
HETATM	27	O	MOL	1	3.467	-3.908	0.995
O							
HETATM	28	H	MOL	1	0.043	-4.856	0.894
H							
HETATM	29	C32	MOL	1	1.248	-3.306	1.414
C							
HETATM	30	C12	MOL	1	3.241	1.499	1.283
C							
HETATM	31	C48	MOL	1	0.719	2.435	-2.738
C							
HETATM	32	H	MOL	1	-4.792	0.789	-0.126
H							
HETATM	33	C13	MOL	1	3.225	1.552	-1.251
C							
HETATM	34	C7	MOL	1	-0.796	-0.013	-3.873

C							
HETATM	35	C39	MOL	1	2.725	-0.732	-2.492
C							
HETATM	36	O	MOL	1	-3.543	3.756	1.096
O							
HETATM	37	H	MOL	1	-3.528	1.023	-3.153
H							
HETATM	38	H	MOL	1	-1.596	-4.157	-2.133
H							
HETATM	39	C26	MOL	1	-1.520	1.169	-3.211
C							
HETATM	40	C33	MOL	1	-1.223	-3.346	1.410
C							
HETATM	41	C31	MOL	1	-1.290	3.123	-1.469
C							
HETATM	42	C29	MOL	1	-1.329	3.084	1.567
C							
HETATM	43	C57	MOL	1	-2.450	-2.874	0.662
C							
HETATM	44	O	MOL	1	-4.567	-2.393	1.548
O							
HETATM	45	C8	MOL	1	-0.089	3.559	0.808
C							
HETATM	46	H	MOL	1	-2.026	1.649	-4.073
H							
HETATM	47	C46	MOL	1	-0.876	2.372	2.853
C							
HETATM	48	O	MOL	1	-1.036	-3.629	3.755
O							
HETATM	49	C14	MOL	1	3.196	-1.567	1.173
C							
HETATM	50	O	MOL	1	1.085	3.284	3.994
O							
HETATM	51	O	MOL	1	-4.521	-2.382	-1.821
O							
HETATM	52	H	MOL	1	0.866	-0.107	4.729
H							
HETATM	53	H	MOL	1	1.851	1.404	4.221
H							
HETATM	54	C49	MOL	1	0.796	-2.471	-2.855
C							
HETATM	55	C18	MOL	1	-3.314	-1.708	1.164
C							
HETATM	56	O	MOL	1	1.599	4.514	2.079
O							
HETATM	57	H	MOL	1	3.054	3.608	-0.899
H							
HETATM	58	H	MOL	1	-0.898	-3.241	-3.593
H							

HETATM	59	H	MOL	1	-1.661	4.075	-1.898
H							
HETATM	60	C24	MOL	1	1.524	1.281	-3.326
C							
HETATM	61	O	MOL	1	4.503	2.143	1.693
O							
HETATM	62	H	MOL	1	3.100	3.543	1.011
H							
HETATM	63	C54	MOL	1	2.404	2.731	-0.719
C							
HETATM	64	C3	MOL	1	-3.743	-0.914	-0.083
C							
HETATM	65	H	MOL	1	1.576	-4.272	1.846
H							
HETATM	66	C59	MOL	1	-2.428	-2.847	-0.864
C							
HETATM	67	C58	MOL	1	2.492	-2.807	-0.853
C							
HETATM	68	C2	MOL	1	-3.704	0.596	-0.030
C							
HETATM	69	C53	MOL	1	-2.587	2.665	0.808
C							
HETATM	70	C47	MOL	1	-0.782	-2.643	2.698
C							
HETATM	71	C41	MOL	1	-2.739	0.663	-2.463
C							
HETATM	72	H	MOL	1	-3.664	0.803	3.193
H							
HETATM	73	H	MOL	1	-1.585	-4.329	1.768
H							
HETATM	74	O	MOL	1	-2.034	-1.933	-4.669
O							
HETATM	75	C44	MOL	1	0.706	2.398	2.862
C							
HETATM	76	H	MOL	1	3.572	0.971	-3.209
H							
HETATM	77	C42	MOL	1	-2.857	-0.963	2.448
C							
HETATM	78	C52	MOL	1	2.403	2.706	0.821
C							
HETATM	79	O	MOL	1	-2.207	1.433	4.594
O							
HETATM	80	H	MOL	1	-3.108	-3.748	0.839
H							
HETATM	81	C25	MOL	1	1.564	-1.250	-3.341
C							
HETATM	82	C55	MOL	1	-2.522	2.640	-0.734
C							
HETATM	83	H	MOL	1	-1.658	4.058	1.973

H								
HETATM	84	H	MOL	1	1.043	-3.358	3.432	
H								
HETATM	85	C23	MOL	1	-1.563	-1.418	3.160	
C								
HETATM	86	C9	MOL	1	-0.070	3.589	-0.699	
C								
HETATM	87	O	MOL	1	-3.894	-1.303	3.446	
O								
HETATM	88	O	MOL	1	2.097	1.916	-4.535	
O								
HETATM	89	C40	MOL	1	-2.852	0.593	2.475	
C								
HETATM	90	C43	MOL	1	-2.841	-0.865	-2.617	
C								
HETATM	91	O	MOL	1	-1.217	0.175	-5.288	
O								
HETATM	92	C11	MOL	1	0.035	-3.821	-0.885	
C								
HETATM	93	H	MOL	1	-3.250	3.415	-1.040	
H								
HETATM	94	H	MOL	1	-0.176	4.650	0.984	
H								
HETATM	95	O	MOL	1	2.304	-1.834	-4.486	
O								
HETATM	96	H	MOL	1	4.718	-0.983	-0.057	
H								
HETATM	97	C15	MOL	1	3.179	-1.508	-1.281	
C								
HETATM	98	C5	MOL	1	-0.806	-0.174	3.624	
C								
HETATM	99	O	MOL	1	4.482	2.151	-1.712	
O								
HETATM	100	H	MOL	1	0.873	3.240	-3.482	
H								
HETATM	101	C16	MOL	1	-3.347	1.368	1.253	
C								
HETATM	102	O	MOL	1	-1.243	3.374	3.899	
O								
HETATM	103	C50	MOL	1	-0.795	2.387	-2.712	
C								
HETATM	104	C28	MOL	1	1.172	3.186	1.599	
C								
HETATM	105	H	MOL	1	-0.970	-0.275	4.716	
H								
HETATM	106	O	MOL	1	3.816	0.935	3.538	
O								
HETATM	107	H	MOL	1	3.277	-3.541	-1.113	
H								

HETATM	108	C17	MOL	1	-3.217	1.379	-1.224
C							
HETATM	109	C51	MOL	1	-0.725	-2.461	-2.824
C							
HETATM	110	C34	MOL	1	1.298	-3.325	-1.658
C							
HETATM	111	H	MOL	1	1.517	4.124	-1.888
H							
HETATM	112	H	MOL	1	-1.951	-1.768	4.134
H							
HETATM	113	C22	MOL	1	-1.617	1.078	3.282
C							
HETATM	114	O	MOL	1	-0.063	-5.264	-1.163
O							
HETATM	115	O	MOL	1	2.105	-1.822	4.470
O							
HETATM	116	C6	MOL	1	0.777	-0.004	-3.899
C							
HETATM	117	C4	MOL	1	0.700	-0.140	3.633
C							
HETATM	118	H	MOL	1	-1.046	3.122	-3.505
H							
HETATM	119	C56	MOL	1	2.501	-2.850	0.692
C							
HETATM	120	C35	MOL	1	-1.192	-3.260	-1.621
C							
HETATM	121	C37	MOL	1	2.740	0.795	-2.504
C							
HETATM	122	H	MOL	1	4.677	1.843	2.613
H							
HETATM	123	H	MOL	1	-3.196	4.590	0.722
H							
HETATM	124	H	MOL	1	-4.685	2.785	1.638
H							
HETATM	125	H	MOL	1	-4.365	-1.824	-3.413
H							
HETATM	126	H	MOL	1	4.312	2.921	-2.278
H							
HETATM	127	H	MOL	1	0.275	3.812	4.187
H							
HETATM	128	H	MOL	1	-4.097	-2.255	3.344
H							
HETATM	129	H	MOL	1	2.810	2.528	-4.277
H							
HETATM	130	H	MOL	1	1.406	-2.205	5.037
H							
HETATM	131	H	MOL	1	1.137	-4.952	-2.817
H							
HETATM	132	H	MOL	1	0.843	-5.621	-1.033

H								
HETATM	133	H	MOL	1	-2.204	3.239	4.074	
H								
HETATM	134	H	MOL	1	-1.488	1.788	5.157	
H								
HETATM	135	H	MOL	1	1.974	4.361	2.975	
H								
HETATM	136	H	MOL	1	-1.316	-1.839	-5.331	
H								
HETATM	137	H	MOL	1	-2.156	-0.119	-5.342	
H								
HETATM	138	H	MOL	1	1.145	0.883	-5.626	
H								
HETATM	139	H	MOL	1	3.658	-3.912	1.951	
H								
HETATM	140	H	MOL	1	-4.931	-2.845	-1.062	
H								
HETATM	141	H	MOL	1	2.064	-1.280	-5.264	
H								
HETATM	142	H	MOL	1	-1.984	-3.860	3.770	
H								
HETATM	143	H	MOL	1	3.623	0.400	4.336	
H								
TER								
CONNECT	1	21	12	33	30			
CONNECT	2	44						
CONNECT	3	66	51	64	90			
CONNECT	4	116	138					
CONNECT	5	49						
CONNECT	6	110	131					
CONNECT	7	20						
CONNECT	8	28	40	29	92			
CONNECT	9	97						
CONNECT	10	20	115	14	117			
CONNECT	11	34	74	109	90			
CONNECT	12	97	49	1	96			
CONNECT	13	108						
CONNECT	14	10	29	70	84			
CONNECT	15	66						
CONNECT	16	23	117	75	53			
CONNECT	17	64						
CONNECT	18	35						
CONNECT	19	31	111	86	63			
CONNECT	20	49	10	7	23			
CONNECT	21	1						
CONNECT	22	54						
CONNECT	23	20	16	106	30			
CONNECT	24	90	125					
CONNECT	25	101	124					

CONECT	26	86			
CONECT	27	119	139		
CONECT	28	8			
CONECT	29	14	119	8	65
CONECT	30	1	61	78	23
CONECT	31	103	60	19	100
CONECT	32	68			
CONECT	33	99	1	63	121
CONECT	34	91	11	116	39
CONECT	35	81	18	121	97
CONECT	36	69	123		
CONECT	37	71			
CONECT	38	120			
CONECT	39	34	103	71	46
CONECT	40	73	70	43	8
CONECT	41	103	82	59	86
CONECT	42	83	47	69	45
CONECT	43	55	80	40	66
CONECT	44	55	2		
CONECT	45	86	94	104	42
CONECT	46	39			
CONECT	47	75	102	42	113
CONECT	48	70	142		
CONECT	49	20	12	119	5
CONECT	50	75	127		
CONECT	51	3	140		
CONECT	52	117			
CONECT	53	16			
CONECT	54	110	109	81	22
CONECT	55	43	77	64	44
CONECT	56	104	135		
CONECT	57	63			
CONECT	58	109			
CONECT	59	41			
CONECT	60	116	31	88	121
CONECT	61	30	122		
CONECT	62	78			
CONECT	63	78	33	57	19
CONECT	64	3	55	17	68
CONECT	65	29			
CONECT	66	3	43	15	120
CONECT	67	97	119	110	107
CONECT	68	32	108	64	101
CONECT	69	82	36	42	101
CONECT	70	40	14	85	48
CONECT	71	37	108	39	90
CONECT	72	89			
CONECT	73	40			
CONECT	74	11	136		

CONECT	75	50	104	16	47
CONECT	76	121			
CONECT	77	87	55	85	89
CONECT	78	62	104	63	30
CONECT	79	113	134		
CONECT	80	43			
CONECT	81	116	35	95	54
CONECT	82	108	41	69	93
CONECT	83	42			
CONECT	84	14			
CONECT	85	77	70	112	98
CONECT	86	45	19	26	41
CONECT	87	77	128		
CONECT	88	60	129		
CONECT	89	113	101	77	72
CONECT	90	71	24	3	11
CONECT	91	34	137		
CONECT	92	110	120	8	114
CONECT	93	82			
CONECT	94	45			
CONECT	95	81	141		
CONECT	96	12			
CONECT	97	67	12	35	9
CONECT	98	113	105	117	85
CONECT	99	33	126		
CONECT	100	31			
CONECT	101	25	89	69	68
CONECT	102	47	133		
CONECT	103	41	31	118	39
CONECT	104	78	45	75	56
CONECT	105	98			
CONECT	106	23	143		
CONECT	107	67			
CONECT	108	82	71	13	68
CONECT	109	54	120	58	11
CONECT	110	54	92	6	67
CONECT	111	19			
CONECT	112	85			
CONECT	113	89	79	47	98
CONECT	114	92	132		
CONECT	115	10	130		
CONECT	116	34	4	60	81
CONECT	117	52	16	98	10
CONECT	118	103			
CONECT	119	67	29	27	49
CONECT	120	109	66	92	38
CONECT	121	60	35	33	76
CONECT	122	61			
CONECT	123	36			

CONECT	124	25
CONECT	125	24
CONECT	126	99
CONECT	127	50
CONECT	128	87
CONECT	129	88
CONECT	130	115
CONECT	131	6
CONECT	132	114
CONECT	133	102
CONECT	134	79
CONECT	135	56
CONECT	136	74
CONECT	137	91
CONECT	138	4
CONECT	139	27
CONECT	140	51
CONECT	141	95
CONECT	142	48
CONECT	143	106
END		